(4)

GROUNDWATER FATE OF AROMATIC HYDROCARBONS AT INDUSTRIAL SITES: A COAL TAR SITE CASE STUDY

by

Allison Ann MacKay

S.M., Civil and Environmental Engineering, Massachusetts Institute of Technology, 1993
B.A.Sc., Engineering Science, University of Toronto, 1991

Submitted to the Department of Civil and Environmental Engineering
In Partial Fulfillment of the Requirements of the Degree of

DOCTOR OF PHILOSOPHY
in Civil and Environmental Engineering

at the

MASSACHUSETTS INSTITUTE OF TECHNOLOGY
February 1998

Signature of the Author _____
Department of Civil and Environmental Engineering
January 16, 1998

Certified by _____
Philip M. Gschwend
Professor of Civil and Environmental Engineering
Thesis Supervisor

Accepted by _____
Joseph M. Sussman
Chairman, Departmental Committee on Graduate Studies

GROUNDWATER TRANSPORT OF AROMATIC HYDROCARBONS AT INDUSTRIAL SITES: A COAL TAR CASE STUDY

By

Allison Ann MacKay

Submitted to the Department of Civil and Environmental Engineering on
January 16, 1998 in Partial Fulfillment of the Degree of
Doctor of Philosophy in Civil and Environmental Engineering

Abstract

The fate of groundwater contaminants in anthropogenic fill materials was investigated at a coal tar site, Site YYZ. This site was representative of other contaminated sites with a history of industrialization at which wastes from process operations form the local subsurface solids. The solids composing the groundwater-bearing unit at Site YYZ were reactants (oil), byproducts (tar, coke) and wastes (gas purification box waste) used and produced during 100 years of gas manufacture operations at this site. The *in situ* groundwater transfer and reaction processes acting upon aromatic hydrocarbons in the subsurface at this site were hypothesized by comparing the groundwater fingerprints of individual compound concentrations to measured aqueous concentrations of these hydrocarbons in coal tar-equilibrated water. In general, the groundwater concentrations agreed with tar-equilibrated aqueous concentrations, indicating the source of aromatic hydrocarbons in the groundwater was equilibrium dissolution of the nonaqueous phase liquid tar.

The first field evidence of colloid-enhanced solubilization of hydrophobic organic colloids was found at Site YYZ. At some monitoring wells, groundwater polycyclic aromatic hydrocarbon (PAH) concentrations were greater than measured for aqueous equilibrium with tar by a factor which increased with compound hydrophobicity. Two thirds of the PAH mass in excess of dissolved solubility was associated with particles that could be settled from solution over 5 months. The remaining excess PAH mass was associated with 4 mg_C/L suspended organic carbon that was stable over 5 months, but could be precipitated at pH1, suggesting that PAHs were associated with humic acid-like molecules. About 5 mg_C/L of humic and fulvic acids were present in the groundwater at all monitoring wells sampled. The presence of colloids in the groundwater will increase the off-site flux of hydrophobic PAHs over flux estimates assuming only dissolved equilibrium with coal tar.

Evidence of bioattenuated xylene, naphthalene and methylnaphthalene concentrations was found at the shallow monitoring wells. The compound depletion patterns and groundwater ion concentrations were consistent with aromatic hydrocarbon removal by sulphate reducers. Biodegradation acted to decrease the off-site flux of these compounds, relative to tar-water equilibrium at Site YYZ.

Solid-water partitioning to carbon-containing anthropogenic fill solids isolated from Site YYZ was also quantified. The overall partition coefficients for fill solids mixtures were described by summing the sorption contributions of the individual materials, using sorbent-specific partition coefficients. Predictions of overall partitioning made on a carbon basis, assuming a natural organic carbon partition coefficient, were up to two orders of magnitude

different from measured values. An octanol water partition coefficient (K_{ow})-based linear free energy relationship for predicting sorbent-specific partitioning to wood was developed from an investigation of monoaromatic hydrocarbon sorption to wood chips, where log K_{lignin} = 0.71 log K_{ow} + 0.08. Accurate predictions of groundwater transport through anthropogenic fill solids at industrial sites must account for the composition of the fill matrix.

Thesis Supervisor: Dr. Philip M. Gschwend
Title: Professor

Acknowledgements

Funding for this research was provided by Baltimore Gas and Electric Company.

This thesis could not have been completed without the help of many others.

Thanks to Herb Hoffman, formerly of Baltimore Gas and Electric, Ian MacFarlane of EA Engineering, Science and Technology, and Rick Walden and Lee Malinowski of Baltimore Gas and Electric for technical and field support. Peter Dow, Mike and Ed of Environmental Drilling Inc. applied their expertise to obtain cores and install wells in the uncohesive fill. Extra big thanks to John MacFarlane, Freddi Eisenberg and Chris Swartz for their help and companionship while field sampling in the unseasonable, inclement weather I seemed to attract.

Thanks to my thesis advisor Phil Gschwend for helping me to strive for excellence in scientific questioning and for clarity in my thought expression. Phil and the other members of my thesis committee, Harry Hemond and Dennis McLaughlin provided many insights to help bring stacks of raw data together into a coherent story.

Thanks to members of the Gschwend group, Parsons Lab and the Gas Turbine Lab for some necessary diversions from research during my years at MIT, and for providing, perhaps unknowingly, sparks of motivation along the way. In my final months, I enjoyed the camaraderie of Tory Herman, Randi Carlson, and Chris Swartz who also suffered from the common task of having to manipulate the English language, instead of lab equipment.

My development as a scientist benefitted greatly from interesting conversations with Tory Herman and Lynn Roberson about "the way everything else works" .

I especially thank my best friend Ken Gordon for his unwavering support, awesome cooking and the coolest camping trips ever. What a challenge we have met together - double PhDs!!

Table of Contents

List of Tables

Appendix B

List of Figures

Chapter 1.

INTRODUCTION

Introduction

An important class of sites with contaminated subsurface solids and groundwater are industrial sites with a history of manufacturing operations. These are sites which have been industrialized for many years, especially before environmental regulations mandated secure landfill disposal of hazardous wastes, or before it was economical to recycle byproduct wastes. During this time many waste products may have been buried at these industrial sites, not only contaminating the subsurface, but also forming the hydrologic units through which infiltrating precipitation or groundwater moves. Because our understanding of groundwater transport processes has been developed through study of natural aquifers systems, we pose the question, "To what extent is our understanding of groundwater transport and reaction processes applicable to predict the transport of contaminants through these anthropogenic fill solids at industrial sites?"

This thesis addresses this question in a study to characterize the fate processes acting upon groundwater contaminants in a water-bearing unit composed of anthropogenic fill at a former manufactured gas plant site, Site YYZ. (Former manufactured gas plants are also referred to as "coal tar" sites because of the prevalence of this byproduct in the subsurface solids.) It is recognized that a unique combination of physical and chemical processes act upon the groundwater contaminants at this site; however, in a study of 25 former manufactured gas plant sites, all exhibited similar hydrology and contamination (Luthy *et al.*, 1994). Over 1000 manufactured gas plants were in operation in the United States prior to World War II (Environmental Research and Technology Inc and Koppers Company Inc, 1984). Coking plants employed similar production methods, and hence the same contaminants and waste products may be expected at these sites too. One common characteristic of manufactured gas plant sites was the use of fill materials to create "made land" near water bodies (Luthy *et al.*, 1994). There are likely many other industrial sites which followed this practice. Thus, results from this field study will be applicable at many sites due to the nature of the contamination or the subsurface solids.

History of Manufactured Gas Production and the Nature of Site Contamination

The history of gas operations at Site YYZ is outlined to provide an understanding of the reactant, product, and waste materials utilized and produced during gas manufacture. Reactant and product materials that are used and produced in large quantities during process operations will tend to compose fill materials and subsurface contamination at industrial sites. At Site YYZ, the property shoreline was expanded riverward over time by filling in the wetland with gas manufacture wastes (Figure 1.1). Building rubble from a local fire was also buried at this site.

Site YYZ is located in the mid-Atlantic region of the United States and operated as a manufactured gas plant facility from the mid-1800s until 1960. Manufactured gas, also known as town gas, was initially used for lighting, then later for heating and cooking when the manufacture process was modified to produce a gas of higher heating value. Natural gas supplanted manufactured gas as the major gaseous fuel source for heating in the 1950s with the introduction of interstate gas transmission pipelines. Manufactured gas plants could not remain competitive with this cheaper alternative gas source and most ceased operation about this time (Environmental Research and Technology Inc and Koppers Company Inc, 1984). A liquified natural gas distribution center currently operates at Site YYZ.

Manufactured gas was so named because it was produced from the destructive distillation of coal. In 1792, William Murdoch distilled coal in an iron retort and produced a gas for illumination. Within the next thirty years, large scale gas production was refined and the formation of gas production and distribution companies began throughout Europe and the Eastern and Midwestern US (American Gas Centenary, 1916).

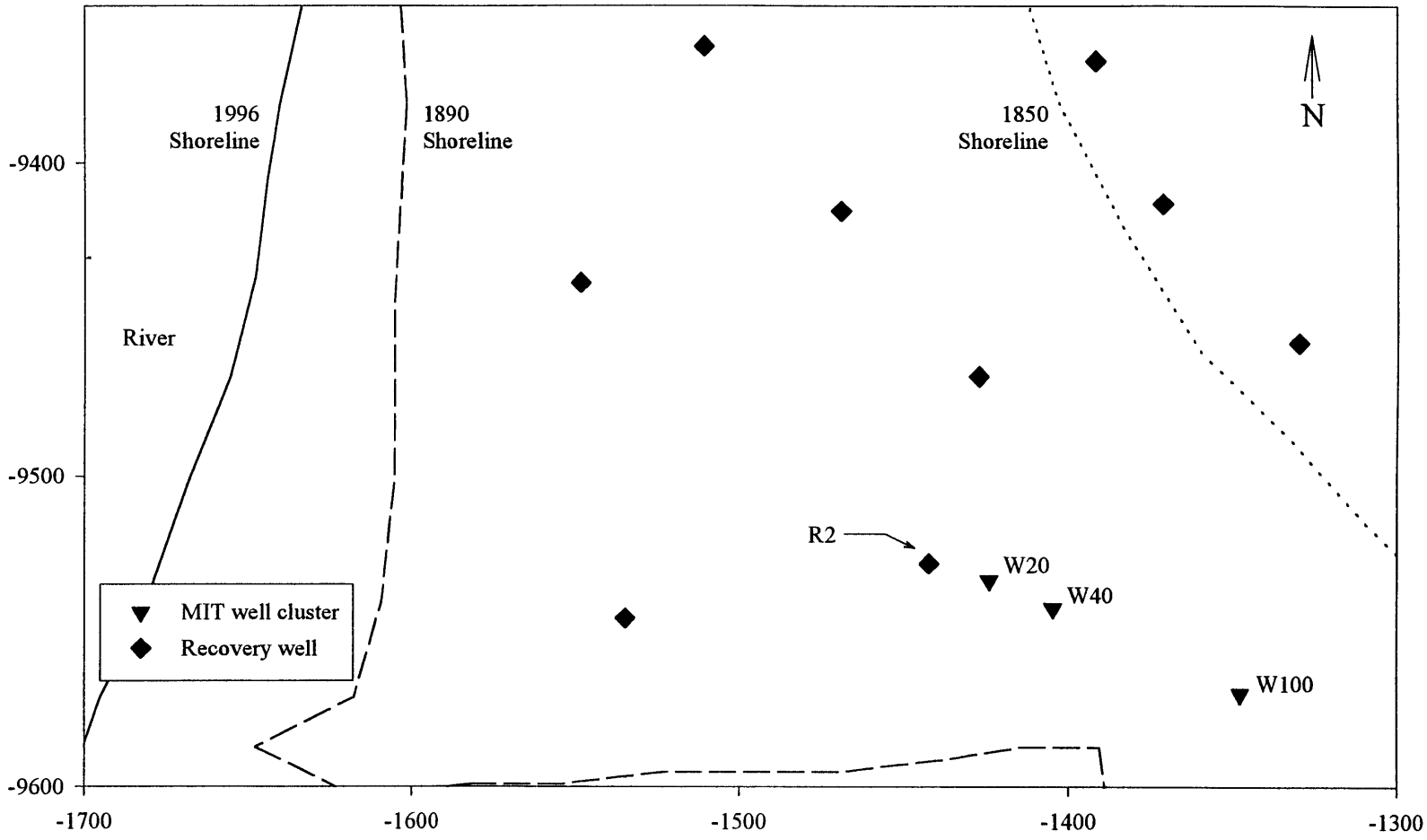

Figure 1.2. Map of Site YYZ detailing the study region. Axes denote distance (ft) from an arbitrary origin. The approximate locations of the historic shorelines in this landfilled region are noted.

Manufactured gas, a mixture of hydrogen, carbon monoxide and low molecular weight hydrocarbons, was produced by three processes. Coal gas was produced by heating bituminous coal in a closed vessel (up to 800°C) until all of the volatile materials were evolved as gas (Powell, 1945). Water gas, the most prevalent form of manufactured gas, was produced by alternately reacting coal with air and steam, thus increasing the heat content over coal gas by the addition of hydrogen. The heating value was further enriched by cracking petroleum oils in the hot gases (Environmental Research and Technology Inc and Koppers Company Inc, 1984; Morgan, 1945). Oil gas production was similar to the second step of water gas production (Environmental Research and Technology Inc and Koppers Company Inc, 1984). Coal gas was produced at Site YYZ until 1902 when production was switched to water gas. In 1949 gas production was subsequently converted to oil gas.

The destructive distillation of coal produced many waste products. Water gas production is summarized in Figure 1.2, explicitly noting the waste streams generated and their destinations. First, coal was not completely converted to volatile products. In addition to the gas, light oils, heavy tars, aqueous ammonia solutions (called liquor) and solid char residues (ash and coke) were also produced during gasification (Environmental Research and Technology Inc and Koppers Company Inc, 1984; Powell, 1945). The relative abundances of these gasification products varied somewhat as a function of gasification temperature: gas production increased from 6 to 18% by weight of coal, and coke production decreased from 81 to 74% with an increase in gasification temperature from 500 to 1100°C. Tar, oil and liquor production remained approximately constant at 5, <1, and 6%, respectively, by weight of coal gasified (Rhodes, 1945). When total gas production is considered, these amount to significant quantities of waste from manufacturing gas. In 1939, water gas production in the US was 4200×10^9 L (Morgan, 1945). Assuming a 12% conversion efficiency of coal to gas (on a weight basis) and an average gas density of 0.7 g/L (Environmental Research and Technology Inc and Koppers Company Inc, 1984), 1.3×10^6 metric tons of tar and 21×10^6 metric tons of coke were produced as byproducts in this year alone.

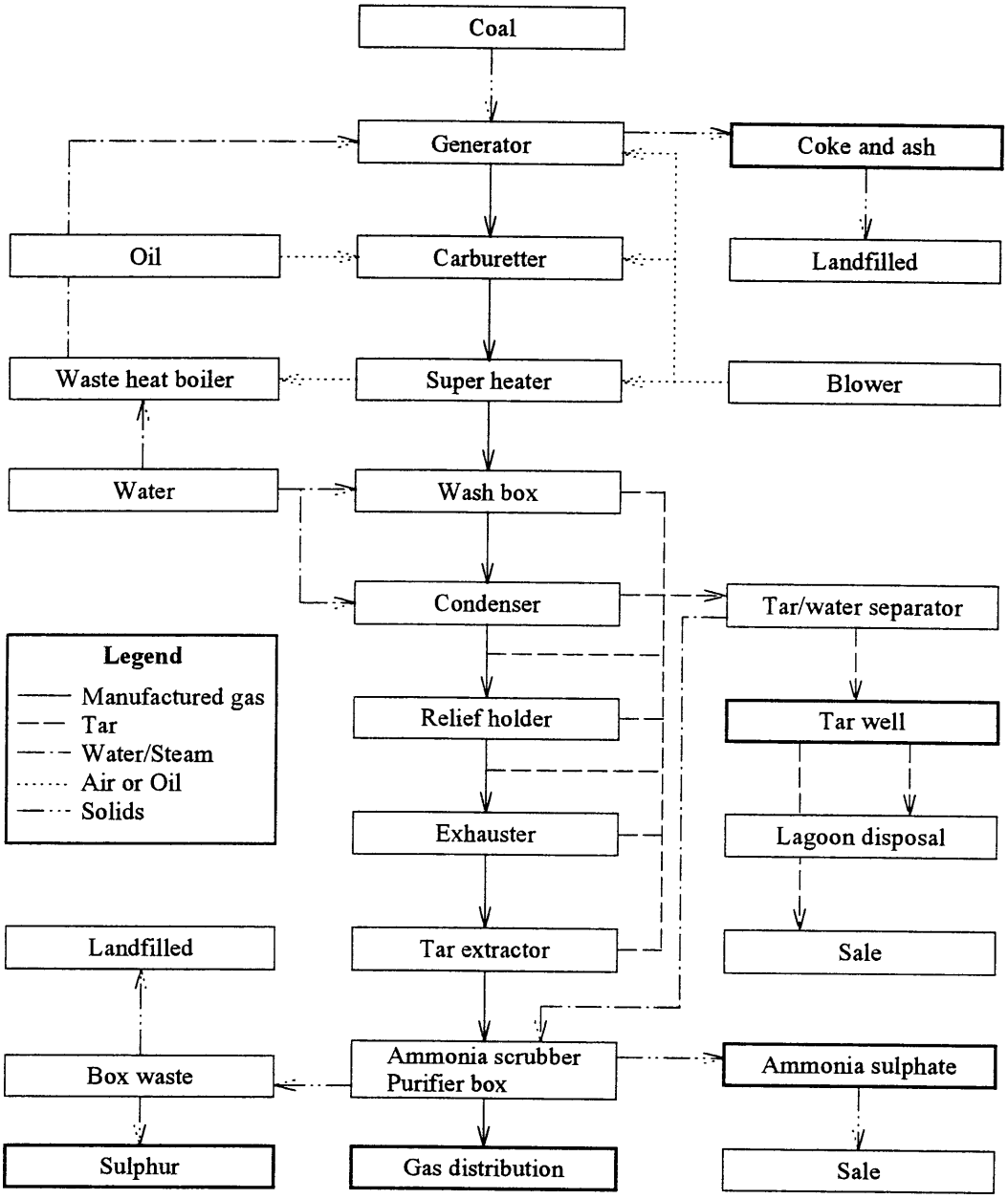

Figure 1.2. Material flow diagram for water gas production. Products of manufactured gas are noted in bold boxes. Adapted from Morgan (1945) and Environmental Research and Technology Inc. and Koppers Company Inc. (1984).

Wastes were also generated from the clean up of the gas stream. The hot gases exiting the retort contained unwanted impurities of hydrogen sulphide, hydrogen cyanide and ammonia. Hydrogen sulphide and hydrogen cyanide were removed by passing the gases through purifier boxes containing a mixture of iron oxides and wood chips. The purifier boxes were regenerated with air until the build up of ferrocyanide complexes prevented further use. Ammonia was scrubbed from the gas by passing it through sulphuric acid.

Some of the manufactured gas waste products had commercial value. By the turn of the century, coal tar had become an important raw material for chemical synthesis (*e.g.* naphthalene, tar acids and tar bases) and for the manufacture of creosote and road tars. Spent oxides or "box waste" could be sold for sulphur recovery (Gollmar, 1945). Ammonia sulphate from gas scrubbing was feedstock for fertilizer use (Wilson, 1945).

Waste products with no commercial value were land-filled. Until 1900 there was little market for coal tars, and tars generated up to this point were probably disposed on-site in sludge pits, tar ponds and disposal wells. Ash wastes had little use and were most likely landfilled. The use and disposal of light oils and coke are not clear (Environmental Research and Technology Inc and Koppers Company Inc, 1984).

Groundwater contamination at former manufactured gas plants resulted from the on-site disposal of tars, oxide wastes, ash and coke. Coal tars are viscous dense organic liquids composed of mono- and polycyclic aromatic hydrocarbons. Many of these compounds are potential carcinogens and are EPA priority pollutants. Oxide wastes are acidic solid wastes containing cyanides and heavy metals (Environmental Research and Technology Inc and Koppers Company Inc, 1984). Ash is primarily composed of aluminum, silicon and calcium oxides. All of these wastes have been observed to some extent in the subsurface at Site YYZ.

Research Outline

The purpose of this thesis was to understand some of the groundwater fate processes and characteristics of the fill solids which were unique to this, and other industrial sites, with water-bearing units composed of anthropogenic fill materials. The fate processes acting upon the groundwater contaminants at Site YYZ are discussed in Chapter 2. The subsurface source and fate of dissolved coal tar constituents were assessed by comparing the observed

groundwater concentrations of aromatic hydrocarbons with measured coal tar-equilibrated aqueous concentrations of compounds with a range of six orders of magnitude in solubility. Field observations were made under both ambient and induced groundwater gradient conditions. The physical-chemical characteristics of groundwater colloids which enhanced the groundwater solubilities of hydrophobic compounds at Site YYZ are described in Chapter 3.

Characteristics of the solids composing the anthropogenic fill at Site YYZ are summarized in Chapters 4 and 5. Chapter 4 presents some of the issues that may be important for modelling flow through fill solids. An extensive hydraulic characterization of these materials was not undertaken as part of this thesis. Chapter 5 presents the physical-chemical properties of the distinct fill materials found at Site YYZ, with respect to their chemical composition and their capacity to sorb nonpolar organic contaminants.

Wood was recognized as a material that may be buried as fill at many sites with a history of industrialization. Results from a study of monoaromatic hydrocarbon sorption to wood are presented in Chapter 6. A free energy relationship to predict wood sorption from octanol water partition coefficients is also presented.

The experimental results of this thesis are summarized again in Chapter 7 to introduce a discussion of future research areas which will broaden the understanding of contaminant transport at industrial sites with hydrologic units composed of anthropogenic fill. Some general guidelines for remedial investigation of these sites are also suggested.

Two appendices summarize results that were not central to the understanding of contaminant transport at this industrial site. The applicability of Raoult's Law to predicting equilibrium dissolution of coal tar is discussed in Appendix A. Appendix B presents a reverse phase separation method for quantifying *in situ* colloid-associated contaminants.

References

Consolidated Gas Electric Light and Power Company of Baltimore (1916). *American Gas Centenary 1816-1916.*

Environmental Research and Technology Inc; Koppers Company Inc (1984). *Handbook on Manufactured Gas Plant Sites.*

Gollmar, H. A. (1945). "Removal of sulfur compounds from coal gas." In *Chemistry of coal utilization*. H. H. Lowry, Ed. New York, John Wiley & Sons, Inc. **II:** 947-1007.

Luthy, R. G.; Dzombak, D. A.; Peters, C. A.; Roy, S. B.; Ramaswami, A.; Nakles, D. V.; Nott, B. R. (1994). "Remediating tar-contaminated soils at manufactured gas plant sites." *Environmental Science and Technology* **28**: 266A-276A.

Morgan, J. J. (1945). "Water gas." In *Chemistry of Coal Utilization*. H. H. Lowry, Ed. New York, John Wiley & Sons, Inc. **II:** 1673-1749.

Powell, A. R. (1945). "Gas from carbonization - Preparation and properties." In *Chemistry of Coal Utilization*. H. H. Lowry, Ed. New York, John Wiley & Sons, Inc. **II:** 921-946.

Rhodes, E. O. (1945). "The chemical nature of coal tar." In *Chemistry of Coal Utilization*. H. H. Lowry, Ed. New York, John Wiley & Sons, Inc. **II:** 1287-1370.

Wilson, P. J. (1945). "Ammonical liquors." In *Chemistry of Coal Utilization*. H. H. Lowry, Ed. New York, John Wiley & Sons, Inc. **II:** 1371-1481.

Chapter 2.

AROMATIC HYDROCARBONS IN GROUNDWATER AT A COAL TAR SITE

Abstract

The phase transfer and reaction processes acting upon aromatic hydrocarbons in the groundwater at a coal tar site were hypothesized by comparing the groundwater fingerprint of individual compound concentrations to measured aqueous concentrations in coal tar-equilibrated water. The source of aromatic hydrocarbons in the groundwater was the dissolution of residual nonaqueous phase liquid coal tar. Dissolution occurred under equilibrium conditions at this site. Evidence for colloid-enhanced solubilization of polycyclic aromatic hydrocarbons (PAHs) was found at some monitoring wells. PAH concentrations in the groundwater were elevated above tar-water equilibrium by sorption to colloid particles and suspended organic matter. Concentrations of xylenes, naphthalene and methylnaphthalenes were biologically attenuated at the shallow wells. Sulphate and sulphide were the only redox couple present in sufficient abundance to account for the loss of aromatic hydrocarbons, suggesting that sulphate reducers were important degraders at this site. An induced groundwater gradient had no effect on compound fate processes or groundwater chemistry compared to ambient gradient conditions.

Introduction

Fingerprinting may be used as a tool for probing groundwater fate processes and the efficacy of groundwater clean-up approaches (Sidebar 2.1). Site investigations begin with a hypothesized conceptual model of the governing transport equations for the contaminants present. This conceptual model, including source and sink terms, may be used to predict the distribution of contaminants in space and in time. The predicted distribution of compounds is likely not exact when compared to actual field data; however, if the governing transport equations are correct, the relative distributions of compounds in the conceptual model will match the relative distributions in the field data set. When the field data does not match the conceptualized compound distributions, deviations between the data sets which vary systematically with compound physical-chemical properties (*e.g.*, octanol-water partition coefficient, Henry's Law partition coefficient, Hammett constant) may be used to hypothesize additional fate processes that occur at the field site. Better predictions of remediation effectiveness or compound transport can be made once these additional processes are included in the conceptualized site model.

The use of trends in compound physical-chemical properties to investigate groundwater fate processes is only possible with analyses of individual compounds, and not with bulk measures of groundwater contamination (*e.g.*, total petroleum hydrocarbons (TPH), volatile organic compounds). When multi-component plumes exist, one compound may account for the majority of the mass in a bulk measure. Thus monitoring TPH, for example, only describes the space or time trends of one, or several, of the most abundant compounds. Information gained from the relative distributions of less abundant or less soluble plume constituents would be lost. Monitoring multi-constituent fingerprints may involve more intensive and expensive data collection and analysis; however, judicious use of these methods may save on future remediation costs. For example, fingerprinting has been used to identify natural attenuation of monoaromatic hydrocarbons (Thierrin *et al.*, 1995; Beller *et al.*, 1995) and halogenated solvents. At these sites implementation of remedial measures may be unnecessary. The presence of nonaqueous phase liquids (NAPL) was also deduced from the

Sidebar 2.1. Multi-component fingerprint analysis.

Fingerprinting is a method by which the relative ratios of organic compound concentrations in an environmental sample are used to deduce transformation processes occurring in the environmental system.

Example Application

Assume compounds A, B and C have the same physical-chemical properties (*e.g*, chemical formula, octanol-water partition coefficient) and differ only in the degradation rates in reaction **X** with C reacting twice as fast as B and four times as fast as A. If the source of A, B and C had a known composition given by the solid line (below), an environmental sample with the composition given by the dashed line would suggest that reaction **X** was occurring in the environmental system since concentrations of A, B and C are depleted to increasingly greater extent relative to the known source.

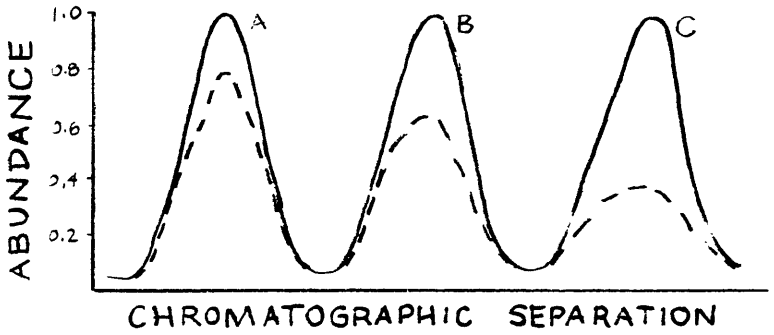

Fingerprinting may be used to deduce groundwater fate processes by gathering data over time, or space, and comparing relative compound distributions.

Conceptual Model

Since A, B and C have the same physical-chemical properties, the distributions of compound concentrations relative to the known source concentration should be the same for each and overlay one another when plotted in time or space.

Actual Distribution

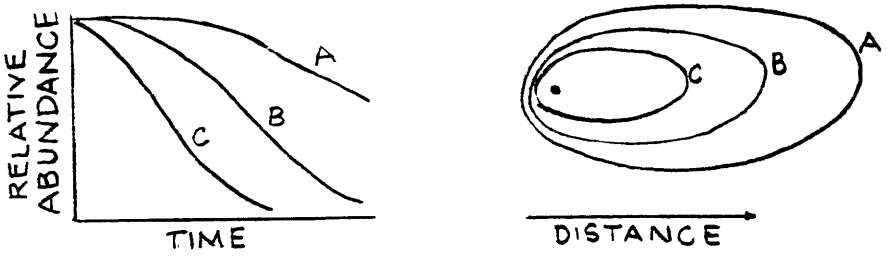

If the relative concentration distributions were obtained as shown above, these data would suggest that reaction **X** was a groundwater fate process acting on these compounds. Other data could then be gathered to support this hypothesis (*e.g.*, concurrent appearance of reaction products).

relative compound distributions in time (MacKay *et al.*, 1996) and space (Jackson and Mariner, 1995). Site remediation with unamended pump-and-treat could be eliminated from consideration as a clean-up scheme at these sites due to the long times necessary for dissolution of the NAPL.

This chapter details the use of fingerprinting to deduce the fate processes affecting mono- and polycyclic aromatic hydrocarbons (MAHs and PAHs) under ambient and induced gradient flow at a coal tar site. Residual tar was found in subsurface solids at this site (Chapter 5). Thus, the source of aromatic hydrocarbons in the groundwater was hypothesized to be equilibrium dissolution of coal tar. The conceptualized contaminant concentrations were the aqueous concentrations of aromatic hydrocarbons measured from a batch equilibration of purified water and site coal tar. The extent to which field measurements of individual compound concentrations deviated from the conceptual model was quantified by calculating the ratio of the observed (field) concentration to the measured (batch tar-water equilibration) concentration. This value was referred to as the enhancement (or depletion) factor when the observed concentration was greater (or less) than the measured concentration.

Field observations focussed on individual MAH and PAH compounds such that the range of physical-chemical properties of these contaminants would yield insight to hypothesize their fates at this site. Comparison of contaminant concentrations and groundwater quality parameters before and after inducing flow indicated that the gradient had little effect on aromatic hydrocarbon concentrations. However, several unique physical and chemical processes were found to act upon these compounds under both ambient and induced gradient flow. First, coal tar dissolution was hypothesized to occur under equilibrium conditions at this field site. Secondly, concentrations of hydrophobic polycyclic aromatic hydrocarbons were present above expected tar-water equilibrium solubilities, suggesting enhancement by the presence of colloids in the groundwater. Finally, concentrations of mono- and diaromatic hydrocarbons were biologically attenuated at this site.

Site Description

The coal tar site (Site YYZ) was located in the mid-Atlantic United States and is a former manufactured gas plant at which remedial actions are being undertaken to abate groundwater contamination. Briefly, the shallow unconfined water-bearing unit has been contaminated by a surface fuel oil spill. Oil percolated through the vadose zone and is now distributed on the water table. A series of wells have been installed to depress the local water table and induce flow of the oil to these wells for recovery. Prior to the oil spill, however, the groundwater and subsurface solids at this site had also been contaminated by wastes from gas manufacture, primarily coal tar. Therefore, a "pump-and-treat" remediation of the groundwater and solids at depth within the zone of influence is occurring as a result of the flow induction. This study focussed upon the changes in chemical and physical processes acting upon gasification contaminants resulting from this "pump-and-treat", well below the zone of oil contamination. It was possible to do so because the bulk of the groundwater flow was at depth in this water-bearing unit (Chapter 4).

The field study at Site YYZ was conducted in a water-bearing unit composed of anthropogenic fill materials. As operations expanded at the site, the western boundary was extended by filling in the river as depicted in Figure 2.1. The region of the field study is located just west of the original predevelopment shoreline in "made land" that was extended out over the time period to 1890. Ash, slag and other solid wastes (*e.g.*, wood chips) from gas manufacture were considered suitable fill materials at the time and were used as fill at Site YYZ. In addition, building debris from a local fire was also used. Evidence of these materials were noted in drilling logs from the field study region and observed in a boring obtained during this study (Chapter 5). The silty historic river bottom forms a semi-confining aquitard at the base of this unconfined water-bearing unit.

The ambient groundwater gradient was estimated from head distributions in fully penetrating, large diameter (0.3 m) extraction wells (Figure 2.1). The fully screened wells gave head measurements that were averaged through the depth of the fill material. The wide well diameters minimized effects of diurnal head variations. A plane was fit through the reported values and the ambient head gradient was found to be 0.006 in the WSW (254°) direction (SigmaPlot, Jandel Scientific). The ambient pore water velocity was estimated to be

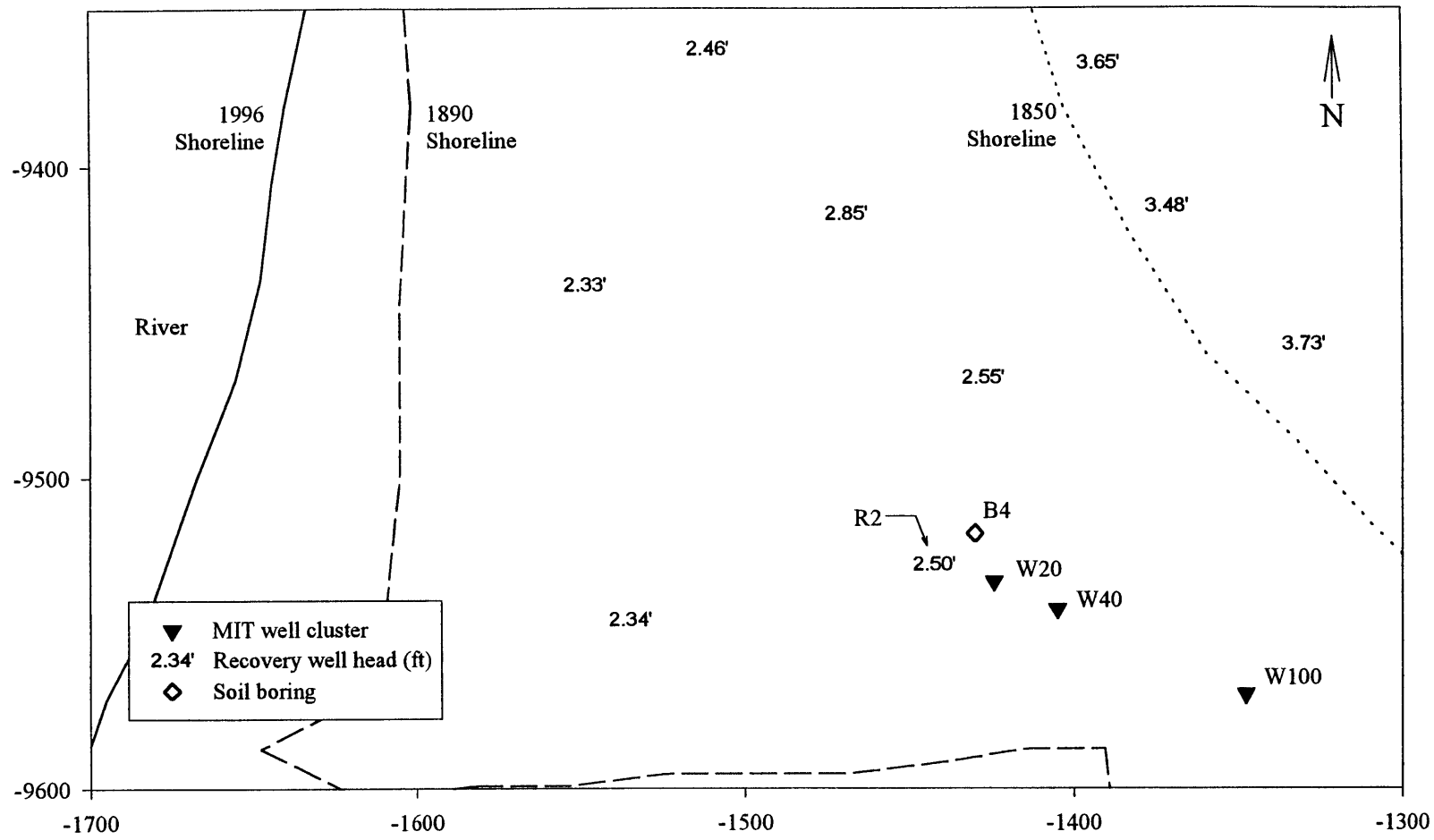

Figure 2.1. Map of Site YYZ detailing the field study area. Axes denote distance (ft) from an arbitrary origin. The approximate locations of the historic shorelines in this landfilled region are noted. April 10, 1996 ambient head measurements (ft relative to mean sea level) in the recovery wells are noted at the well location.

0.6 to 2 m/d with a porosity of 0.3 and a fill hydraulic conductivity of 15 to 30 m/d (Chapter 4).

The induced gradient at the MIT monitoring wells was calculated with a conservation of mass equation. A gradient was induced by pumping extraction well R2 at a rate of 27 L/min from April 12, 1996. Assuming equal radial flow, this volumetric flowrate was converted to a velocity at a distance, r, from the pumping well by dividing by a cylindrical area of height saturated thickness, b, and radius r:

$$v = \frac{Q}{2\pi r b \theta} \tag{1}$$

where Q (m^3/d) was the volumetric flowrate, and b (m) was the saturated zone thickness of 3 m. At the W20, W40, and W100 well clusters, the estimated induced pore water velocities were 1.2, 0.6 and 0.2 m/d, respectively.

Methods

Well Installation

The effect of an induced gradient on the fate of organic groundwater contaminants was investigated to the southeast of R2. The monitoring well locations were chosen to minimize the hydraulic effects of other wells in the recovery system so that R2 induced flow could be more easily characterized. Additionally, information was known about the fill solids in this region from the B4 boring. It was thought that there would not be any potentially mobile coal tar present above residual saturation in the area since tar processing occurred on the south border of Site YYZ.

A series of multi-level monitoring well clusters were installed at increasing distances (20, 40, 100 ft) from R2 in Dec. 1994 (Figure 2.1). All wells were 5 cm in diameter and constructed of stainless steel with 0.6 m screens (0.05 cm slots). Wells were installed using a hollow stem auger drilled continuously to the well screen depth, using no drilling fluids. The deepest well was installed first, just above the historic river silt. The medium and shallow wells were positioned with the screen bottom 0.30 m above the next deepest well. The shallowest well screen was located at least 1.2 m below the ambient water table and fuel oil

affected capillary zone. Coarse sand was used to backfill the well screens and the fill material collapsed above the sand. A bentonite seal was installed at the ground surface. No well development was conducted; however, the first ground water samples were not taken until Dec. 1995. Subsequent sampling events occurred on April 10 and 18, 1996, and in May and September, 1996.

Monitoring well nomenclature identifies the distance from the recovery well R2 and the depth of the well screen. Wells were denoted shallow (S), medium (M) and deep (D). For example, W40M is the medium depth well located 40 ft from R2. No W20D well exists as the silty historic river bottom was shallower at this location and only two wells could be installed with the screen placement criteria.

Groundwater Sampling

Slow pumping methods (Backhus *et al.*, 1993) were utilized to collect groundwater samples with minimum entrainment of immobile particles. First, wells were "scoped" with methylene chloride-rinsed aluminum tubing to determine the presence of coal tar in the wells. Tar depth was quantified according to the height of tar staining on the retrieved tubing after standing in the well for 10 min. Sample lines were installed with polypropylene and viton packers (QED, Ann Arbor, MI) to isolate the screened portion of the sampling wells. Sample line intakes were set at least 0.5 m above the tar when it was present in the bottom of the well. Sampling apparatus were allowed to stand overnight to minimize installation disturbances when pumping was begun. Groundwater samples were collected by peristaltic pumping at 28 - 34 mL/min. The pump was located downstream of the well and sample bottle such that groundwater only contacted aluminum tubing or glass (Figure 2.2). Turbidity was periodically monitored in the field by removing a flow-through cell off line for measurements with a calibrated turbidimeter (DRT-15CE, HF Scientific, Inc). Conductivity (HI8333, Hanna Instruments), pH (Orion), and redox potential (platinum electrodes, Orion) were also monitored in the field. Dissolved oxygen and sulphide were measured by colorimetric assay (Chemettes, Chemetrics, Calverton, VA). When turbidity levels became constant, samples for volatile aromatic compounds were collected in 40 mL amber VOA vials and PAH samples were collected in 2 L amber bottles. PAH samples were spiked at the site with an internal recovery standard of deuterated phenanthrene in methanol. Methylene

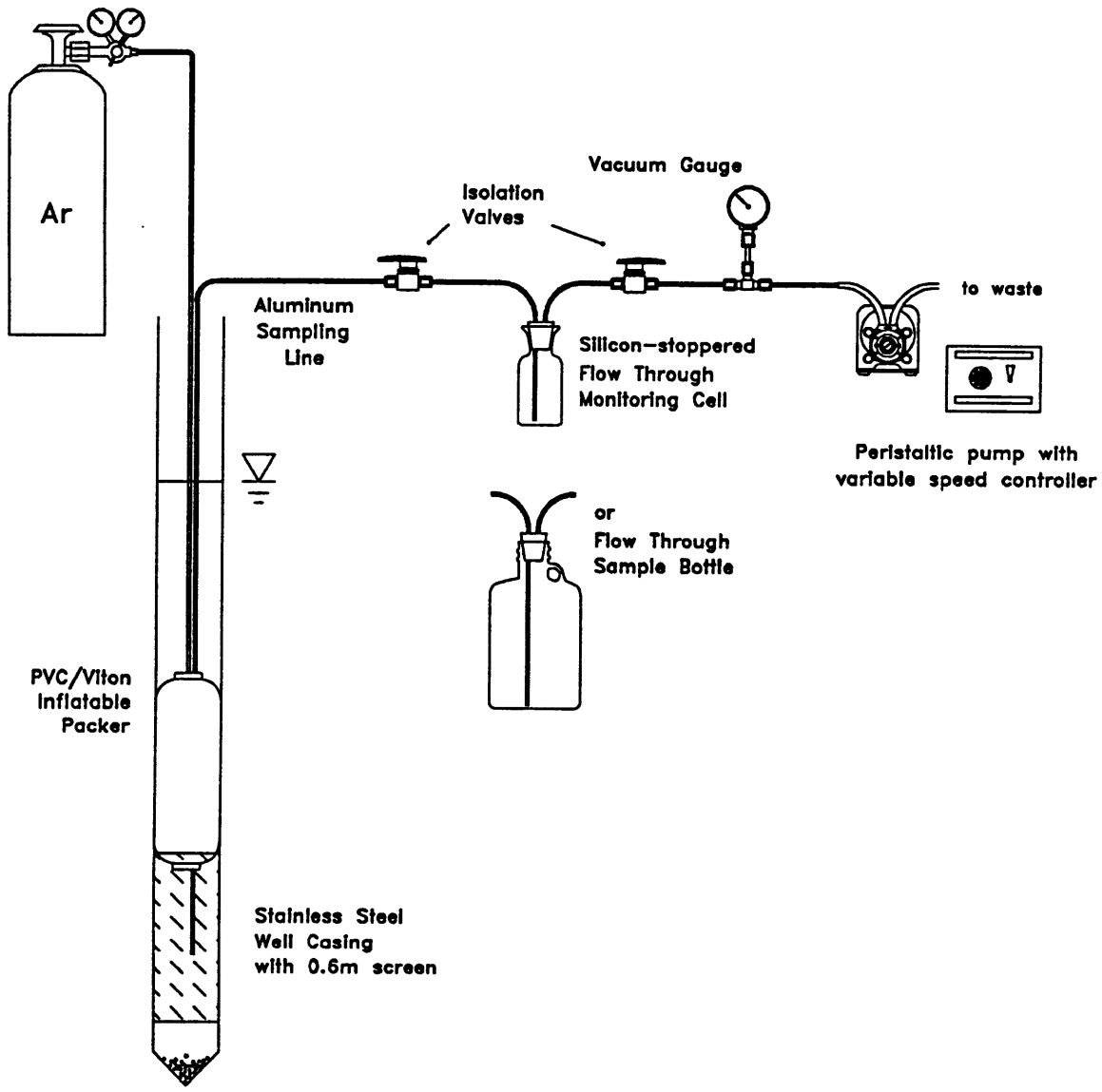

Figure 2.2. Groundwater sampling apparatus.

chloride (100 mL) was then added to the bottles to poison the water and to begin the extraction process. Groundwater for inorganic analyses was also collected and stored in 60 mL BOD bottles. Filter samples were obtained for microscopic observation of suspended particles. Small volumes of groundwater (0.5 - 2 mL) were filtered through 25 mm diameter filters (30 nm pore size, Nuclepore, Pleasanton, CA) in acid-washed Swinnex filter holders (Millipore, Bedford, MA). RO water (10 mL) was rinsed through the filters, and filters were stored in a desiccator. BOD bottles and VOA vials were kept refrigerated or in a chilled cooler until return to the lab.

Chemicals and Glassware

Solvents used for extraction of groundwater and dissolution of compounds were methylene chloride and methanol (Omnisolve, EM Science, Gibbstown, NJ) and hexane (Ultra-Resi, J.T. Baker, Phillipsburg, NJ). Recovery standards, internal standards and quantification standards of deuterated phenanthrene and *p*-terphenyl (Ultra Scientific, North Kingstown, RI), 1-bromo-4-fluorobenzene and 1,4-difluorobenzene (Aldrich, Milwaukee, WI) and m-terphenyl (Ultra Scientific) were used as received. External standards for PAHs were obtained as EPA 525 PAH Mix A (Supelco, Bellefonte, PA). Standards for quantification of volatile compounds were made up from neat compounds: benzene, toluene, ethylbenzene, *p*-xylene, *o*-xylene (all ChemService, West Chester, PA), naphthalene (J.T. Baker), 1- and 2-methylnaphthalene (Aldrich). Inorganic compounds included sodium sulphate (Mallinkrodt, Paris, KY); silica gel (100-200 mesh, EM Science); mercuric chloride (Fluka, Switzerland); sodium chloride, potassium phosphate monobasic, and sodium fluoride (all Mallinkrodt, Paris, KY); sodium nitrate and sodium nitrite (Sigma, St. Louis, MO); and 1000 mg/L stock solutions of iron, aluminum, calcium and silicon (Fisher Scientific, Fairlawn, NJ). Hydrochloric, phosphoric (Mallinkrodt) and nitric (Ultrex II, J.T. Baker) acids were used for acidification.

All glassware was soap and water washed, rinsed with reverse osmosis (RO) water and soaked in chromic/sulphuric acid cleaning solution (Fisher Scientific) for a minimum of 2 hours. Acid-soaked glassware was RO water, methanol, and methylene chloride rinsed.

Volatile Compound Analysis

Volatile organic compound samples were analyzed within 1 day upon return to the laboratory by direct aqueous injection gas chromatography (GC) or by purge and trap/GC. Cold on-column injections of aqueous samples were made to a Carlo Erba HRGC with a flame ionization detector (FID) held at 300°C. A 19 m, 5 μm film thickness column (0.32 ID, RTX-5, Restek, Bellefonte, PA) was used for chromatographic separation. The temperature program started at 103°C and ramped at 8°C/min to 200°C. Compounds were quantified with external standards.

September 1996 samples were analyzed by purge and trap/GC. A 300 μL sample was injected into 5 mL of RO water and purged for 7 min with helium at 10 mL/min. Purge gases were concentrated on a Tenax®/silica gel/charcoal trap. The trap was desorbed at 175°C for 4 min at a flowrate of 20 mL/min. The desorbed sample was transferred directly to the head of the GC capillary column through a 0.32 mm internal diameter deactivated fused silica line held at 150°C. The trap was reconditioned by baking at 225°C for 5 min. Compounds were separated with a 60 m, 1 μm film thickness DB5 capillary column (J&W Scientific, Folsom, CA) and detected by FID with a base temperature of 250°C. The temperature program began at 35°C with a ramp of 10°C/min to 200°C and the temperature was held at 200°C for 10 min. Blanks were run between each sample or standard injection. Internal purge standards of 1-bromo-4-fluorobenzene and 1,4-difluorobenzene were used to monitor compound recoveries. Purge standards did not vary for blanks, standards or samples, so no corrections were made to sample concentrations. The coefficient of variation between all purge standard injections was 10% (n = 13).

PAH Analysis

At the lab, groundwater samples were spiked with an internal recovery standard of *p*-terphenyl in methanol without disturbing the methylene chloride layer in the bottle. Groundwater was first extracted in the sample bottle and poured into a 2 L separatory funnel. The methylene chloride layer was drained off, and the water was extracted twice more with 80 mL volumes of methylene chloride. One aliquot of methylene chloride was used to rinse the walls of the empty sample bottle before being added to the separatory funnel. All extracts for each sample were combined and dried with sodium sulphate which had been baked at

450°C for 8 h. The dried extracts were concentrated to about 5 mL with a Kuderna-Danish concentrator. Extracts (or a subfraction for wells with high compound abundances) were then transferred into hexane by concentrating under a stream of nitrogen to a final volume of 1 mL.

PAH compounds were separated by silica gel column chromatography. Silica gel was baked at 450°C for 8 h. Fully activated silica gel (2 g) was wet packed and rinsed under pressure with hexane in glass columns. Groundwater extracts in hexane were applied to the column and compounds eluted under pressure with the following series: fraction 1: 15 mL hexane; fraction 2: 9 mL hexane + 5 mL hexane:methylene chloride (8:1); fraction 3: 13 mL hexane:methylene chloride (8:1) + 2 mL methylene chloride; fraction 4: 7 mL methylene chloride; fraction 5: 10 mL methylene chloride: methanol (9:1). The PAHs were contained in fraction 3 which was subsequently concentrated under a gentle stream of nitrogen.

Fraction 3 extracts were analyzed by capillary gas chromatography (Carlo Erba HRGC). An injection standard of *m*-terphenyl was added just prior to analysis to quantify the volume of the extract. A 30 m DB5-MS column (0.32 mm ID, 0.25 μm film thickness, J&W Scientific, Folsom, CA) was used for compound separation after cold on-column injection. The temperature program began at 70°C with a ramp of 12°C/min to 120°C, followed by a ramp of 3°C/min to 175°C, and a ramp of 8°C/min to 300°C and a final hold time of 5 min at 300°C. Compounds were detected by a flame ionization detector and quantified by measuring peak heights or integrating peak areas and comparing to known external standards. Phenanthrene and anthracene concentrations were corrected with deuterated phenanthrene recoveries and high molecular weight PAHs were corrected for recovery with *p*-terphenyl.

The compound detection limit with this analytical method was a groundwater concentration of 2×10^{-6} mg/L for a 2 L groundwater sample, assuming 100% recovery. *P*-terphenyl internal standard recoveries averaged 71 ± 20%. This 28% variability in internal standard recoveries was taken to be an estimate of the analytical variability in compound concentrations measured in groundwater samples.

Verification of Compound Identities

Compound identities were also verified by gas chromatography-mass spectrometry detection (HP 5995) by matching the temperature program as closely as possible to the above programs. The mass spectrometer was run with an electron ionization voltage of 70 eV. Cold on-column injections were made to a DB5-MS column (above). For PAH identification, a temperature program beginning at 70°C, with a ramp of 6°C/min to 300°C and a 15 minute hold time at 300°C was used. Mass-to-charge ratios were collected between 200-350 amu to increase detection limits of high molecular weight PAHs, integrating for 3 ms and averaging once. For volatile compounds, 3 mL of groundwater were transferred to a 15 mL vial. The vials were shaken for 5 min and 1 mL of headspace was withdrawn and injected on the GC/MS with a temperature program of 35°C for 5 min followed by a ramp at 8°C/min to 200°C with a hold time of 15 min. Mass-to-charge ratios of 50-170 amu were monitored.

Tar Analysis

Tar was pumped from W40M during the April 1996 sampling trip after the extraction well was turned on. A subsample of this tar was removed from the bottle, and a water phase allowed to separate. The glass tip of a 50 μL micropipettor (VWR Scientific) was immersed below the tar-water interface to ensure that only tar was sampled. The outer surface of the glass tip was wiped free of tar and the tar expelled below the surface of 50 mL of methylene chloride. This dilution was analyzed for PAHs and volatile aromatic compounds on the Carlo Erba HRGC with a DB5-MS column. The temperature program began at 35°C with a ramp of 8°C/min to 300°C.

Tar-Water Equilibration

Aqueous concentrations of tar components in equilibrium with coal tar were determined experimentally by mixing 3 mL of tar with 2 L of RO water. Sodium chloride (1 g/L) was added to match the groundwater conductivity, and mercuric chloride (10 mg/L) was added to inhibit biodegradation of components. The two phases were mixed with a stir bar for 2 days and the dispersed tar droplets were allowed to settle for 2 months before sampling. The aqueous phase was carefully siphoned into a separatory funnel using aluminum tubing primed with RO water. The aqueous phase was spiked with deuterated phenanthrene and *p*-terphenyl. The equilibrated water was extracted three times with

methylene chloride. The solvent extracts were combined and analyzed as described for PAHs. A small aliquot of tar-equilibrated water was also removed for purge-and-trap analysis of volatile aromatic compounds, as described.

Inorganic Compounds

Levels of inorganic anions in the groundwater were determined by ion chromatography (Dionex Ion Chromatograph 16). A 1 mL sample was delivered to the AS4A-SC column (Dionex,) and eluted with 0.003 M sodium bicarbonate/0.0024 M sodium carbonate buffer at a rate of 2 mL/min. Ions were quantified with external standards.

Groundwater cation concentrations were determined by graphite furnace atomic absorption spectrophotometry (Perkin Elmer 4100ZL). Standards were made up in Q-water (Millipore, Bedford, MA).

Carbon Analysis

Alkalinity titrations were performed by Gran titration with 0.02 N hydrochloric acid and an Orion pH meter. Total inorganic carbon was calculated assuming all the alkalinity to be bicarbonate ions and applying equilibrium dissociation constants (Morel and Hering, 1993).

Total non-purgeable organic carbon was determined by high temperature oxidation (Shimadzu, 8 μL syringe). Samples were acidified with phosphoric acid and purged with argon for 10 to 15 min prior to analysis. Purgeable organic carbon was determined by integrating the purge-and-trap chromatogram, using a benzene response factor (ng/area) for all peaks present except the naphthalenes for which the naphthalene response factor was used, due to the inefficient naphthalene stripping.

Surface Tension

Groundwater surface tension measurements were made by the falling drop method (Harkins and Brown, 1919). Measurements of RO water surface tension were made to verify this method. A value of 72.2 ± 0.1 dyne/cm (n = 5) was calculated for RO water and compares with the reported value of 72 dyne/cm at 25°C (CRC Handbook of Chemistry and Physics, 1989).

Electron Microscopy

Groundwater filters were observed by scanning electron microscopy (Cambridge Instruments). Particle composition was determined by energy dispersive X-ray analysis (Link Analytical) of carbon-coated filters. Particle size distributions were calculated from measurements of particle diameters of particles at random locations on the filter. Due to the time consuming nature of these manual measurements, only 30 particles were measured on each filter.

Results

Method Evaluation/Sample Quality

Groundwater sample quality was first evaluated to determine that artifacts from the groundwater sampling procedure were minimized. No conclusions can be drawn about the groundwater fate of aromatic hydrocarbons if representative samples were not obtained. It is generally thought that groundwater from the aquifer unit is being sampled after turbidity measurements have reached asymptotic levels (Backhus *et al.*, 1993). Groundwater turbidities were monitored at wells W20S, W20M, W40S and W40M through 5 to 9 days of continuous slow pumping over April 9-18, 1996 (Figure 2.3) to obtain data about turbidity variations at these wells.

Asymptotic turbidity levels at all of the wells sampled in April 1996 appeared to be less than 2 NTU. Turbidities fell within this range for these wells at all other sampling times, except at W40M in Dec. 1995. At that time it was thought that the sampling lines would freeze if pumping was continued overnight to allow turbidity stabilization. The last turbidity measurement before groundwater samples were obtained from W40M that day was 28 NTU. The long term asymptotic turbidity of groundwater at the W100 cluster is not known, but at each sampling time sufficient groundwater was pumped to reach asymptotic turbidities over a 12 to 24 h timescale. If the data collected for the W20 and W40 well clusters was representative of the W100 cluster, the turbidity levels approached on the timescale of a day were likely the same as those that would have been approached after longer term (*i.e.*, weekly) pumping.

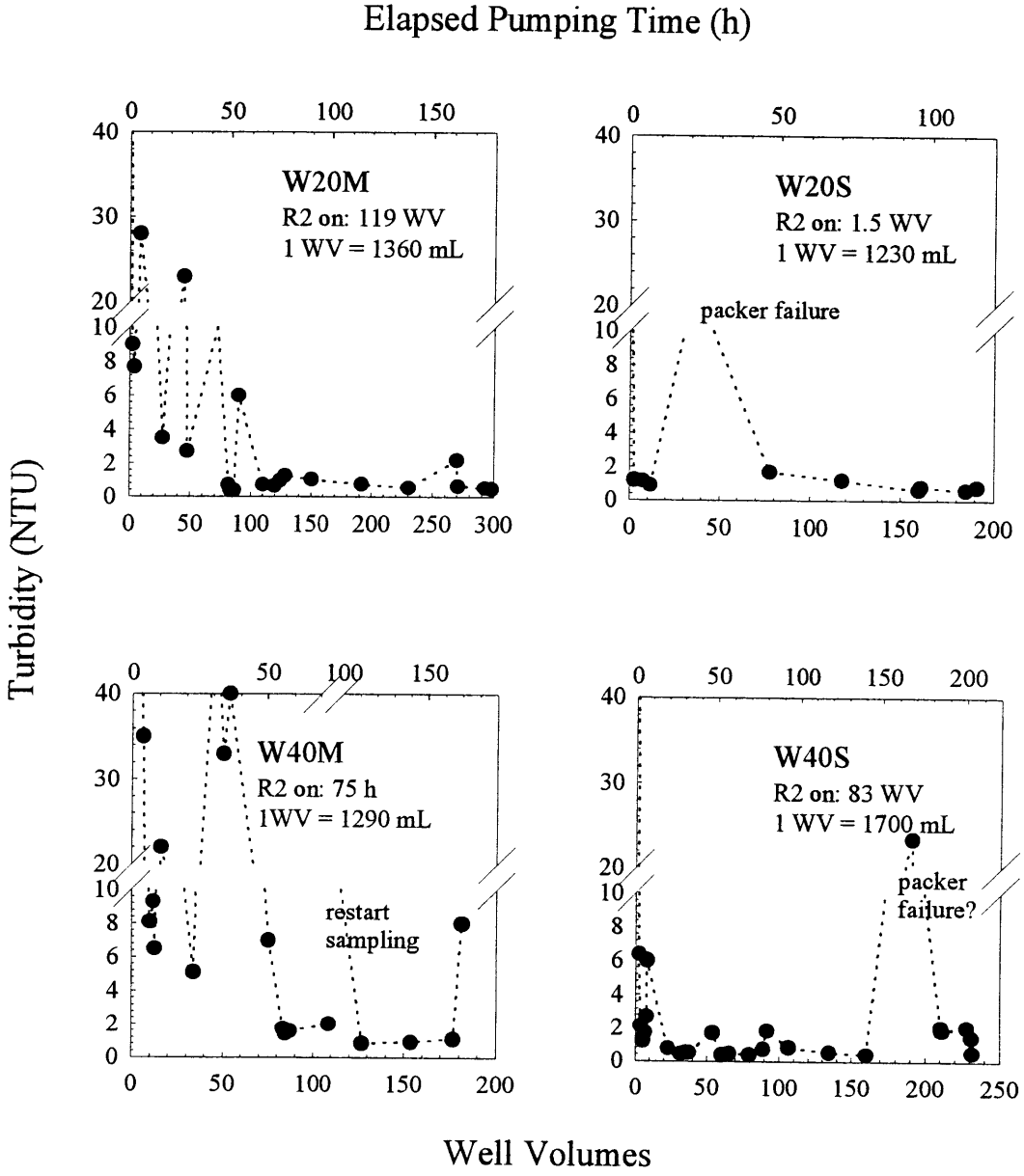

Figure 2.3. Groundwater turbidity during continuous slow pumping from Apr. 9 to 18, 1996. Turbidities are plotted as functions of both well volumes turned over (lower x-axis) and elapsed pumping time (upper x-axis). The initiation of induced gradient flow is noted on each figure. Instrument readings of turbidities below 10 NTU generally varied by ± 0.2 NTU.

The size distribution of particles in a groundwater sample also provides an indication of sampling artifacts. Slow pumping was employed to minimize shearing of the aquifer formation. High flowrates (*i.e.*, shear rates) cause the release of particles from the aquifer solids that would be immobile under the ambient groundwater gradient. If the fate of particle reactive or hydrophobic compounds, such as polycyclic aromatic hydrocarbons, are of interest, a groundwater sample obtained under high shear conditions may contain compound species which were not mobile under the ambient groundwater gradient.

Groundwater particles obtained on filters from Site YYZ were generally less than 1 μm in diameter (Figure 2.4). Thus most of the particles in the groundwater samples were likely mobile. Filter samples obtained after several hours of pumping wells in Dec. 1995 did contain larger particles, up to 40 μm in diameter (Figure 2.5). Energy dispersive X-ray analysis of these particles showed only a silicon peak. Dec. 1995 was the first time that the monitoring wells were sampled so these particles were likely dislodged from the surrounding sand pack during sample line installation. There was also concern at this date that sample lines might freeze so the packers were not allowed to stand overnight before sampling. These large particles were not observed at the other sample dates and it may be that well disturbance artifacts were allowed settle by setting packers the night prior to sampling.

The sampling distribution of the mean particle sizes were calculated from the frequency distributions for a population with an unknown variance. The mean diameter in Dec. 1995 was between 0.5 and 1.1 μm with a probability of 90%. With the same probability, the mean particle diameter was between 0.5 and 0.8 μm at W40S in Dec. 1995 and between 0.8 and 1.4 μm at W20M in Sept. 1996. As the cumulative distribution suggests (Figure 5.4), there was no significant difference between groundwater particles at W20M and W40S in Dec. 1995. After pumping was initiated at R2, the cumulative particle size distribution at W20M shifted to larger diameters; however, the range of mean particle diameter in Sept. 1996 overlapped the range of mean particle diameter computed for the pre-pumping Dec. 1995 sample date.

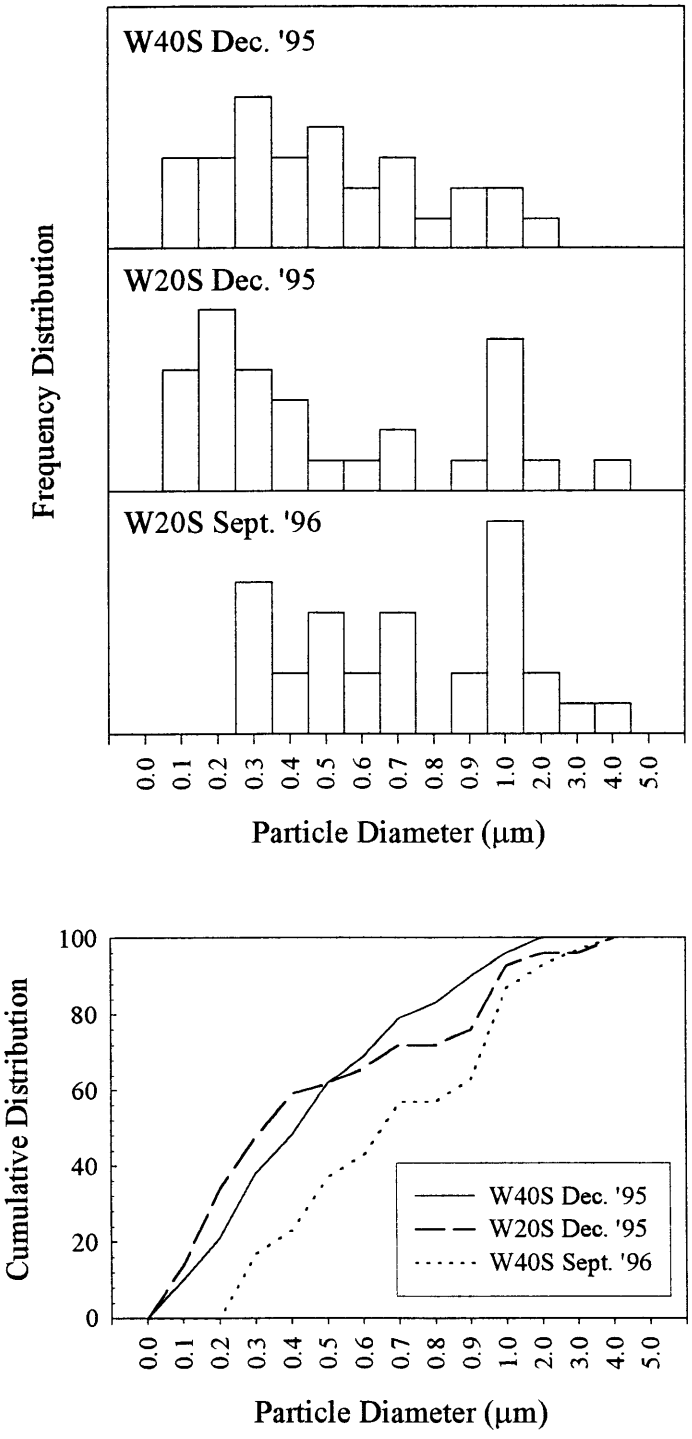

Figure 2.4. Particle size distributions of groundwater particles collected on Nuclepore filters. Particles were counted by scanning electron microscopy.

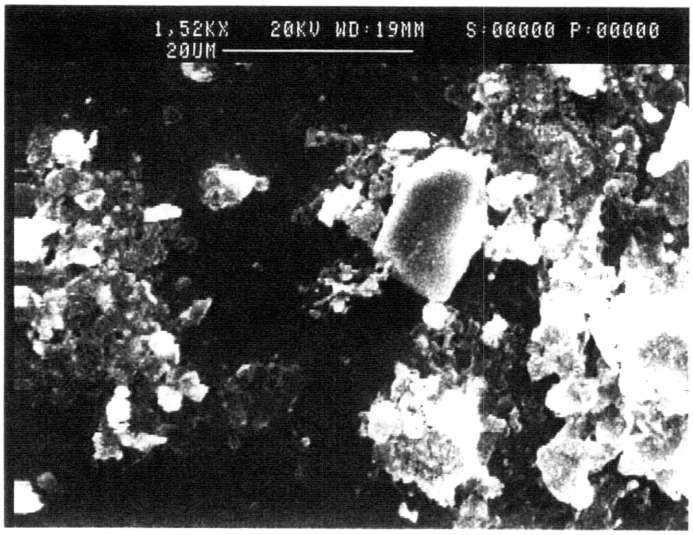

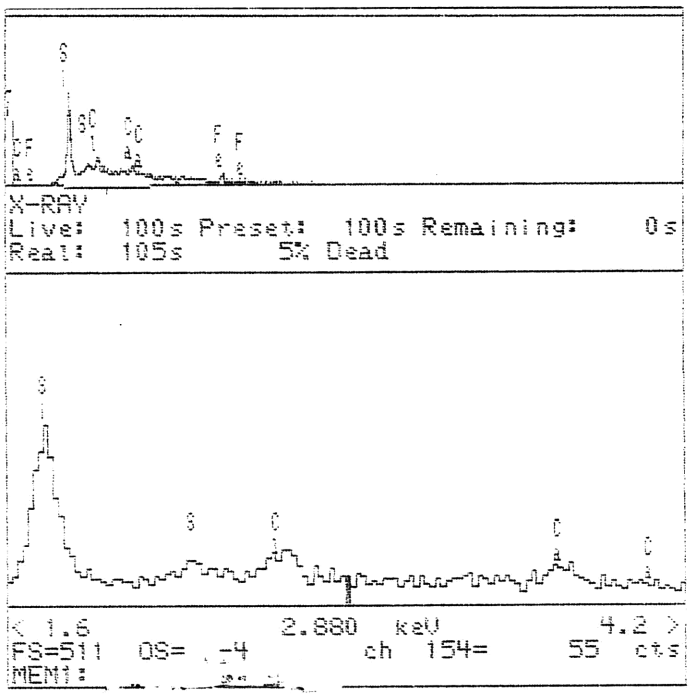

Figure 2.5. Scanning electron micrographs of groundwater particles.

Groundwater Quality Parameters

Water quality parameters (pH, conductivity, redox potential) showed little change over the entire sampling period from December 1995 until September 1996. Representative values are reported from Sept. 1996 (Table 2.1). The groundwater was mildly acidic and was reducing. The shallow wells consistently had the lowest redox potentials at each cluster and the presence of hydrogen sulphide was noted in winter, spring and fall.

Groundwater turbidity levels at Site YYZ were generally low, but varied over time and location. As noted, the asymptotic turbidity levels at all of these wells appear to be less than 2 NTU; however, turbidities did show considerable variability over time (*e.g.*, W20M, W40M, Figure 2.3). The timescales for these transient bursts to decline back to asymptotic levels may be shorter than suggested by Figure 2.3 because turbidity measurements were made only periodically. The increased turbidities at W20S (20 h) and W40S (170 h) likely resulted from packer failures. The integrity of the W20S packer was checked immediately after the 12 NTU value was reported. At this time the packer was loose in the well, suggesting that the higher turbidity may have been generated in the well with the expulsion of pressurized air upon packer failure. The packer in W40S was also loose at the end of sampling, although it is not known when over the last 100 h that it failed. (Failed packers were left in place because their large diameter still limited exchange of fluids between the screened interval and the standing water above in the well casing.) All other turbidity spikes were not correlated with known turbidity release events, and thus represent the natural variability of turbidity levels at this site.

High values of inorganic and organic carbon were found at all monitoring wells. The high alkalinity values and acidic pHs indicated very elevated dissolved carbon dioxide in the groundwater. Up to one third of the total organic carbon in the groundwater was contributed by volatile coal tar constituents. Of the remaining non-purgeable organic carbon, only about 2 mg/L was chromatographable with the temperature program used for PAH analysis. The residue remaining after evaporating an aliquot of the methylene chloride groundwater extract was less than 2 mg/L. Thus, the bulk of the nonvolatile organic carbon was not organic solvent extractable and is presumably composed of fulvic and humic acids.

Table 2.1. Physical and chemical groundwater parameters from September, 1996.

	W20M	W20S	W40M	W40S	W100D	W100M	W100S
pH	5.4	5.5	5.6	5.4	5.3	5.5	5.6
Turbidity (field) (NTU) (*prior to 2L sample)	1.4 (78*)	2.3	0.5	1.6	7.2	7.8	4.3
Conductivity (field) (mS)	1.95	1.37	1.76	1.32	1.50	2.23	2.44
Redox Potential (field) (mV, H° scale)	-51	-82	-31	-110	-16	+29	-76
Dissolved Oxygen (μM)	<1	<0.3	<0.3	6	<6	5	<0.3
S^{2-}_{Total} (μM)	<80	1600	<80	1600	<80	<80	800
SO_4^{2-} (μM)	2000	300	<1	1400	NA	20	1400
NO_3^- (μM)	4000	<1000	<300	<2100	NA	100	<2700
PO_4^{3-} (μM)	19	18	100	<3	NA	<3	<5
Alkalinity (meq/L)	27.2	15.7	19.2	14.6	15.4	18.6	15 1
CO_2 (calc'd) (atm)	$10^{+0.84}$	$10^{+0.51}$	$10^{+0.5}$	$10^{+0.57}$	$10^{+0.7}$	$10^{+0.58}$	$10^{+0.39}$
Nonpurgeable organic carbon (mg/L)	45	34	34	28	33	33	40
Purgeable organic carbon (mg/L)	13	3	16	4	16	14	17

NA - not analyzed

Table 2.1 (cont.). Physical and chemical groundwater parameters from September, 1996.

	W20M	W20S	W40M	W40S	W100D	W100M	W100S
Al_{Total} (μM)	30	20	4	7	17	31	80
$Al_{Dissolved}$ (μM)	1	1.4	2	1	9	2	10
Ca_{Total} (μM)	2400	7200	5000	5500	4200	4700	5500
Fe_{Total} (μM)	13	37	40	5	100	370	83
$Fe_{Dissolved}$ (μM)	3	70	3	3	12	4	7
Si_{Total} (μM)	NA	NA	1500	NA	NA	NA	1600
$Si_{Dissolved}$ (μM)	NA	NA	1000	NA	NA	NA	1300

NA - not analyzed

Mineral Phases

The composition of filterable material at Site YYZ could not be determined by energy dispersive X-ray (EDX) analysis of these filters. A representative EDX spectrum is shown and did not show any elemental peaks beyond the background from the bare membrane filter (Figure 2.6) The sparse abundance of material collected on groundwater filters may have been insufficient to determine submicron particle composition by EDX analysis. It is also possible that filterable material was organic in composition and thus gave no signal with a beryllium EDX window. High carbon content (50-90% by weight) coke was observed in the soil boring (Chapter 5). Perhaps coke fines are mobile in the groundwater but give no detectable EDX signal due to their virtually pure carbon content.

MINEQL (Schecher and McAvoy, 1994) calculations were made to determine the possible solids present in the groundwater at each well with groundwater compositions given by the total species measured and reported in Table 2.1. These calculations indicated that under equilibrium conditions the only solids present would be gibbsite from the precipitation of aluminum. Indeed, dissolved aluminum concentrations determined after sample filtration were less than total aluminum concentrations (Table 2.1).

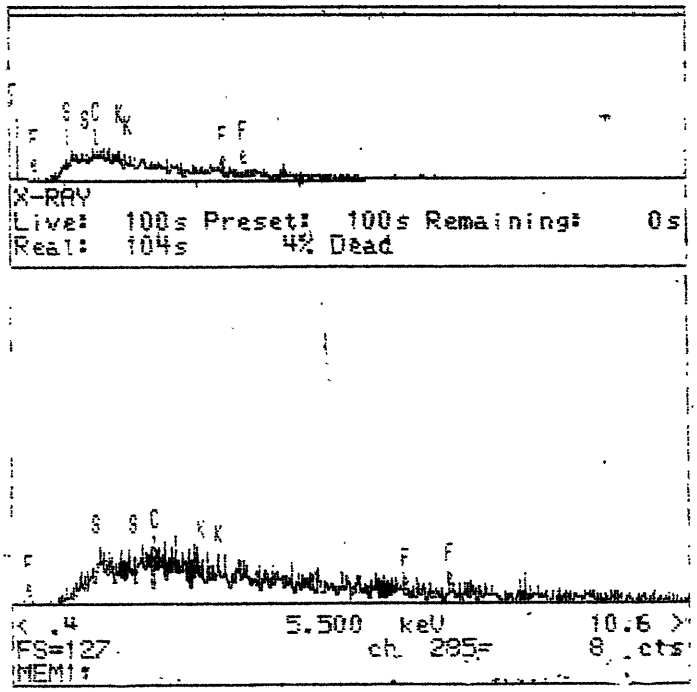

Figure 2.6. Representative energy dispersive X-ray spectrum of groundwater particles. The spectral locations of the primary calcium, aluminum, silicon and iron peaks are noted.

Aromatic Hydrocarbons in Groundwater

Concentrations of aromatic hydrocarbons in coal tar and coal tar-equilibrated water are reported in Table 2.2. Numerical values of aromatic hydrocarbon concentrations at W40M and W40S are also included in this table. Values for W40S are the average ± the standard deviation of three groundwater samples obtained over a 36 hour period.

Groundwater concentrations of aromatic hydrocarbons were graphically compared to measured batch equilibrium aqueous concentrations. An enlarged sample plot is shown for W40S (Figure 2.7). Here data are plotted with bidirectional error bars representative of the 28% variability in internal standard recoveries of *p*-terphenyl. Data from 3 samples taken over a 36 h time period prior to extraction well pumping were included to demonstrate variability between concentrations in replicate samples. In addition to the experimental data, lines denoting agreement of observed concentrations with tar-water equilibrium (1:1) and observed concentrations which differ by a factor of 2 (2:1 and 0.5:1) from tar-water equilibrium are also shown. The range of concentrations of most of the compounds generally fell within the 2:1 and 0.5:1 lines. (The low volatile organic compound concentrations are addressed later in the discussion section.) If the variability among individual samples taken over a short time period at W40S is representative of the heterogeneity of samples obtained at the other wells, then compound concentrations which differ from measured tar-water equilibrium by a factor of 2 are likely not significantly different than tar-water equilibrium levels.

The comparisons of observed groundwater concentrations to measured batch equilibrium concentrations at all sample dates are shown in Figures 2.8 to 2.12. One-to-one lines are also plotted for comparison with the equilibrium dissolution case. Points which fall below the 1:1 line are depleted with respect to equilibrium tar dissolution and points which fall above are enhanced over solubility in the presence of tar. For clarity, error bars were not included in these figures.

Table 2.2. Aqueous and tar concentrations of mono- and polycyclic aromatic hydrocarbons. Subcooled liquid solubilities are from Miller *et al.*, 1985, except for 2-methylnaphthalene, chrysene, and benzo(ghi)perylene which were calculated from the Yalkowsky equation (Schwarzenbach *et al.*, 1993). W40S groundwater concentrations are the average and standard deviation of 3 samples obtained over a 36 hour period.

Compound and Figure Abbreviation		Tar Concentration (mg/L)	Calculated Equilibrium Aqueous Conc. (mg/L)	Measured Equilibrium Aqueous Conc. (mg/L)	W40S Apr. 10, 1996 Groundwater Conc. (mg/L)	W40M Apr.10, 1996 Groundwater Conc. (mg/L)
benzene				1.1	3 ± 0.02	5.4
toluene				0.02	< 0.1	< 0.05
ethylbenzene		4900	1.36	1.21	1.4 ± 0.1	0.5
m, *p*-xylene	MX	990	0.32	0.28	< 0.05	0.4
o-xylene	OX	3200	1.0	0.87	0.073 ± 0.006	1.1
naphthalene	NA	55 700	7.8	10.5	0.4 ± 0.1	4.8
2-methylnaphthalene	2MN	29 000	1.0	2.09	< 1	3
1-methylnaphthalene	1MN	23 700	0.76	1.46	< 1	4
phenanthrene	PH	19 700	0.11	0.073	0.063 ± 0.0007	0.12
2-methylphenanthrene		3900				
anthracene	AN	5000	0.027	0.012	0.011 ± 0.001	0.02
fluoranthene	FL	6500	8.7×10^{-3}	3.3×10^{-3}	$3.8 \times 10^{-3} \pm 5 \times 10^{-4}$	0.015
pyrene	PY	9300	6.4×10^{-4}	1.4×10^{-3}	$2.5 \times 10^{-3} \pm 5 \times 10^{-4}$	0.011

Table 2.2 (cont.). Aqueous and tar concentrations of mono- and polycyclic aromatic hydrocarbons.

Compound and Figure Abbreviation		Tar Concentration (mg/L)	Calculated Equilibrium Aqueous Conc. (mg/L)	Measured Equilibrium Aqueous Conc. (mg/L)	W40S Apr. 10, 1996 Groundwater Conc. (mg/L)	W40M Apr.10, 1996 Groundwater Conc. (mg/L)
benz(a)anthracene	BA	3900	6.9×10^{-4}	7.7×10^{-4}	$3.8 \times 10^{-4} \pm 5 \times 10^{-5}$	7.9×10^{-3}
chrysene	CH	3600	9.6×10^{-4}	6.8×10^{-4}	$4.2 \times 10^{-4} \pm 3 \times 10^{-5}$	6.3×10^{-3}
benzo(b&k)fluoranthene		4300		2.4×10^{-4}	$1.8 \times 10^{-4} \pm 5 \times 10^{-5}$	3.4×10^{-3}
benzo(e)pyrene		3700		1.9×10^{-4}	$1.4 \times 10^{-3} \pm 1.4 \times 10^{-3}$	3.4×10^{-3}
benzo(a)pyrene	BaP	3600	1.1×10^{-4}	3.5×10^{-4}	$1.7 \times 10^{-4} \pm 9 \times 10^{-4}$	5.8×10^{-3}
indeno(123-cd)pyrene	IP	1200		6.2×10^{-5}	$7 \times 10^{-5} \pm 4 \times 10^{-5}$	2×10^{-3}
benzo(ghi)perylene	BP	1200	6×10^{-5}	1.6×10^{-4}	$6 \times 10^{-5} \pm 3 \times 10^{-5}$	2×10^{-3}

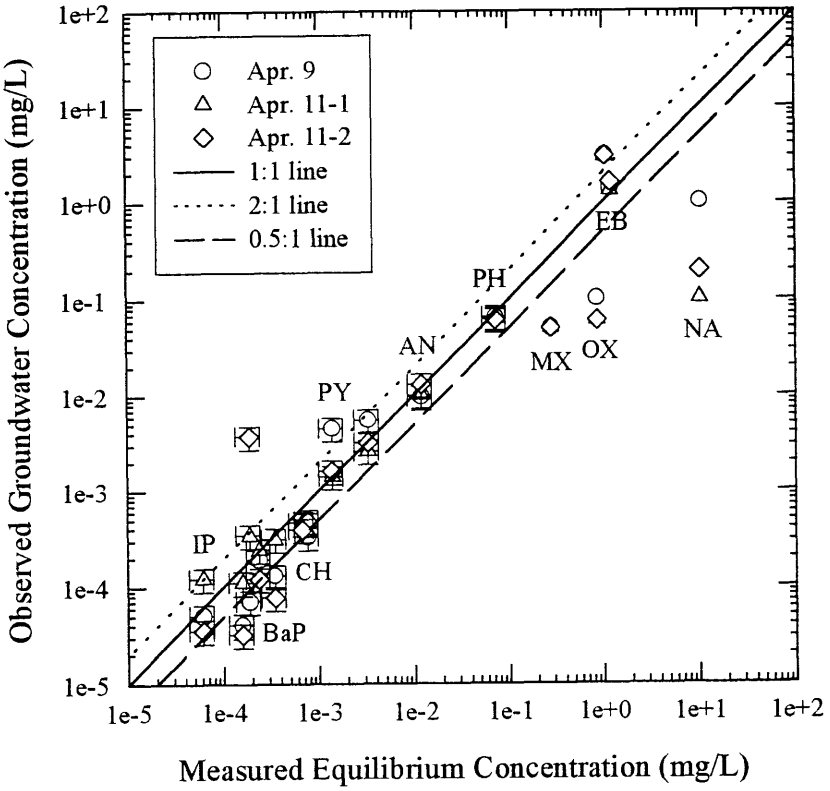

Figure 2.7. Replicate observations of groundwater mono- and polycyclic aromatic hydrocarbon concentrations at W40S. Observed concentrations are plotted against measured aqueous concentrations in equilibrium with W40M coal tar. Error bars represent analytical variability and are smaller than the data symbols where not visible. Compound identities are aligned above or below the respective data points and are abbreviated in Table 2.2.

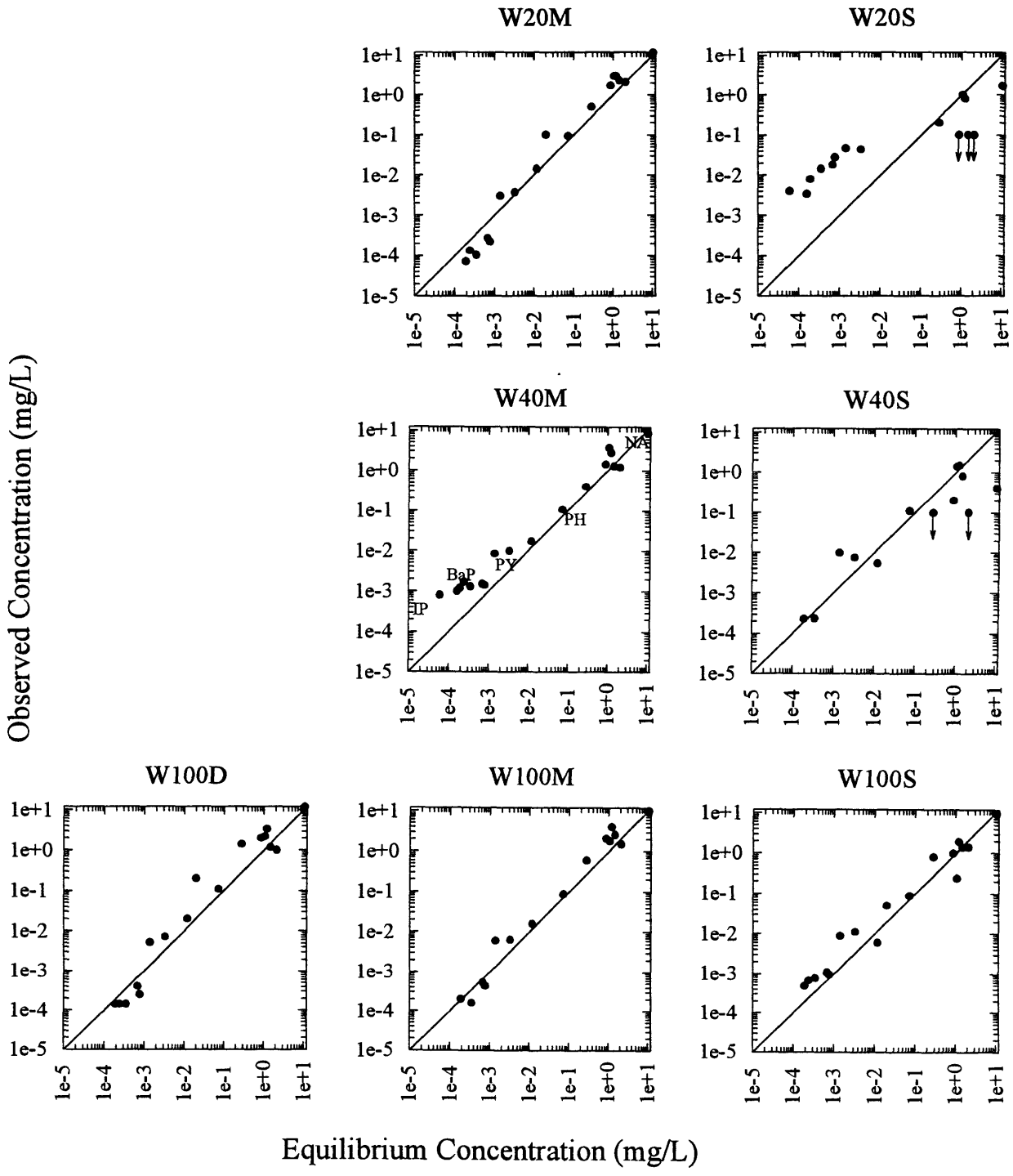

Figure 2.8. Aromatic hydrocarbon groundwater concentrations, Dec. 1995. Concentrations below detection limits are noted with an arrow and a symbol at the detection limit.

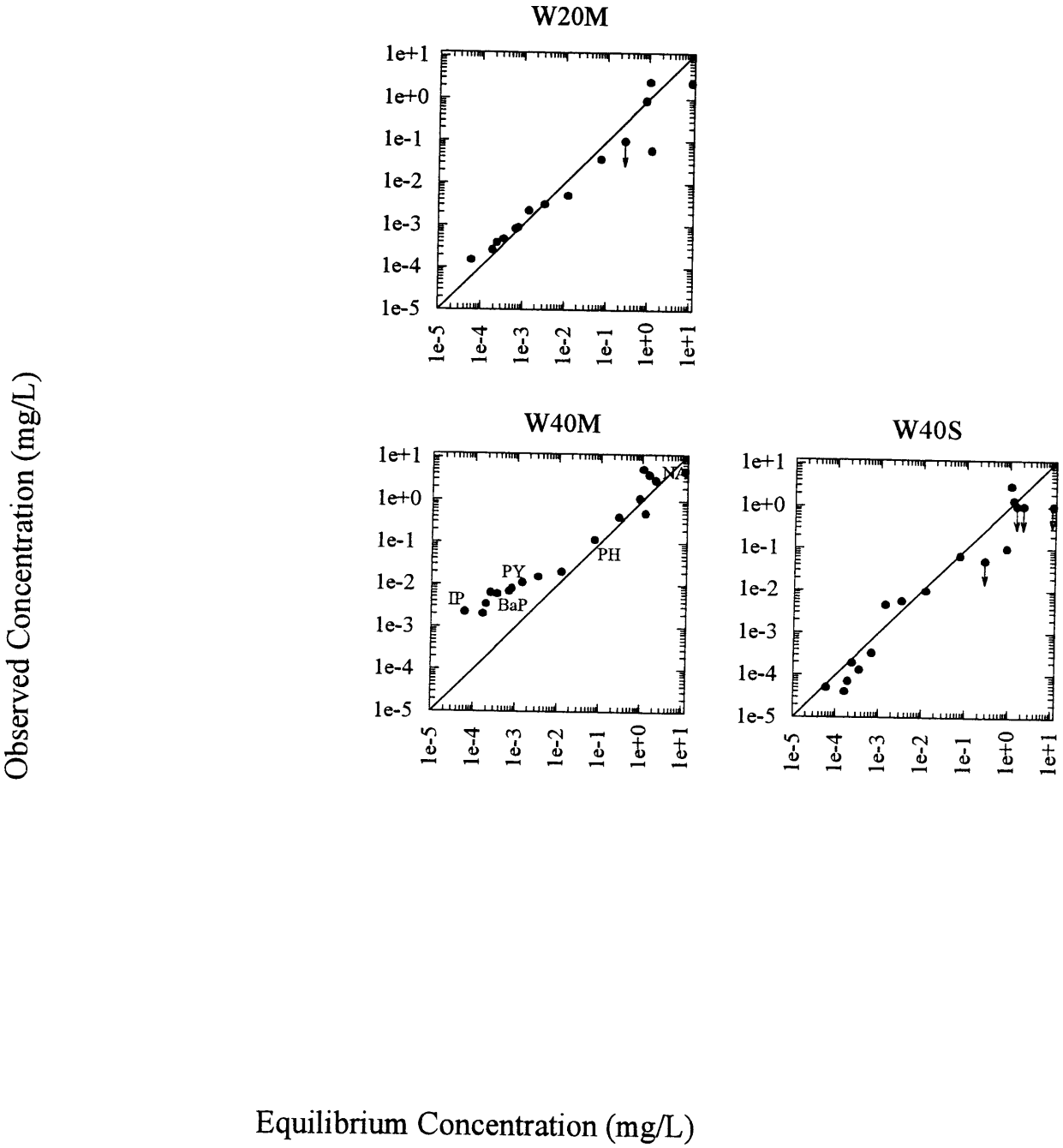

Figure 2.9. Aromatic hydrocarbon groundwater concentrations, Apr. 10, 1996. Concentrations below detection limits are noted with an arrow and a symbol at the detection limit.

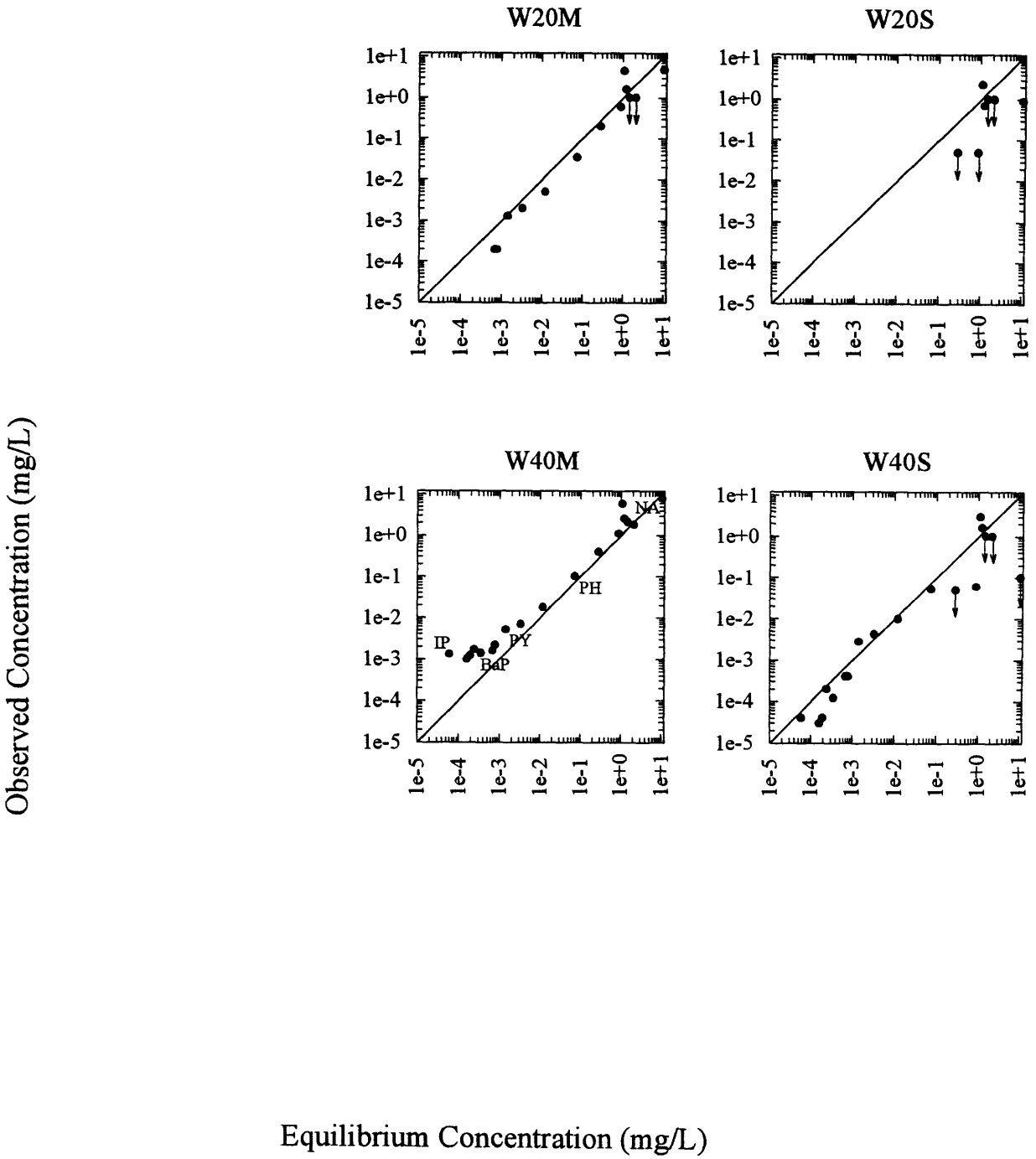

Figure 2.10. Aromatic hydrocarbon groundwater concentrations, Apr. 18, 1996. Concentrations below detection limits are noted with an arrow and a symbol at the detection limit.

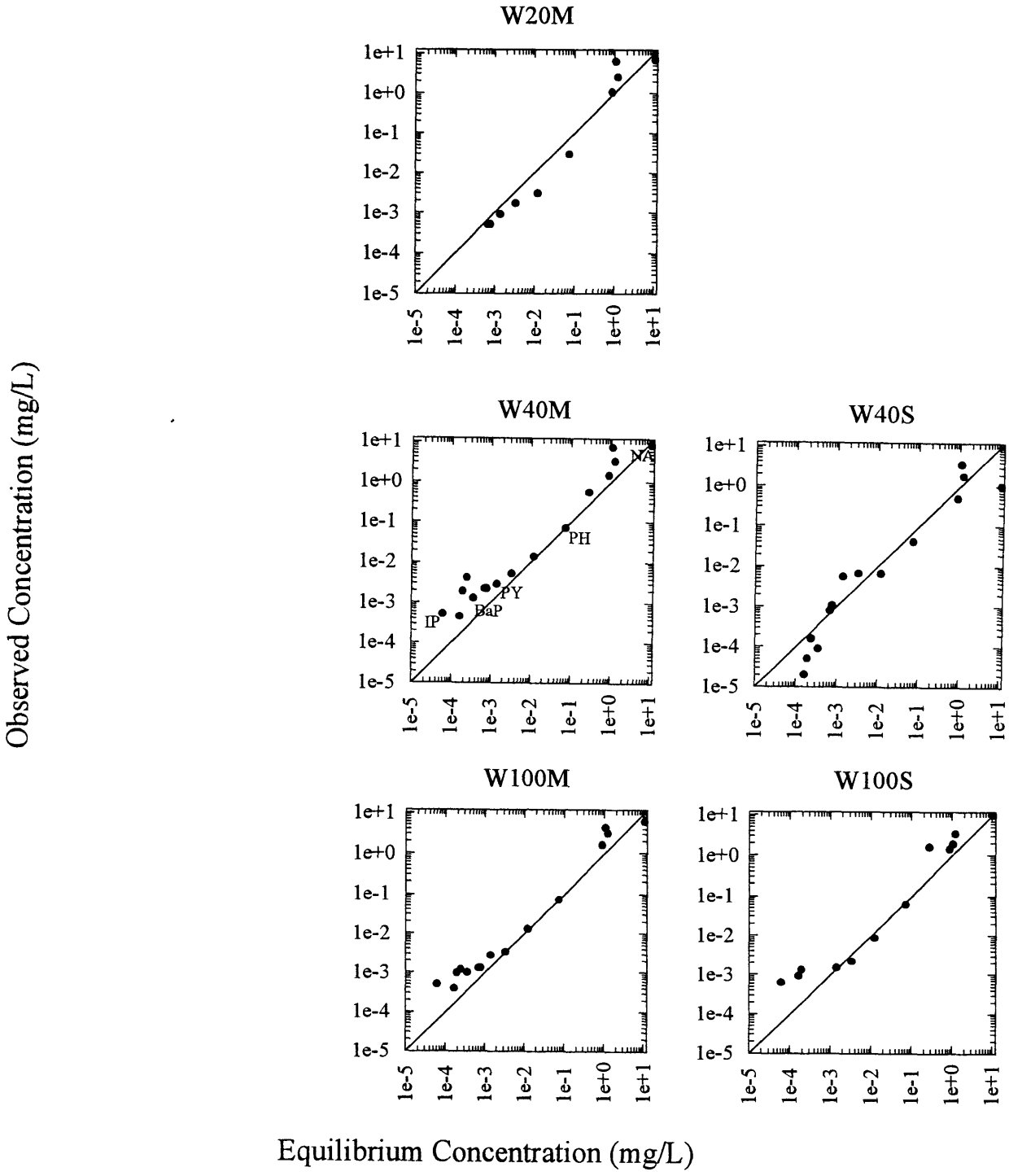

Figure 2.11. Aromatic hydrocarbon groundwater concentrations, May, 1996. Concentrations below detection limits are noted with an arrow and a symbol at the detection limit.

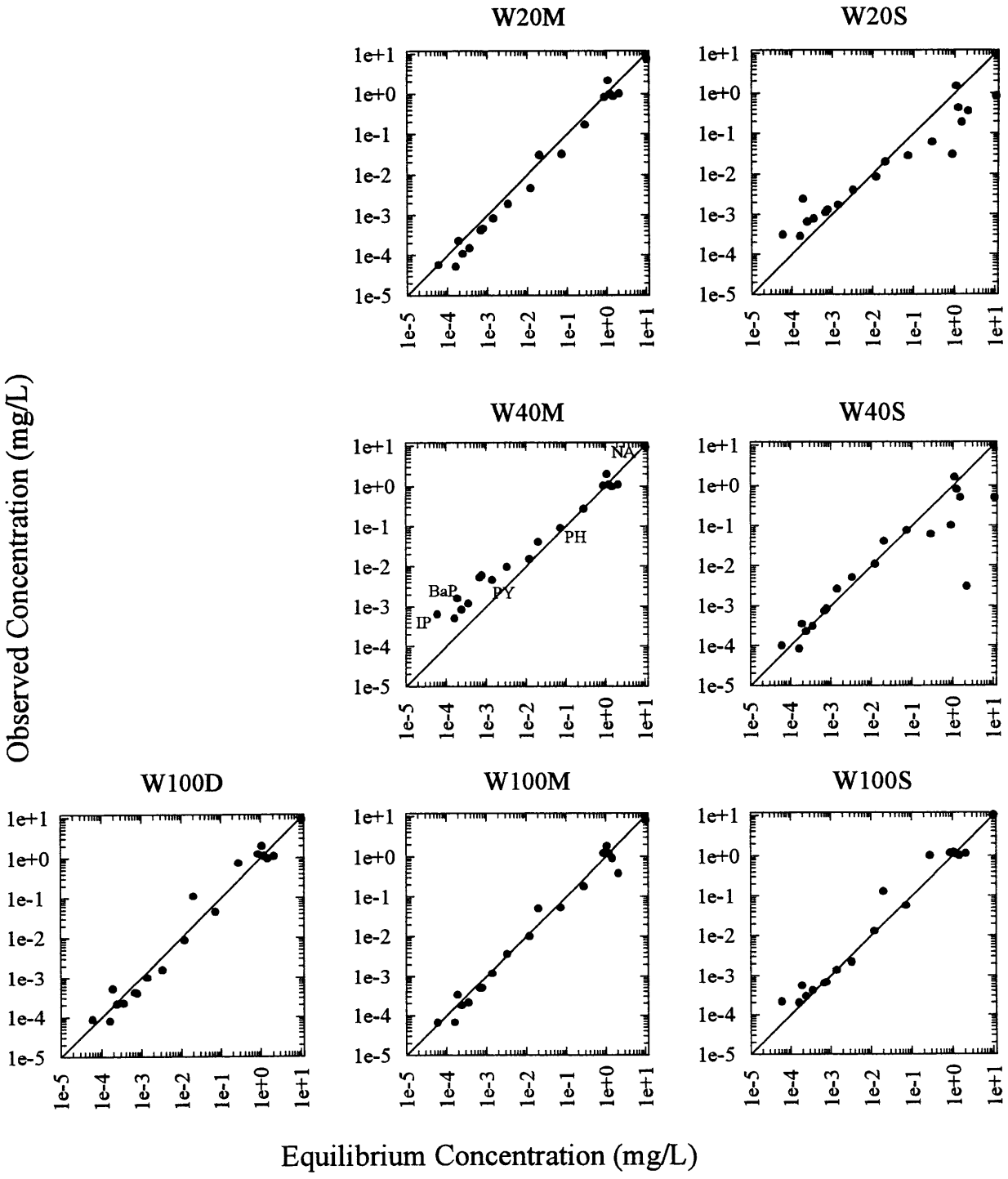

Figure 2.12. Aromatic hydrocarbon groundwater concentrations, Sept., 1996. Concentrations below detection limits are noted with an arrow and a symbol at the detection limit.

Discussion

Changes in Groundwater Chemistry from an Induced Groundwater Gradient

Pumping of the extraction well, R2, increased the groundwater hydraulic gradient at Site YYZ above the ambient level. Over a 4 hour period after starting R2, the vacuum required to peristaltic pump groundwater at the W20 and W40 well clusters increased, indicating a decline in the watertable. By Apr. 18, groundwater levels had decreased about 0.3 m from the pre-pump levels at the W20 cluster and about 0.15 m at the W40 cluster. The induced gradient was linearly approximated to be 0.025 between the clusters.

Turbidity is likely the first groundwater quality parameter to show a response to the induced gradient. A turbidity pulse may be released in response to the increased shear from the higher velocities created by pumping. If the composition of fill solids at Site YYZ is similar at all of the well clusters, the greatest turbidity release would be expected at W20 since the local groundwater velocity increased by a factor of 3 with the onset of pumping. Sampling at W20S was initiated coincident with the start-up of R2 and showed turbidity levels less than 2 NTU (Figure 2.3). There appeared to be a slight increase in turbidity values at W20M after R2 began pumping (Figure 2.3). Turbidity increased from 0.65 NTU to 0.95 and 1.25 NTU after 5 and 7 hours of pumping, respectively; however, these fluctuations were less than the levels observed during pre-pumping monitoring and were not maintained with continued pumping. Similar trends were observed at W40S and W40M in response to pumping from R2 pumping. (Groundwater sampling was suspended at W40M for 3 days to remove tar from the bottom of this well when R2 was started.). Thus the induced gradient did not cause sustained turbidity releases from the fill solids, relative to pre-pumping levels.

Particle size distributions of suspended material in Site YYZ groundwater also did not appear to change as a result of the induced gradient. Particle sizes were determined by microscopic observation of groundwater filters. Problems with insufficient sample volume and incomplete salt removal limited the comparisons that could be made by this method with filters from the April 1996 sampling event. Filters from Dec. 1995 (pre-pumping) and Sept. 1996 (pumping) sampling events were compared instead. The W20 cluster was expected to show the greatest change in groundwater velocity as a result of pumping. Little difference was seen between particle sizes at W20S at these two dates or between W20S and W40S

(Figure 2.4). Due to the time consuming nature of the microscopic counting, no replicate measurements were made to quantify the statistical spread of these distributions. The less than 2 NTU turbidity measurements made at these wells at sampling times subsequent to R2 pumping are likely stronger evidence that the induced gradient had little effect on the mobile particle load in Site YYZ groundwater.

There were no differences in groundwater quality parameters between pumping and pre-pumping sample dates. Changes in groundwater quality parameters may indicate that the upgradient "origin" of groundwater at a monitoring well had changed as a result of the induced gradient. This does not appear to be occurring at Site YYZ.

Groundwater concentrations of selected aromatic hydrocarbons were plotted as a function of time to determine if their levels had changed in response to pumping. Sample plots are shown in Figures 2.13 and 2.14. R2 pumping was initiated between Apr. 9 and Apr. 18, but no systematic trends in compound concentrations were observed between pre-pumping and pumping sample dates. For example, pyrene concentrations declined with time at W20M and W40S, but naphthalene concentrations increased (W20M) or remained constant (W40S). Possible phenomena which might result in changes in contaminant concentrations in response to an induced gradient are rate-limited solid-water mass transfer, or an imbalance between compound biodegradation and advection rates. No processes such as these appeared to affect aromatic hydrocarbon concentrations in the groundwater at Site YYZ up to 5 months after pumping was initiated.

The groundwater fate of aromatic coal tar constituents at Site YYZ was investigated with no differentiation between fates under ambient and induced gradient conditions since no apparent changes in groundwater quality parameters or aromatic hydrocarbon concentrations were observed between pre-pumping and pumping sample dates.

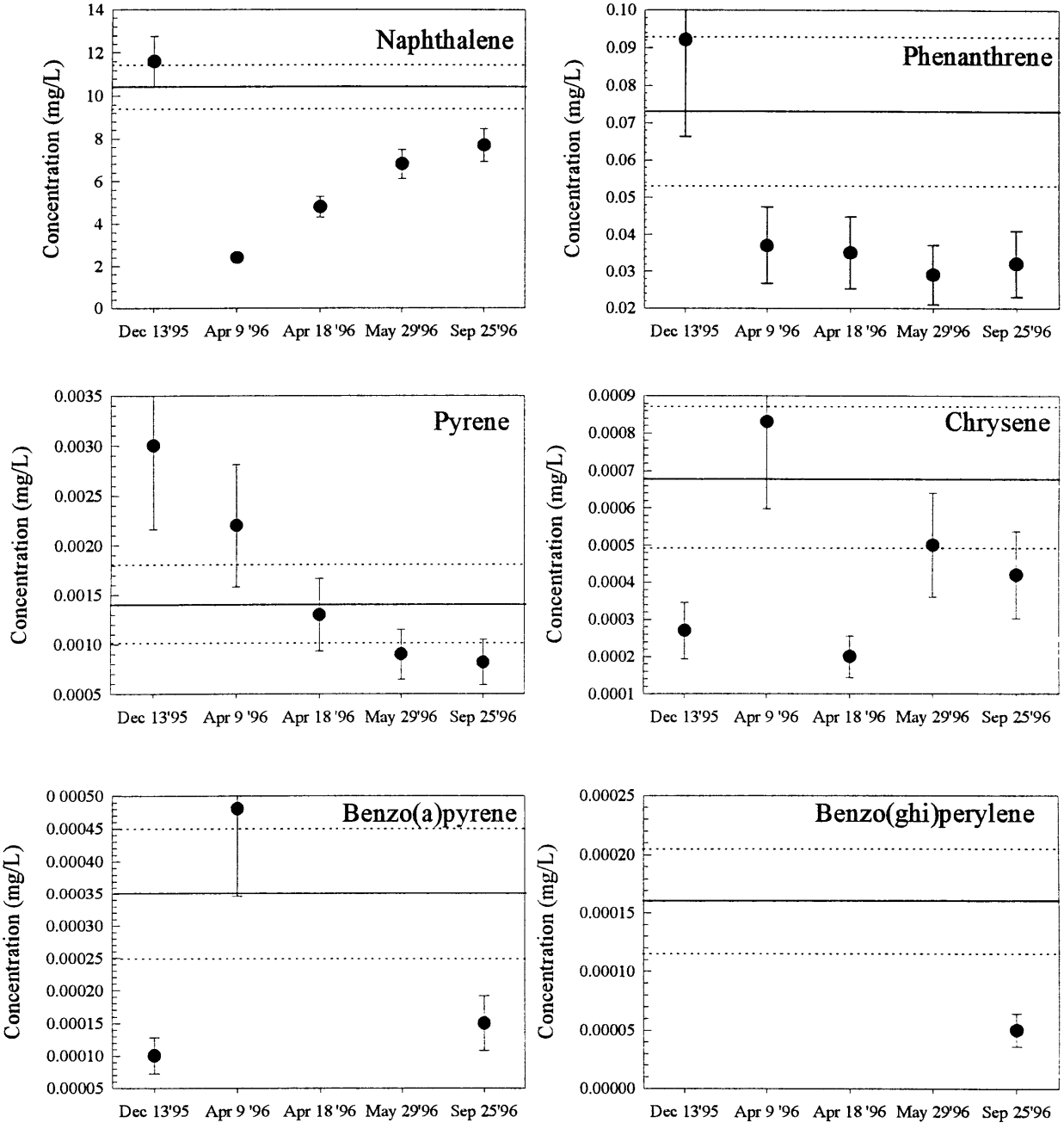

Figure 2.13. Aromatic hydrocarbon concentrations at well W20M as a function of sample date. The error bars denote the analytical variability in the individual measurements. For comparison, the measured tar-water equilibrium concentration is denoted as a solid line in each plot. The dotted lines denote the analytical variability of the tar-water equilibrium concentrations.

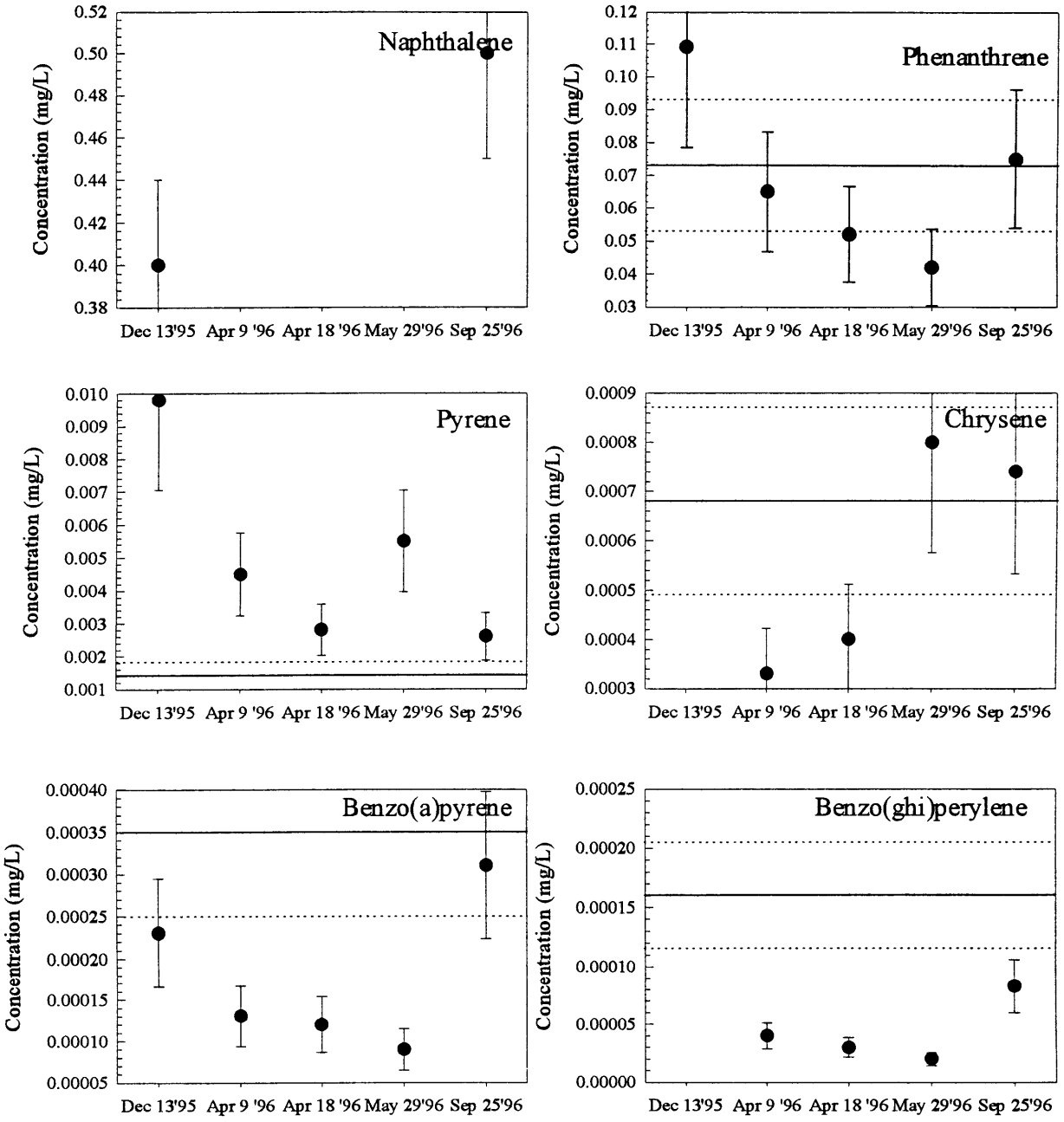

Figure 2.14. Aromatic hydrocarbon concentrations at well W40S as a function of sample date. The error bars denote the analytical variability in the individual measurements. For comparison, the measured tar-water equilibrium concentration is denoted as a solid line in each plot. The dotted lines denote the analytical variability of the tar-water equilibrium concentrations.

Fate of Coal Tar Constituents at Site YYZ

Equilibrium Coal Tar Dissolution

Aqueous concentrations of mono- and polycyclic aromatic hydrocarbons indicate that the groundwater at Site YYZ was in equilibrium with coal tar at the outset of this study. Over a range of 6 orders of magnitude in compound aqueous solubility, aromatic hydrocarbon concentrations generally fell on the 1:1 line when plotted against the corresponding laboratory-measured concentrations of tar-equilibrated water (Figures 2.8 to 2.12). (Deviations from the 1:1 line greater than can be accounted for with analytical error are discussed later.) It was only by observing such a wide range of compound solubilities that this equilibrium conclusion could be made. Use of volatile compounds alone may not have indicated groundwater-tar equilibrium at Site YYZ. Groundwater concentrations of monoaromatic hydrocarbons and naphthalenes at some of the wells (W40S, W20S, Sept. 1996) were much lower than expected in the presence of tar; however, equilibrium solubility values were observed for most of the higher molecular weight compounds at these wells.

In this study, sampled groundwater showed PAH concentrations consistent with equilibrium coal tar dissolution, indicating that equilibrium nonaqueous phase liquid (NAPL) dissolution occurs at field sites. There is little evidence in the literature of field-scale NAPL dissolution. Expected equilibrium groundwater concentrations of NAPL constituents have been observed for the Bemidji crude oil spill (Eganhouse *et al.*, 1996) and at other coal tar sites (Backhus and Gschwend, 1994; Groher *et al.*, 1990). Generally, however, at sites where the presence of nonaqueous phase liquids was strongly suspected, aqueous compound concentrations of up to only 1% of compound solubility have been reported (Jackson and Mariner, 1995; Anderson *et al.*, 1992).

Laboratory studies have suggested that nonaqueous phase liquids dissolve under mass transfer-limited conditions (Powers *et al.*, 1994; Geller and Hunt, 1993; Powers *et al.*, 1992); however, microscopic mass transfer limitations are likely unimportant at the macroscopic field scale. The groundwater velocities at the monitoring well clusters at Site YYZ were high, even under ambient conditions (0.3 - 0.6 m/d). According to laboratory studies, these pore water velocities should result in mass transfer-limited NAPL dissolution (Geller and Hunt,

1993; Powers *et al.*, 1992). In addition, dissolution from coal tar may be further hindered by the presence of skins on aged tar blobs (Luthy *et al.*, 1993). These NAPL dissolution studies were conducted in small columns of 5 to 15 cm dimensions (Geller and Hunt, 1993; Powers *et al.*, 1992). At larger flow scales, longer contact times between the groundwater and the nonaqueous phase may allow constituent concentrations to build up to equilibrium levels. Mathematically, equilibrium concentrations have been predicted to occur after 10 cm travel distances at pore water velocities of 0.86 m/d (Miller *et al.*, 1990). Equilibrium concentrations have been observed experimentally for a 15 cm source region within a 0.75 m^3 flow system (Anderson *et al.*, 1992). The coal tar distribution upgradient of the study area at Site YYZ is not known, but groundwater may have been in contact with dissolving tar for up to 300 m before it flowed past the monitoring wells, allowing equilibrium aqueous hydrocarbon concentrations to build up at this field site.

Lower-than-equilibrium concentrations of NAPL constituents at other field sites likely result from hydraulic dilution. Dilution would affect all constituents of a multi-component NAPL similarly, with slight variations according to compound diffusivities. Observed groundwater concentrations would fall below the 1:1 line on a plot versus expected concentration by an equal amount, independent of compound solubility. Thus ratios of compound concentrations would remain constant in the presence of a multi-component NAPL source. At one field site with a two-component NAPL source, ratios of aqueous compound concentrations were constant, despite being below expected equilibrium concentrations (Jackson and Mariner, 1995). As the scale of groundwater observation points grow beyond the scale of the NAPL distribution in the subsurface, hydraulic dilution likely becomes more important. Equilibrium solute concentrations fall off sharply away from residual nonaqueous phase liquid sources (Jackson and Mariner, 1995; Whelan *et al.*, 1994; Anderson *et al.*, 1992). Thus, the lack of hydraulic dilution at Site YYZ suggests that all of the monitoring wells are located in close proximity to coal tar sources and tar is widely distributed through the fill solids at Site YYZ.

Facilitated Transport

Monitoring wells that had enhanced groundwater concentrations of PAHs, that is, in excess of tar-water equilibrium values, showed an increasing ratio of observed-to-equilibrium concentrations with increasing compound hydrophobicity. This trend was most clearly noted at wells W40M and W20S (Figures 2.8 and 2.12) at which the lowest solubility compounds deviated the greatest from their expected values in equilibrium with tar (Table 2.3). The fact that the observed enhancements in groundwater concentrations at this site increase with compound hydrophobicity (or particle reactivity) is suggestive of a second phase present in the groundwater which can facilitate the transport of these coal tar PAHs.

We again address whether the enhanced load of groundwater PAHs was truly mobile at this site or whether the observed groundwater concentrations were an artifact of our sampling procedure. As discussed previously, groundwater turbidities and particle sizes suggest that it is unlikely that our sampling procedure introduced non-mobile particles to our groundwater samples and caused the elevated PAH concentrations. One potential artifact that was not addressed that in the previous discussion was the presence of mobile nonaqueous phase liquids.

Mobile NAPL may flow into and be retained within monitoring wells at Site YYZ and other NAPL-contaminated sites. Care must be taken to ensure that this phase is not inadvertently sampled in addition to the groundwater, causing higher than true contaminant concentrations in the groundwater sample. With tar concentrations of PAHs many orders of magnitude greater than their equilibrium aqueous concentrations, the entrainment of only a small amount of tar (*i.e.*, 10-100 μg/L quantities, see Table 2.3) in a groundwater sample may greatly elevate PAH concentrations. The contribution of entrained tar to observed concentrations becomes greater for PAHs with increasingly lower aqueous solubilities. If droplets of tar were entrained from the monitoring wells while groundwater pumping, the elevated polycyclic aromatic hydrocarbon concentrations should correlate with the presence of tar in monitoring wells.

Table 2.3. Calculated enhancements in polycyclic aromatic hydrocarbon concentrations at wells W20S and W40M in Sept., 1996. Compound abbreviations are given in Table 2.2.

	PY	BA	BaP	BP
OBSERVED GROUNDWATER CONCENTRATION ENRICHMENT ABOVE TAR-WATER EQUILIBRIUM				
W20S	1	2	2	2
W40M	3	8	14	12
PHYSICAL PROPERTIES				
log K_{ow}	5.13	5.91	6.50	7.1
K_{oc} (mL/g)†	$10^{4.76}$	$10^{5.55}$	$10^{6.14}$	$10^{6.75}$
K_{tar} (mL/g) (this thesis)	$10^{6.8}$	$10^{6.7}$	$10^{7.0}$	$10^{6.9}$
$E = C_{groundwater}/C_{equilibrium} = 1 + (phase)K_p$				
QUANTITY OF ORGANIC MATTER NECESSARY TO EXPLAIN ENRICHMENTS				
10 mg/L organic carbon	2	4	15	56
1 mg/L tar	7	8	14	12

† $\log K_{oc} = \log K_{ow} + 0.42$ (Schwarzenbach *et al.*, 1993).

No clear correlation was found between the extent of concentration enhancement for a particular PAH and the presence of tar in the monitoring wells. Tar was always observed at the bottom and on the sides of W40M and enhanced groundwater concentrations of the most hydrophobic PAHs were always observed at this well (Figure 2.8 to 12), even in Dec. 1995 when no tar was observed on the surfaces of the retrieved packer and sampling line. In Dec. 1995, both the presence of tar and concentration enhancements were observed at W20S. Similar depths (6") of tar were also observed at W100M at this sample date, but no enhancement of PAH concentrations were observed at that well (Figure 2.8). At later sampling dates, PAHs elevated above measured tar-water equilibrium concentrations were observed at W100S and W100M (May '96) and W20S (Sept. '96), but no evidence of tar was found on the scope lines or the retrieved packer assemblies. If droplets of tar were entrained from the bottom of the monitoring wells during groundwater sampling, no elevation in PAH concentrations should have been observed at these latter three wells, but elevated PAH concentrations should have been observed at W100M in Dec. '95. Thus, entrainment of mobile tar does not appear to explain these concentration enhancements.

The observed groundwater concentrations at this site are the first field evidence of enhanced mobile loads of organic contaminants. The groundwater transport of PAHs at Site YYZ is presumably facilitated relative to dissolved species. Possible means to allow enhanced mobile loads of PAHs include the presence of inorganic particles, cosolvents, and organic or organic-coated colloids in the groundwater. In order to investigate which of these mechanisms is facilitating transport of PAHs at this site, we considered the theoretical expression for the expected enhancement of PAH concentrations over equilibrium conditions when a carrier phase is present in the groundwater:

$$E = \frac{C_{groundwater}}{C_{equilibrium}} = 1 + (phase)K_p \qquad (2)$$

where E is the enhancement factor, $C_{groundwater}$ (mg/L) is the groundwater concentration, $C_{equilibrium}$ (mg/L) is the aqueous concentration in equilibrium with tar, (phase) (kg/L) is the abundance of the carrier phase in the groundwater, and K_p (L/kg) is the equilibrium phase-water partition coefficient. Where the right-hand-side of Eq. 2 is dominated by the second

term, the enhancement factors of various PAHs should vary as their partition coefficients, K_p. Since partitioning to the carrier phase is driven by a compound's aqueous activity coefficient, K_p values for a series of organic compounds will have similar relative values for any partitioning mechanism and so enhancement factors alone cannot be used to discern the mechanism facilitating PAH transport. Additional supporting data is also required.

We first address whether cosolvents and surface active compounds could cause PAH enhancements at Site YYZ. Both of these mechanisms would enhance compound solubilities by lowering the groundwater surface tension. The surface tension of groundwater sampled at W40M was calculated to be 70.6 ± 3 dyne/cm (n=5). Within the measurement variability, this value did not differ from the surface tension measured for RO water. Much greater variability between individual measurements was observed for the groundwater sample than the RO water which suggests that there are surface active species present in the groundwater at this well. The magnitude of this surface tension effect on the solubility of benzo(a)pyrene was estimated with the Yalkowsky equation (Schwarzenbach *et al.*, 1993):

$$\log \frac{C_{mix}^{sat}}{C_{w}^{sat}} = \frac{N(\sigma_{air\,RO} - \sigma_{air\,gw})(HSA)}{2.303RT} \qquad (3)$$

where C_{mix} and C_w (mg/L) are the aqueous concentrations in the presence and the absence, respectively, of the surface active agent, N is Avagadro's number, $(\sigma_{air\,RO} - \sigma_{air\,gw})$ (erg/cm^2) is the difference in surface tensions between the two water samples, R (erg/mol/K) is the gas constant, T (K) is the temperature, and HSA (cm^2) is the molecule hydrophobic surface area, here approximated as 250 Å^2 (Schwarzenbach *et al.*, 1993). A difference of 1.4 erg/cm^2 (1 dyne/cm = 1 erg/cm^2) in surface tensions gives an increased benzo(a)pyrene (BaP) concentration of 2.6 in the groundwater relative to RO water containing no surface active species. The observed BaP enhancement factor at W40M was 14 in Sept. '96 when the surface tension measurement was made. Thus, concentrations of polycyclic aromatic hydrocarbons enhanced above tar-water equilibrium values were not explained by lowered groundwater surface tensions alone.

The amount of cosolvent or surfactant required to enhance the benzo(a)pyrene concentration by a factor of 14 above dissolved equilibrium with tar was estimated. A polar, methanol-like cosolvent would need to be present at gram per liter quantities to explain this enhancement (Schwarzenbach *et al.*, 1993; Groher, 1989); however, only mg/L quantities of organic carbon were measured in groundwater. On a carbon basis, surfactants and biosurfactants enhance can elevate compound solubilities at much lower concentrations, but not without a dramatic decrease in surface tension. For example, 50 mg/L of rhamnolipid biosurfactants increased the apparent solubility of octadecane by a factor of 10^4, but lowered the surface tension of water from 72 dyne/cm to 30 dyne/cm (Zhang and Miller, 1992). Thus, surface active species are not important contributors to the enhancement of groundwater PAH concentrations at Site YYZ.

Inorganic particles are also potential mediators of hydrophobic compound transport in groundwater. At Site YYZ, mineral surfaces of suspended particles are likely organic-carbon coated, and thus groundwater solubilities of PAHs would be enhanced by partitioning into these coatings. Filterable iron and aluminum were present at levels of 2 - 360 μM and 2 - 60 μm, respectively, in the groundwater (Table 2.1). Aluminum did not correlate with silicon, thus clays were not predominant. Silica colloids may be also be present since silicon levels were close to equilibrium with amorphous silica (Morel and Hering, 1993), and dissolved levels were lower than total concentrations. At the groundwater pH, negatively charged silica colloids would not sorb organic matter. The mineral particles with the potential to act as carrier phases in Site YYZ groundwater were iron and aluminum oxides. Studies of humic acid sorption to iron (Tipping, 1981) and aluminum (Davis, 1982) oxides would predict these surfaces to be humic-coated at the iron, aluminum and non-purgeable organic carbon levels (assuming is all capable of binding to mineral surfaces) in the groundwater at this site.

If organic-coated mineral particles are important facilitating phases for polycyclic aromatic hydrocarbons, a correlation would be expected between the amount of iron and aluminum oxides in the groundwater and the enhancement factors of PAH compounds. Unfortunately, only W40M had PAH concentrations that were elevated by more than a factor of 2 above tar-water equilibrium in Sept. 1996 when iron and aluminum measurements were also made (Table 2.4). The lowest amount of filterable aluminum were observed at this

monitoring well and the filterable iron was in the middle of the range observed at all of the wells. Most of the monitoring wells had BaP enhancement factors between 0.4 and 1, but they exhibited a wide range in filterable solids concentrations. Thus, the concentration of iron or aluminum oxides was not a good predictor of enhanced groundwater concentrations.

Benzo(a)pyrene concentration enhancements were also plotted against turbidity measurements (Figure 2.15) at all wells. Although turbidity is a bulk measure of suspended solids, data was available from each of the well locations at all of the sampling dates. Energy dispersive X-ray analysis suggested that the filtered groundwater particles may have had high carbon contents. If these particles accounted for the bulk of the suspended solids in the groundwater, they may form an important sorptive phase because of their carbon-rich composition. As with the specific mineral particles, BaP concentrations exceeding tar-water equilibrium levels were not found at wells with the highest turbidities. Even at a single well location, W40M, which consistently had elevated PAH concentrations, benzo(a)pyrene enhancement factors did not show a correlation with turbidity. Either particles are not important sorptive phases for polycyclic aromatic hydrocarbons, or only a subclass of particles quantified by the turbidity measurements were facilitating enhanced PAH concentrations.

Table 2.4. Enhancements in polycyclic aromatic hydrocarbon concentrations in Sept., 1996. Enhancement factors were calculated with Equation 2. Compound abbreviations are given in Table 2.2

Well ID	PY	CH	BaP	BP
W20S	0.6	0.6	0.4	0.3
W20M	1	2	2	2
W40S	2	1	1	0.5
W40M	3	8	14	12
W100S	1	0.9	1	1
W100M	0.9	0.7	0.6	0.4
W100D	0.7	0.6	0.6	0.5

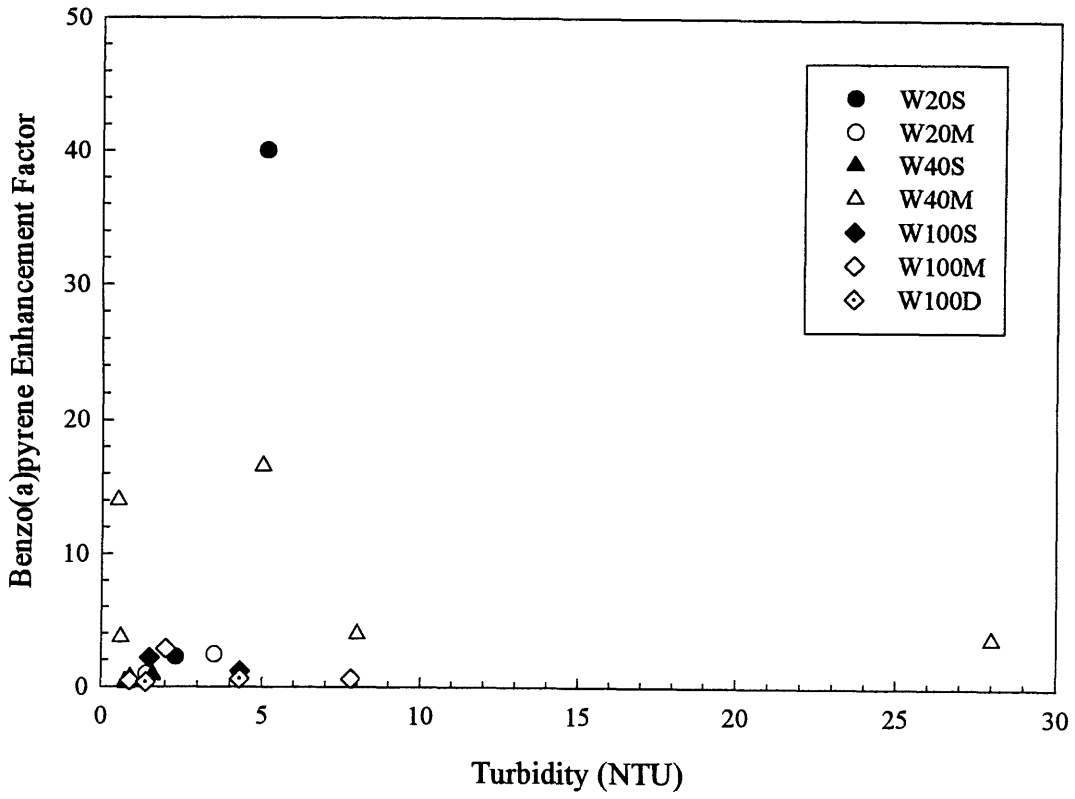

Figure 2.15. Benzo(a)pyrene enhancement factors as a function of turbidity. Enhancement factors were calculated with Equation 2.

Organic matter in the groundwater was present at high enough concentrations for organic (or organic-coated) colloids to facilitate PAH transport at Site YYZ. Enhancements in groundwater concentrations over solubility levels may occur from the partitioning of PAHs to suspended organic matter (as has been shown in the laboratory (Chiou *et al.*, 1987)) or to organic-coated suspended mineral particles (Murphy *et al.*, 1990). The abundance of organic matter required to yield the observed enhancement factors for the most hydrophobic PAHs were estimated with organic carbon-water (K_{oc}) and tar-water (K_{tar}) partition coefficients. (Calculations with K_{tar} were made because partition coefficients for anthropogenically-impacted sediments were greater than estimated with K_{oc} partition coefficients likely because of the presence of nonpolar petroleum hydrocarbons (Kile *et al.*, 1995). At Site YYZ, suspended organic matter may also be very nonpolar and exhibit tar-like partition coefficients.) Organic carbon was present in groundwater at W40M at concentrations greater than required for humic-type materials to enhance PAH concentrations to the extent observed at this well (Tables 2.1 and 2.3). About one third of the organic carbon measured in the groundwater would have to be active as a sorbing phase at this well. Finally, only small amounts of tar would be required to enhance PAHs to the extent observed at all wells (for comparison, tar is about 95% by weight carbon, assuming pyrene is representative of tar composition). From these estimates of the magnitude of partition coefficients, we can only conclude that there is sufficient organic matter present in the groundwater to allow facilitated transport of PAHs to occur at this site.

Further study was undertaken to investigate the nature of the groundwater colloid phases. A series of separation methods, detailed in Chapter 3, were quantified the particle bound and suspended organic colloid-associated PAHs. Over 65% of the pyrene mass in excess of the dissolved mass in equilibrium with coal tar was associated with settled particles in W40M groundwater (Chapter 3). The pyrene was likely particle-associated and not in tar droplets because enhanced PAH concentrations were not correlated with the presence of tar in monitoring wells. The particulate phase was not quantified for allow for estimation of the pyrene particle-water partition coefficient with Eq. 2. Such estimation would indicate whether the particles were more likely tar-coated or organic matter-coated. With the exception of W100S, all monitoring wells at which elevated concentrations of PAHs have been observed

have contained mobile tar at some time. The elevated groundwater PAH concentrations may result from colloidal particles in close proximity to subsurface coal tar deposits which become tar-coated. Mobile tar that flowed into (and out of) the monitoring wells may indicate the proximity of subsurface tar. Poor core recoveries during monitoring well drilling prevented quantification of the NAPL content of the subsurface solids at the monitoring well locations.

A second explanation for polycyclic aromatic hydrocarbon association with settled particles is that the particles were coke fines. X-ray analysis of filterable solids gave no detectable element peaks and carbon could not be detected with the beryllium window would not detect carbon. A high fluorescence background was observed when coke particles were placed in water (Chapter 5), suggesting that aromatic hydrocarbons were desorbed from the coke (the emission spectra was similar to phenanthrene, the most soluble PAH), and thus could be extracted from coke fines suspended in groundwater samples. Again, the composition of the fill solids near the well screens is not known to verify the presence of coke in the subsurface near W40M.

Suspended organic colloids were present in groundwater at each of the monitoring well clusters at levels of about 5 mg_C/L (Chapter 3), but it was unclear to what extent they enhanced groundwater concentrations of polycyclic aromatic hydrocarbons. The fluorescence quenching capacity of the groundwater was removed by acidification and centrifuge ultrafiltration, or by the addition and precipitation of alum. Both of these groundwater treatments suggested that humic acid-like organic matter was quenching the probe fluorescence; however, this evidence was not supported by extractions of unaltered water samples containing both the dissolved and colloid-associated PAH compounds (Chapter 3, Appendix B). More thorough fluorescence measurements (*e.g.*, probe lifetime measurements, nonsorbing probes) are required to verify static probe quenching by association with organic colloids.

Further study is required to determine whether it is tar, natural organic matter, or a combination of both, that is enhancing groundwater PAH concentrations at Site YYZ. Since the groundwater is at equilibrium with the dissolving coal tar, the suspended sorptive phase also likely achieved equilibrium with dissolved tar constituents. Thus, the effect of a mobile sorbing phase on transporting PAHs was readily observable as groundwater concentrations

that were greater than expected aqueous equilibrium concentrations in the presence of tar. Enhanced transport of PAHs has been suggested at another coal tar site with high concentrations of chrysene and benz(a)anthracene (Backhus *et al.*, 1993). The enhanced groundwater concentrations we see for many compounds provide very strong evidence for facilitated transport of organic contaminants at this coal tar site.

Biodegradation

Monitoring wells W20S and W40S had order of magnitude lower concentrations of high solubility compounds (*m*+*p*- and *o*-xylene, naphthalene, and methylnaphthalenes), relative to the tar-water equilibrium case (Figures 2.8 to 2.12). Over the entire sampling period, *o*-xylene always showed smaller depletion factors (*e.g.*, $C_{groundwater}/C_{equilibrium} = 0.03$) than ethylbenzene (0.36) and the combined *m*- and *p*-xylene isomers (0.21) at W20S. Similarly, at W40S, 2-methylnaphthalene was preferentially removed ($C_{groundwater}/C_{equilibrium} \leq 0.001$) compared to the 1-methylnaphthalene isomer (0.3). Volatilization losses of these compounds to the vadose zone would not discriminate within these isomer sets, nor would volatilization be expected since W20S and W40S are screened 0.9 and 1.2 m, respectively, below the water table. These compounds also do not readily undergo redox reactions in groundwater. Therefore, there is likely a biological sink for low molecular weight aromatic hydrocarbons in the field study area at Site YYZ.

A mass balance approach was employed to investigate the reasonableness of a biological attenuation hypothesis. For any removal process, a mass balance of the reactants and products can be conducted to determine whether their relative ratios support the hypothesized removal mechanism. When biodegradation occurs, the required reactants and expected products are as follows:

$$\begin{matrix} substrate \\ compound \end{matrix} + \begin{matrix} electron \\ acceptor \end{matrix} \rightarrow CO_2 + \begin{matrix} reduced \\ electron \\ acceptor \end{matrix} + products \qquad (4)$$

Over time (or distance travelled), the groundwater would be depleted of substrate compounds (if not continually replenished by a source) and electron acceptors. Carbon dioxide, reduced electron acceptors and other partially mineralized products would build up. Differences in

groundwater composition may be expected between wells where biological removal of coal tar constituents is occurring and those where no compounds are removed. For example, greater CO_2 levels were present in W40S as compared to W40M which showed no loss of volatile compounds.

The mass balance calculation was performed to assess whether biological removal of naphthalene (by far, the predominant hydrocarbon degraded) could occur at Site YYZ. The bulk of the purgeable organic compounds depleted from wells W20S and W40S (Table 2.1) resulted from the loss of 10 mg/L of naphthalene, relative to the equilibrium tar dissolution case. Complete mineralization of naphthalene would produce 30 mg/L of carbon dioxide or a partial pressure of $10^{-1.7}$ atm. The observed partial pressures of carbon dioxide were much greater with values of $10^{+0.5}$ and $10^{+0.6}$, respectively, at W20S and W40S. The presence of elevated CO_2 levels is consistent with active biological degradation; however, similar CO_2 levels were also observed at the other wells which showed no losses of naphthalene.

(High levels of carbon dioxide in groundwater may result from the removal of other compounds which were not monitored by our analytical methods, such as methane. Site YYZ is still an active natural gas distribution center and leaking underground pipelines may be a source of methane for microbial degradation. Alternatively, the source of elevated CO_2 levels may be from the dissolution of inorganic carbonate sources in contact with the low pH groundwater. MINEQL calculations indicated that under equilibrium conditions, the groundwater was not saturated with respect to iron or calcium carbonate solids; however, this does not preclude the presence of carbonates in the fill solids which may have kinetically-limited dissolution. A lime kiln was located near the field study area in 1870 to generate lime for gas purification. Wastes from lime generation or gas purification may have been disposed in the study area. Certainly gas purification wastes were found in the fill while drilling R2.)

The stoichiometric requirements for complete mineralization of naphthalene were calculated under aerobic and nitrate-, sulphate- and iron-reducing conditions (Figure 2.16). If naphthalene removal occurred under any one of these degradation pathways, at least the

Aromatic Hydrocarbon Biodegradation

substrate + electron acceptor → CO_2 + reduced electron acceptor + metabolites

0.08 mM naphthalene

electron acceptor	req'd (mM)	obs'd (mM)
O_2	0.9	$< 6\times10^{-3}$
NO_3^-	0.8	< 2
SO_4^{2-}	0.5	1.4
Fe^{3+}	3.7	2×10^{-3}

reduced electron acceptor	obs'd (mM)
H_2O	
N_2	ND
S^{2-}	1.6
Fe^{2+}	3×10^{-3}

Figure 2.16. Stoichiometric electron acceptor requirements for the complete mineralization of naphthalene. The required (req'd) amounts of electron acceptors are compared with observations (obs'd) from W40S groundwater in Sept. 1996. (ND - not determined.)

required amount of electron acceptor would have needed to be present in the groundwater prior to degradation. After naphthalene removal, the reduced electron acceptor species should be present in the groundwater at levels at least as great as required for the electron acceptor.

Sufficient electron acceptors were present in the groundwater for biological removal of low molecular weight tar constituents. Not enough oxygen was available for aerobic degradation of naphthalene. The levels of dissolved iron (presumably Fe^{2+} in the reducing groundwater) were not high enough at W20S and W40S for iron reduction to have resulted in significant naphthalene mineralization. Nitrate reducers were also not significant sinks for aromatic hydrocarbons at this site. The endpoint for nitrate reduction was taken to be nitrogen gas. Measurements of nitrate suffered from high detection limits; however, nitrate levels in the groundwater sampled on the eastern site boundary, the upgradient source of groundwater to the study region, were below 0.1 mM (EA Engineering Science and Technology Inc, 1993), insufficient for complete removal of naphthalene by nitrate reduction. Sulphate levels did exceed the stoichiometric requirements at W20S, W40S, and W100S and sulphate concentrations on the eastern site boundary ranged from 0.5 to 5 mM (EA Engineering Science and Technology Inc, 1993). In addition, total sulphide levels sampled at W20S and W40S were consistent with the reduction of 0.5 mM sulphate for naphthalene removal. (Note that disposed purification wastes may also be a source of sulphide, although groundwater was undersaturated with respect to iron sulphide according to MINEQL calculations.) Therefore, the levels of electron acceptors and reduced species are consistent with sulphate-reduction being the predominant biological removal process.

The aromatic hydrocarbon depletion pattern was also consistent with a sulphate-reducing consortia present in the fill at Site YYZ. At wells W20S and W40S, groundwater benzene concentrations were always at least as great as measured in equilibrium with coal tar. The xylenes always had greater relative removals (*i.e.*, lower $C_{groundwater}/C_{equilibrium}$) than ethylbenzene, although groundwater concentrations of ethylbenzene were depleted by 0 to 50%. The ratio of groundwater-to-equilibrium concentrations of naphthalene were always less than for the xylenes. Preferential removal of xylenes over ethylbenzene under sulphate-reducing conditions has been observed in the field at the site of a fuel spill (Beller *et al.*, 1995). Naphthalene had a faster removal rate by sulphate-reducers than toluene or *p*-xylene,

in a field tracer study (Thierrin *et al.*, 1995). No benzene removal was observed in either of these studies. The degradation of monoaromatic hydrocarbons and naphthalene under denitrifying conditions has only been studied in laboratory microcosms, but with conflicting removal patterns (Kao and Borden, 1997). Naphthalene was not degraded under denitrifying conditions (Flyvberg *et al.*, 1993; Kuhn *et al.*, 1988). When monoaromatic hydrocarbon degradation was observed, ethylbenzene was removed in preference to xylenes (Kao and Borden, 1997). Toluene has been degraded under both sulphate- and nitrate-reducing conditions; however, the detection limits for toluene in Site YYZ groundwater were greater than the low concentration measured in aqueous equilibrium with coal tar.

Sulphide concentrations at W100S were also present at stoichiometric proportions according to the above naphthalene mineralization scheme, yet no removal of naphthalene was observed. This observation may indicate that biological removal of xylenes and naphthalenes was not occurring in the immediate vicinity of the monitoring wells. If biological removal was occurring upstream from the monitoring wells, groundwater that was advected to W100S may have passed another tar source, allowing build-up of tar compounds to equilibrium levels. If groundwater advected to W20S and W40S had not subsequently contacted tar, depleted levels of volatile compounds would still be exhibited, while high molecular weight PAHs with no biological sink would still be at tar-water equilibrium concentrations.

Alternatively, biological removal rates of mono- and diaromatic hydrocarbons may be slower than tar dissolution. The depleted groundwater pattern at W20S and W40S may reflect a local residual tar source that has been depleted of these compounds. (The removal of naphthalene (0.07 mol/mol of the original tar composition) would not produce an increase in groundwater concentrations of higher molecular weight PAHs at these wells detectable by our analytical methods.) If tar was pooled near W100S, a large reservoir of naphthalene may be replenishing the groundwater. As noted, evidence of biological activity (sulphate and sulphide) was observed at this well although all tar constituents were present at expected aqueous solubilities in the groundwater.

Groundwater pumping may induce gradients that disrupt the biological processes occurring under ambient flow conditions. First, the residence time of water flowing past a microbial community may decrease, causing incomplete compound removal (*i.e.*, lower

depletion factors before pumping). At Site YYZ, this effect would be most greatly influenced at the W20S cluster since pumping is estimated to at least triple the pore water velocity here. No changes in compound depletion factors were observed at W20S. Secondly, pumping may cause changes in flow patterns, drawing water into the area of differing composition than is necessary to sustain biodegradation. No relevant groundwater quality parameters were measured at the monitoring well clusters prior to Sept., 1996 to determine if water composition had changed in response to pumping. As noted, reducing conditions and hydrogen sulphide were noted at the shallow wells both before and during R2 pumping. Thus, after 4.5 months time, the induced gradient had no effect on compound attenuation within the field study area at Site YYZ.

We conclude that sufficient levels of electron acceptors and reduced species are present in groundwater at Site YYZ for the biological removal of xylenes and naphthalenes by sulphate reduction. Degradation of these mono- and diaromatic hydrocarbons by sulphate-reducers has been demonstrated in the laboratory and the field (Ball and Reinhard, 1996; Thierrin *et al.*, 1995); however, no clear patterns of aromatic hydrocarbon degradation are evident for specific microbial consortia (*e.g.*, sulphate reducers *v.* nitrate reducers) when the anaerobic biodegradation literature is taken as a whole. For example, xylenes may (Thierrin *et al.*, 1995) or may not (Flyvberg *et al.*, 1993) be removed when toluene is degraded under sulphate reducing conditions. The apparent differences in biodegradability of certain aromatic hydrocarbons between studies may have resulted from impure cultures or other lacking nutrients. Further work with known reactant inputs, allowing quantitative mass balance (*e.g.* laboratory culture studies, field tracer tests), is needed to more conclusively demonstrate biological attenuation at Site YYZ.

Summary of Results and Implications for Off-Site Transport and Remediation

Critical implications for the transport and remediation of aromatic hydrocarbons at Site YYZ would have been missed without the quantification of compounds with a range of six orders of magnitude in compound solubilities. At this site, use of a bulk measure of groundwater contamination, such as total petroleum hydrocarbons, would have only captured the distribution of naphthalenes, since they were the most abundant compounds, By including

compound specific analyses of many polycyclic aromatic hydrocarbons, the source of groundwater contamination was found to be the equilibrium dissolution of residual coal tar. Thus, the rate-limitation to remediation of the aromatic hydrocarbons in the groundwater at Site YYZ is the presence of this nonaqueous phase liquid. Groundwater concentrations in the fill solids are still in equilibrium with tar 50 years after the last tar production, and hence the last possible on-site disposal, and will continue to be a source of contamination to the adjacent river from many years. If the risk posed to aquatic organisms by groundwater discharge of aromatic hydrocarbons to the river is greater than acceptable levels, it may be abated by a hydraulic curtain. There are no other remedial technologies which will enable source (residual tar) removal on the scale required for this site.

Analysis of individual aromatic hydrocarbon concentrations also showed two other fate processes which will affect the flux of contaminants to the river from Site YYZ. First, the presence of colloids in the groundwater will increase the flux of hydrophobic PAHs over the flux calculated assuming tar equilibration with groundwater containing no colloids. The field data gathered in this study suggested that there are temporal and spatial variations in the presence of groundwater colloids at Site YYZ. In order to calculate the increased risk posed by colloid-associated polycyclic aromatic hydrocarbons, groundwater concentration measurements would need to be made at shoreline wells adjacent to the river bed seepage face and a model of colloid transport through the river bed sediment would also be required. Once in the river system, hydrophobic aromatic hydrocarbons will associate with particles and settle to the sediment bed, exposing benthic dwelling and feeding organisms.

The second process occurring in the anthropogenic fill at Site YYZ is biological degradation of mono- and diaromatic hydrocarbons. In this case, the flux of these compounds to the river may be decreased relative to calculations assuming aqueous tar water equilibrium. Again the spatial variability of microbial populations in the fill solids is must be knownn to predict the full extent of biodegradation of groundwater aromatic hydrocarbons between the MIT monitoring wells and the river. The sink for one and two-ringed aromatic hydrocarbons in the river is volatative exchange to the atmosphere because of their high Henry's law constants.

References

CRC Handbook of Chemistry and Physics (1989). Boca Raton, FL, CRC Press, Inc.

Anderson, M. R.; Johnson, R. L.; Pankow, J. F. (1992). "Dissolution of dense chlorinated solvents into ground water: 1. Dissolution from a well-defined residual source." *Ground Water* **30**: 250-256.

Backhus, D. A.; Gschwend, P. M. (1994). "Groundwater contamination by polycyclic aromatic hydrocarbons: A case study of a coal-tar contaminated site." In *Groundwater Contamination and Control.* U. Zoller, Ed. New York, Marcel Dekker: 315-335.

Backhus, D. A.; Ryan, J. N.; Groher, D. M.; MacFarlane, J. K.; Gschwend, P. M. (1993). "Sampling colloids and colloid-associated contaminants in ground water." *Ground Water* **31**: 466-479.

Ball, H. A.; Reinhard, M. (1996). "Monoaromatic hydrocarbon transformation under anaerobic conditions at Seal Beach, California: Laboratory studies." *Environmental Toxicology and Chemistry* **15**: 114-122.

Beller, H. R.; Ding, W.-H.; Reinhard, M. (1995). "Byproducts of anaerobic alkylbenzene metabolism useful as indicators of in situ bioremediation." *Environmental Science and Technology* **29**: 2864-2870.

Chiou, C. T.; Kile, D. E.; Brinton, T. I.; Malcolm, R. L.; Leenheer, J. A.; MacCarthy, P. (1987). "A comparison of water solubility enhancements of organic solutes by aquatic humic materials and commercial humic acids." *Environmental Science and Technology* **21**: 1231-1234.

Davis, J. A. (1982). "Adsorption of natural dissolved organic matter at the oxide/water interface." *Geochimica et Cosmochimica Acta* **46**: 2381-2393.

EA Engineering Science and Technology Inc (1993). *Site Characterization Report for the BG&E Spring Gardens Facility.*

Eganhouse, R. P.; Dorsey, T. F.; Phinney, C. S.; Westcott, A. M. (1996). "Processes affecting the fate of monoaromatic hydrocarbons in an aquifer contaminated by crude oil." *Environmental Science and Technology* **30**: 3304-3312.

Flyvberg, J.; Arvin, E.; Jensen, B. K.; Olsen, S. K. (1993). "Microbial degradation of phenols and aromatic hydrocarbons in creosote-contaminated groundwater under nitrate-reducing conditions." *Journal of Contaminant Hydrology* **12**: 133-150.

Geller, J. T.; Hunt, J. R. (1993). "Mass transfer from nonaqueous phase organic liquids in water-saturated porous media." *Water Resources Research* **29**: 833-845.

Groher, D.; Gschwend, P. M.; Backhus, D.; MacFarlane, J. K. (1990). "Colloids and sampling groundwater to determine subsurface mobile loads." In *Proc.: Environmental Research Conference on Groundwater Quality and Waste Disposal.* I. P. Muraka ,S. Cordle, Eds.. Palo Alto, CA, Electric Power Research Institute**:** 18.1-18.10.

Groher, D. M. (1989). *An Investigation of Factors Affecting the Concentration of Polycyclic Aromatic Hydrocarbons in Groundwater at Coal Tar Waste Sites.* M.S. Thesis, Massachusetts Institute of Technology.

Harkins, W. D.; Brown, F. E. (1919). "The determination of surface tension (free surface energy), and the weight of falling drops: The surface tension of water and benzene by the capillary height method." *Journal of the American Chemical Society* **41**: 499-524.

Jackson, R. E.; Mariner, P. E. (1995). "Estimating DNAPL composition and VOC dilution from extraction well data." *Ground Water* **33**: 407-414.

Kao, C.-M.; Borden, R. C. (1997). "Site-specific varability in BTEX biodegradation under denitrifying conditions." *Ground Water* **35**: 305-311.

Kile, D. E.; Chiou, C. T.; Zhou, H.; Li, H.; Xu, O. (1995). "Partition of nonpolar organic pollutants from water to soil and sediment organic matters." *Environmental Science and Technology* **29**: 1401-1406.

Kuhn, E. P.; Zeyer, J.; Eicher, P.; Schwarzenbach, R. P. (1988). "Anaerobic degradation of alkylated benzenes in denitrifying laboratory aquifer columns." *Applied and Environmental Microbiology* **54**: 490-496.

Luthy, R. G.; Ramaswami, A.; Ghoshal, S.; Merkel, W. (1993). "Interfacial films in coal tar nonaqueous-phase liquid-water systems." *Environmental Science and Technology* **27**: 2914-2918.

MacKay, A. A.; Chin, Y.-P.; MacFarlane, J. K.; Gschwend, P. M. (1996). "Laboratory assessment of BTEX soil flushing." *Environmental Science and Technology* **30**: 3223-3231.

Miller, C. T.; Poirier-McNeill, M. M.; Mayer, A. S. (1990). "Dissolution of trapped nonaqueous phase liquids: Mass transfer characteristics." *Water Resources Research* **26**: 2783-2796.

Morel, F. M. M.; Hering, J. G. (1993). *Principles and Applications of Aquatic Chemistry.* New York, John Wiley and Sons, Inc.

Murphy, E. M.; Zachara, J. M.; Smith, S. C. (1990). "Influence of mineral-bound humic substances on the sorption of hydrophobic organic compounds." *Environmental Science and Technology* **24**: 1507-1516.

Powers, S. E.; Abriola, L. M.; Weber, W. J., Jr. (1992). "An experimental investigation of nonaqueous phase liquid dissolution in saturated subsurface systems: Steady state mass transfer rates." *Water Resources Research* **28**: 2691-2705.

Powers, S. E.; Abriola, L. M.; Weber, W. J., Jr. (1994). "An experimental investigation of nonaqueous phase liquid dissolution in saturated subsurface systems: Transient mass transfer rates." *Water Resources Research* **30**: 321-332.

Schecher, W. D.; McAvoy, D. C. (1994). "MINEQL+: A chemical equilibrium program for personal computers." In Hallowell, ME, Environmental Research Software.

Schwarzenbach, R. P.; Gschwend, P. M.; Imboden, D. M. (1993). *Environmental Organic Chemistry.* New York, NY, John Wiley & Sons, Inc.

Thierrin, J.; Davis, G. B.; Barber, C. (1995). "A groundwater tracer test with deuterated compounds for monitoring *in situ* biodegradation and retardation of aromatic hydrocarbons." *Ground Water* **33**: 469-475.

Tipping, E. (1981). "The adsorption of aquatic humic substances by iron oxides." *Geochimica et Cosmochimica Acta* **45**: 191-199.

Whelan, M. P.; Voudrias, E. A.; Pearce, A. (1994). "DNAPL pool dissolution in saturated porous media: Procedure development and preliminary results." *Journal of Contaminant Hydrology* **15**: 223-237.

Zhang, Y.; Miller, R. M. (1992). "Enhanced octadecane dispersion and biodegradation by a *Pseudomonas* rhamnolipid surfactant (biosurfactant)." *Applied and Environmental Microbiology* **58**: 3276-3282.

Chapter 3.

MECHANISMS OF GROUNDWATER SOLUBILITY ENHANCEMENTS OF AROMATIC HYDROCARBONS AT A COAL TAR SITE

Abstract

The colloid phases enhancing the mobile concentrations of polycyclic aromatic hydrocarbons (PAHs) above tar-water solubility at a coal tar site were investigated by applying a series of separation methods to groundwater samples. Over 65% of the enhanced *in situ* pyrene mass was associated with settleable particles or tar droplets. The quenching of pyrene fluorescence was decreased by groundwater treatments of acidification followed by ultrafiltration and by addition of aluminum sulphate (alum), suggesting that humic acids quenched pyrene fluorescence in unaltered groundwater. About 5 mg_C/L of humic and fulvic acids were present in groundwater at all monitoring wells sampled, but no enhancement in PAH concentrations were detected over tar-water equilibrium solubility at these wells.

Introduction

In a recent investigation, polycyclic aromatic hydrocarbons were present in groundwater at concentrations greater than expected for equilibrium dissolution of coal tar (Chapter 2). Predictive calculations indicated that the only colloid phase present in sufficient abundance to cause these solubility enhancements was organic matter. These calculations could not discern between facilitating organic matter present as suspended macromolecules, mineral particles with organic coatings, or tar droplets. The purpose of this study was to investigate which, if any, of these organic colloids may be enhancing groundwater polycyclic aromatic hydrocarbon (PAH) concentrations over dissolved compound equilibrium with tar.

A series of separation methods were applied to groundwater samples based on the expected behaviors of suspended organic matter, organic-coated minerals, and tar droplets under various separation strategies. These are summarized in Table 3.1. More than one type of organic colloid may be removed by a single treatment, thus the order of application is important. Tar and some bacteria may remain adhered to the walls of sample collection vessels if the aqueous solution is carefully decanted. Particles with organic coatings can then be separated from suspended organic matter by centrifuging the decanted sample. After centrifugation, the supernatant could be treated to remove all, or some, of the humic substances by precipitation with aluminum oxide floc, or acidification and ultrafiltration. At each separation stage, a subsample of the two fractions could be collected for quantification of the *in situ* compound concentrations in each, a direct measure of colloid-association. Alternatively, each fraction could be tested for the capacity to quench the fluorescence of a probe compound, an indirect measure of the potential for colloid-association.

The sequential separation steps summarized in Table 3.1 were applied to groundwater samples from Site YYZ. Compound-colloid associations were quantified by the distributions of *in situ* pyrene among fractions. Pyrene fluorescence quenching in separated fractions was also measured. The nature of the organic colloids enhancing groundwater PAH concentrations was hypothesized from the separation methods which yielded fractions which contained *in situ* pyrene or which quenched pyrene probe fluorescence.

Table 3.1. Effect of separation methods on the removal of organic colloids from solution. A 'Y' denotes removal by the treatment process. An 'N' denotes no effect.

Separation Treatment	Organic Colloid				
	Humic Acid	Fulvic Acid	Coat'd part.	Tar drop	Bac-teria
Adheres to sampling apparatus	N	N	N	Y	Y
Settled by centrifugation	N	N	Y	Y	Y
Removed by ultrafiltration	Y	Y/N	Y	Y	Y
Precipitated by acidification	Y	N	N	N	N
Precipitated with aluminum oxide floc	Y	Y	N	N	N

Methods

Chemicals

Pyrene (Aldrich, Milwaukee, WI) and internal standards of *p*-terphenyl and *m*-terphenyl (Ultra Scientific, North Kingstown, RI) were greater than 99% pure and used as received. Methylene chloride, hexane and methanol solvents were OmniSolve (EM Science, Gibbstown, NJ). Chromerge and aluminum sulphate were obtained from Fisher Scientific (Fairlawn, NJ). Sodium carbonate was from Mallinckrodt (Paris, KY) and potassium hydrogen phthalate was from Sigma (St. Louis, MO). Hydrochloric (Fisher) and phosphoric (Mallinckrodt) acids were also used.

Sample Treatments

Groundwater samples were collected in September 1996 (W40M) and June 1997 (W20S, W20M, W100S, W100M) (see Chapter 2 for well locations). Samples were collected in foil-wrapped BOD bottles by slow pumping methods (Chapter 2). They were stored at 4°C for 2 weeks (June '97) or 5 months (Sept. '96) before use. Fluorescence quenching studies were undertaken with samples from W40M and W100S. A duplicate sample from W40M was fractionated for quantification of *in situ* pyrene distribution. Only alum-precipitated organic matter was measured in the remaining samples from June '97.

Fractionated Extractions of Groundwater

The *in situ* pyrene was quantified in separated fractions of W40M groundwater. Mineral solids were allowed to settle out of solution over the 5 month storage period. (All particles greater than 0.4 μm in diameter would settle in this time, assuming a particle density of 1.5 g/cm^3, omitting the effect of Brownian motion on particle resuspension. A diameter of 1.2 μm was calculated with a density of 1.05 g/cm^3.) The first step of the fractionation was to gently siphon the supernatant from the BOD bottle, leaving a small, undisturbed volume of water containing the settled solids. (The siphon tube was a piece of aluminum tubing primed with purified water, introducing less than 8 mL to the 270 mL transferred volume.) The small volume of water remaining in the original sample bottle was spiked with an internal standard of *p*-terphenyl and extracted in the bottle with methylene chloride. This extract was

denoted the "settled solids + walls" fraction and contained pyrene associated with settled solids and tar droplets which were adhered to the glass.

The siphoned supernatant contained the dissolved compounds plus those associated with stable colloids. This fraction was subdivided by acidifying the groundwater to pH 1 with hydrochloric acid. The sample was allowed to stand for 3 days while acid-precipitated material settled out. The siphoning procedure described above was repeated. The remaining volume was spiked, extracted and referred to as the "pH 1 precipitate" fraction. The second siphoned supernatant contained dissolved pyrene and organic colloids not precipitated under acidic conditions. This volume of water was also spiked with *p*-terphenyl and extracted with methylene chloride. This fraction was called the "pH 1 dissolved" fraction.

The fractionated methylene chloride extracts were transferred to hexane and analyzed by capillary gas chromatography. The gas chromatograph was a Carlo Erba HRGC equipped with a 30 m DB5-MS column (0.32 mm ID, 0.25 μm film thickness, J&W Scientific, Folsom, CA) to which cold on-column injections were made. An injection standard of *m*-terphenyl was added to the extract just prior to cold on-column injection to quantify the volume of the extract. The temperature program began at 70°C with a ramp of 12°C/min to 120°C, followed by a ramp of 3°C/min to 175°C, and a ramp of 8°C/min to 300°C with a final hold time of 5 min at 300°C. Compounds were detected by a flame ionization detector (300°C) and quantified by measuring peak heights or integrating peak areas and comparing to known external standards. Pyrene concentrations were internal standard corrected with *p*-terphenyl recoveries.

Fluorescence Quenching

Pyrene fluorescence measurements were made with a Perkin Elmer LS50B fluorometer. The excitation wavelength was 334 nm with a slit width of 4 nm and the emission wavelength was 373 nm, also with a slit width of 4 nm. The absorbances at these two wavelengths were measured on a Beckman DU 640 spectrophotometer to correct for the inner filter effect (Gauthier *et al.*, 1986). Fluorescence measurements were made with water samples siphoned from the collection vessels to include only the colloid species most stable over a 5 month period. Background fluorescence readings of a 3 mL water sample were taken before pyrene addition. Four 50 μL aliquots of a pyrene in methanol stock solution

were added to the cuvette. The cuvette was allowed to stand for 10 min after each addition before fluorescence measurements were made. In all cases, fluorescence response was linear and quantified as the slope of a plot of background-corrected fluorescence versus pyrene concentration. A duplicate sample with 3 mL of oxygen-free (< 0.3 μM, Chemettes, Chemetrics, Calverton, VA) purified water (18 MΩ, Aries purification system, Vaponics, Rockland, MA) was treated identically to quantify pyrene fluorescence in the absence of quenchers. Because these were single point measurements at only one quencher concentration, the linearity of a Stern Volmer plot was verified by a dilution series to minimize coagulation artifacts by colloid concentration. Groundwater was diluted with oxygen-free 18 MΩ water. All sample manipulations were made in an argon or nitrogen atmosphere. Between water samples, cuvettes were chromerged for 30 minutes, followed by a rinsing sequence of 18 MΩ water, methanol, methylene chloride, methanol and 18 MΩ water.

Organic Carbon Measurements

Total organic carbon (TOC) in water samples was determined after removal of inorganic carbon. Samples were acidified to pH 3 with phosphoric acid and bubbled with nitrogen or argon for 10 minutes. TOC was measured by high temperature oxidation with a Shimadzu TOC-5000 Organic Carbon analyzer externally calibrated with potassium hydrogen phthalate standards. Triplicate measurements were made. The mean ± the standard deviation of these analyses is reported.

Removal of Organic Carbon

Acid precipitation. Solution pH was lowered to pH 1 by the addition of hydrochloric acid. The acid precipitated material was separated from acid-stable organic carbon by centrifuge ultrafiltration. Centricon 3 (Amicon, Beverley, MA) filter cartridges with a nominal cutoff of 3000 Daltons were used. Before use, the filters were washed with methanol, followed by repeated washes with 18 MΩ water until the TOC of the filtrate was indistinguishable from 18 MΩ water. Acidified samples were ultrafiltered by centrifuging for 2 hours at 800 *g*.

Alum precipitation. Surface reactive organic carbon was removed from solution by addition of alum (aluminum sulphate). Under mildly acidic conditions, a heavy aluminum hydroxide floc formed which settled from solution, removing organic carbon which had sorbed to it.

Alum (10 mg) and sodium carbonate (5 mg to adjust pH) were added to 10 mL of water in a centrifuge tube. The sample was shaken vigorously for 30 s and allowed to stand for 30 min for floc formation. The floc, and associated organic matter, was separated from the supernatant by centrifuging at 800 *g* for 15 minutes. The concentration of alum removed all organic carbon from an 8 mg_C/L solution of Aldrich humic acid.

Calculation of Partition Coefficients

Partition coefficients of colloidal materials were calculated from enhancement factors:

$$E = \frac{C_T}{C_w} = 1 + (OC)K_{oc} \quad (1)$$

where E is the enhancement factor, C_T (μg/mL) is the total compound concentration in a bulk (dissolved plus colloid-associated) water sample, C_w (μg/mL) is the dissolved concentration, (OC) (g/mL) is the colloid concentration, and K_{oc} (mL/g) is the colloid-water partition coefficient. While this equation has been written with organic carbon (OC) notation, it is also applicable to mineral solid or tar-enhanced solubilities. In the case of fluorescence quenching, the total compound concentration is given by the probe fluorescence of a sample from which the colloid phase has been removed (F_0) and the dissolved concentration is the probe fluorescence in the sample (F_1), assuming the colloid-associated probe is fully quenched.

Results and Discussion

Fractionated Extractions of Groundwater

Pyrene concentrations were elevated above dissolved concentrations in both of the colloid-containing fractions of fractionated W40M groundwater (Table 3.2). The masses in each fraction were summed to give the pyrene concentration which would have been obtained by an extraction of the bulk water sample. This concentration (0.0036 ± 0.001 mg/L) was in agreement with the concentration of pyrene (0.0046 ± 0.0013 mg/L) determined from an extraction of 2 L of fresh W40M groundwater (Chapter 2).

The separation of the colloid fractions in W40M groundwater was likely not perfect because gravitational settling and siphoning were used for separation. The concentration of pyrene in the final "pH 1 dissolved" fraction was 0.0013 mg/L and a concentration of 0.0014 mg/L was measured in equilibrium with coal tar (Chapter 2). Thus, all colloid-associated pyrene appears to have been removed and the "dissolved" fraction truly contains only dissolved pyrene. Because the pyrene concentration was not elevated in the "pH 1 dissolved" fraction, fulvic acids are likely not important sorbing colloid phases.

The importance of settled solids plus tar and acid-precipitated organic matter on the enhancement of groundwater pyrene concentrations was calculated. In order not to suspend settled particles, a volume of water containing dissolved and stable organic colloid-associated pyrene was also extracted with the settled solids and walls. The portion of the pyrene mass reported in Table 3.2 for this fraction which originated from the inclusion of dissolved and organic colloid-associated pyrene in this volume was calculated to be 5%. This fraction was calculated by dividing the product of the settled solids and walls volume (0.01 L) and the effective pyrene concentration of the pH 1 dissolved and pH 1 precipitate ($(0.3 \times 10^{-3} + 0.28 \times 10^{-3})$ mg/(0.23 + 0.039) L) by the mass of pyrene in the settled solids and wall fraction (0.044 mg/L × 0.01 L). In the case of the "pH 1 precipitate", 18% of the pyrene mass was actually dissolved and not colloid-associated. With these corrections, about 65% $((0.95\times43)/(0.95\times43 + 0.82\times27)$ of the pyrene in excess of dissolved solubility in equilibrium with tar was associated with the bottle walls or settled solids. The remainder of the excess pyrene mass was associated with colloids that were stable over 5 months, but could be acid-precipitated.

Table 3.2. Distribution of pyrene in fractionated W40M groundwater. The fractionation method is described in the Fractionated Extractions of Groundwater section. Bulk groundwater values are the sum total from each of the separated fractions.

Separated fraction	Pyrene concen-tration (mg/L)	Volume of extract (L)	Mass of pyrene (mg)	Mass fraction of total pyrene (%)
pH 1 dissolved	0.0013	0.230	0.3×10^{-3}	30
pH 1 precipitate	0.0071	0.039	0.28×10^{-3}	27
Settled solids + walls	0.044	0.010	0.44×10^{-3}	43
Bulk groundwater	0.0036	0.279	1.02×10^{-3}	100

The distribution of pyrene in colloid fractions assumed perfect separation of settled particles. It is possible that the "pH 1 precipitate" was settleable particles that had been entrained in the transfer step. They would have settled from solution over the 3-day stand time in response to gravity not acidification. Total organic carbon concentrations were not measured in any of the fractions to verify colloid conservation or enhancement in any of the fractions. If the colloid separation steps did achieve the proposed separation, the pyrene enhancement factors calculated from these separations should agree with those obtained from fluorescence quenching studies on groundwater samples subjected to selective organic carbon removal by ultrafiltration and precipitation.

Fluorescence Quenching

Static quenching of the probe compound must be verified before fluorescence quenching can be applied to quantify colloid-association. The presence of dissolved species, such as oxygen, can quench pyrene fluorescence in solution, incorrectly suggesting colloid-association of the pyrene. One way to differentiate between static and dynamic quenching of a probe compound is with a Stern-Volmer plot (Figure 3.1). If the probe is statically quenched, the fluorescence will be quenched according to Eq. 1 and a plot of F_0/F_1 versus the quencher concentration (OC) will be linear. Such a plot for W40M groundwater was linear (Figure 3.1); however, the concentration range of organic carbon was too narrow to discern plot nonlinearities.

The Stern-Volmer plot can be interpreted in a second way if dynamic quenching of the probe fluorescence was occurring. In this case, the quenched fluorescence is related to the quencher concentration with the following equation:

$$\frac{F_0}{F_1} = 1 + k_q \tau(Q) \qquad (2)$$

where k_q ($M^{-1}s^{-1}$) is the quenching rate constant, τ is the fluorescence lifetime of the probe, and (Q) (M) is the quencher concentration. The dynamic quencher in the W40M groundwater was assumed to be the low, but detectable levels of oxygen present. The quenching rate

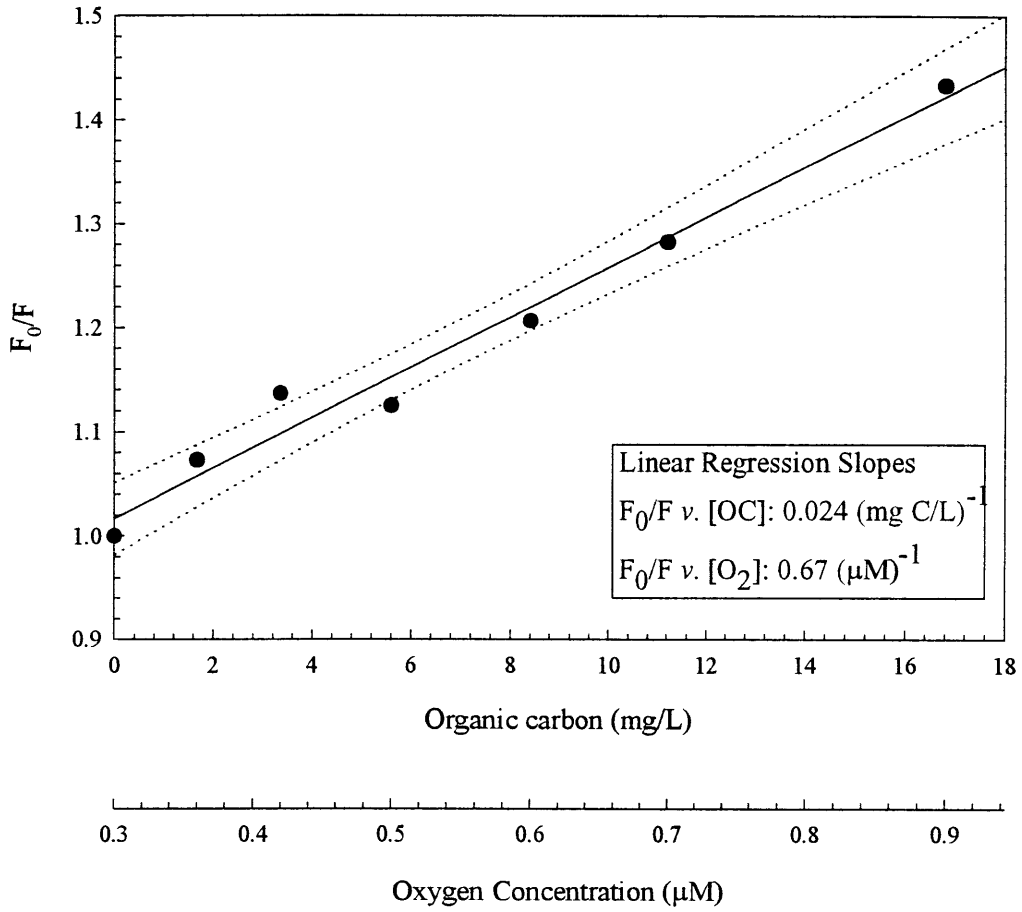

Figure 3.1. Stern-Volmer plot of quenched pyrene fluorescence in W40M groundwater. Quencher concentrations were varied by dilution with oxygen-free 18 MΩ water.

constant for oxygen is estimated to be 1×10^{10} $M^{-1}s^{-1}$ (Lakowicz, 1983) and the fluorescence lifetime of pyrene is 200×10^{-9} s. With oxygen as the quenching species, the slope of the Stern-Volmer plot was 670 000 M^{-1}. A quenching rate constant of 3.4×10^{12} $M^{-1}s^{-1}$ was estimated for oxygen with the pyrene fluorescence lifetime. This rate constant is faster than the diffusion rate constant for oxygen, the fastest rate at which pyrene fluorescence could be quenched by oxygen. Thus, it is likely that pyrene is statically quenched in W40M groundwater and single-point fluorescence measurements are sufficient to quantify colloid-association.

Pyrene fluorescence was quenched by humic acid-like organic colloids in W40M groundwater. First, the fluorescence of pyrene in W40M groundwater was decreased relative to a control of 18 MΩ water (Table 3.3), indicating the presence of a colloid phase in the groundwater. Ultrafiltration removed some of the quenching phase and the pyrene fluorescence was slightly greater than in the unaltered groundwater, but did not approach the fluorescence in 18 MΩ water. Thus, the colloid phase was able to pass through a nominal 3000 Dalton filter. Some organic-coated mineral particles or large suspended molecules may have been retained on the filter surface, accounting for 1 mg_C/L of organic matter. Mineral particles were not expected to be significant because the water sample was siphoned from a BOD bottle which had been stored for 5 months. When the groundwater was acidified to pH 1 and then ultrafiltered, the probe fluorescence did approach the levels of fluorescence in colloid-free water. Acidification of the water sample would cause humic acid-like molecules to coagulate and be more efficiently removed from solution by the ultrafiltration. A change in organic carbon concentration was observed between the unfiltered acidified groundwater and the filtrate. The groundwater absorbance at 280 nm also decreased from 0.73 (ultrafiltered) to 0.5 (pH 1 ultrafiltered). (Water that was in equilibrium with tar had an absorbance of 0.45 at 280 nm, and thus the groundwater absorbance after acidification and ultrafiltration likely resulted from dissolved aromatic hydrocarbons.) The calculated molar absorptivity of the removed organic matter was 690 $M^{-1}cm^{-1}$. This molar absorptivity is of the same magnitude as reported for humic materials (Chin *et al.*, 1991) and is much less than the

Table 3.3. Pyrene fluorescence in W40M groundwater after various treatments to remove organic colloids.

Sample	Slope (fluorescence *v.* pyrene concentration)	TOC (mg C/L)
18 MΩ water	3.1 ± 0.1, 3.2 ± 0.1	1.9 ± 0.4
Ultrafiltered 18 MΩ water	3.9 ± 0.3	3.1 ± 0.1
Unaltered W40M groundwater	2.2 ± 0.1	19 ± 1.5
Ultrafiltered W40M groundwater	2.4 ± 0.1	17 ± 0.02
pH 1 W40M groundwater	not measured	20 ± 0.9
Ultrafiltered pH 1 W40M groundwater	3.4 ± 0.2	13 ± 0.4

molar absorptivity of polycyclic aromatic hydrocarbons (*c.f.*, benz(a)anthracene absorptivity of 10^4 $M^{-1}cm^{-1}$ (Schwarzenbach *et al.*, 1993)). Thus, pyrene fluorescence appears to be quenched by 4 to 7 mg_C/L of organic colloids which are humic acid-like in nature.

The magnitude of the organic colloid-water partition coefficient and its enhancement of pyrene solubility was calculated. The enhancement factor was calculated by Eq. 1 from the ratio of fluorescence in the colloid-free solution to the fluorescence in the colloid-containing solution. The values of F_0 and F_1 were taken from the ultrafiltered pH 1 groundwater and the unaltered ultrafiltered groundwater because there was a known amount of organic carbon removed from the later sample which accounted for the increased probe fluorescence between the two samples. The enhancement factor of 1.4 was slightly less than that calculated from the distribution of pyrene mass between the dissolved and organic colloid phases of the fractionated extractions (Table 3.4). Therefore, both the fractionated extractions and the fluorescence quenching results were consistent with the presence of humic acid in the groundwater which enhanced the concentrations of PAHs at Site YYZ above dissolved levels in equilibrium with tar.

Pyrene fluorescence quenching studies with fresh W100S groundwater produced similar enhancement factors and partition coefficients as those observed for W40M groundwater. First, pyrene fluorescence in unaltered groundwater was lower than in 18 MΩ water (Table 3.5). A control for quenchers removed by centrifugation was contaminated by organic carbon (TOC 190 mg_C/L). Sufficient sample remained to make duplicate measures of the change in groundwater organic carbon concentration after centrifugation, but not to remeasure pyrene fluorescence quenching. The organic carbon concentration in centrifuged groundwater was not less than in the unaltered groundwater; thus, little pyrene sorbing material was likely removed from solution solely by centrifugation. After removal of humic substances by alum precipitation, W100S groundwater did not quench pyrene fluorescence relative to the colloid-free 18 MΩ water control. About 4 mg_C/L was removed by alum precipitation, increasing the fluorescence from 210 fluorescence units to 299 fluorescence units. Again, the enhancement factor was calculated to be 1.4 with a corresponding partition coefficient of 10^5 mL/g_{oc} (Table 3.4).

Table 3.4. Pyrene solubility enhancements by groundwater organic colloids. Partition coefficients were calculated by applying Eq. 1.

Sample	Enhancement factor	[OC] (mgC/L)	log K_{oc}
W40M fractionated extractions	$E = \frac{\text{pH 1 precipitate + pH 1 diss'd)}}{\text{pH 1 dissolved}}$ = ((0.28 + 0.3)µg / 269mL) / 0.0013µg/mL = 1.7		
W40M fluorescence quenching	$E = \frac{\text{pH 1 ultrafiltrate}}{\text{dissolved + colloidal ultrafiltrate}}$ = 3.4 / 2.4 = 1.4	4	5
W100S fluorescence quenching	$E = \frac{\text{alum precipitated supernatant}}{\text{bulk supernatant}}$ = 299 / 210 = 1.4	4	5

Table 3.5. Pyrene fluorescence quenching by W100S groundwater.

Sample	Pyrene fluorescence	TOC (mgC/L)
18 MΩ water	270	
Unaltered W100S groundwater	210	48 ± 1
Centrifuged W100S groundwater	151*	54 ± 1.5
Alum precipitated W100S groundwater	299	44 ± 1

*Likely reflects glassware contamination, rather than quenchers in the groundwater sample.

The pyrene partition coefficients for organic colloids at Site YYZ were compared to literature values. Colloid-water (Chin and Gschwend, 1992) and sediment-water partition coefficients (Kile *et al.*, 1995) for samples from contaminated marine environments were greater than those observed for samples from pristine environments. By analogy, groundwater colloids at this coal tar site may reflect the hydrocarbon-rich nature of the contaminant source, being much less polar, and hence more sorptive, than groundwater colloids in pristine aquifers. Such trends have been observed for colloids in other contaminated aquifers. Organic matter upgradient of a crude oil spill (Hawley, 1996) and a sewage plume (Backhus and Gschwend, 1990) did not quench the fluorescence of perylene probes, while organic colloids within the plumes at both sites measurably quenched perylene fluorescence. No upgradient samples were obtained for comparison of pyrene fluorescence quenching by groundwater colloids within and outside of the contaminant plume at Site YYZ. Nevertheless, this site is another example of a contaminated aquifer with groundwater organic matter that has the capacity to sorb hydrophobic organic contaminants.

Correlation of Organic Carbon with Enhancement Factors

If the polycyclic aromatic hydrocarbon concentrations in Site YYZ groundwater are enhanced by humic acids over dissolved levels in equilibrium with tar, the enhancement factors of PAHs at various wells should correlate with the amount of acid-precipitated organic matter. Unfortunately, there were no preserved Sept. '96 groundwater samples remaining from other wells to test this hypothesis. The amount of alum-precipitated organic carbon was measured for all of the wells sampled in June '97 (Table 3.6). Centrifugation alone had little effect on changing the concentration of organic carbon in these groundwater samples, except at W100M where about 3 mg_C/L appeared to be particle associated. Alum precipitation removed from 4 (W20M, W100M) to 7 mg_C/L (W20S, W100S); however, insignificant enhancements in PAH concentrations were observed at these wells (Appendix B). Alum precipitation removes both humic and fulvic acids (VanBenschoten and Edzwald, 1990; Edwards and Amirtharajah, 1985). If all of the carbon precipitated with the alum was fulvic acid, no enhancement in PAH concentrations would be expected. (Pyrene showed no association with fulvic acids at W40M.) An upper bound of 1 mg_C/L of humic acids was estimated to be present in the

Table 3.6. Organic carbon content of groundwater samples from June 1997.

Sample	Unaltered (mgC/L)	Centrifuged (mgC/L)	Alum precipitated (mgC/L)
W20M	39.7 ± 0.7	40.2 ± 0.6	35.5 ± 0.4
W20S	24.4 ± 0.6	25 ± 0.2	19.0 ± 0.7
W100M	28 ± 0.6	24.9 ± 0.05	20.3 ± 0.5
W100S	28.7 ± 0.7	27.8 ± 0.1	21.2 ± 1.3

groundwater by reverse phase separation (Appendix B). Polycyclic aromatic hydrocarbons associated with this level of humic acid would not be detectable as concentrations greater than tar-water equilibrium by the extraction of groundwater samples.

While the preceding arguments about the nature of the alum-precipitated organic carbon are consistent with no observable PAH concentration enhancements, they do not explain the fluorescence quenching observed with W100S groundwater. The octanol water partition coefficient (K_{ow}) for benzo(a)pyrene (10^6, (Miller *et al.*, 1985)) is 0.8 orders of magnitude greater than the pyrene K_{ow} ($10^{5.2}$, (Miller *et al.*, 1985)). To a first approximation, the benzo(a)pyrene K_{oc} for Site YYZ groundwater colloids would also be about 6 times greater than the pyrene K_{oc}, with an estimated value of $10^{5.8}$. The corresponding enhancement factor calculated for benzo(a)pyrene with Eq. 1 would then be 3.5 with 4 mg C/L organic colloids present in the groundwater. According to the analytical precision of the liquid-liquid extraction of 2 L groundwater samples (Chapter 2), an enhancement by a factor of 3.5 in the concentration of benzo(a)pyrene above tar-equilibrium solubility levels should be readily detectable but was not observed with bulk groundwater extractions (Appendix B). The June '97 analyses only used 300 mL groundwater sample volumes rather than 2 L samples, as used at the other sample dates (Chapter 2). Methylene chloride was added to these samples in the lab, immediately prior to extraction, while 100 mL of methylene chloride was added to the 2 L samples in the field. Perhaps the solvent water contact times were not great enough to extract colloid-associated compounds. The 2 L groundwater samples contacted this solvent reservoir for a minimum of 48 hours before separatory funnel extraction.

An alternate explanation of the discrepancy between the fluorescence quenching results and the liquid-liquid extractions of the June '97 samples was that pyrene fluorescence was not quenched by association with organic matter. As noted, a dynamic quencher or static inorganic quencher would reduce pyrene fluorescence, but would not sorb polycyclic aromatic hydrocarbons from dissolving coal tar. Clearly, the alum treatment did remove the pyrene quencher. At the pH of precipitation (pH 6), the aluminum hydroxide floc was positively charged, thus a nonsorbing pyrene quencher must be negatively charged. If such a quencher was present in the W40M groundwater, it would have also have had to precipitate at pH 1 and be removed by ultrafiltration. The only difference in the groundwater chemistry between

the two wells was the presence of mM levels of sulphide and sulphate at W100S (Chapter 2). Negatively charged polymeric sulphide species would have been removed from the groundwater with the addition of alum, but it is unknown to what extent they would quench pyrene fluorescence.

More study is required to verify that the pyrene fluorescence was quenched by association with organic colloids in Site YYZ groundwater. The complex groundwater matrix at this site may contain moieties that can quench the fluorescence of pyrene, but not sorb polycyclic aromatic hydrocarbons desorbing from coal tar. Measuring the pyrene fluorescence lifetime in solution or the use of other, non-sorbing fluorescent probes, in addition to pyrene, may help to elucidate whether quenchers other than organic matter are present in the groundwater at this site.

Conclusion

The fact that the enhancement factors and pyrene partition coefficients determined for 2 water samples by 2 different methods were so consistent with one another suggests the presence of organic colloids in the groundwater at this site. On the basis of the fractionated extractions of *in situ* pyrene, however, the major contributor of polycyclic aromatic hydrocarbon concentration enhancements above tar-water equilibrium levels was particles coated with organic-matter or tar, or tar droplets, and not organic colloids. About 5 mg_C/L of organic macromolecules was present at most wells, but the detection of colloid-enhanced PAH groundwater concentrations by comparison of groundwater and tar-water equilibrium extractions may not have been sensitive enough to detect organic-colloid enhancements.

References

Backhus, D. A.; Gschwend, P. M. (1990). "Fluorescent polycyclic aromatic hydrocarbons as probes for studying the impact of colloids on pollutant transport in groundwater." *Environmental Science and Technology* **24**: 1214-1223.

Chin, Y.-P.; Gschwend, P. M. (1992). "Partitioning of polycyclic aromatic hydrocarbons to marine porewater organic colloids." *Environmental Science and Technology* **26**: 1621-1626.

Chin, Y.-P.; McNichol, A. P.; Gschwend, P. M. (1991). "Quantitation and characterization of porewater organic colloids." In *Organic Substances and Sediments in Water*. R. A. Baker, Ed. **:** 107-126.

Edwards, G. A.; Amirtharajah, A. (1985). "Removing color caused by humic acids." *Journal of the American Water Works Association* 77(3): 50-57.

Gauthier, T. D.; Shame, E. C.; Guerin, W. F.; Seitz, W. R.; Grant, C. L. (1986). "Fluorescence quenching method for determining equilibrium constants for polycyclic aromatic hydrocarbons binding to dissolved humic materials." *Environmental Science and Technology* **20**: 1162-1166.

Hawley, C. M. (1996). *A Field and Laboratory Study of the Mechanisms of Facilitated Transport of Hydrophobic Organic Contaminants*. M.S. Thesis, University of Colorado.

Kile, D. E.; Chiou, C. T.; Zhou, H.; Li, H.; Xu, O. (1995). "Partition of nonpolar organic pollutants from water to soil and sediment organic matters." *Environmental Science and Technology* **29**: 1401-1406.

Lakowicz, J. R. (1983). *Principles of Fluorescence Spectroscopy*. New York, Plennum Press.

Miller, M. M.; Wasik, S. P.; Huang, G. L.; Shiu, W. Y.; Mackay, D. (1985). "Relationships between octanol-water partition coefficient and aqueous solubility." *Environmental Science and Technology* **19**: 522-529.

Schwarzenbach, R. P.; Gschwend, P. M.; Imboden, D. M. (1993). *Environmental Organic Chemistry*. New York, NY, John Wiley & Sons, Inc.

VanBenschoten, J. E.; Edzwald, J. K. (1990). "Chemical aspects of coagulation using aluminum salts- II. Coagulation of fulvic acid using alum and polyaluminum chloride." *Water Research* **24**: 1527-1535.

Chapter 4.

HYDRAULIC PROPERTIES OF FILL SOLIDS

Abstract

The hydraulic conductivity of the anthropogenic fill solids in the water-bearing unit at Site YYZ was calculated to be 100 m/d from analysis of tidally induced groundwater fluctuations in the anthropogenic fill. A local hydraulic conductivity was calculated to be 30 m/d from particle size distributions of fill solids, suggesting that the hydraulic properties of these fill materials do not vary over lengthscales from a few centimeters to tens of meters. The groundwater velocity under ambient flow conditions was 0.6 to 2 m/d in the WSW (254°) direction. The groundwater velocity induced by pumping R2 was in the NE (295°) direction with magnitudes of 1.2, 0.6, and 0.2 m/d at the W20, W40, and W100 well clusters, respectively.

Introduction

Knowledge of the hydraulic properties of an aquifer is required in order to model the transport of groundwater contaminants. These hydraulic properties, such as porosity, hydraulic conductivity and head gradients, are determined from a combination of laboratory measurements and static or dynamic field tests. The hydraulic conductivity and storativity of an aquifer, in particular, cannot be measured directly with field tests. Rather, changing head levels in monitoring wells are recorded as a function of time or distance in response to aquifer forcing. The data collected are compared to theoretical expressions for head changes in time and space as functions of conductivity and storativity (*i.e.*, type-curve matching). These theoretical relationships were developed for natural, geologically-deposited aquifers. Saturated zone solids composed of anthropogenic fill materials have the potential for differing hydraulic characteristics than geologic media of the same scale. The extent to which the hydraulic properties of and flowpaths in anthropogenic water-bearing units can be estimated from the responses of geologically-deposited media is not known.

The purpose of this chapter was to determine the hydraulic properties (conductivity, flow velocity) for the anthropogenic fill material at Site YYZ. The focus of this thesis was on the physical-chemical sources and sinks affecting the groundwater transport of organic contaminants, not on the physical flow field *per se*. Thus, the unique physical structure of the fill solids and its effect on flowpaths in the fill region was not investigated as part of this work. However, the possible unique characteristics of fill solids and the ways in which they may differ from geologic media are discussed in general.

General Characteristics of Fill Solids

The primary contrast between fill solids and geologic media is the difference between their depositional environments. The depositional environments give rise to the hydraulic properties of these two aquifer types and determine which, if any, hydrology theories for geologic media are applicable to fill solids. Landfilling likely occurs over a period of time, yielding pockets of material that were formed at the same time, but are somewhat discontinuous from those added prior and later. In contrast, the geologic processes through which natural aquifers are formed tend to have distinct bedding planes which dominate the

groundwater flow direction. The bedding plane in natural aquifer sediments is generally horizontal and gives rise to anisotropic hydraulic conductivities (Bouwer, 1978). Fill materials that were deposited intermittently may be more isotropic with less preference for horizontal-over-vertical flow in response to head gradients.

A second difference between anthropogenic water-bearing units and natural aquifers is the scale of their areal extent. Industrial sites are likely on the scale of tens of hectares (10^4 m^2) while geologic deposits and formations can cover thousands for meters in dimension. (One anthropogenic exception is landfills which can be much larger in dimension than industrial sites. Landfills are intentionally sited to not penetrate the saturated zone (Fetter, 1994); however, the transport of infiltrating precipitation may still be affected by the same depositional characteristics as discussed here for saturated fill solids.) The large scale of geologic media allows correlations of aquifer properties to be developed. For example, natural aquifer sediments formed by glacial outwash show decreasing particle size with distance from the terminus (Fetter, 1994). Such data can be used to determine the change in hydraulic conductivities over distance in the aquifer and the scale over which conductivity can be assumed relatively homogeneous (Thompson, 1994). It is unlikely that any sorting of solids occurs as filled land is made. Geologic features in natural aquifers may also remain constant over great distances. Again, the sporadic nature of landfilling may inhibit the formation of such continuous features. Thus, anthropogenic water-bearing units have the potential to be very heterogeneous, depending upon the range in particle sizes of the waste materials that were landfilled.

The nature and arrangement of fill materials (*e.g.* coarse building rubble *v.* fine ash) suggests the relevant hydrologic model for understanding and predicting contaminant transport through these solids. The disparate-sized anthropogenic materials can assume two primary forms of organization as they are deposited. First, fine-grained materials can fill in the intra- and interparticle porosity of large particles. The resultant water-bearing formation is structurally similar to an unsorted glacial till. Approaches for determining hydraulic conductivities and flow fields in glacial tills may be applicable to such anthropogenic fill solids. The second fill organization has a limited amount of interparticle mixing, and the variously-sized anthropogenic materials form randomly distributed pockets of varied

permeability in the fill. In this case, the resultant water-bearing unit has structural characteristics in common with a random dual-porosity fractured aquifer system (*e.g.*, Barrenblatt model (Sen, 1995)) with flow occurring predominantly through the coarse solids, around zones of fine-textured material. This type of fill structure may also include cases of non-Darcian flow through anthropogenic solids with high intraparticle porosity that do not consolidate (*e.g.*, cinder blocks). Such flow channels would have characteristics similar to karstic systems, although on a much smaller scale, in which groundwater flow is modelled as pipe flow (Ford and Williams, 1989).

These are a few examples of fill characteristics which may be important when understanding the hydraulics of anthropogenic water-bearing units. Each site with anthropogenic fill is likely unique. The extent to which hydrologic models must be modified, or less typical hydrologic models (*e.g.*, dual-porosity fractures) used to interpret and predict groundwater flow fields depends upon the size distribution of the fill solids. For example, made land could be created by landfilling sand which would be homogeneous, in contrast to building rubble which may have non-Darcian flow.

We now focus on Site YYZ as a specific example of an industrial site with a water-bearing unit composed of anthropogenic fill. Our goal was to calculate the groundwater velocity under ambient and induced gradient conditions. Boring logs demonstrated the patchiness of the fill solids at this site. Nevertheless, local hydraulic conductivities (from particle size analysis) were of the same order of magnitude as regional values (from pump tests) at this site.

Site YYZ Hydraulics

Conceptual Picture of Site YYZ Hydrology

A conceptual picture of the groundwater flow within the study region at Site YYZ was developed from boring observations. The boring locations are shown on a map of the study area (Figure 4.1). A cross section profile of the fill material depicts the patchiness of the fill solids distribution (Figure 4.2). Further evidence of the extreme heterogeneity of this water bearing unit was indicated by the variability of the core recoveries. B4 was a 7-m continuous

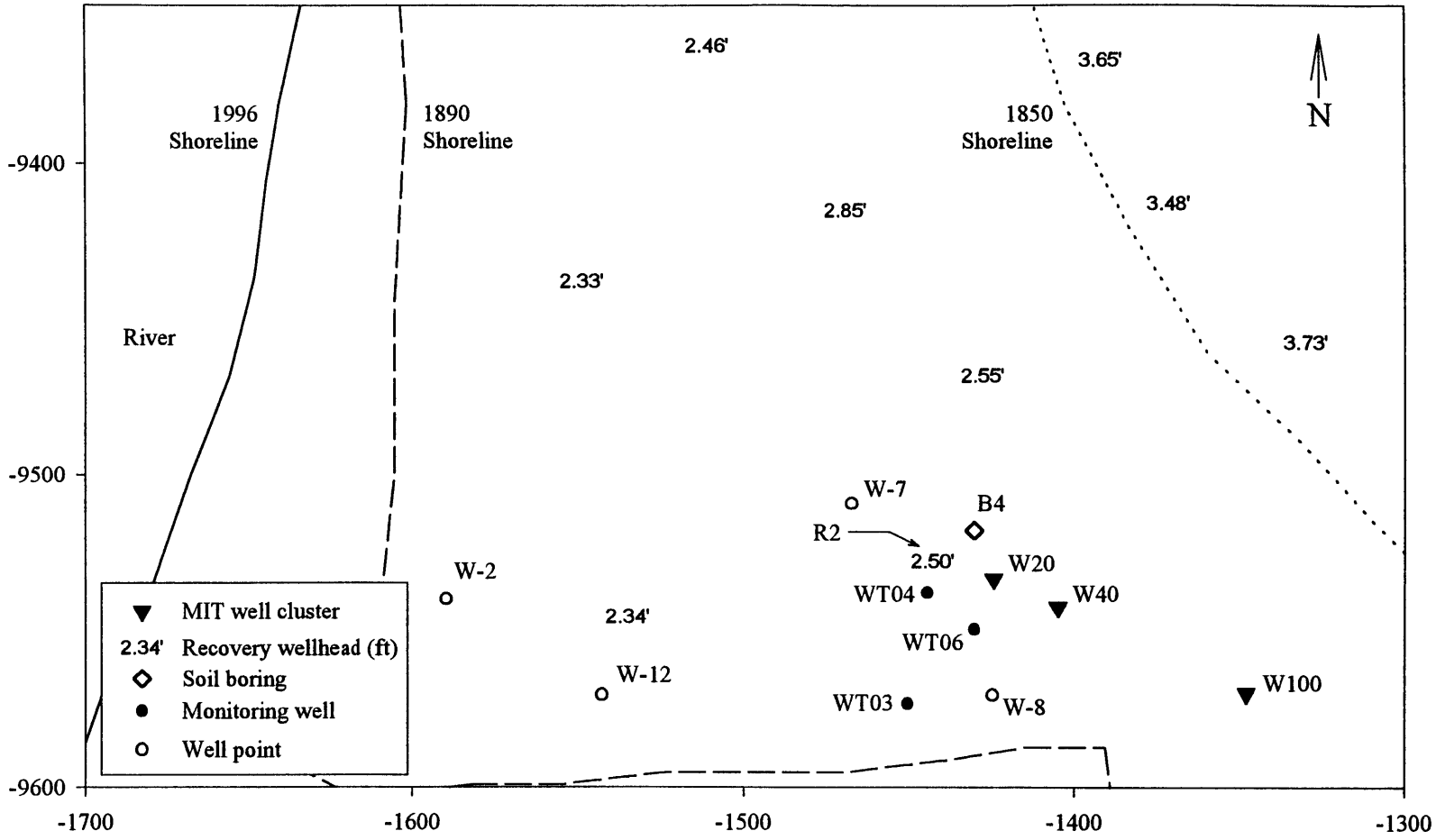

Figure 4.1. Map of Site YYZ detailing the field study area. Axes denote distance (ft) from an arbitrary origin. The approximate locations of historic shorelines in this landfilled region are noted. April 10, 1996 ambient head measurements (ft relative to mean sea level) in the recovery wells are noted at the well location.

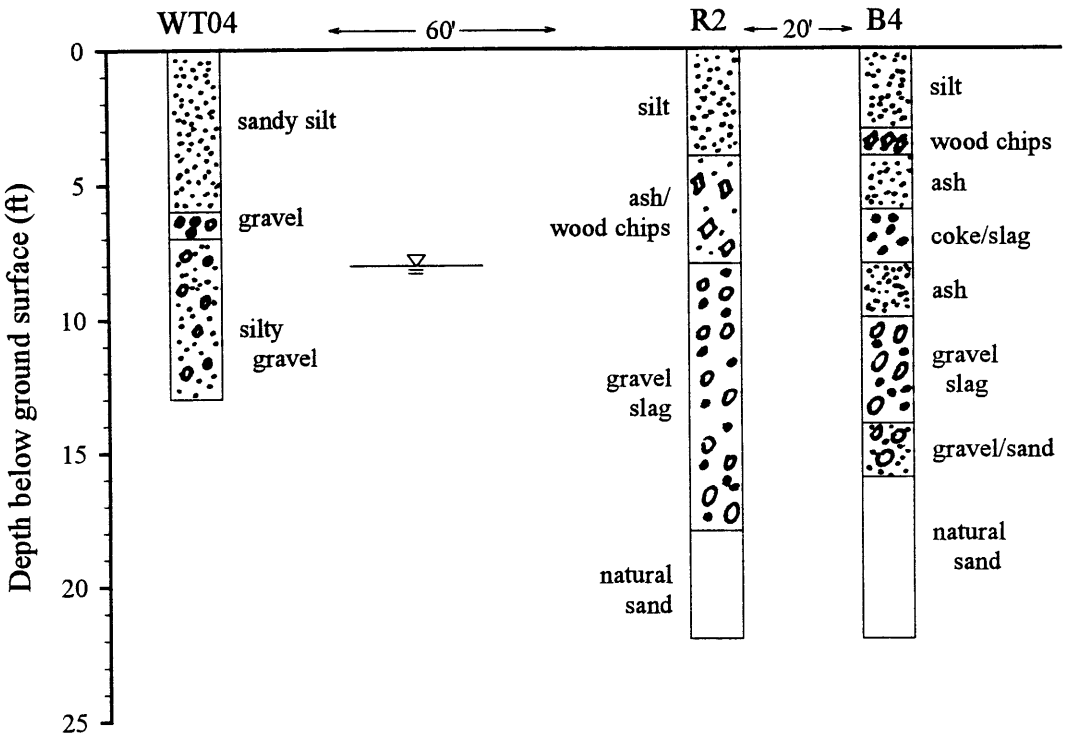

Figure 4.2. Cross-section of fill material in the field study area at Site YYZ. Depth profiles were constructed from qualitative observations of B4 material and drilling logs (locations are noted in Figure 4.1). The density of the graphic fill pattern decreases with coarseness of anthropogenic solids. Note the exaggerated vertical scale. The approximate water table depth is also noted.

boring with a total recovery of 7 m. A duplicate boring made within 2 m of the B4 location recovered only 0.6 m of material.

The coarser anthropogenic solids in this water-bearing unit were generally, located at depth, above the natural sand and silt. Shallower solids near the water table were finer in texture. The qualitative observations from the cross section profile were substantiated with particle size analysis of solids from boring B4 (Figure 4.3). Again, greater amounts of coarse material were found deeper in the saturated zone. These results suggest that most of the groundwater flow occurs at the base of this water-bearing unit and an induced gradient would primarily draw water at depth from this unconfined unit.

Hydraulic Conductivity

The hydraulics at Site YYZ under ambient and induced gradient conditions were determined from static head measurements and tidal forcing in the study area. The parameters obtained from these measurements were used to determine an average pore water velocity in this region according to Darcy's Law:

$$v = \frac{K_h}{\theta}\frac{dh}{dx} \qquad (1)$$

where v (m/d) is the pore water velocity, K_h (m/d) is the hydraulic conductivity, θ is the porosity, and dh/dx (m/m) is the head gradient per unit distance. For the purpose of this study, we were interested in a bulk measure of velocity from which the mean residence time (order of magnitude value) of groundwater in this region could be calculated.

Hydraulic conductivities were first estimated from particle size analysis of the fill solids from B4. Solids were obtained by split spoon sampling ahead of a hollow stem auger. Core segments were obtained in acrylic liners with a 0.6 m, 7.5 cm diameter split spoon. Solids were removed from each segment and wet sieved through brass screens (63, 125, 250 and 500 μm) with reverse osmosis water containing 2 g/L sodium chloride and adjusted to pH 6 to match the ionic strength and pH of the groundwater. Sieved solids were dried at 105°C for 24 h and weighed. Sufficient amounts of fill solids were retained in the cores that porous medium flow (Darcy's Law) was assumed to occur on a local scale. Hence, hydraulic

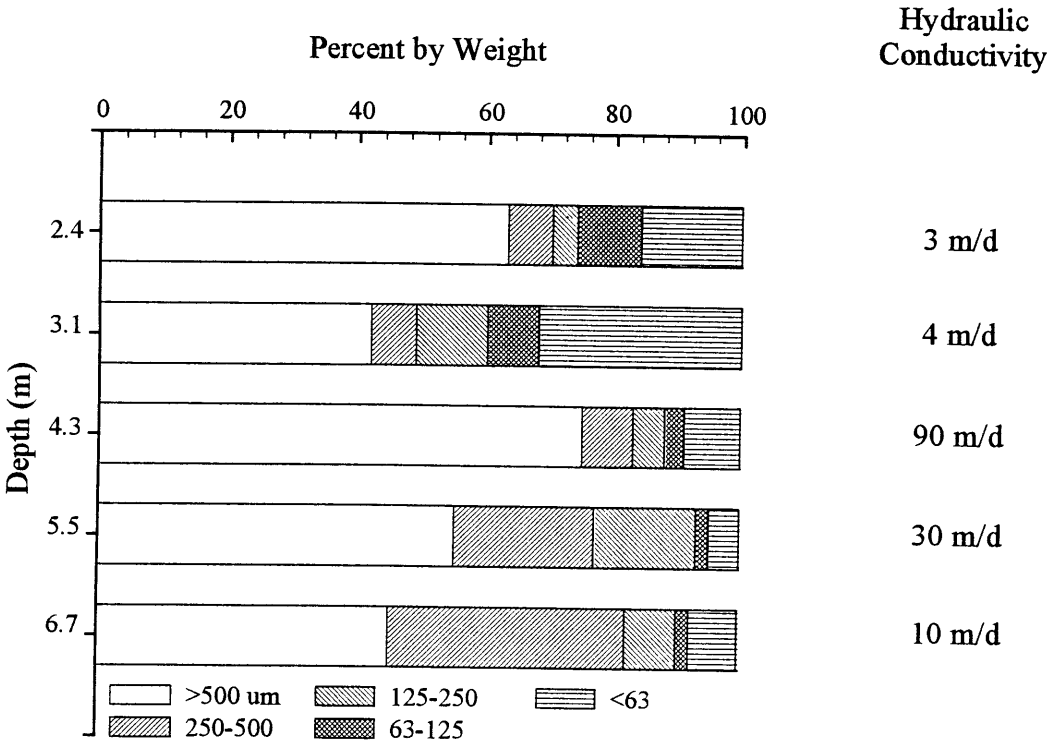

Figure 4.3. Particle size analysis of anthropogenic fill materials from boring B4. Hydraulic conductivities were estimated from the cumulative particle size distributions according to the relationship developed by Bedinger, 1961. The water table was at a depth of 2.4 m at the time of this core sampling.

conductivities were estimated from cumulative size distributions using the relationship developed by Bedinger (1961).

Hydraulic conductivity values calculated from particle size analysis support the conceptual picture that the bulk of groundwater flow occurs near the bottom of the water-bearing unit (Figure 4.3). Values range from 3 m/d at the water table to one order of magnitude greater at depth in the water-bearing unit. This highly conductive material was a mixture of gravel and slag. The estimated K_h values suggest that this mixture behaves as a coarse sand (Bouwer, 1978). Assuming predominantly horizontal flow, the arithmetic average hydraulic conductivity is 30 m/d at this point location.

The transmissivity (and hence hydraulic conductivity) of the anthropogenic fill solids was also determined over a greater zone of influence with analysis of tidal-induced fluctuations in groundwater heads. The river adjacent to Site YYZ is tidally influenced and is in hydraulic communication with the anthropogenic water-bearing unit. The properties of the groundwater aquifer attenuate the amplitude and introduce a time lag into the head fluctuations relative to the tidal cycling (Erskine, 1991):

$$h = h_0 \exp\left(-x\sqrt{\frac{\pi S}{t_0 T}}\right)\sin\left(\frac{2\pi t}{t_0} - x\sqrt{\frac{\pi S}{t_0 T}}\right) \qquad (2)$$

where h (m) is the groundwater head relative to the mean sea level; h_0 (m) is the amplitude of the tidal oscillation; S is the aquifer storage; T (m^2/d) is the aquifer transmissivity; t_0 (d) is the period of the tidal oscillation; x (m) is the distance from the shoreline, and t (d) is the time. Aquifer parameters can be calculated from measures of the time lag as a function of the distance from the shoreline:

$$Time\ lag = x\sqrt{\frac{t_0 S}{4\pi T}} \qquad (3)$$

or from measures of the amplitude attenuation as a function of distance:

$$\textit{Tidal efficiency factor} = \exp\left(-x\sqrt{\frac{\pi S}{t_0 T}}\right). \quad (4)$$

In 1987 tidal fluctuations were monitored in the river and in well points (W-2, W-12, W-7, W-8) for 75 hours (Figure 4.4). Fill solid transmissivity was calculated from both the average amplitude attenuations, and the average time lags (EA Engineering Science and Technology, 1987) observed over this time period at these well points for a tidal period of 0.5 d (Figure 4.5). A storativity value of 0.03, representative of the fill at the depth of the well points (EA Engineering Science and Technology, 1993), was used in the calculation. The transmissivity was calculated to be 310 m^2/d by equating the slope of the time lag plot *v.* distance with Eq. 3. The slope of a log-linear plot of amplitude ratio *v.* distance (Eq. 4) gave a transmissivity of 390 m^2/d for this fill material. With an average saturated zone thickness of 3 m, the hydraulic conductivity was between 100 and 130 m/d.

The local hydraulic conductivity (30 m/d) was is excellent agreement with the tidal analysis value (100 m/d) that was averaged over the study region. This suggests that in the study region, the hydraulic properties of these fill solids do not vary on the scale of 10s of centimeters (core) to 10s of meters (tidal analysis). If the fill solids were significantly fractured or exhibited preferential flow through channels, the tidal analysis would have yielded hydraulic conductivities several orders of magnitude greater than from the particle size analysis (Ford and Williams, 1989).

Groundwater Velocity

The ambient groundwater gradient was estimated from recovery well head measurements made while R2 was not pumping (Figure 4.1). The recovery wells are full-screened and fully-penetrate the fill material. Thus, heads in these wells reflect flow throughout the depth of the fill and capture the more conductive, deeper zone. Tidal

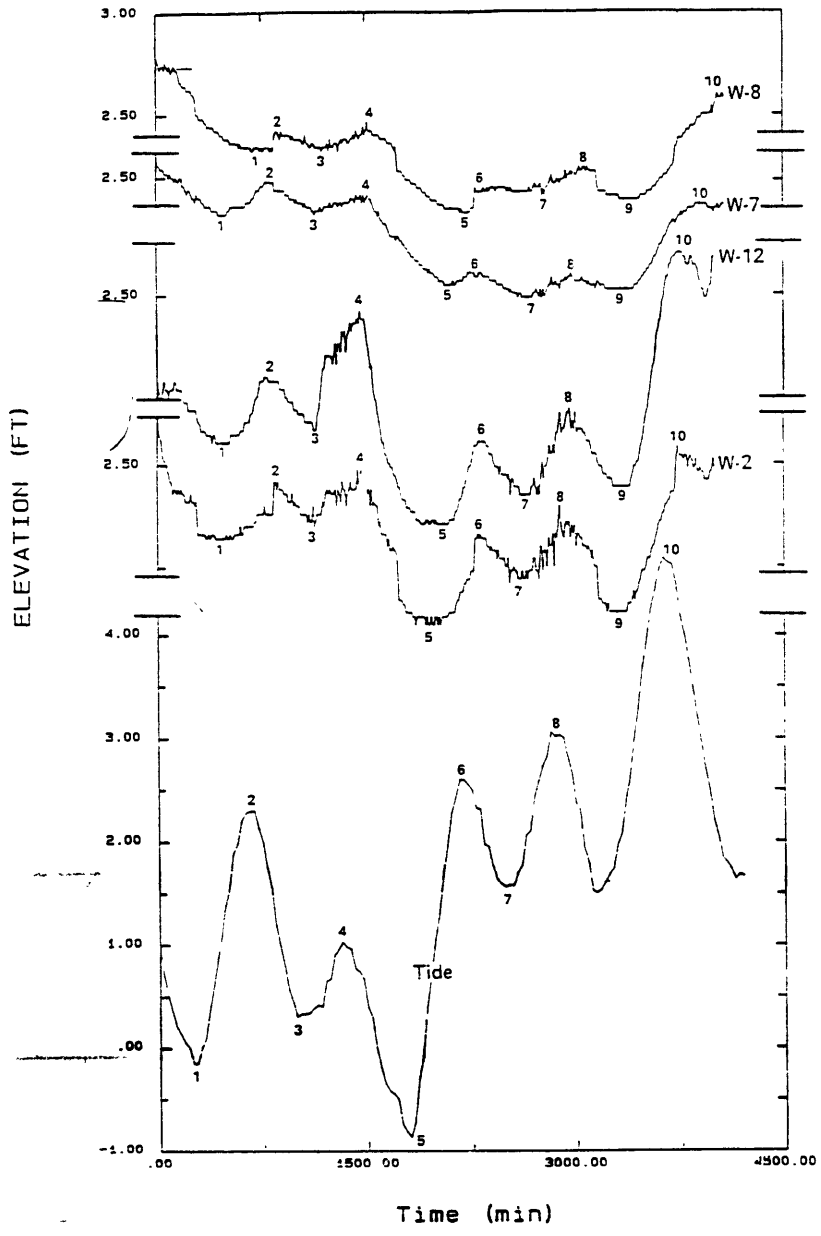

Figure 4.4. Tidal fluctuations in the river and well points (refer locations in Figure 4.1) (EA Engineering Science and Technology, 1987).

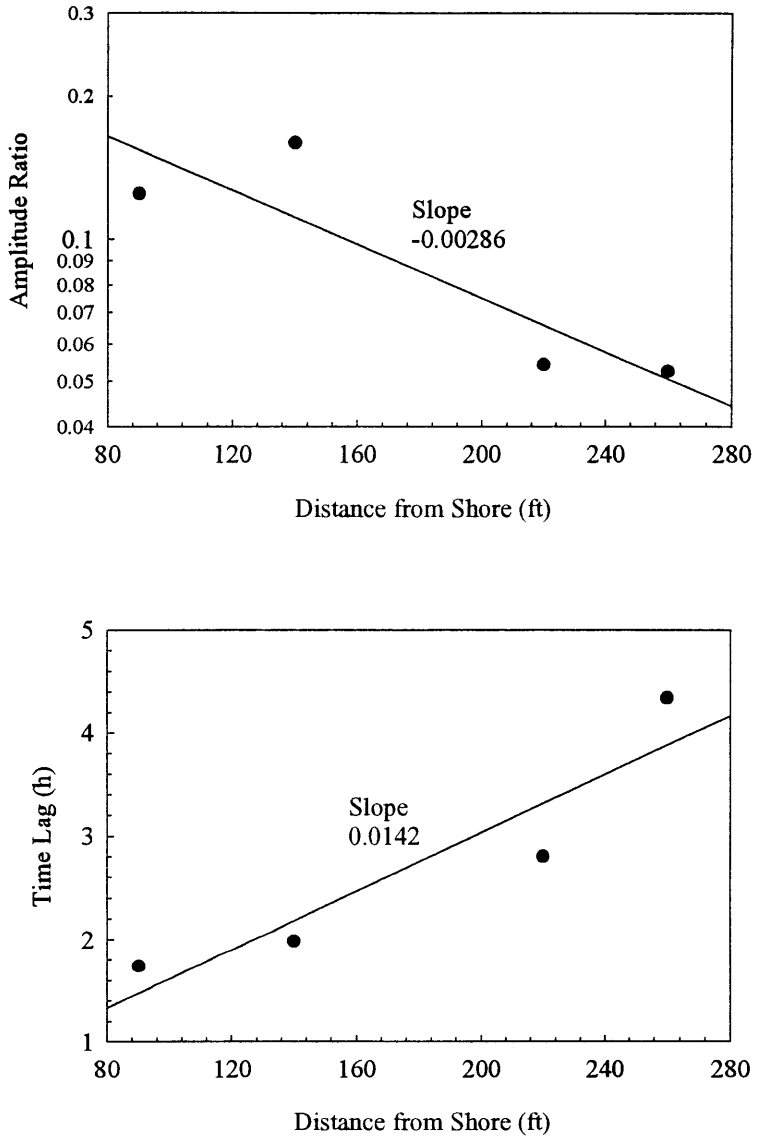

Figure 4.5. Analysis of tidal head fluctuations in the anthropogenic fill at Site YYZ. Well point locations are shown in Figure 4.1. Data from EA Engineering, Science and Technology, 1987.

fluctuations were damped in these wide diameter wells, as compared to shallow well points which showed tidal amplitudes of 0.1 ft at 140 ft from the shore. A plane was fit through the head measurements (SigmaPlot, Jandel Scientific). From this best fit, the head gradient was found to be 0.006 in the WSW (254°) direction.

The gradient in the field study region is consistent with a site wide head gauging conducted in 1987 (EA Engineering Science and Technology Inc, 1993). Groundwater heads decreased from east to west at Site YYZ with the gradient becoming much less steep in the highly transmissive fill material. Heads across the site were slightly higher to the north of the study region. These head variations induce the slight southwesterly direction to the gradient in the study area; but as a whole, groundwater generally discharges to the river to the west.

The tidal fluctuations of the river may increase the residence time of groundwater in the study region by causing flow reversal. Near the end of the monitoring period the absolute height of the river level became greater than the groundwater head in the study region (*i.e.*, step input function) (Figure 4.4). Heads in the near shore wells (W-2, W-12) also increased in absolute value, although to a lesser extent than the river, indicating inflow to this region from the river. Note that heads in wells located east of the 1870 shoreline were greater than the river level, maintaining a net westward flow of groundwater. Thus, the reversed near-shore gradient caused by a rising tidal cycle may slow groundwater efflux from the fill material. The increased absolute head in the river, and hence inflow, to the fill material occurred at the tidal maxima over the 75 h monitoring period. The minima for these cycles were below the heads in the study region. Due to the backflow, a more precise description of the net gradient in the study region should therefore include a head measure of the river level.

The ambient groundwater velocity in the study region was calculated ignoring effects of groundwater reversal due to tidal influences. The location of the MIT monitoring wells far from the river would minimize head variations due to tidal fluctuations, and thus flow reversal of the groundwater would be damped relative to near shore locations. The hydraulic conductivity of the fill material is 30 to 100 m/d, the porosity is assumed to be 0.3 and the head gradient is 0.006. The ambient porewater velocity is thus 0.6 to 2 m/d.

The induced gradient at the MIT monitoring wells was calculated with a conservation of mass equation. R2 was pumped at a rate of 27 L/min from Apr. 12, 1996. Assuming

equal radial flow, this volumetric flowrate was converted to a velocity at distance, r, from the pumping well by dividing by a cylindrical area of height saturated thickness, b, and radius, r:

$$v = \frac{Q}{2\pi r b \theta} \tag{5}$$

At the W20, W40 and W100 well clusters, the induced pore water velocities are 1.2, 0.6 and 0.2 m/d, respectively. The resultant velocity vectors under induced gradient flow are shown in Figure 4.6. The effect of the induced gradient was to increase the magnitude of the groundwater velocity by a factor of 3 times at the W20 cluster, 2 times at the W40 cluster and 1.3 times at the W100 cluster over a pre-pumping ambient velocity 0.6 m/d.

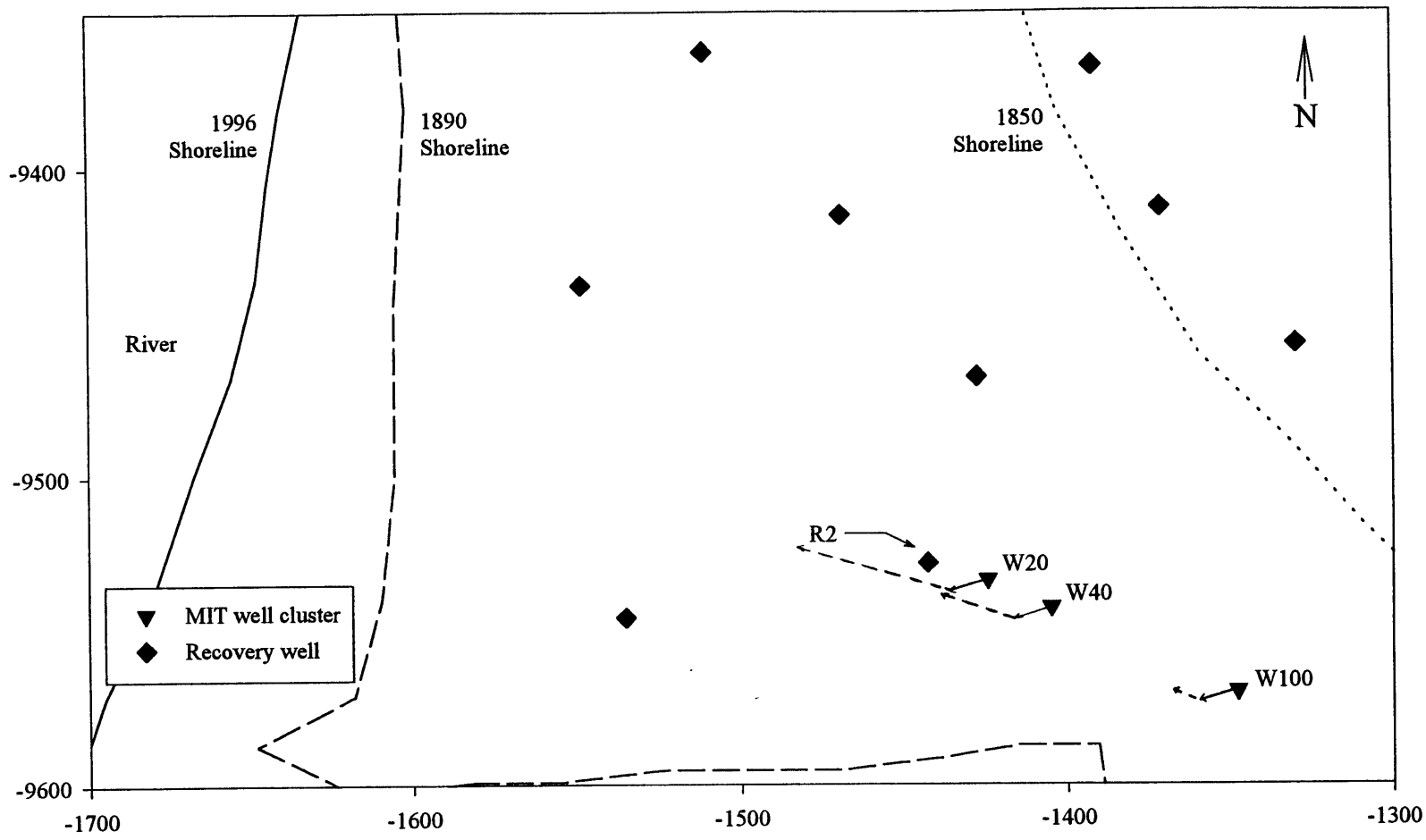

Figure 4.6. Ambient (solid arrows) and induced (dotted arrows) groundwater velocities at the MIT monitoring well clusters.

References

Bedinger, M. S. (1961). *Relation between median grain size and permeability in the Arkansas River Valley, Arkansas*. U.S.G.S. Prof. Paper 424-C, pp. 31-32.

Bouwer, H. (1978). *Groundwater Hydrology*. New York, McGraw-Hill.

EA Engineering Science and Technology (1987). *Investigation and Remedial Alternatives for the Area Near Tanks 10 and 11 and the North Tank Field at the Baltimore Gas and Electric Company Spring Gardens Facility*.

EA Engineering Science and Technology (1993). *Pumping Test Conducted in the Oil Recovery Area During March 1989*.

EA Engineering Science and Technology Inc (1993). *Site Characterization Report for the BG&E Spring Gardens Facility*.

Erskine, A. D. (1991). "The effect of tidal fluctuation on a coastal aquifer in the UK." *Ground Water* **29**: 556-562.

Fetter, C. W. (1994). *Hydrogeology*. Englewood Cliffs, NJ, Prentice Hall.

Ford, D. C.; Williams, P. W. (1989). *Karst Geomorphology and Hydrology*. Boston, Unwin Hyman.

Sen, Z. (1995). *Applied Hydrology for Scientists and Engineers*. Boca Raton, CRC Press.

Thompson, K. D. (1994). *The Stochastic Characterization of Glacial Aquifers Using Geologic Information*. PhD Thesis, Massachusetts Institute of Technology.

Chapter 5.

SORPTION OF HYDROPHOBIC COMPOUNDS TO FILL SOLIDS

Abstract

Industrial sites with water-bearing units composed of anthropogenic fill can contain a variety of organic-carbon containing materials, in addition to natural organic matter. Fill materials from a former manufactured gas plant site contained natural solids, box waste (containing wood), wood fibres, and nonaqueous phase liquids. The total carbon content of the fill solids (5 to 55% by weight) were several orders of magnitude greater than observed for natural aquifer materials (less than 0.1% by weight). Solid-water partition coefficients (K_d) for tar-containing natural solids and box waste and for coke were not accurately predicted by total carbon measurements (f_{oc}) and natural organic matter carbon-normalized partition coefficients (K_{oc}). K_d (= $f_{oc}K_{oc}$) values differed by factors of 2 to several orders of magnitude from measured values. The overall partition coefficient for a mixture of organic-carbon containing sorbents must be calculated from the sum of the individual component sorption:

$$K_d^{TOT} = \sum_{i=1}^{n} f_i K_i$$

where *i* denotes the individual sorbent phases, f_i is the mass fraction, and K_i is the sorbent-specific partition coefficient. Partition coefficients (K_d^{TOT}) which accounted for the fraction of individual sorbent components and component-specific partition coefficients were in good agreement with measured values for tar-containing natural solids and box waste, but not coke wastes. Coke sorption was an adsorptive process and was underestimated by use of activated carbon as a model sorbent due to coke surface saturation by the sorbate. The gross compositions of sorbent mixtures were quantified with elemental mass balance equations.

Introduction

The groundwater transport of organic contaminants is governed by the tendency for a compound to associate with the aquifer solids or to remain dissolved in the groundwater. The solid-water partition coefficients for aquifer solids (Schwarzenbach and Westall, 1981), and other environmental particles such as soils and sediments (Karickhoff *et al.*, 1979), have been correlated with the fraction of organic carbon in these sorbents. Research has since been directed towards developing linear free energy relationships relating the organic carbon-normalized partition coefficients of these environmental solids to physical-chemical properties of the sorbates (*e.g.*, octanol-water partition coefficient (Karickhoff *et al.*, 1979), solubility (Schwarzenbach *et al.*, 1993)). Subsequently, partition coefficients at other sites of study could be estimated with a measurement of the carbon content of the aquifer solids and a sorbate-specific carbon-normalized partition coefficient calculated from a linear free energy relationship:

$$K_d = f_{oc} K_{oc} \tag{1}$$

where K_d (mL/g) is the partition coefficient, f_{oc} (g_{oc}/g_s) is the fraction organic carbon, and K_{oc} (mL/g_{oc}) is the carbon-normalized partition coefficient. This approach for estimating K_d values is supported by research in which little variability among carefully measured soil and sediment K_{oc} values was observed for samples obtained from regions throughout the world (Kile *et al.*, 1995). The accuracy of partition coefficient estimates made with Eq. 1 is dependent upon how well the linear free energy relationship used to calculate K_{oc} represents the true organic carbon partition coefficient.

The broad applicability of Eq. 1 to predict partition coefficients at industrial sites may be limited by the composition of anthropogenic fill solids at these sites. The partition coefficients used to develop Eq. 1 and subsequent linear free energy relationships were measured in systems in which the partitioning media were natural organic macromolecules, or humic substances. Anthropogenic fill may be composed of other organic carbon-containing media, such as wood or nonaqueous phase liquids, for which a sorbate's tendency to partition from the aqueous phase differs from natural organic matter. Partition coefficients for these

solids may still be predicted with an approach similar to Eq. 1, but with modified definitions of the correlating sorbent parameter (*i.e*, f_{oc}) or the linear free energy relationship.

There is evidence in the literature that some organic carbon-containing sorbents other than natural organic matter require modified forms of Eq. 1 to predict sorbate partition coefficients. For example, wood is a sorbent for which the fraction organic carbon must be scaled to account for nonsorbing polymeric components (Severtson and Banerjee, 1996). The wood partition coefficient does not correlate with the total carbon content which is relatively constant among wood species, but it does correlate with the lignin content, and hence the fraction of total carbon which composes lignin. Other sorbents exhibit carbon-normalized partition coefficients that are greater than those calculated with natural organic matter free energy relationships. One example is coal for which K_{oc} values are 1 to 1.5 orders of magnitude greater than for natural organic matter-containing soils and sands (Grathwohl, 1990).

Anthropogenic fill solids at industrial sites may contain mixtures of many different organic carbon-containing materials. In these cases, the bulk partition coefficient would be the sum of the individual partition coefficients for each of the discrete sorbents:

$$K_d = \sum_{i=1}^{n} f_{oc}^{i} K_{oc}^{i} \qquad (2)$$

where *i* denotes each sorbent type. The summed contribution of individual sorbents was required to estimate the partition coefficient for soil contaminated with transformer oil (Boyd and Sun, 1990) in which the discrete sorbents were natural soil organic matter and oil. In a second example, polycyclic aromatic hydrocarbon partitioning in marine sediments was predicted by accounting for organic matter and soot components in the solid phase (Gustafsson *et al.*, 1997).

Scope of investigation

The study presented in this chapter had two objectives. The first was to characterize the variety of organic carbon-containing materials found in a typical anthropogenic fill. Solids were collected from a water-bearing unit composed of anthropogenic fill at a former

manufactured gas plant (Site YYZ, Chapter 2). The source of the fill material was gas production wastes and rubble from a local fire.

The second objective of this research was to determine the extent to which partition coefficients for this anthropogenic fill could be estimated from Eq. 1 (*i.e.*, bulk carbon measurement and calculated organic matter K_{oc}) or Eq. 2 (*i.e.* quantification of individual sorbents with sorbent-specific partition coefficients). Naphthalene or pyrene sorption isotherms were measured for samples of anthropogenic fill that formed lenses of discrete sorbent types. The measured partition coefficients were compared to estimated values calculated with Eq. 1 and Eq. 2. As part of this study, multi-element analysis was investigated as a method to quantify the relative proportions of various sorbents in a bulk mixture.

Methods

Chemicals

Naphthalene (J.T. Baker, Phillipsburg, NJ) and pyrene (Aldrich, Milwaukee, WI) were used as received. Solutions were made up in reverse osmosis (RO) water (Ionics, Bridgewater, PA). Methanol and methylene chloride solvents were 'Ultra-resi Analyzed' (J.T. Baker). Pentane (J.T. Baker) and acetone (OmniSolv, EM Science, Gibbstown, NJ) were also used. Mercuric chloride was from Fluka Chemie (Switzerland) and acetanalide was from Perkin Elmer (Norwalk, CT).

Solids Collection

Anthropogenic fill material was obtained from a water-bearing unit at Site YYZ, a former manufactured gas plant site. The water-bearing unit was constructed by filling a water body over a period of decades with waste materials from the gas operations (Chapter 1). Continuous cores were obtained by hollow stem auger and split spoon sampling (Chapter 2, boring B4, Figure 2.1). Undisturbed samples were collected ahead of an auger drilled to depth with a 0.6 m, 7.5 cm diameter split spoon. Core solids were collected in acrylic liners which were promptly capped and subsequently stored at 4°C. To avoid contamination of core samples, no drilling fluids were used.

Solids Characterization

Anthropogenic fill solids in the acrylic cores were first visually characterized, noting the materials that formed distinct lenses of 10 to 15 cm thickness. The total carbon content and the nonaqueous phase liquid content of the solids were quantified as a function of depth.

Fraction Organic Carbon

Bulk subsamples from 0.6 m intervals of the B4 core were dried, ground and analyzed for carbon content by high temperature combustion (CHN 2400, Perkin Elmer, Norwalk, CT). Carbon contents of isolated core materials (*e.g.*, wood chips, coke) were also analyzed.

Nonaqueous Phase Liquids

The amount of nonaqueous phase liquids in the fill solids was quantified by short-exposure solvent extraction. Subsamples from 0.6 m intervals of the boring were extracted with 1:1 pentane/acetone (v/v) in centrifuge tubes for 10 min. These short contact times were used to remove entrapped nonaqueous phase liquids, but to minimize the removal of sorbed constituents. The solid and solvent phases were separated by centrifugation at 840 *g* for 15 min. The total nonaqueous phase liquid content of the solids was estimated by two methods (1) drying aliquots of the pentane extract to constant weight and (2) integrating the total hydrocarbon content of the pentane extract gas chromatogram (described below).

Polycyclic Aromatic Hydrocarbons

Polycyclic aromatic hydrocarbon concentrations in the fill solids were quantified by gas chromatographic analysis (Carlo Erba Fractovap) of the pentane extracts. Cold on-column injections were made to a 30 m, 0.25 μm film thickness DB5 capillary column (J&W Scientific, Folsom, CA). The temperature program began at 70°C and increased at 6°C/min to 300°C. The flame ionization detector base was held at 300°C. Compound concentrations were quantified with external standards. A subsample of the capillary zone oil, obtained from free phase on the top of the 3 - 3.7 m core section, was diluted in hexane and analyzed with this temperature program.

Sorption Isotherms

Sorbents

Anthropogenic solids were removed from the cores in which they formed 'lenses' of 10 to 15 cm thickness. Samples were removed from the center of the core. The solids

contacting the core liner were discarded to minimize sorption artifacts in the event that oil in the bore hole had coated the inside of core liners retrieved from depths below the water table. The solids of study were: (a) natural estuarine sediments; (b) box waste, and (c) coke. The natural solids were isolated from the deepest core which had penetrated the sediments of the former water body. These solids were primarily quartz with some residual coal tar streaking observed in these solids.

The box wastes isolated from the site had been impregnated with tar. Box waste was used to remove tar and impurities, such as hydrogen cyanide and hydrogen sulphide, from the production gases. The isolated box waste had a strong coal tar odor and consisted of wood chips with discontinuous mineral coatings. The mineral coatings had an orange-brown color suggesting that they may have been iron oxides; however the composition of the mineral component was not characterized.

The coke was a product of gas generation: the solid residue remaining after liberating gases from heated coal. Large (5-7 cm) diameter porous chunks of coke were removed from the core and crushed to facilitate isotherm measurements. The crushed coke was wet-sieved multiple times to remove fines and the 710-1000 μm fraction used for isotherms.

Analysis

Fluorescence

Naphthalene and pyrene fluorescence measurements were made with a Perkin Elmer LS50B Luminescence Spectrophotometer using quartz cuvettes. The excitation and emission wavelengths were 268 nm and 322 nm, respectively, for naphthalene and 313 nm and 373 nm, respectively, for pyrene. Excitation and emission slits were set to 5 nm. Self-absorbance was corrected by the method of Gauthier *et al.* (1986) using absorbance measurements made with a Beckman DU640 Spectrophotometer. Turbidity interferences were checked with absorbance measurements at 600 nm.

Gas Chromatography

Direct aqueous injections to a Carlo Erba HRGC 5160 gas chromatograph were used to quantify naphthalene concentrations for the tar-impregnated box waste due to large amounts of background interference from fluorescing compounds. Cold on-column injections were made to a 19 m RTX-5 (Restek, Bellefonte, PA) capillary column with 5 μm film thickness

and 0.32 mm inner diameter. The carrier gas was hydrogen with a flowrate of 3 mL/min. The GC was temperature programmed from 100°C to 250°C at 10°C/min. Compounds were detected with a flame ionization detector with a base temperature of 250°C. Methanol extracts were analyzed under these operating conditions, except the temperature program began at 65°C. Compound concentrations were quantified with external standards.

Tar Content

The tar contents of the natural solids and the tar-impregnated box waste were determined following the method of Boyd and Sun (1990). The solids were Soxhlet-extracted for 24 h with 5% methanol in methylene chloride. The extract was evaporated to dryness to determine the mass of residue removed from the solids. An aliquot of this residue was analyzed for carbon content.

Elemental Analysis

Elemental analysis for carbon, hydrogen and nitrogen were determined with a Perkin Elmer 2400 CHN Elemental Analyzer by oxidation at 1300°C. Samples were dried and ground to a fine powder before analysis. Acetanilide, individual sorbents (natural solids, wood, coke) plus known mixtures of these sorbents were analyzed for CHNO by Galbraith Laboratories (Knoxville, TN).

Surface Area

Surface area measurements were made by Porous Materials Inc. (Ithaca, NY) using multi-point krypton BET isotherms.

Experimental

A fluorescence method was used to determine sorption isotherms for (a) naphthalene to natural solids and extracted box waste and (b) pyrene to coke. Moist natural solids were added to equilibration vessels to minimize sorption artifacts due to drying. Moisture contents were determined by drying sample aliquots at 105°C for 24 h after determining isotherm measurements. The vials were filled with reverse osmosis water and contained no headspace. Biodegradation was prevented with 10 μg/mL mercuric chloride. For each isotherm point, two duplicates and a positive control, containing no solids, were spiked with naphthalene from a methanol stock solution, or pyrene from a 10% methylene chloride in methanol stock solution. The maximum amount of organic solvent added to the vials was less than 0.7% of

the water volume. Negative controls, containing solids but no sorbate, were used to account for background fluorescence leached from the solids in the course of the equilibration. In addition, several replicate vials and controls were set up at the middle concentration to monitor fluorescence with time and determine when sorption equilibrium was attained. When supernatant fluorescence of the sorbent-containing vial was no longer decreasing, the isotherm vials were centrifuged at 840 *g* for 30 minutes to separate the phases. Fluorescence of the supernatant was measured.

A single point isotherm was determined for native naphthalene in the tar-containing box waste. Five replicates and two positive controls were set up. Supernatant concentrations were monitored over 15 d by direct aqueous injection (1 μL) gas chromatography. When supernatant concentrations were no longer increasing tubes were centrifuged at 840 *g* for 30 min and analyzed.

Solid-to-water ratios were chosen to have about 50% mass sorbed at equilibrium based on preliminary isotherm points. Solid-to-water ratios and equilibration times are summarized in Table 5.1. Amber vials with teflon-lined solid screw caps (Supelco, Bellefonte, PA) were used for extracted box waste and coke (15 mL) and natural solids (8 mL). Centrifuge tubes (55 mL, Pyrex) with foil-lines solid caps containing teflon liners were used for tar-containing box waste. All equilibration flasks were foil-wrapped or stored in boxes to minimize photodegradation of sorbates.

Mass Balance

Mass balances were performed for several samples. The supernatant was removed and the solids were extracted with 5 mL methanol. Methanol extracts were quantified by GC and FID. Mass recoveries of naphthalene ranged from 50 (extracted box waste) to greater than 80% (natural solids and box waste).

Equations

Sorption isotherms were determined by plotting the solids concentration, C_s, against the aqueous concentration, C_w, at equilibrium. The solids concentration was calculated by

Table 5.1. Experimental conditions for sorption isotherms.

Sorbate-Sorbent Pair	Solid-to-Water Ratio (g/mL)	Equilibration Time (d)
Naphthalene & Natural solids	7.5×10^{-2}	9
Naphthalene & Box Waste	9×10^{-2}	15
Naphthalene & Extracted box waste	2.7×10^{-3}	30
Pyrene & Coke waste	1.2×10^{-3}	54

difference from the positive controls:

$$C_s = \frac{F_{pc}V_{pc} - (F_w V_w - F_{nc}V_{nc})}{\beta M_s} \quad (3)$$

where F denotes a fluorescence measurement, V (mL) the aqueous phase volume, and M (g) the mass. The subscripts *pc*, *nc*, *w*, and *s* refer to the positive control, the negative control, sample aqueous phase and solid phase, respectively. The fluorescence response factor, β (FU·mL/μg), was obtained from standard curves and used to convert to concentration measurements. Isotherms were fit to both the linear sorption equation:

$$C_s = K_d C_w \quad (4)$$

and the Freundlich equation:

$$C_s = K_f C_w^n \quad (5)$$

where K_d (mL/g) is the solid-water partition coefficient, K_f ($\mu g^{1-n} \cdot mL^n/g$) is the Freundlich coefficient, and *n* is the Freundlich exponent. Least squares fits were made to Eq. 4 and the log-transformed Eq. 5 with SigmaPlot (Jandel Scientific). Isotherms were taken to be linear where *n* ($\pm\sigma$) was not significantly different than 1.

The final solids concentration for the coal tar-containing box waste was calculated by difference from the initial solids concentration determined by gas chromatography analysis of the Soxhlet extraction:

$$C_s = C_i - \frac{V_w C_w}{M_s} \quad (6)$$

where C_i (μg/g) is the initial solids concentration solids concentration. A partition coefficient for the tar-containing solids was calculated directly with Eq. 4 for this single-point isotherm measurement.

Results and Discussion

Characterization of Anthropogenic Fill Solids

The most striking characteristic of the anthropogenic fill material at Site YYZ was the high carbon contents of these solids (Figure 5.1). Typical values in natural sand aquifers are less than 1% (Holmen and Gschwend, 1997; Ball *et al.*, 1990). The high carbon values at this site resulted from the inclusion of wood chips (50% carbon by weight) and coke wastes (80-95% carbon by weight) in the fill. Various carbon-containing solids were distributed through the core as follows: (1) wood chips at 1.2, 3, and 5.2 m; (2) coke at 2.4 and 3.6 m; (3) oil at 2.4, 3, and 3.6 m, and (4) coal tar at 4.2 m. Below 5.5 m the natural sands underlying the historic river silt were encountered. The carbon contents of these sands were low (0.001) and within the range of other natural aquifer solids.

The abundance of nonaqueous phase liquids (NAPLs) in the fill material decreased with depth from a maxima near the water table as determined by the residue on evaporation of pentane/acetone extracts (Figure 5.1). The high value at the water table coincided with the occurrence of fuel oil in the capillary fringe at Site YYZ (Chapter 2), thus high residues on evaporation would be expected at this depth. In fact, 40 mg/g of oil would correspond to about 40% of the soil porosity, sufficient to be detected as free product in a monitoring well (Mercer and Cohen, 1990). Oil was observed in shallow, water table monitoring wells within the study region at Site YYZ.

Nonaqueous phase liquids were also quantified as total petroleum hydrocarbons. Total petroleum hydrocarbons have been used as surrogate measures of NAPL concentration at sites with fuel contamination (Huntley *et al.*, 1994; Durnford *et al.*, 1991). The hydrocarbon masses in Site YYZ fill solids were calculated by integrating the total area under the gas chromatograms of the pentane extracts. Total petroleum hydrocarbon measures of the NAPL content of these solids were less than the residue after evaporation of the pentane extracts, except at depths of 4.9 and 5.5 m (Figure 5.1). The quantity of total hydrocarbons measured with this method is biased towards those compounds that can be resolved with the chromatographic method. For example, only one third of the total compound mass of coal tar liquid isolated from well W40M (refer Figure 2.1, Chapter 2) could be chromatographed

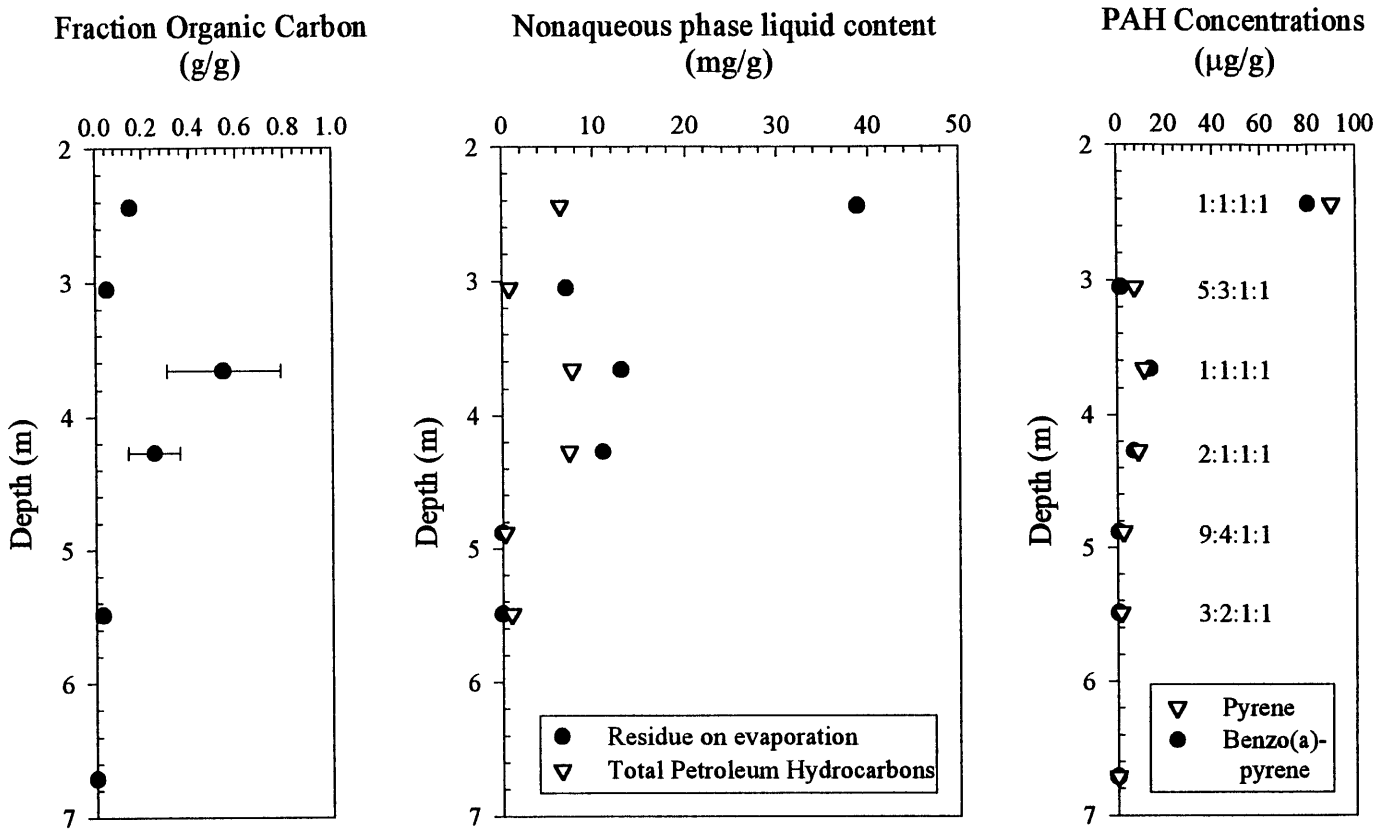

Figure 5.1. Depth profiles of organic carbon, nonaqueous phase liquids and aromatic hydrocarbons in the B4 boring, 1993. Note the change in units of measure between profiles. Organic carbon values are averages of triplicate measurements, with error bars denoting the deviation in measurements. Relative ratios of PAH concentrations (phenanthrene:pyrene:benz(a)anthracene:benzo(a)pyrene) are noted with the solid phase PAH concentrations. The water table depth was 2.4 m at the time of boring.

under our analysis conditions, while all of the mass of isolated oil could be chromatographed. If the pentane/acetone extracts removed a coal tar NAPL from the solids, the mass of total hydrocarbons per gram of solids would be less than the residue on evaporation. The total petroleum hydrocarbons as a function of depth in the fill solids did not appear to constitute a constant fraction of the extract residue. Total hydrocarbon concentrations do not show the same sharp decline in concentration from the water table as extract residues; however, both the pentane extract residues and the total petroleum hydrocarbons were lowest at depths just above the natural sediments.

For denser than water nonvolatile nonaqueous phase liquids like coal tar, the residue on evaporation of a solvent extract will give a better estimate of the total mass of nonaqueous phase liquids in a solid sample than a total petroleum hydrocarbon measure. Some of the volatile compound mass will be lost during the evaporation procedure. This mass will likely introduce less error to the final measurement of NAPL content than the unknown fraction of the NAPL mass that can not be quantified by a chromatographic method. About 10% of the mass of the W40M coal tar was composed of compounds more volatile than dimethylnaphthalenes, while two thirds of the mass could not be chromatographed. Better measures of the nonaqueous phase liquids could also be attained with a more nonpolar solvent than used here. Acetone was added to the pentane to promote disaggregation of the fill solids so that entrapped NAPL droplets could dissolve into the solvent. The solubility of isolated coal tar and oil in this solvent mixture was not measured, but tar and oil were soluble in methylene chloride. Thus, methylene chloride extracts were used to quantify the nonaqueous phase liquid contents of solids used for sorption isotherm measurements.

The composition of the nonaqueous phase liquids (NAPLs) in the fill solids was further investigated by comparison of the chromatographic "fingerprints" of the pentane extracts with NAPLs (oil and coal tar) isolated from Site YYZ. The oil and tar each had distinctive chromatographic signatures (*e.g.*, unresolved compounds, ratios of polycyclic aromatic hydrocarbons). The chromatograph of the isolated oil was 75% by weight unresolved complex mixture (UCM), from which polycyclic aromatic hydrocarbon (PAH) compounds could not be resolved. In contrast, the tar chromatograph had distinct PAH compound peaks with little unresolved complex mixture (< 7% by weight) and were the

primary source of PAHs in the extracts. For comparison the total mass of compounds with a molecular weight of 252 (*e.g.*, benzo(a)pyrene) was 11 400 mg/L_{tar} for tar and only 700 mg/L_{oil} in the oil. At all depths in the fill solids, distinct chromatographic peaks of polycyclic aromatic hydrocarbons were observed, suggesting that coal tar was distributed throughout the depth of the anthropogenic fill at Site YYZ. The concentrations of pyrene and benzo(a)pyrene mirrored the profile of the nonaqueous phase liquid content determined by pentane/acetone extract residues (Figure 5.1). The ratios of individual PAH compounds (phenanthrene-to-pyrene-to-benz(a)anthracene-to-benzo(a)pyrene) in the W40M tar were 5:2:1:1 (Tar Analysis, Chapter 2). The ratios of individual PAH concentrations (phenanthrene:pyrene:benz(a)anthracene:benzo(a)pyrene) at 2.4, 3.7 and 4.3 m depths differed from the isolated coal tar suggesting that some weathering of the residual tar had occurred (*e.g.*, removal of phenanthrene relative to benzo(a)pyrene).

Sorption Isotherms

The high carbon contents of the fill solids and the prevalence of organic carbon in sorbents other than natural organic matter prompted an interest in characterizing the solid-water partition coefficients of anthropogenic fill materials at Site YYZ. By comparison of the total carbon content alone, Eq. 1 suggests that partition coefficients in this water-bearing unit could be orders of magnitude different than for natural aquifers, overlooking the fact that sorbent-specific K_{oc} values may differ from natural organic matter carbon partition coefficients. Sorption isotherms were measured for isolated natural solids, box waste, and coke, as well as for solvent-extracted box waste. The experimental results were compared to estimates of solid-water partition coefficients accounting for the nature of the organic carbon-containing sorbents. The inadequacy of using the total carbon content of the solids and a natural organic matter-derived K_{oc} (Eq. 1) was also demonstrated. Partition coefficients calculated with this approach (Eq. 1) are subsequently referred to as traditional partition coefficients (K_{trad}) because, until recently, no distinction has been made natural organic carbon and other carbon-containing sorbents present in the solid phase. These experimental results and calculations are summarized in Table 5.2 and are discussed more thoroughly in the following sections.

Table 5.2. Summary of observed and estimated partition coefficients for anthropogenic fill materials.

Sorbate-Sorbent Pair	Method of Calculation	Sorbate-Specific Partition Coefficient (mL/g)	Sorbent Mass Fraction (g/g)	Estimated K_d (mL/g)	Meas'd K_d (mL/g)
Naphthalene & Natural solids	Sorbent specific	$K_{oc} = 10^{2.93}$ $K_{tw} = 10^{3.7}$	f_{oc}= 0.0071 f_{tar}= 0.0011	6 ± 5.5 11.5	10
	Traditional	$K_{oc} = 10^{2.93}$	f_{oc}= 0.0078	6.6	
Naphthalene & Box waste	Sorbent specific	$K_{tar} = 10^{3.7}$ $K_{lignin}=10^{2.76}$	f_{tar} = 0.34 f_{lignin}=0.033	20 ± 2700 2720	2400
	Traditional	$K_{oc} = 10^{2.93}$	f_{oc} = 0.24	200	
Naphthalene & Extracted box waste	Sorbent specific	$K_{lignin}=10^{2.76}$	f_{lignin}=0.033	20	300‡ for C_w= 1 µg/mL
	Traditional	$K_{oc} = 10^{2.93}$	f_{oc} = 0.11	90	
Naphthalene & Coke waste†	Sorbent specific	$K_{GAC}=10^{2.44}$ (mL/m^2)	f_{COKE}= 0.46 (m^2/g)	130	0‡ for C_w= 1 µg/mL
	Traditional	$K_{oc} = 10^{2.93}$	f_{oc} = 0.8	6800	
Pyrene & Coke waste†	Sorbent specific	$K_{GAC}=10^{3.2}$ (mL/m^2)	f_{COKE}= 0.46 (m^2/g)	740‡ for C_w= 0.1 µg/mL	5900‡ for C_w= 0.1 µg/mL
	Traditional	$K_{oc} =10^{4.76}$	f_{oc} = 0.8	46 000	

† GAC - granular activated carbon. See Coke Wastes text for description of calculation.

‡ Single point values of K_d for these nonlinear isotherms were calculated at the specified concentrations for comparison with linear K_d values.

Natural Solids

A naphthalene sorption isotherm was measured for a bulk sample of natural solids from Site YYZ. A bulk sample refers to the inclusion of coal tar (as evidenced by tar streaking in the solids) as a sorbent medium, in addition to natural organic matter. The naphthalene sorption isotherm for these solids appeared linear (Figure 5.2). The Freundlich fit of the log-transformed data had an exponent of $n = 2$; however, the quality of a nonlinear fit was not sufficiently better than a linear to justify the use of a more complex sorption isotherm. The partition coefficient for natural solids was the slope of the linear regression and had a value of 10 ± 1 mL/g for naphthalene.

The measured partition coefficient for natural solids was compared to the predicted sorption of naphthalene. The total partition coefficient for these solids was hypothesized to be the sum of the contributions of the natural organic matter and the residual tar:

$$K_d^{NS} = f_{oc} K_{oc} + f_{tar} K_{tw} \tag{7}$$

where f_{oc} (g_{oc}/g_s) is the fraction organic matter carbon; K_{oc} (mL/g_{oc}) is the natural organic carbon partition coefficient; f_{tar} (g_{tar}/g_s) is the fraction of tar, and K_{tw} (mL/g_{tar}) is the tar-water partition coefficient. The fraction organic carbon was determined by difference from the carbon content of the bulk solids (0.0078 g_{oc}/g_s) and the carbon removed by Soxhlet extraction (0.63 g_{oc}/g_{res} × 0.0011 g_{res}/g_s) to be 0.0071 g_{oc}/g_s. The original carbon partition coefficient was estimated from a free energy relationship developed for polycyclic aromatic hydrocarbons (Schwarzenbach *et al.*, 1993) with data from Karickhoff (1981). The K_{oc} for naphthalene was 850 mL/g ($K_{ow} = 10^{3.35}$ (Miller *et al.*, 1985)). The fraction tar was assumed to be the residue removed by Soxhlet extraction (0.0011 g_{res}/g_s). Isolated tar from Site YYZ had a measured tar-water partition coefficient of $10^{3.7}$ mL/g_{tar}. Substituting each of these values into Eq. 7 yielded a calculated naphthalene partition coefficient of 12 mL/g for these natural solids. This is in excellent agreement with the observed value of 10 ± 1 mL/g. (The calculated K_d^{NS} could be further tuned by adjusting the fraction of tar in Eq. 7. The carbon content of the Soxhlet extracted residue was 0.63 g_C/g_s. Reported values of tar carbon contents are typically greater than 80% (Electric Power Research Institute, 1993). This suggests that the

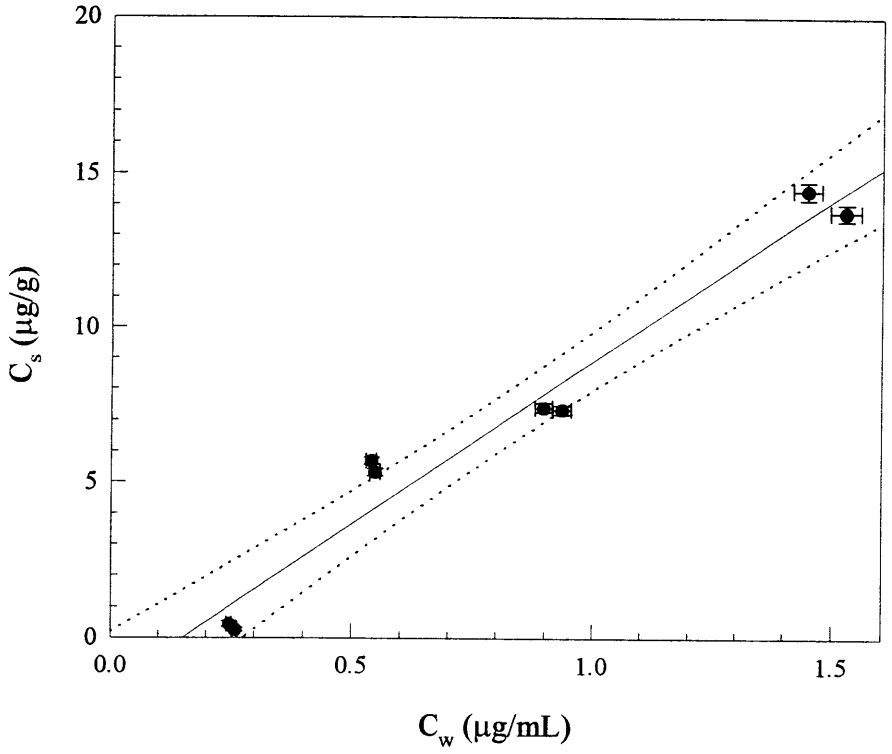

Figure 5.2. Naphthalene sorption to natural solids. Error bars were calculated from propagating analytical uncertainty in Eq. 3, and where not visible, are smaller than the data symbols.

extracted tar may have been 'diluted' by mineral fines retained in the residue. If the tar content of the extracted residue were only 80% (0.63/0.8) of the residue mass, the predicted K_d for these solids would decrease to 10 mL/g.)

The partition coefficient for natural solids was also calculated by ignoring the inclusion of residual tar in these solids. The total carbon content for the natural solids was 0.0078 g_{oc}/g_s and the naphthalene K_{oc} was 850 mL/g. A traditional calculation of the partition coefficient for natural solids gave a solid-water partition coefficient of 6.6 mL/g and underestimated the observed partition coefficient. Partition coefficient estimates have often been considered sufficient if they predict true solid-water partition coefficients to within a factor of 2 (Garbarini and Lion, 1986; Karickhoff *et al.*, 1979). By this criteria, our K_{trad} would be sufficient to predict partitioning to these tar-containing natural solids. However, for solids with greater fractions of residual nonaqueous phases, it becomes increasingly important to account for their contribution to the bulk sorption of hydrophobic compounds. Residual saturations of up to 0.04 g_{res}/g_s have been observed for heavy oils (Hunt *et al.*, 1988) (assuming residual saturation of 20%, porosity of 0.3, solids density of 2.5 g/cm^3, oil density of 1.1 g/cm^3), and partition coefficients for hydrocarbon liquids are almost an order of magnitude greater than organic matter K_{oc} values (*e.g.*, naphthalene hexane-water partition coefficient of 4300 mL/g_{oc} (Schwarzenbach *et al.*, 1993), average naphthalene tar-water partition coefficient of 9900 mL/g_{oc} (Lee *et al.*, 1992)).

Box Waste

The box waste was also a composite sorbent made of wood chips and mineral deposits. The box waste isolated from Site YYZ also contained large amounts of tar, characterized first by a distinctive tar odor, and later quantified by Soxhlet extraction. Only a single-point isotherm was measured for the desorption of native naphthalene. The naphthalene partition coefficient for this tar-impregnated box waste was 2400 mL/g.

A partition coefficient for box waste was predicted assuming naphthalene partitioning from the wood and the tar to the aqueous phase. Organic compound partitioning to mineral phases in aqueous media is unimportant when organic carbon contents exceed 0.001 (g_{oc}/g_s) (Schwarzenbach and Westall, 1981). Mineral partitioning was thus assumed not to contribute

to the overall partition coefficient for box waste. The partitioning of organic sorbates to wood is dominated by lignin partitioning. The naphthalene partition coefficient for tar-coated box waste was calculated with the following equation:

$$K_d^{BW} = f_{tar} K_{tw} + f_{lignin} K_{lignin} \quad (8)$$

where f_{lignin} (g/g_s) is the fraction lignin in the solids and K_{lignin} (mL/g) is the naphthalene lignin-water partition coefficient. The fraction of tar was again assumed to be the Soxhlet-extracted residue, 0.34 g_{res}/g_s, with a K_{tw} of $10^{3.9}$ mL/g_{tar} for naphthalene. The fraction lignin was calculated on a carbon basis since the box waste was not pure wood. The total carbon content of the extracted wood was 0.11 g_{oc}/g_s. Wood is typically 30% lignin by weight (Parham and Gray, 1984) and wood (Wegner *et al.*, 1992) and lignin (Xing *et al.*, 1994; Garbarini and Lion, 1986) are both about 50% carbon by weight. The equivalent f_{lignin} in Eq. 8 was thus 0.033 g_{oc}/g_s. The K_{lignin} value was also calculated on a carbon basis from a lignin-octanol free energy relationship (Chapter 6). K_{lignin} for naphthalene is $10^{2.76}$. The partition coefficient for tar-impregnated box waste was calculated to be 2700 mL/g and is in agreement with the observed value of 2400 mL/g. Sorption to this box waste was dominated by tar-water partitioning of naphthalene: the wood component partition coefficient was estimated to be only 20 mL/g.

An estimate of the box waste partition coefficient by the traditional method underestimated the observed value by a factor of 10. The total carbon content of the box waste was 0.24 g_{oc}/g_s and with a naphthalene K_{oc} of 850 mL/g, the K_{trad} was only 200 mL/g. This box waste was a clear example of a nonaqueous phase-containing sorbent for which the NAPL content must be quantified to correctly estimate sorbate partitioning.

Solvent-Extracted Box Waste

Naphthalene sorption to box waste which had been solvent-extracted to remove the tar component was also quantified. Again, the mineral component was assumed to be an insignificant contributor to the overall sorption of naphthalene by extracted box waste. Thus, the sorption isotherm for extracted box waste was hypothesized to reflect wood sorption. The extracted box waste sorption isotherm for naphthalene was nonlinear with a Freundlich exponent of 0.68 ± 0.02 (Figure 5.3). This nonlinearity may have resulted from an inadvertent experimental artifact. The presumed wood-dominated extracted box waste isotherm was measured before a study of nonpolar organic compound sorption to wood particles was undertaken (Chapter 6). In the wood study the times for water-saturation by wood were found to exceed the times for organic compound sorption. Care was not taken in this investigation to ensure that the extracted box waste was water-saturated before commencing the isotherm experiment. Although there was no difference between the aqueous fluorescence of the sorbent-containing vessels after 9 days and 14 days, this apparent equilibrium may have resulted from naphthalene uptake slowed by the rate of water penetration into the dry sorbent matrix. If water had only penetrated a small portion of the wood tissue, the effective lignin phase would have been smaller than anticipated and the local sorbed naphthalene concentration greater than expected. A Freundlich exponent less than 1 suggests that the sorbed concentration would plateau at high aqueous concentrations. Such a trend has been observed for sorption of stearic acid and phenol to saturated wood particles (Stamm and Millet, 1941). Plateau-like behavior may have been artificially induced if only a small portion of the wood tissue were water-saturated.

The sorptivity of the extracted box waste was greater than calculated, even if the naphthalene isotherm was not at sorptive equilibrium. The calculated wood-dominated partition coefficient for extracted box waste (Eq. 8, omitting the tar term) fell below the observed data points (Figure 5.3). For comparison, the sorbed concentration in equilibrium with a 1 μg/mL aqueous concentration was estimated to be 20 $\mu g/g_s$. The actual sorbed concentration had a minimum value of 300 $\mu g/g_s$, a factor of 15 greater than the calculated

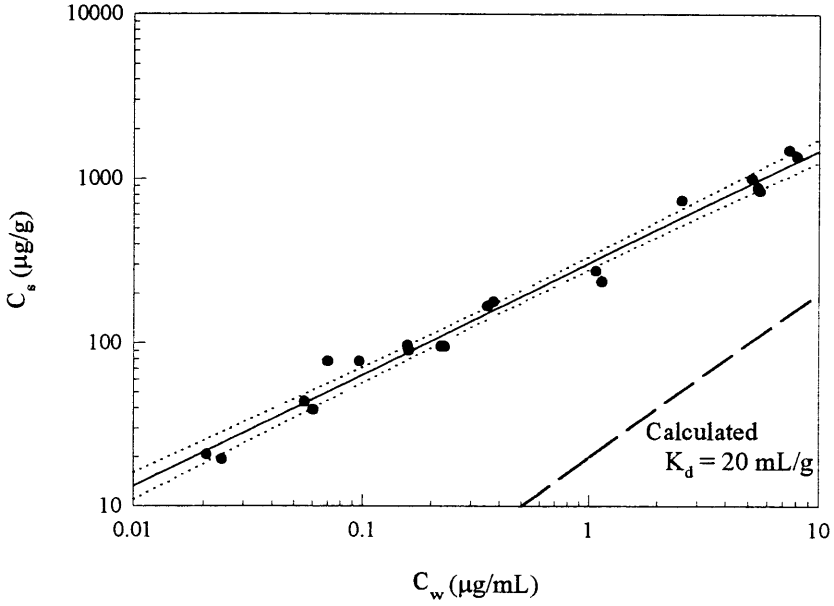

Figure 5.3. Naphthalene sorption to extracted box waste. Error bars were calculated by propagating analytical variability in Eq. 3, and where not visible, error bars are smaller than the data symbols.

value. This difference between the observed and calculated sorbed concentrations suggests that the model assumed for sorptive uptake by extracted box waste was incorrect. Two alternate models are (1) incomplete tar extraction and (2) structural alteration of the wood sorbent during gas purification.

The amount of tar required to increase the sorption of the extracted box waste above the wood-only isotherm was estimated. A single point effective partition coefficient of 300 mL/g was assumed for a naphthalene solids concentration of 300 μg/g and an aqueous concentration of 1 μg/mL. Since both the tar and wood were here assumed to compose the extracted box waste, Eq. 8 was used to estimate the remaining mass of tar. With previous values of K_{tw}, f_{lignin} and K_{lignin}, the fraction of tar needed for an effective partition coefficient of 300 mL/g was estimated to be 3% by weight of the extracted box waste. It is possible that tar which had soaked into the porous wood structure was not effectively removed during the short contact times of the Soxhlet extraction. Compounds take longer to diffuse out of wood particles in nonpolar solvents that do not swell the wood tissue than wood particles in aqueous media (Behr *et al.*, 1953). Surficial tar would be effectively removed from the box waste by Soxhlet extraction, but tar that had penetrated into the wood structure may not have been effectively solubilized during the 10 minute contact times between solvent turnovers. Once exposed to aqueous solution, the extracted box waste may have begun to swell, allowing access of the naphthalene sorbate to internal tar deposits.

The structure of the wood matrix in the purifier boxes may have been altered during the purification process causing changes which increased its sorptivity. The carbon-normalized sorption capacity of wood is increased when it is pyrolyzed and converted to activated carbon (Rael *et al.*, 1995). The temperature (40-50°C) and the relative humidity (65%) for optimal operation of the purifier boxes (Gollmar, 1945) do not favor carbonization of the wood matrix; however, fires were known to occur during the regeneration of the mineral reagents with the infusion of air through the purifier boxes (Gollmar, 1945). Also, the operating conditions of the purifier boxes tended toward acidic pHs from the gas impurities (*e.g.*, H_2S, HCN). Under acidic conditions cellulose can be hydrolysed and thus the lignin content of the wood matrix may be elevated above natural wood species. A lignin content of 0.52 g_{oc}/g_s on a carbon basis would be required to give an effective partition

coefficient of 300 mL/g. This value exceeds the carbon content of the extracted box waste solids, thus enhanced lignin contents of the wood matrix do not explain the high naphthalene sorption to extracted box waste.

Possible alterations to the wood support matrix are secondary to understanding the groundwater transport of contaminants through box waste-rich solids at coal tar sites because transport is likely dominated by tar-water partitioning. The order of gas passage through multiple purifier boxes was rotated as the purification reagents became spent (Gollmar, 1945). Thus, all matrix materials would have filtered tar from the process gas during their placement as the first purification boxes of the sequence. Analysis of a typical box waste reported the solids to be about 1% by weight tar and about 5% by weight organic matter fibres (Environmental Research and Technology Inc and Koppers Company Inc, 1984). At these proportions, the tar would dominate the partitioning between these solids because of its higher tar-water partition coefficients, relative to lignin-water or organic matter-water partition coefficients. At other industrial sites, however, alterations of wood structure by industrial processes or weathering during burial may give differing sorption characteristics than observed for kiln-dried wood.

Coke Wastes

A pyrene sorption isotherm was obtained for coke wastes isolated from Site YYZ fill solids. Naphthalene showed no detectable sorption so a more hydrophobic compound was used. The sorption isotherm for pyrene after 54 days of equilibration was nonlinear with a Freundlich exponent of 1.3 ± 0.2 (Figure 5.4). A Freundlich exponent greater than 1 suggests an increased affinity of pyrene for pyrene sorption at high concentrations, perhaps due to interactions between sorbed molecules at high surface coverages (Parfitt and Rochester, 1983). At the highest isotherm concentration, about 100 μg/g of pyrene was sorbed to the coke. This sorbed concentration corresponded to about 3×10^{17} molecules per gram of coke. The cross-sectional area of a pyrene molecule is 7×10^{-19} m^2 (calculating the molecular radius from the pyrene density of 1.3 g/cm^3 (1989)), and thus the surface coverage of the coke was 0.2 m^2 of pyrene per gram of coke. The specific surface area of coke was measured to be 0.46 m^2/g by krypton sorption. The smaller size of krypton gas molecules may have allowed krypton to penetrate coke micropores that were not accessible to pyrene molecules in aqueous solution, and thus the coke surface may have been near saturation with respect to pyrene coverage.

The sorption of pyrene to coke was estimated from a model of pyrene sorption to activated carbon. The microscopic structure of coke (Pierson, 1993) - randomly oriented crystalline aromatic nuclei - is similar to that of activated carbon (Mattson and Mark, 1971), and thus sorption sites on the coke surface may be similar to those on activated carbon. If the sorption mechanism were the same for these two sorbents, the relative strength of pyrene interaction with these sorbents could then be scaled according to their relative surface areas. A partition model for coke was assumed:

$$\begin{aligned} K_{d_{C_w}} &= f_{COKE} K_{GAC} \\ &= f_{COKE}\left(\frac{K_f}{f_{GAC}} C_w^{n_{GAC}-1}\right) \end{aligned} \tag{9}$$

where f_{COKE} (m^2/g) and f_{GAC} (m^2/g) are the specific surface areas of the coke and granular activated carbon (GAC), respectively; K_f ($\mu g^{1-n} \cdot mL^n/g$) is the Freundlich parameter for GAC;

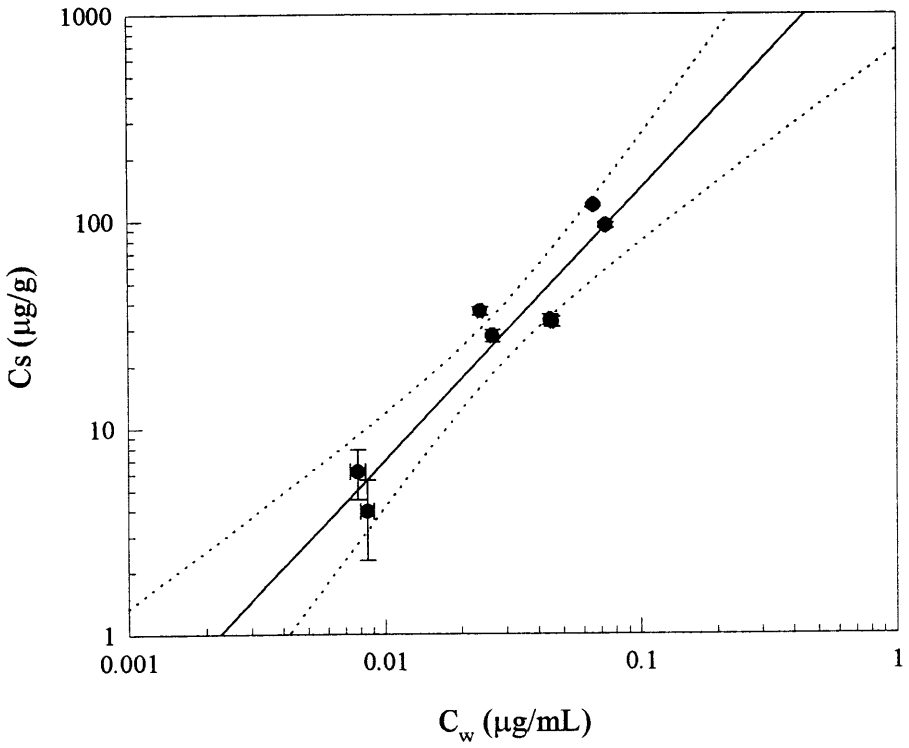

Figure 5.4. Pyrene sorption to coke waste. Error bars were calculated by propagating analytical variability in Eq. 3, and where not visible, are smaller than the data symbols.

n is the Freundlich exponent for GAC, and C_w (μg/mL) is the solution concentration that the partition coefficient is evaluated at. K_{GAC} was estimated to be 1600 mL/m^2 with values from the high concentration pyrene isotherm determined by Walters and Luthy (1984) (f_{GAC} = 1000 m^2/g; K_f = 389 000 μg^{1-n}·mL^n/g; n = 0.389). With the specific surface area of 0.46 m^2/g, and an aqueous concentration of 0.1 μg/mL, the pyrene partition coefficient for coke was calculated to be 740 mL/g. This value is about an order of magnitude lower than measured (5900 mL/g at an aqueous concentration of 0.1 μg/mL) for the coke isotherm.

The difference between the measured coke partition coefficient and the partition coefficient estimated from pyrene sorption to activated carbon may be due to differences in sorbent-sorbate interactions for these two solid phases. The abundance of surface sorption sites was much lower for coke due to its smaller surface area (*c.f.*, 1000 m^2/g for 74 μm diameter activated carbon (Walters and Luthy, 1984)), leading to near saturated surface coverage at the sorbed concentrations of the isotherm measurement. Less than 1% of the activated carbon surface would have been covered at sorbed pyrene concentrations in this range. Additional sorptive interactions, resulting from high sorbate surface coverages, may not have been represented in the activated carbon sorption isotherm.

For comparison, the traditional partition coefficient was also calculated for pyrene sorption to coke. The coke was 80% carbon by weight. A natural organic carbon partition coefficient for pyrene was calculated to be 57 500 mL/g$_{oc}$ from the linear free energy relationship developed with data from Karickhoff (1981) (Schwarzenbach *et al.*, 1993). The traditional partition coefficient for coke was calculated to be 46 000 mL/g for pyrene. A similar calculation for naphthalene yielded a value of 6800 mL/g. Both of these estimates are at least several orders of magnitude greater than the measured uptake of these sorbates by coke. These calculations demonstrate that, while the partition mechanism for coke is not fully understood, a carbon-based model for predicting solid-water exchange to coke is not accurate for this sorbent.

Sorbent Quantification

Each of the sorbents isolated from the anthropogenic fill materials at Site YYZ required unique expressions to estimate the overall solid-water partition coefficient. In each

case, applying a total carbon measurement and a calculated organic carbon partition coefficient (Eq. 1) inaccurately estimated the observed compound partitioning. However, one benefit of applying a single K_{oc} value and a bulk f_{oc} measure to estimate partition coefficients is the simplicity in making a single carbon measurement. In this way, many samples can be quickly analyzed to characterize the spatial heterogeneity of partition coefficients within a region of investigation. A similarly simple measurement technique is necessary to quantify the abundance of various organic carbon-containing sorbents in a mixture.

We investigated the use of elemental analysis, including carbon, hydrogen, nitrogen and oxygen, to separate the amounts of individual components within a mixture. The ratio of carbon-to-oxygen content varied greatly for the sorbents investigated here, ranging from about 1 for natural organic matter to about 40 for coke (Table 5.3). Inclusion of hydrogen and nitrogen would allow further differentiation, such as between organic matter and wood, because of differing ratios relative to carbon (Steelink, 1985). This method was tested by analyzing samples of individual sorbent matrices (wood, natural solids, coke) for their elemental (CHNO) composition. Known mixtures of these sorbents were also analyzed for their elemental composition. Mass balance equations were then written for each of the elements, equating the total mass observed in the mixture with the unknown mass contribution from sorbents with known compositions (Figure 5.5). The set of matrix equations was solved for the mass fraction of each sorbent within the mixture, subject to the constraint that the sum of the mass fractions totalled 1.

A sample calculation is shown in Figure 5.5 for a sorbent mixture with equal masses of carbon from natural organic matter, wood, and coke. An equation for hydrogen was not considered as one of the three elemental mass balance equations because its value was below the detection limit for the mass of the mixtures. The elemental composition of the individual sorbents and the mixture are also given (Figure 5.5). The mass balance constraint was introduced into the solution by setting $M_{NOM} = 1 - M_{WOOD} - M_{COKE}$. The mass balance equations were rewritten, substituting this expression of M_{NOM}, to give 3 equations with 2 unknowns. The modified set of matrix equations was solved by minimizing the norm of the error vector using Matlab. The error vector was calculated as the difference between the

Table 5.3. Elemental composition of organic-carbon containing anthropogenic fill solids.

Solid	C (g/g_s)	H (g/g_s)	N (g/g_s)	O (g/g_s)	C/O Ratio
Natural solids	0.0097	0.005	0.0006	0.01	1.3
Wood	0.47	0.033	< 0.5	0.37	1.7
Coke waste	0.8	0.013	0.015	0.025	43

$$[C]_{TOT} = M_{WOOD}\,[C]_{WOOD} + M_{NOM}\,[C]_{NOM} + M_{COKE}\,[C]_{COKE}$$

$$[N]_{TOT} = M_{WOOD}\,[N]_{WOOD} + M_{NOM}\,[N]_{NOM} + M_{COKE}\,[N]_{COKE}$$

$$[O]_{TOT} = M_{WOOD}\,[O]_{WOOD} + M_{NOM}\,[O]_{NOM} + M_{COKE}\,[O]_{COKE}$$

PERCENT ELEMENTAL COMPOSITION

Element	Total	Wood	Natural Organic Matter	Coke
C	2.77	46.64	0.97	79.86
N	0.13	< 0.5[†]	0.061	1.49
O	2.05	37	1.03	2.47

FRACTIONAL COMPOSITION

Solid Matrix	Known Composition	Estimated By Linear Optimization
Wood	0.02	0.0280
Natural Organic Matter	0.96	0.9654
Coke	0.02	0.0066

Figure 5.5. Sample elemental mass balance calculation to determine the fractional composition of a sorbent mixture.

right hand side and the left hand side of the modified versions of the equations shown in Figure 5.5.

The mass fractional composition of the mixture calculated with this optimization method was similar to the known composition of the mixture (Figure 5.5). The estimated wood component was 50% greater than the actual value and the coke was underestimated by a factor of 4, in comparison to the true mass fraction. When these fractional compositions were substituted back into the right hand side of the mass balance equations in Figure 5.5 to solve for the bulk elemental weight percentages, the nitrogen value was lower by 50% while the carbon and oxygen values were the same as the values measured in the experimental mixture, within measurement error. This check suggests that the nitrogen were the least well known of the three elements in the elemental analysis and may result from the difficulty in quantifying the low percentages of nitrogen in these sorbents.

The error introduced into a calculation of the overall solid-water partition coefficient by the difference between the true and estimated fractional compositions depends upon the relative magnitudes of the sorbent specific partition coefficients. The sorbent mixtures tested for this elemental mass balance method were found to have less than a factor of 2 difference between the overall partition coefficients calculated with the estimated fractional compositions and the partition coefficients calculated with the known fractional compositions (Table 5.4). For other sorbent mixtures, the imprecision of the elemental mass balance method may give rise to poor estimates of the overall K_d of the mixture.

Conclusion

The sorption isotherm study demonstrated the importance of characterizing the various organic carbon-containing materials in order to accurately predict sorption to, and hence, groundwater transport through, anthropogenic fill materials. For example, coke wastes composed a large fraction of the subsurface solids at Site YYZ, accounting for a total carbon content of 35 to 75% by weight at a depth of 3.6 m; however, no detectable sorption of naphthalene to coke was able to be measured. Thus, naphthalene retardation would be overestimated by several orders of magnitude if this sorbent was not correctly identified and an appropriate sorption isotherm applied. Elemental analysis can be used to determine the

Table 5.4. Evaluation of elemental mass balance method for determining fractional composition of sorbent mixtures. The partition coefficients for naphthalene were calculated with the following equation using parameter values from Table 5.2:
$K_d = f_{WOOD}f_{lignin}K_{lignin} + f_{NOM}f_{oc}K_{oc} + f_{COKE}K_{COKE}$

Estimated Fractional Composition	Known Fractional Composition	K_d from Estimated Composition	K_d from Known Composition
f_{WOOD} - 0.0480 f_{NOM} - 0.9772 f_{COKE} - -0.0201	0.0098 0.9902 0	17	10
f_{WOOD} - 0.0070 f_{NOM} - 0.9868 f_{COKE} - 0.0062	0 0.9880 0.0124	10	9
f_{WOOD} - 0.0280 f_{NOM} - 0.9654 f_{COKE} - 0.0066	0.0183 0.9671 0.0145	13	12

gross composition of solid matrix mixtures. Refinements of this method, such as the inclusion of selective digestion steps, may be necessary to improve the accuracy of solid-water partition coefficient estimates for mixtures containing small mass fractions of materials with large sorbent-specific partition coefficients.

References

CRC Handbook of Chemistry and Physics (1989). Boca Raton, FL, CRC Press, Inc.

Ball, W. P.; Buehlar, C.; Harmon, T. C.; Mackay, D. M.; Roberts, P. V. (1990). "Characterization of a sandy aquifer material at the grain scale." *Journal of Contaminant Hydrology* **5**: 253-295.

Behr, E. A.; Briggs, D. R.; Kaufert, F. H. (1953). "Diffusion of dissolved materials through wood." *Journal of Physical Chemistry* **57**: 476-480.

Boyd, S. A.; Sun, S. (1990). "Residual petroleum and polychlorinated oils as sorptive phases for organic contaminants in soils." *Environmental Science and Technology* **24**: 142-144.

Durnford, D.; Brookman, J.; Billica, J.; Milligan, J. (1991). "LNAPL distribution in a cohesionless soil: A field investigation and cryogenic sampler." *Ground Water Monitoring Review* **11**(Summer): 115-122.

Electric Power Research Institute (1993). *Chemical and Physical Characteristics of Tar Samples From Selected Manufactured Gas Plant (MGP) Sites*. EPRI TR-102184s.

Environmental Research and Technology Inc; Koppers Company Inc (1984). *Handbook on Manufactured Gas Plant Sites*.

Garbarini, D. R.; Lion, L. W. (1986). "Influence of the nature of soil organics on the sorption of toluene and trichloroethylene." *Environmental Science and Technology* **20**: 1263-1269.

Gauthier, T. D.; Shame, E. C.; Guerin, W. F.; Seitz, W. R.; Grant, C. L. (1986). "Fluorescence quenching method for determining equilibrium constants for polycyclic aromatic hydrocarbons binding to dissolved humic materials." *Environmental Science and Technology* **20**: 1162-1166.

Gollmar, H. A. (1945). "Removal of sulfur compounds from coal gas." In *Chemistry of coal utilization*. H. H. Lowry, Ed. New York, John Wiley & Sons, Inc. **II:** 947-1007.

Grathwohl, P. (1990). "Influence of organic matter form soils and sediments from various origins on the sorption of some chlorinated aliphatic hydrocarbons: Implications on K_{oc} correlations." *Environmental Science and Technology* **24**: 1687-1693.

Gustafsson, O.; Haghseta, F.; Chan, C.; MacFarlane, J.; Gschwend, P. M. (1997). "Quantification of the dilute sedimentary soot phase: Implications for PAH speciation and bioavailability." *Environmental Science and Technology* **31**: 203-209.

Holmen, B. A.; Gschwend, P. M. (1997). "Estimating sorption rates of hydrophobic organic compounds in iron oxide- and aluminosilicate clay-coated aquifer sands." *Environmental Science and Technology* **31**: 105-113.

Hunt, J. R.; Sitar, N.; Udell, K. S. (1988). "Nonaqueous phase liquid transport and cleanup: 1. Analysis of mechanisms." *Water Resources Research* **24**: 1247-1258.

Huntley, D.; Hawk, R. N.; Corley, H. P. (1994). "Nonaqueous phase hydrocarbon in a fine-grained sandstone: 1. Comparison between measured and predicted saturations and mobility." *Ground Water* **32**: 626-634.

Karickhoff, S. W. (1981). "Semi-empirical estimation of sorption of hydrophobic pollutants on natural sediments and soils." *Chemosphere* **10**: 833-846.

Karickhoff, S. W.; Brown, D. S.; Scott, T. A. (1979). "Sorption of hydrophobic pollutants on natural sediments." *Water Research* **13**: 241-248.

Kile, D. E.; Chiou, C. T.; Zhou, H.; Li, H.; Xu, O. (1995). "Partition of nonpolar organic pollutants from water to soil and sediment organic matters." *Environmental Science and Technology* **29**: 1401-1406.

Lee, L. S.; Rao, P. S. C.; Okuda, I. (1992). "Equilibrium partitioning of polycyclic aromatic hydrocarbons from coal tar into water." *Environmental Science and Technology* **26**: 2110-2115.

Mattson, J. S.; Mark, H. B. (1971). *Activated Carbon*. New York, Marcel Dekker, Inc.

Mercer, J. W.; Cohen, R. M. (1990). "A review of immiscible fluids in the subsurface: Properties, models, characterization and remediation." *Journal of Contaminant Hydrology* **6**: 107-163.

Miller, M. M.; Wasik, S. P.; Huang, G. L.; Shiu, W. Y.; Mackay, D. (1985). "Relationships between octanol-water partition coefficient and aqueous solubility." *Environmental Science and Technology* **19**: 522-529.

Parfitt, G. D.; Rochester, C. H. (1983). "Adsorption of small molecules." In *Adsorption From Solution at the Solid-Liquid Interface*. G. D. Parfitt ,C. H. Rochester, Eds.. New York, Academic Press: 3-47.

Parham, R. A.; Gray, R. L. (1984). "Formation and Structure of Wood." In *The Chemistry of Solid Wood*. R. Rowell, Ed. Washington, DC, The American Chemical Society. **207:** 3-56.

Pierson, H. O. (1993). *Handbook of Carbon, Graphite, Diamond and Fullerenes*. Park Ridge, NJ, Noyes Publications.

Rael, J.; Shelton, S.; Dayaye, R. (1995). "Permeable barriers to remove benzene: Candidate media evaluation." *Journal of Environmental Engineering* **121**: 411-415.

Schwarzenbach, R. P.; Gschwend, P. M.; Imboden, D. M. (1993). *Environmental Organic Chemistry*. New York, NY, John Wiley & Sons, Inc.

Schwarzenbach, R. P.; Westall, J. (1981). "Transport of nonpolar organic compounds from surface water to groundwater: Laboratory sorption studies." *Environmental Science and Technology* **15**: 1360-1367.

Severtson, S. J.; Banerjee, S. (1996). "Sorption of chlorophenols to wood pulp." *Environmental Science and Technology* **30**: 1961-1969.

Stamm, A. J.; Millet, M. A. (1941). "The internal surface area of cellulosic materials." *Journal of Physical Chemistry* **45**: 43-54.

Steelink, C. (1985). *Humic Substances in Soil, Sediment and Water*. New York, John Wiley and Sons.

Walters, R. W.; Luthy, R. G. (1984). "Equilibrium adsorption of polycyclic aromatic hydrocarbons from water onto activated carbon." *Environmental Science and Technology* **18**: 395-403.

Wegner, T. H.; Baker, A. J.; Bendtsen, B. A.; Brenden, J. J.; Eslyn, W. E.; Harris, J. F.; Howard, J. L.; Miller, R. B.; Petersen, R. C.; Rowe, J. W.; Rowell, R. M.; Simpson, W. T.; Zinkel, D. F. (1992). "Wood." In *Kirk-Other Encyclopedia of Chemical Technology*. J. I. Kroschwitz ,M. Howe-Grant, Eds.. New York, John Wiley and Sons.

Xing, B.; McGill, W. B.; Dudas, M. J. (1994). "Cross-correlation of polarity curves to predict partition coefficients of nonionic organic contaminants." *Environmental Science and Technology* **28**: 1929-1933.

Chapter 6.

SORPTION OF NONPOLAR ORGANIC COMPOUNDS TO WOOD

Abstract

The sorption of nonpolar organic compounds to wood is important for determining the groundwater transport of contaminants in aquifers of anthropogenic fill containing wood wastes. Isotherms for benzene, toluene and *o*-xylene (BTX) sorption to Douglas fir and Ponderosa pine chips were measured. Equilibrium wood partition coefficients for these sorbates were 3 to 17 times less than values estimated on an organic carbon basis (*i.e.*, $K_{wood} = f_{oc}K_{oc}$). A better model to predict wood partitioning accounted for the sorptivity of the wood lignin and the lack of sorption by the cellulose component: $K_{wood} = f_{lignin}K_{lignin}$. A lignin-octanol free energy relationship with an equation of $\log K_{lignin} = (0.72 \pm 0.08) \log K_{ow} + (0.08 \pm 0.19)$ was developed using these lignin-normalized experimental K_{wood} values and literature values of K_{lignin} for other organic sorbates. The characteristic times of sorption kinetics of all sorbate/sorbent pairs were on the order of 100 min for cm-sized wood particles. Estimated characteristic diffusion times were in agreement with experimental values for both physically hindered wood diffusion and homogeneous retarded diffusion models. The clean-up times of wood-containing aquifer solids is not limited by kinetic desorption from cm-sized wood particles.

Introduction

Wood is an absorbent material which may be present as fill at many industrial sites. During recent investigations at a former manufactured gas plant, wood was found in the aquifer solids in the form of building rubble and chip waste from the gas manufacture process (Chapter 5). The practice of burying fill was common at other manufactured gas plants (Luthy *et al.*, 1994), and likely was conducted at a wide variety of other industrial sites as renovations were made or wastes were produced. Wood is also a significant component of solid waste, accounting for up to 25% by weight of material at landfills which accept demolition wastes (Niessen, 1977). Thus, groundwater transport of organic contaminants at these sites may be influenced by the presence of wood in the subsurface solids. However, the sorption of nonpolar organic compounds to wood has not been extensively studied and no model exists to predict the influence of wood on contaminant transport.

The purpose of this study was to investigate the sorption of nonpolar organic compounds to wood. The objectives of this experimental work were two-fold: (1) to determine the equilibrium partition coefficients of structurally intact wood, and (2) to determine the effects of particle size and sorbate hydrophobicity on the time scale of wood sorption kinetics. The specific hypotheses that were tested while meeting these objectives are developed in the following discussion of wood physiology and prior wood sorption studies. Once a conceptual picture of wood sorption has been developed, the objectives will again be summarized, noting our specific analytical approach.

Wood Physiology

Chemical Composition

Wood is a naturally occurring complex polymeric composite. The primary chemical components of wood are cellulose and lignin. Cellulose is a carbohydrate formed from repeating glucose units (Figure 6.1). The degree of polymerization of cellulose chains in wood ranges from 1000 to 5000 units (Stamm, 1964). The hydroxyl groups make cellulose a highly polar substance which is capable of hydrogen bonding. At the molecular scale, parallel cellulose chains in wood cell walls form intermolecular hydrogen bonds to yield a rigid crystalline structure. Cellulose constitutes a significant portion of wood, ranging from 3 to 47 weight percent in hardwoods and 40-44% in softwoods (Thompson, 1996).

Lignin is an amorphous three dimensional polymer which permeates the wood cell wall and interstitial spaces (Pearl, 1967). It is formed by the enzymatic dehydrogenative polymerization of phenylpropanoid monomers (Higuchi, 1980) (Figure 6.1). Hence, lignin has no specified chemical composition and is defined by its structural placement and function in wood cells (Pearl, 1967). Unlike cellulose, lignin is hydrophobic in nature. The chemical properties of lignin in wood are not known because isolation methods alter its structure (Pearl, 1967); however, isolated lignin exhibits a Hildebrand solubility parameter of 10 to 12 $(cal/cm^3)^{1/2}$ (Kopinke *et al.*, 1995; Barton, 1983; Higuchi, 1980; Dellicoli, 1977) (*c.f.* cellulose solubility parameter of 14.5-16.5 $(cal/cm^3)^{1/2}$ (Barton, 1975)). By weight, hardwoods contain 16-24% lignin, and softwoods are 25-31% lignin (Thompson, 1996).

The remainder of the wood structure (about 20%) is composed of hemicellulose. These are polysaccarides of 5 and 6-carbon sugars with short side chains (Parham and Gray, 1984). The irregular nature of these subunits limit the degree of hydrogen bonding that can occur between chains, and hence limits the formation of a crystalline structure.

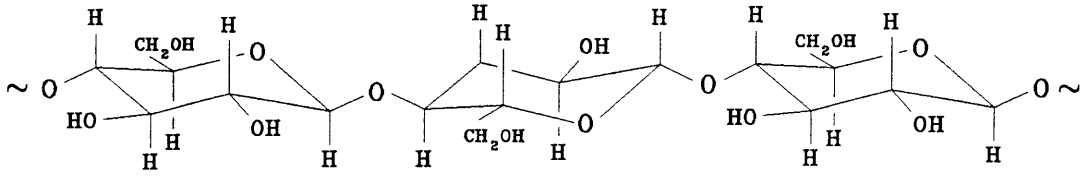

Cellulose

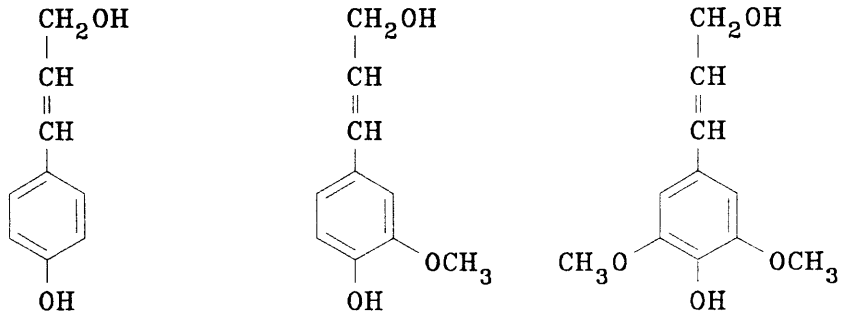

p-coumaryl alcohol

coniferyl alcohol

sinapyl alcohol

Lignin Precursors

Predominant Softwood Lignin Linkage

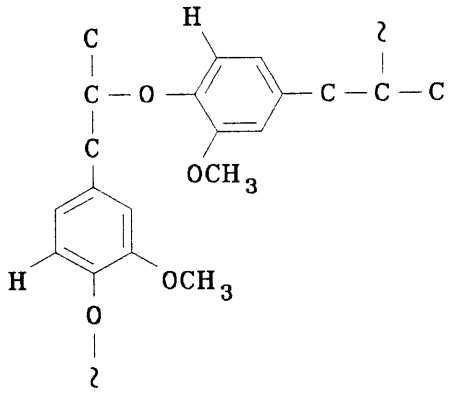

Figure 6.1. The molecular structure of cellulose and lignin polymers.

Physical Structure

Lignin and cellulose have a distinct arrangement in the wood cell walls. The basic microstructure is a lignin-hemicellulose matrix with imbedded crystalline fibrils of cellulose (Siau, 1984) (Figure 6.2). The cell walls also have a macrostructure composed of a primary wall and 3 secondary walls (Figure 6.2). The interstitial region between the cells is referred to as the middle lamella. The relative abundance of lignin and cellulose varies between the cell wall layers, increasing in lignin content through the secondary wall to the middle lamella (Figure 6.2).

The bulk wood structure is composed of regular layers of wood cells, referred to as fibres. Fibres are the rigid cell wall structure remaining after autolysis of the protoplasm. These fibres are oriented in the longitudinal direction of tree growth and enclose a hollow lumen. Softwoods have an average longitudinal dimension of 3500 μm (Siau, 1984), while hardwood fibres have a shorter longitudinal dimension of 1000 to 1500 μm (Stamm, 1964). The ratio of longitudinal to radial dimensions of fibres is about 100 (Siau, 1984; Stamm, 1964) and the cell wall thickness is about 10 μm. The lumina of adjoining cells are connected by pits lining the sides and ends of the cell walls. These pits have a fibrous covering to allow diffusive transfer of nutrients and water in the living wood tissue. Intercell transfer is increased by the presence of ray cells oriented in the radial direction and connected to the longitudinal fibres by pits. Ray cells only constitute 6 to 8% of the total wood porosity (Stamm, 1964). These features are present in both softwoods and hardwoods; however, hardwoods contain additional structures known as vessel elements. Vessel elements are continuous hollow channels, like straws, which transport sap.

Transport processes in hardwoods have been studied less extensively than softwoods because of their more complex physical structure. The subsequent discussion, and our experimental work, focus on softwoods because of their regular fibre structure. Softwoods likely compose the bulk of the buried wood materials at industrial sites. Lumber in the form of construction rubble, or lumber production wastes (sawdust, wood chips) used as sorbents, may have been buried as fill and the primary class of building lumber is pine/fir/spruce. All discussions are with respect to water-saturated wood.

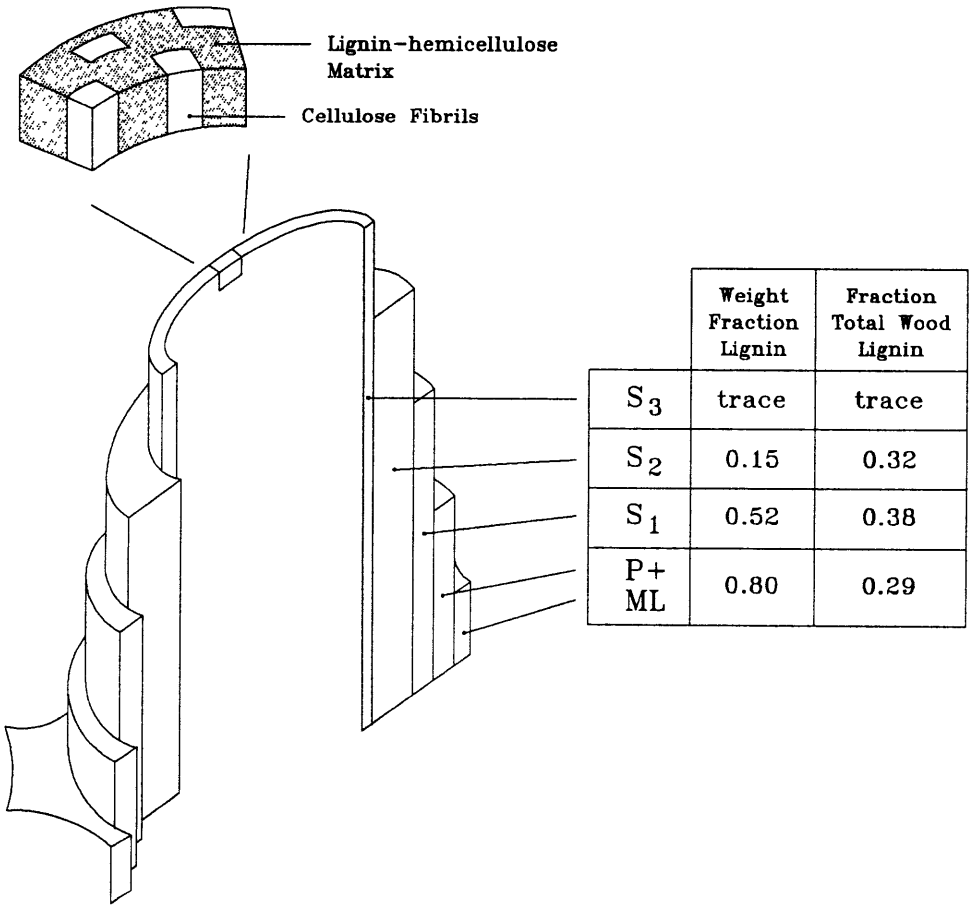

	Weight Fraction Lignin	Fraction Total Wood Lignin
S_3	trace	trace
S_2	0.15	0.32
S_1	0.52	0.38
P+ ML	0.80	0.29

Figure 6.2. The macrostructure and microstructure of the wood cell wall (Siau, 1984). The primary (P) and secondary (S) cell wall layers and middle lamella (ML) are noted. The lignin composition is for Scotch pine (total lignin fraction of 0.28) (Genco, 1996).

Sorption of Nonpolar Organic Compounds to Wood and Wood Components

Organic compound sorption coefficients have been measured for isolated wood components. The magnitude of sorption to isolated cellulose and lignin reflects the respective solubility parameters of these wood components. On an organic carbon basis, cellulose has little measurable uptake of mono-aromatic compounds (Xing *et al.*, 1994; Rutherford *et al.*, 1992; Garbarini and Lion, 1986) or chlorinated solvents (Rutherford *et al.*, 1992; Garbarini and Lion, 1986). By contrast, lignin exhibits linear isotherms for toluene, tricholoethylene and chlorinated phenols (Severtson and Banerjee, 1996; Garbarini and Lion, 1986). Lignin sorption coefficients are of a similar magnitude to those of soil organic matter when normalized to the carbon content. The sorption of organic compounds to hemicellulose has not been studied. These polysaccarides are similar in molecular composition to cellulose so, like cellulose, hemicellulose would likely have little affinity for sorbing organic compounds.

From the above observations for cellulose and lignin, the sorption of organic compounds to intact wood was hypothesized to occur by partitioning into lignin (Severtson and Banerjee, 1996). Thus, a wood-water partition coefficient (K_{wood}) for a compound could be predicted from the lignin content of the wood (f_{lignin}) and the lignin-water partition coefficient (K_{lignin}) of the compound, assuming all the lignin is accessible for sorption:

$$K_{wood} = f_{lignin} K_{lignin} \quad (1)$$

This hypothesis was tested for discrete wood fibres with varying lignin contents. A positive correlation was observed between the fibre partition coefficients of chlorophenols and the lignin fraction of the wood fibres (Severtson and Banerjee, 1996). The slopes of K_{wood} *v.* f_{lignin} plots exactly matched independently measured K_{lignin} values.

The sorption of benzene to intact wood particles in the form of sawdust was also investigated (Rael *et al.*, 1995). If all of the cell wall lignin was accessible in these wood particles, the benzene partition coefficient should be predicted from Eq. 1. The estimated partition coefficient was 16 mL/g (pine f_{lignin} = 0.26 (Petterson, 1984), benzene K_{lignin} = 60 (Xing *et al.*, 1994)); however, the observed isotherm was highly nonlinear with a small

(10^{-4} mL/g) Freundlich parameter (Rael *et al.*, 1995). Eq. 1 greatly overestimated the benzene wood partition coefficient suggesting that the assumption of lignin accessibility was incorrect.

The inability of Eq. 1 to predict K_{wood} for intact wood particles may be due to differences in their structure relative to wood fibres. Most of the wood lignin is found in and near the middle lamella region (Figure 6.2). If sorbates must first penetrate the cellulose-rich secondary cell wall layer they may not be able to access all of the wood lignin. In contrast, the lignin in the wood fibres of Severtson and Banerjee was exposed to the solution phase. The discrete wood fibres were generated from wood chips by pulping, a process in which the middle lamella is dissolved. Pulping also reduces the degree of cellulose polymerization (Stamm, 1964), perhaps allowing sorbate access to lignin within the inner cell wall. The cell wall fragments of the pine sawdust likely also had exposed secondary wall and middle lamella lignin; however, deeper sorbate penetration into the whole lignin matrix may be inhibited by outer regions of crystalline cellulose. Cell wall fractures may have been created as the sawdust particles were generated by mechanical degradation, but no chemical degradation of the wood matrix would have resulted.

Other data suggests that lignin-accessibility should not be hindered in intact wood particles. First, visualization studies of wood impregnated with copper sulphate solutions showed copper to be distributed throughout the cell wall matrix (Fengel, 1971). Second, the model for diffusive transport through wood (described below) suggests that compounds penetrate through the cell wall to some extent. Finally, the rigid crystalline structure of cellulose fibrils may not be maintained under saturated conditions. At the fibre saturation point, the stress at which wood failure occurs is at a minimum relative to wood with lower moisture contents (Bodig, 1982).

Diffusion in Wood

The movement of compounds into the wood sorbent during sorption occurs by diffusion. Thus, the kinetics of sorption reflect the characteristic mass transfer times of the diffusional process. Two possible treatments of this diffusion process are considered. The first model of the wood diffusion coefficient considers the diffusion hinderance of the physical structure of the wood to compounds diffusing through wood particles. The second

model overlooks wood cell structure and treats wood particles as homogeneous porous sorbents.

Physically Hindered Diffusion

A model for compound penetration through saturated wood was developed by Stamm, based upon the porous structure of wood (Stamm, 1964). A schematic picture of softwood macrostructure is shown in Figure 6.3 for a bundle of fibres. There are two pathways for diffusion through each wood fibre in the longitudinal or tangential (or radial) direction: (1) diffusion through the continuous cell wall, or (2) diffusion through the lumen cavity. Compounds move between the lumina of adjoining cells by diffusion through the overlapping cell wall or through the interconnecting pits. As shown in the enlarged detail (Figure 6.3), the pit structure is not an open aperture between adjacent lumina. A membrane composed of cell wall tissue fills most of the pit chamber and is held in place by a porous fibre structure. Pit diffusion may occur through the membrane itself, or through the membrane pores. Stamm postulated that each of these pathways hindered the diffusion of solutes through a piece of wood and referred to these hinderances as "resistances" to diffusion in the longitudinal, tangential or radial direction.

A pictorial representation of Stamm's resistance model for diffusion through wood is shown in Figure 6.4. By analogy to an electric circuit, the wood diffusion coefficient is reduced relative to the solution diffusion coefficient by a factor equal to the reduced conductance of the wood "circuit" relative to a circuit with no resistance (the solution). Stamm's theoretical model was verified by measuring the conductance of wood blocks saturated with a salt solution. The conductance of Western white pine was reduced relative to the solution by a factor that was the same as the factor by which the experimentally measured wood diffusion coefficient was reduced relative to the aqueous diffusion coefficient (Stamm, 1964; Burr and Stamm, 1947). Theoretical equations for the individual resistances depicted in Figure 6.4 were developed with parameters derived from the physical structure of the wood species. Details of the resistance calculations can be found in Stamm (1964) and Behr *et al.* (1953). (They are also reproduced in Appendix C in a sample calculation specific to the experimental Results of this chapter.) The resistance calculations do not account for properties of the penetrant compound. Theoretically calculated ratios of wood-to-aqueous diffusion coefficients show good agreement with experimental measurements for salts (Behr *et al.*, 1953).

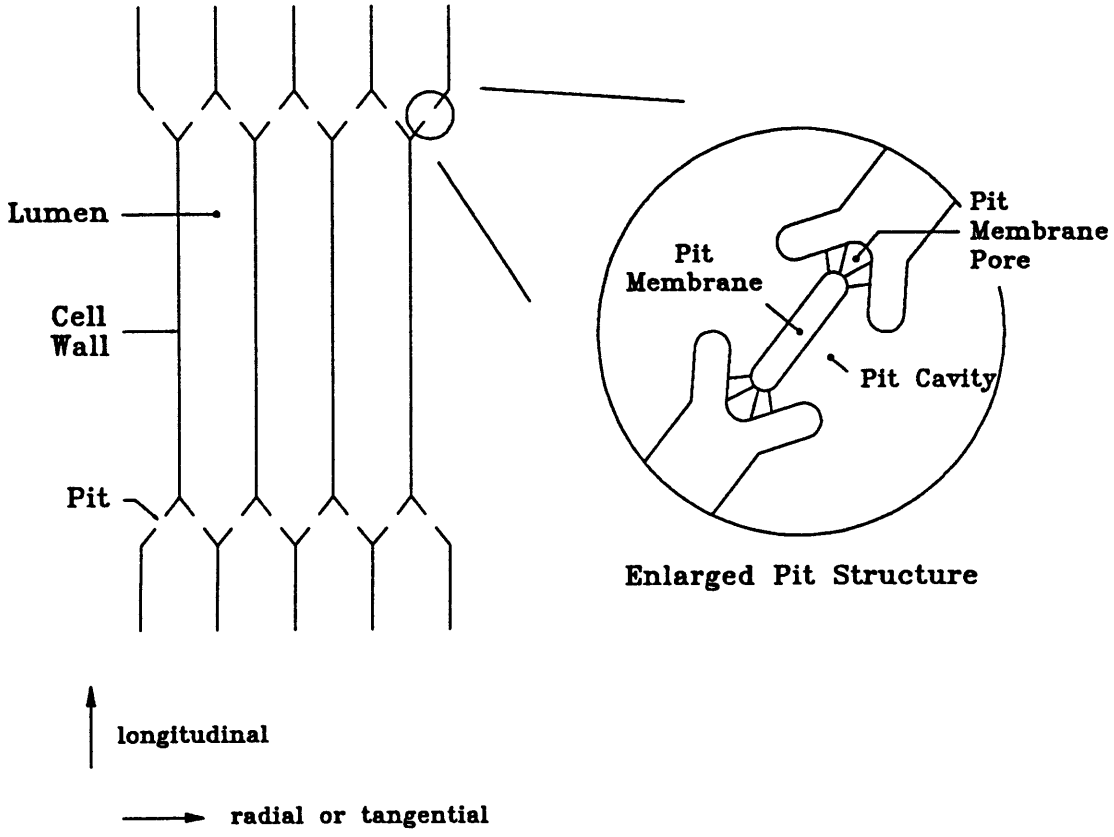

Figure 6.3. Schematic representation of softwood physical structure with enlarged detail of the interconnecting pit structure. The directions of fibre orientation are noted.

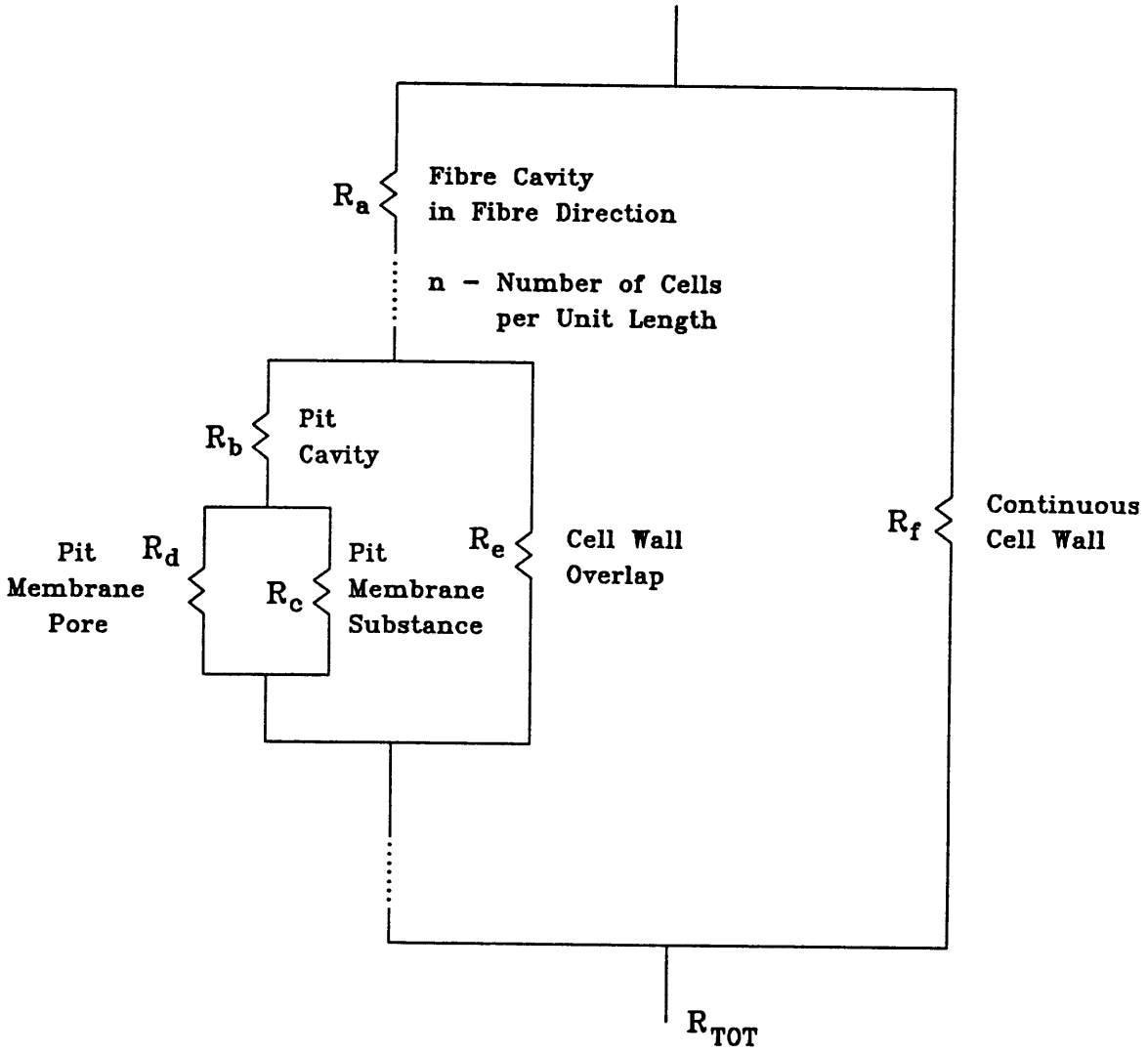

Figure 6.4. Pictorial representation of Stamm's resistance model for diffusion through softwoods. The theoretical equation for the net reduction in the wood diffusion coefficient relative to the aqueous diffusivity is also given (Burr and Stamm, 1947).

The resistance model for diffusion in wood has also been applied to organic compounds. Again, theoretical calculations of wood-to-aqueous diffusion coefficient ratios predicted experimental values for lactose, glycerol, and urea (Stamm, 1964; Cady and Williams, 1935). These organic compounds are highly polar and likely have little tendency to sorb to wood tissue (*e.g.*, urea octanol-water partition coefficient of $10^{-2.1}$ (Hansch *et al.*, 1995)). It is reasonable to assume that sorbing compounds would follow the same diffusion pathways through the wood macrostructure as nonsorbing compounds. In the case of sorbing compounds, diffusion through the cell wall tissue is likely retarded by equilibrium microscale partitioning between the wood tissue and lignin. The cell wall tissue resistances, R_c, R_e and R_f are all inverse functions of the physical dimension (thickness or length) of the tissue structure (Behr *et al.*, 1953) (Appendix C). Microscale partitioning effectively lengthens the diffusive path, and hence the resistances, R_c, R_e, and R_f for a sorbing compound would be increased by a retardation factor that was a function of the lignin content of these tissues and the lignin-water partition coefficient of the sorbate.

The effect of penetrant sorption on the overall ratio of wood-to-aqueous diffusion coefficients is greater for tangential (or radial) diffusion than for longitudinal diffusion. Conductance through the continuous cell wall is less than 4% of the overall wood conductance in either the longitudinal or tangential direction (Burr and Stamm, 1947). The resistance of the fibre cavities in the longitudinal direction is great compared to the pit structures (Burr and Stamm, 1947), thus longitudinal diffusion coefficient would be relatively unaffected by retardation of a sorbing penetrant molecule. In the tangential direction, the resistance of the fibre cavities is much less important than passage between adjacent fibres for which the pit resistance is about twice the resistance of the overlapped cell wall (Burr and Stamm, 1947). Tangential diffusion coefficients could thus be affected by sorbate retardation in lignin-rich cell walls.

Homogeneous Retarded Diffusion

The alternate model for diffusion through wood ignores the resistances of the cell structure. Instead, wood particles are assumed to be homogeneous porous sorbents. Diffusion occurs through the uncharacterized pore space in the wood. In the case of sorbing compounds, the rate of diffusion is slowed by equilibrium microscale partitioning to the solid

sorbent. The effective diffusion coefficient is the aqueous diffusivity reduced by a retardation factor which characterizes the partition process:

$$R = 1 + r_{sw} K_{wood} \quad (2)$$

where r_{sw} (g/mL) is the internal solid-to-water ratio, and K_{wood} (mL/g) is the partition coefficient.

Scope of Investigation

The purpose of the equilibrium sorption study was to test the hypothesis that sorption to intact wood is predicted by the fraction of lignin and the sorbate's lignin partition coefficient (Eq. 1). Three sorbates (benzene, toluene, and *o*-xylene) were chosen for which lignin-water partition coefficients were known (Xing *et al.*, 1994). The sorbents were Douglas fir and Ponderosa pine. The hypothesis that lignin partitioning is limited by penetration through cellulose-rich cell wall regions was also tested with toluene sorption to wood particles of differing sizes.

The second experimental objective was to determine the effects of particle size and sorbate hydrophobicity on wood sorption kinetics. Wood particles were cut to include greater fractions of the wood macrostructure, from cell wall fragments to hundreds of fibres. The effect of sorbate hydrophobicity on uptake times was investigated using the three sorbates and a single wood particle size.

Methods

Chemicals

Neat benzene, toluene and *o*-xylene were used as received from Alltech (Deerfield, IL). Purified water (subsequently referred to as 18 MΩ water) from an Aries water purification system (Vaponics, Rockand, MA) was used to make aqueous solutions. Acetonitrile was 'Baker Analyzed' HPLC solvent (J.T. Baker, Phillipsburg, NJ). Sodium azide was from Fluka (Switzerland). Kiln-dried Douglas fir and Ponderosa pine wood was obtained from Cambridge Lumber and Supply (Cambridge, MA). The wood was sanded before use to remove surficial grit.

Equilibrium Sorption Isotherms

Wood partition coefficients were calculated from 5-point sorption isotherms. Douglas fir sticks (2 cm × 0.1 cm × 0.1 cm, longitudinal × tangential × radial dimensions) and Ponderosa pine chips (1 cm × 0.1 cm × 0.7 cm) were soaked in 18 MΩ water containing 1 mM sodium azide biocide until they reached a constant wet mass. The minimum time of contact was 18 days. The saturated wood particles were blotted with paper towel to remove surficial water and transferred to 50 or 100 mL glass equilibration flasks. The flasks were filled with an aqueous sorbate solution and sealed with glass stoppers to contain no headspace. The stoppers were wrapped with teflon tape and clamped to prevent leakage. The flasks were then wrapped with foil to minimize photodegradation. A wood-free control was assembled in the same manner as the isotherm points to quantify loss mechanisms other than sorption to wood. The flasks were inverted by hand several times daily to mix the solution phase. Equilibration times were from 5 to 21 days (Table 6.1). At this time, the aqueous concentrations were measured and the sorbed concentration calculated by difference from the initial concentration, as detailed in Equations.

Sorption isotherms were determined for benzene, toluene, and *o*-xylene. Aqueous sorbate solutions of various concentrations were made by diluting saturated stock solutions with 18 MΩ water in a glass syringe. Saturated stock solutions were made by equilibrating a neat solvent phase of benzene, toluene or *o*-xylene with 18 MΩ water in a separatory funnel. The presence of the excess solvent phase ensured no compound loss from the saturated aqueous solution between uses. Enough concentrated sodium azide solution was added to the dilute aqueous solution in the syringe to give a final biocide concentration of 1 mM. The syringe, containing glass beads, was shaken with no headspace to mix the solution. The initial concentrations of the dilute aqueous phases for each isotherm point were measured before transfer of the solution from the syringe to the equilibration flasks.

The dry weight and the water content of the wood particles was quantified at the completion of the experiment. The wet wood particles were blotted with paper towel to remove surficial water and weighed. The wood was then dried for 24 h at 103-105°C and reweighed. The water content was the difference between the wet and dry weights of the wood particles.

A minimum of 1 wood-containing flask and 1 wood-free control was also set up by the above method for kinetic monitoring. These flasks were subsampled over time at time intervals of 1×10^n, 3×10^n, and 8×10^n minutes. The first value of n was 1 and sampling continued until aqueous concentrations in the wood-containing flasks remained at constant levels for several successive sampling points. The isotherms were measured at this time.

Aqueous concentrations were quantified by high pressure liquid chromatography (HPLC). Thirty microliter aliquots were injected into a Hewlett Packard 1050 HPLC equipped with a diode array detector. Compounds were eluted isocratically (85% acetonitrile/ 15% 18 MΩ water) through a 250 mm Adsorbosphere C_{18} (5 μm packing, Alltech) column at a flow rate of 1 mL/min. Peak areas were quantified at a detection wavelength of 260 nm, and background corrected for the solvent with a reference wavelength of 550 nm. External standards were made up daily from the saturated stock solutions to calibrate the instrument response.

Wood Sorption Kinetics

Toluene sorption kinetics were monitored for wood particles of various shapes with toluene as the sorbate. Douglas fir and Ponderosa pine shavings were generated by rasping wood. The sawdust was sieved and the fraction that was retained between 1000 to 1400 μm screens was used for the time course experiment. This fraction also included some fines that were stuck to the dry-screened particles. These particles were all broken cell wall fragments with solution-exposed lignin. Larger particles, in the shapes of cubes, sticks and chips, were also cut from the wood and rinsed of fines after being saturated with water. These larger particles all had tangential and radial dimensions of 0.1 to 0.2 cm, except the chips which had a radial dimension of 1 (pine) or 2 cm (fir). The cubes were about 0.3 cm in the longitudinal dimension, less than the length of a softwood fibre. Therefore, longitudinal resistance to mass transfer would not be important for these particles. The Douglas fir sticks and chips had lengths of 2 cm and the Ponderosa pine sticks and chips had lengths of 1 cm. Both longitudinal and tangential resistance to mass transfer would occur in these particles since they were several fibre lengths long and 10s to 100s of fibre diameters thick.

The water-saturated wood particles were transferred to individual flasks as described for the sorption isotherms. In this case only one aqueous toluene concentration was used for

all of the wood particle shapes and the control flask. The stoppers were fitted with ground glass stopcock joints to permit subsampling with a minimum of headspace turnover. Aqueous concentrations were analyzed by HPLC at logarithmically spaced intervals as described for the kinetic isotherm monitoring.

All data from kinetic monitoring are reported on plots of peak area versus time. The HPLC response factor for the calibration standards did not vary over the duration of the time courses. Therefore, peak area was an accurate surrogate for aqueous sorbate concentration. The term aqueous concentration is used in place of peak area in the discussion section.

Equations

Sorption Isotherms

Sorption isotherms were developed from mass balances on the equilibration flasks. At equilibrium, the total mass of sorbate in the initial solution, M_{tot}, was equal to the sorbed mass, M_{wood}, the mass remaining in solution, M_{water}, the mass in the headspace, M_{air}, and the mass dissolved in the water-filled wood porosity, $M_{diss'd}$:

$$M_{tot} = M_{wood} + M_{water} + M_{air} + M_{diss'd} \tag{3}$$

The sorbed compound concentration was calculated by difference from the initial concentration as follows:

$$C_s = \left(\frac{V}{M}\right)\left(C_i - C_w - K_H\left(\frac{V_a}{V}\right)C_w\right) - M_f C_w \tag{4}$$

where C_s (μg/g) is the sorbed concentration; V (mL) is the bulk water volume; M (g) is the dry mass of wood; C_i (μg/mL) is the syringe transfer-corrected initial aqueous concentration; C_w (μg/mL) is the final aqueous concentration; K_H (mL/mL) is the dimensionless Henry's Law constant; V_a (mL) is the headspace volume, and M_f (mL/g) is the mass normalized volume of water-filled wood porosity.

All of the variables in Eq. 4 were measured except Henry's Law constants. K_H values were taken from Schwarzenbach *et al.* (1993). The syringe transfer-corrected initial aqueous concentration was the sorbate concentration measured in the dilution syringe and multiplied

by a factor of 0.92. The sorbate concentrations for 5 wood-free controls were measured immediately before and after transfer to equilibration flasks. The aqueous concentrations in the flasks were found to be only 92 ± 2% of the syringe concentrations. On average, 8% of the sorbate mass was lost for these wood-free controls during syringe transfer, therefore, a constant 8% sorbate loss was also assumed for each of the isotherm flasks. The volume of headspace was determined by the difference in the mass of the equilibration flasks after assembly and prior to isotherm analysis. Losses of sorbate to the 0.2 to 0.6 mL headspace in the flasks were insignificant. Finally, the mass normalized volume of water-filled porosity was calculated by dividing the volume of water lost upon drying the wood particles by the wood dry weight.

Wood partition coefficients were calculated from plots of sorbed concentration versus aqueous concentration. A linear regression was used to fit a linear sorption isotherm to the data:

$$K_{wood} = \frac{C_s}{C_w} \tag{5}$$

where K_{wood} is the wood-water partition coefficient. The linearity of the fits was also verified by fitting the log-transformed data to the log-transformed Freundlich equation:

$$\log C_s = n \log C_w + \log K_f \tag{6}$$

where n is the Freundlich exponent and K_f is the Freundlich coefficient. If the value of n was not significantly different than 1, a linear sorption isotherm was assumed to apply.

Sorption Kinetics

The characteristic time scale for a mass transfer process is the time at which half of the equilibrium sorbed mass has been removed from solution. The mass transfer times that were experimentally measured in the kinetic time courses are referred to as $t_{1/2}$ values in order to distinguish them from characteristic times that are theoretically calculated. Experimental $t_{1/2}$ values were calculated by first fitting a linear equation to the changing aqueous concentrations (before the equilibrium plateau) on a linear-log plot of peak area *v.* time. The

time at which the peak area of the best-fit line was equal to the midpoint of the first measured peak area and the equilibrium plateau was the $t_{1/2}$ value.

Characteristic time scales for mass transfer processes were also theoretically calculated. The important sorptive uptake mechanism for the wood was diffusive mass transfer. The characteristic time at which half of the equilibrium sorbed mass has been removed from solution was assumed a function of a characteristic diffusion length scale and a diffusion coefficient:

$$t = \frac{l^2}{D_{eff}} \tag{7}$$

where l (cm) is the characteristic length and D_{eff} (cm^2/s) is the mass transfer process-specific diffusion coefficient.

Results and Discussion

Equilibrium Sorption Isotherms

Wood-water partition coefficients

Benzene, toluene and *o*-xylene (BTX) were sorbed by particles of Douglas fir and Ponderosa pine wood. The aqueous concentrations of these compounds decreased to a significantly greater extent in flasks with wood particles than in controls containing no wood (Figure 6.5). Compound mass recovered from successive desorptions of the wood particles was greater than 93% of the sorbed mass calculated by difference between the initial and final aqueous concentrations. Thus, solute concentrations in the wood-containing flasks did not decrease by degradation by bacteria or fungi introduced into the solution with the wood. The decrease in aqueous concentrations, relative to the controls, was greater than the decrease calculated for dilution into the water-filled porosity alone. For both woods and all sorbates, the fraction of sorbate mass remaining in the aqueous phase at equilibrium (f_w) was less than would have remained had the bulk sorbate concentration been diluted by diffusion into the water-filled pore spaces of the wood particles. For example, the volume of water in the wood particles for the Ponderosa pine-benzene couple was 13% of the water volume in the

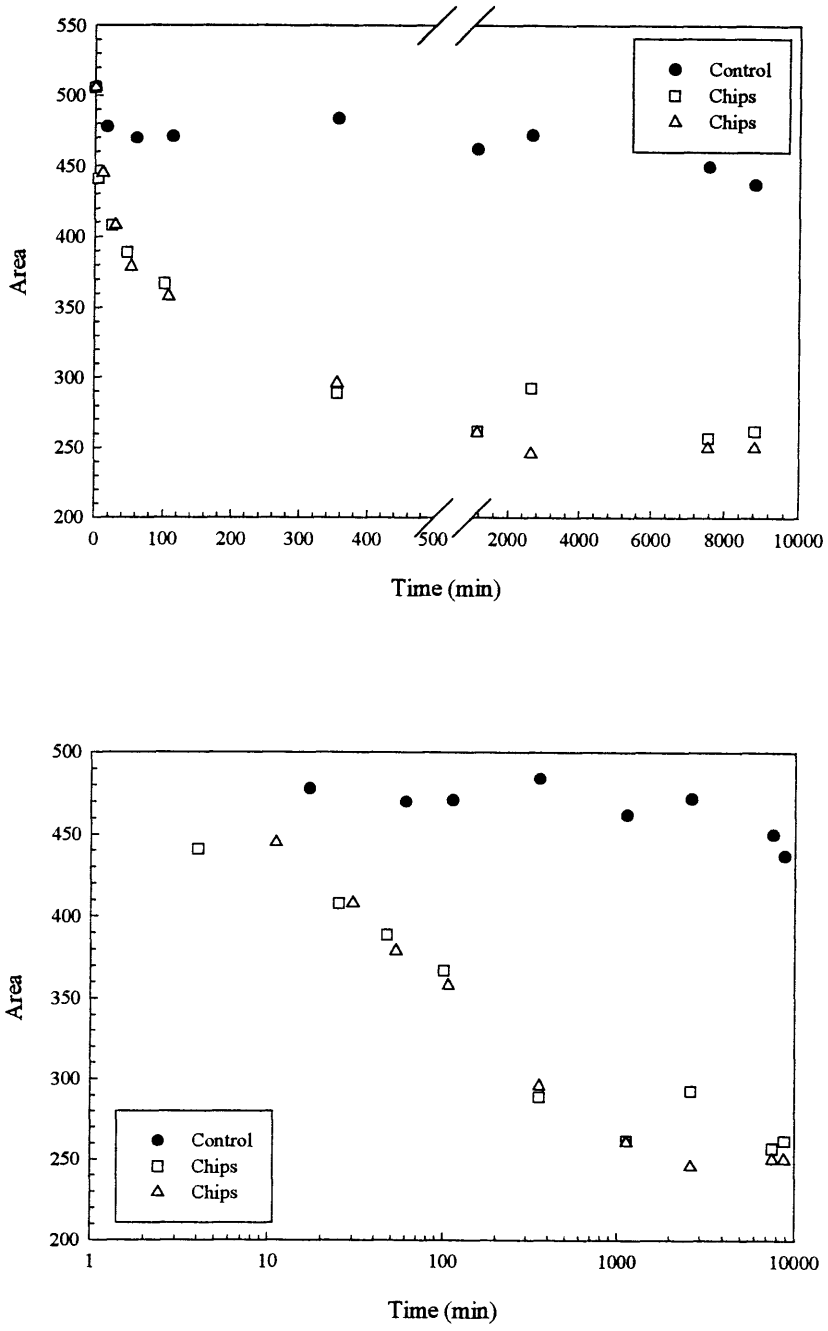

Figure 6.5. Change in aqueous toluene peak area as a function of time for duplicate flasks containing Ponderosa pine chips.

equilibration flask. The concentration of benzene in the bulk solution would be diluted to 88% (1/1.13) of its initial concentration solely by diffusion into the benzene-free pore space water. The observed fraction of benzene mass in the aqueous phase at equilibrium was 54% of the initial mass, indicating that wood uptake in addition to pore space dilution had occurred. An effect of sorbate hydrophobicity on f_w was observed for Douglas fir for which the same solid-to-water ratios were used for each of the isotherms (Table 6.1). The fraction of mass remaining in the aqueous phase decreased with increasing compound hydrophobicity, consistent with sorptive uptake of alkylated benzenes by wood.

The sorptive uptake of toluene was also not limited by sorbent particle size. The fraction of toluene mass remaining in the aqueous phase at equilibrium was 0.56 for Ponderosa pine cubes and sticks and 0.51 for cubes. The equilibrium "accessibility" of the partitioning phase appeared to be independent of wood particle size.

Sorption isotherms were plotted for each of the sorbates and each of the softwoods (Figures 6.6 and 6.7). Errors in the aqueous concentrations were determined from the variability in peak areas of replicate injections and the error in the HPLC sorbate response factor. Errors in aqueous concentration measurements were propagated through Eq. 4 to give the error in solids concentrations. Final control concentrations were 90 ± 3% of the initial transfer-corrected concentrations. No corrections for leakage losses from wood-containing flasks were made.

Most of the sorption isotherms had Freundlich exponents which were not significantly different than 1 when the log-transformed data was fit to Eq. 5. The exceptions were toluene sorption to Ponderosa pine (0.9 ± 0.04) and *o*-xylene sorption to Douglas fir (0.8 ± 0.1). The linear plot of the Douglas fir-*o*-xylene isotherm also had a nonzero intercept. Both of these isotherm characteristics likely resulted from analytical limitations. The equilibrium aqueous phase concentrations of *o*-xylene that were less than 2 μg/mL were near the HPLC detection limit. For these 3 data points, the fraction of compound mass in the water was only 10% while, f_w was 0.39 ± 0.03 for the other data points. If the aqueous phase concentration was underestimated, the solids concentration would be correspondingly overestimated when calculated by difference from the starting concentration. This shift in concentrations would lead to an apparent nonzero isotherm intercept and a nonlinear Freundlich isotherm fit.

Table 6.1. Experimental conditions and partition coefficients for equilibrium isotherms.

	Benzene	Toluene	*o*-Xylene
DOUGLAS FIR			
Equilibration time	8 d	9, 22 d†	5, 15 d†
Average f_w (n = 8)	0.63 ± 0.01	0.57 ± 0.02	0.39 ± 0.03
Porosity dilution‡	0.04	0.04	0.04
K_{wood} (mL/g)	17 ± 0.8	23 ± 1	34 ± 4
K_{lignin} (mL/g)	60	80	110
PONDEROSA PINE			
Equilibration time	12 d	9 d	14 d
Average f_w (n = 9)	0.54 ± 0.03	0.45 ± 0.05	0.48 ± 0.03
Porosity dilution‡	0.13	0.09	0.06
K_d (mL/g)	8.8 ± 0.3	18 ± 2	33 ± 1
K_{lignin} (mL/g)	30	60	110
PHYSICAL CONSTANTS AND PARTITION COEFFICIENTS			
K_{ow} (Miller *et al.*, 1985)	135	450	1350
K_{oc} (Schwarzenbach *et al.*, 1993)	54	180	550
$K_{wood} = f_{oc}K_{oc}$ (mL/g)	30	60	110

† Second value is duplicate measure of same isotherm flasks that were measured at the earlier time point.

‡ Porosity dilution = (Total volume of water in wood particles)/(Bulk volume of water in flask)

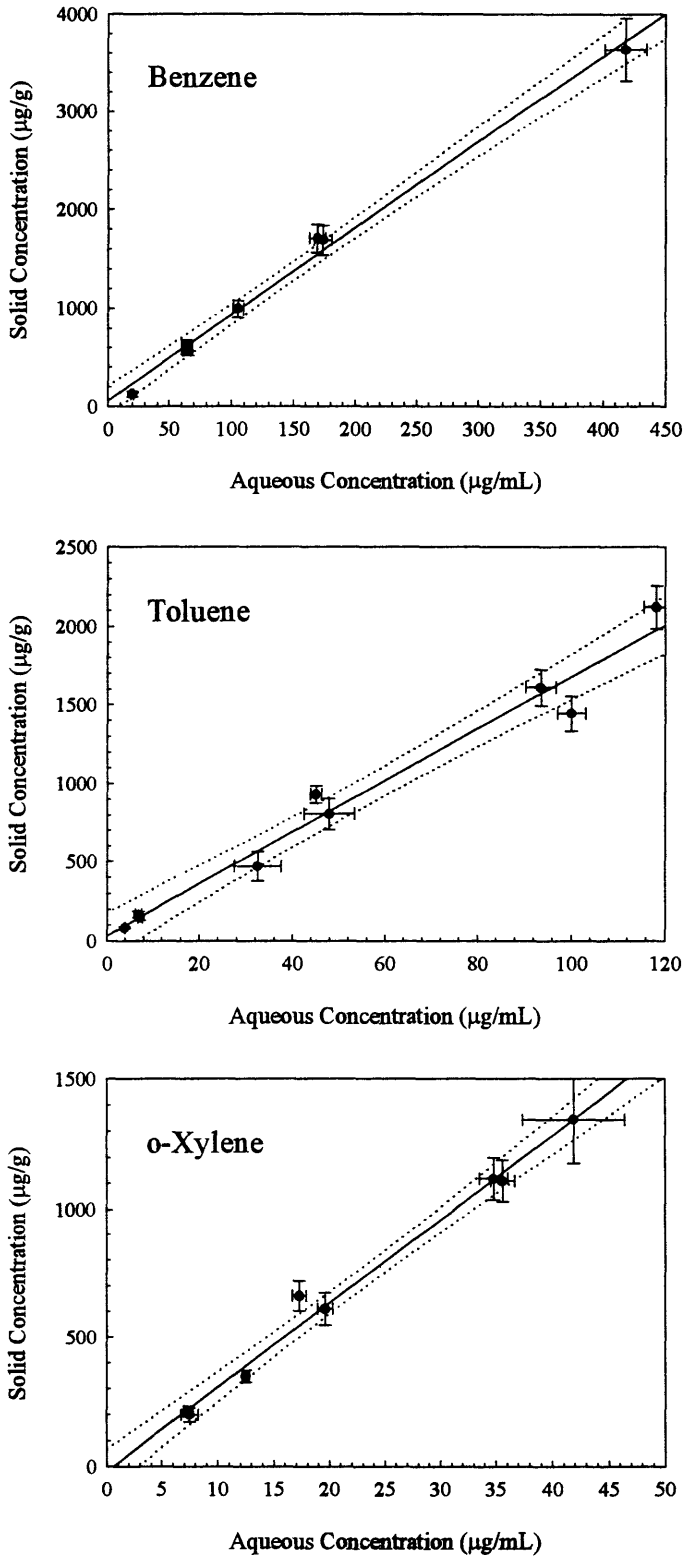

Figure 6.6. Ponderosa pine sorption isotherms. Partition coefficient values are reported in Table 6.1.

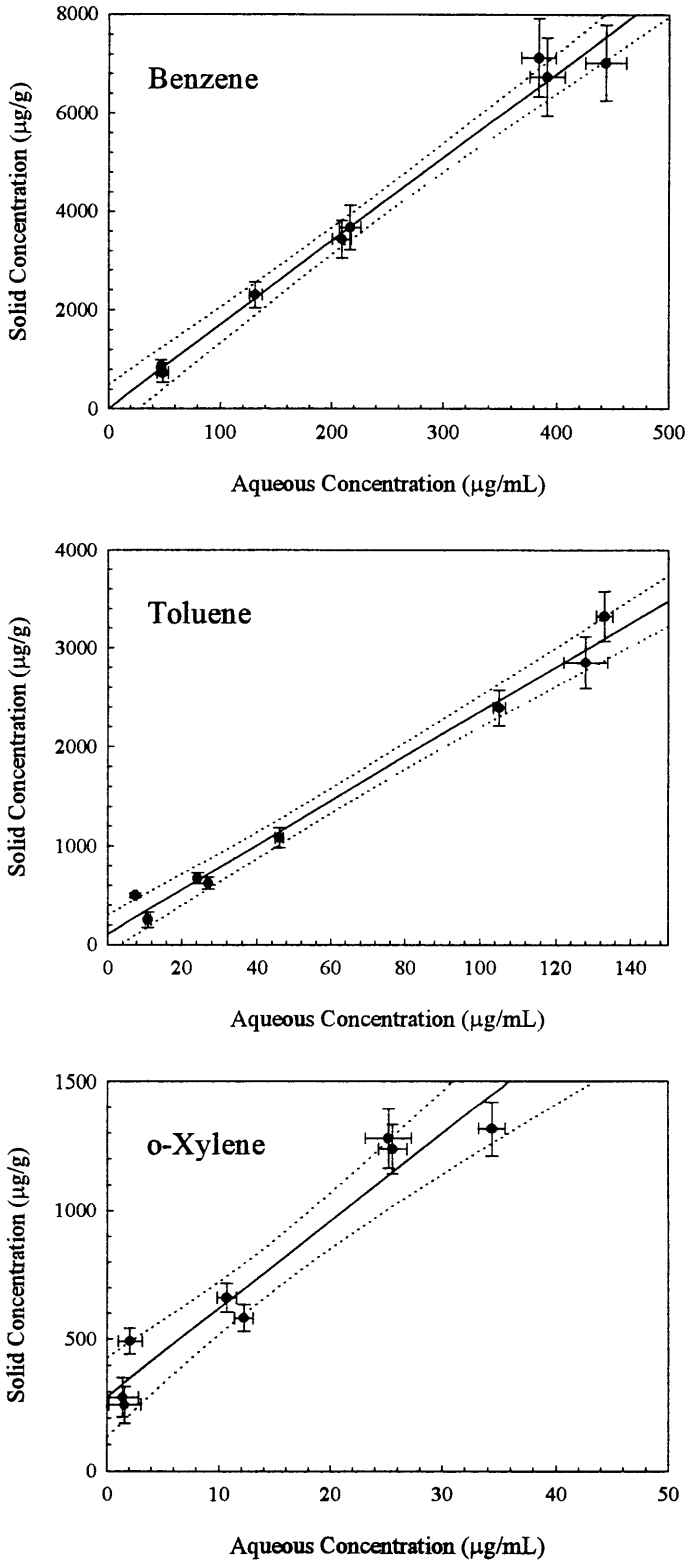

Figure 6.7. Douglas fir sorption isotherms. Partition coefficient values are reported in Table 6.1.

Wood partition coefficients, K_{wood}, were calculated from the slopes of the sorption isotherms (Table 6.1). The partition coefficients for Ponderosa pine approximately doubled from benzene to toluene to *o*-xylene. This trend was consistent with the hydrophobicities of these compounds: the octanol-water partition coefficients approximately triple with the addition of each methyl group to benzene. The wood-water partition coefficients for Douglas fir also increased with hydrophobicity, but not in regular multiples. Benzene and toluene had about the same K_{wood}, while the *o*-xylene K_{wood} was about 50% greater than for toluene. Both of the species of wood did exhibit partition coefficients of similar magnitude.

The lignin-normalized partition coefficients for the wood-BTX pairs were compared to literature values for these sorbates. The range in lignin contents of softwoods is 25-31% by weight (Thompson, 1996). This not a wide enough range to calculate K_{lignin} for undigested wood from a plot of K_{wood} *v.* f_{lignin} (Eq. 1). Rather, we normalized our experimental K_{wood} values directly by dividing by the fractional lignin content. Douglas fir and Ponderosa pine are both about 30% lignin by weight (Parham and Gray, 1984). The resultant K_{lignin} partition coefficients are reported in Table 6.1.

The calculated K_{lignin} values for benzene, toluene, and *o*-xylene showed good agreement with literature partition coefficients for isolated lignins. Xing *et al.* (1994) reported lignin-water partition coefficients for an organosolv lignin of 60, 140, and 330 mL/g for benzene, toluene, and *o*-xylene, respectively. K_{lignin} values for these compounds were 30, 90, and 180 mL/g for an alkali lignin. The toluene partition coefficient for an alkali pine lignin was 100 mL/g (Garbarini and Lion, 1986). If the K_{wood} values for Douglas fir and Ponderosa pine were estimated with alkali lignin partition coefficients, they would have agreed with our measured values to within a factor of 2 or less.

Predictions of wood partition coefficients on an organic carbon basis greatly overpredict our experimental values. Traditionally, partition coefficients for soils and sediments are estimated from the sorbent fraction organic carbon, f_{oc}, and an organic carbon-normalized partition coefficient, K_{oc} (*i.e.*, $K_d = f_{oc}K_{oc}$) (Karickhoff *et al.*, 1979). This method was applied to Douglas fir and Ponderosa pine wood using K_{oc} values estimated from an octanol water partition coefficient linear free energy relationship (Table 6.1) (Schwarzenbach

et al., 1993). The average carbon content of wood is 50% (Wegner *et al.*, 1992) so a value of 0.5 was used for both woods. The calculated partition coefficients, K_d, overestimated the measured values by 2 to 3 times for benzene, 5 times for toluene and 7 to 8 times for *o*-xylene (Table 6.1). This result is not surprising given that only the lignin polymeric wood component has been demonstrated to sorb organic compounds (Xing *et al.*, 1994; Garbarini and Lion, 1986). The carbon content of the wood used to estimate K_d included both lignin carbon and cellulosic carbon which does not contribute to sorption. Douglas fir and Ponderosa pine are about 30% lignin by weight (Parham and Gray, 1984). Since lignin is about 50% carbon by weight (Xing *et al.*, 1994; Garbarini and Lion, 1986), the true sorbing f_{oc} should be $0.5 \times 0.3 = 0.15$, or a factor of 3 less than the f_{oc} used to compute the Table 6.1 K_d values. Accounting for the sorptive capacities of the wood polymers, the wood partition coefficients were estimated to be 8, 30, and 80 for benzene, toluene, and *o*-xylene, respectively. These refined partition coefficient estimates are much closer in value to the wood partition coefficients measured for Douglas fir and Ponderosa pine, but the ratio of calculated-to-measured values is not constant, suggesting that lignin has a different octanol-water free energy relationship than natural organic matter.

Linear Free Energy Relationship for Lignin-Water Partition Coefficients

A linear free energy relationship (LFER) relating lignin and octanol water partition coefficients was developed. Such a free energy relationship is constructed assuming that the same interaction occurs between the sorbate and lignin as between the sorbate and octanol. Lignin exhibits noncompetitive compound uptake with a low (1.8 - 2.6 kcal/mol) heat of sorption (Severtson and Banerjee, 1996), suggesting that organic compounds sorb to lignin by a partitioning mechanism, such as compounds distribute between octanol and water. This argument has been used to develop LFERs for natural organic matter sorption (Chiou *et al.*, 1979). Organic matter macromolecules in an aqueous solution are free to adopt configurations that contain hydrophobic pockets into which organic solutes can partition. In contrast, the function of lignin is to impart rigidity to the wood structure (Parham and Gray, 1984). This may limit the extent to which organic molecules can partition into this polymer. As a note, Severtson and Banerjee (1996) measured heats of sorption and sorptive

competitiveness on wood fibres. These fibres were generated in a pulping process which may have chemically degraded the lignin so that it could more easily form hydrophobic pockets for sorbate molecules. However, intact lignin partition coefficients measured in this experiment compared well with values for highly digested alkali lignin (Xing *et al.*, 1994). This agreement suggests that the tertiary structure of the lignin in intact softwoods does not alter its sorptivity. The linearity of the Douglas fir and Ponderosa pine isotherms was more evidence suggestive of partitioning between lignin and water.

Lignin-water partition coefficients, K_{lignin}, were plotted versus octanol water partition coefficients (Figure 6.8). The regression of the free energy relationship had a slope of 0.71 ± 0.08 and an intercept of 0.08 ± 0.19. If the lignin LFER is converted to a carbon basis by dividing by the 50% carbon content, the resultant equation is:

$$\log K_{lignin}^{oc} = 0.71 \log K_{ow} + 0.38 \qquad \textbf{(8)}$$

This organic carbon-normalized LFER is similar to the free energy relationship for substituted benzenes developed by Schwarzenbach and Westall (1981). The equation for natural aquifer sediment organic matter was $\log K_{oc} = 0.72 \log K_{ow} + 0.49$. The similarity between the free energy relationship slopes of lignin and sediment organic matter is consistent with the diagenic formation of organic matter. Lignin and other plant materials are precursors for natural organic matter in terrestrial systems (Kumada, 1987).

There was remarkable agreement between the K_{lignin} values for several forms and sources of lignin. The individual LFER slopes for Ponderosa pine (0.6) and isolated lignin (lignin O and A slopes = 0.7) were not significantly different than for the whole data set; however, the Douglas fir data had a regression slope of 0.3. The data sets for individual lignins were limited to only three compounds. Thus, it is not clear whether lignin partition coefficients for Douglas fir were distinct from the other wood and lignins. A slope of 0.3 suggests highly unfavorable interactions of the sorbates with this wood, relative to octanol. Certainly the saturated Douglas fir was more rigid than the Ponderosa pine, if the tertiary structure of intact wood is important to sorption. However, as previously noted, K_{lignin} measurements for compounds with a wider range of K_{ow} values is needed to conclude if there

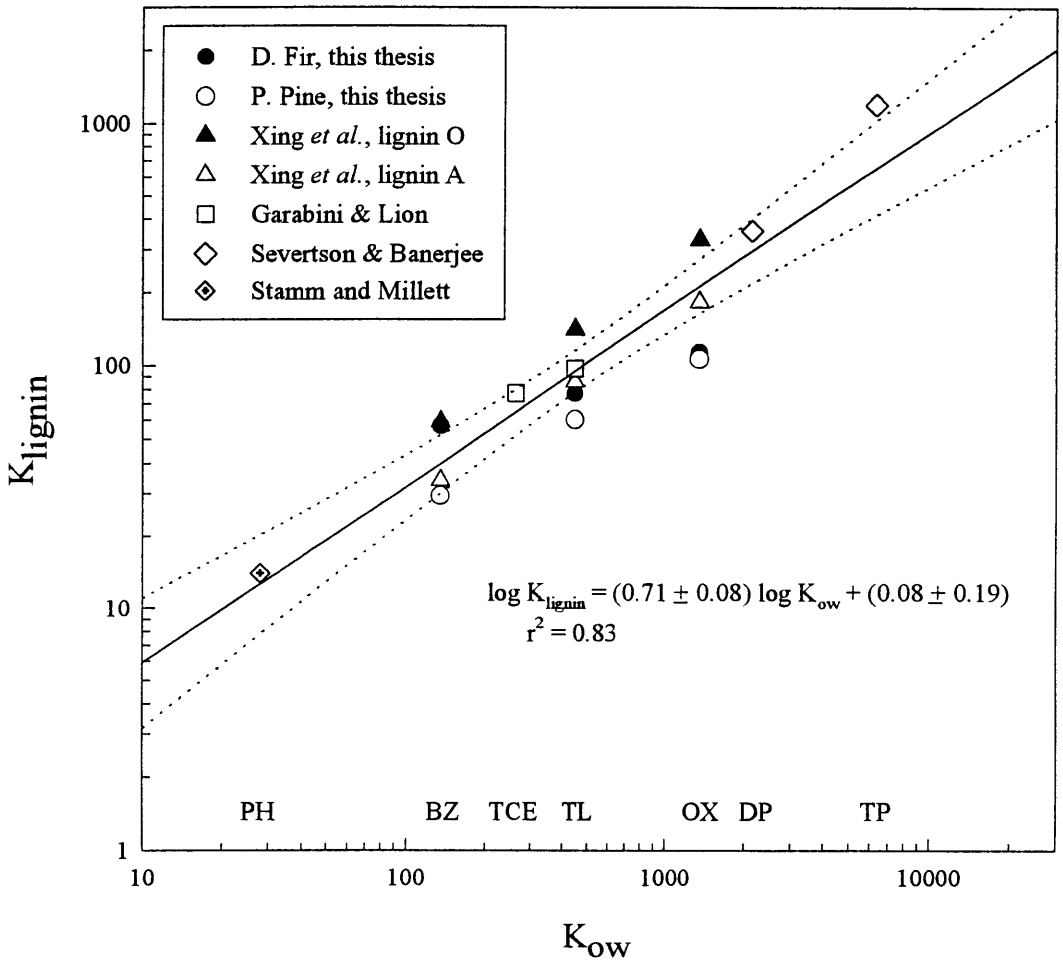

Figure 6.8. Lignin-octanol linear free energy relationship. Experimental and literature data are plotted for phenol (PH), benzene (BZ), trichloroethylene (TCE), toluene (TL), *o*-xylene (OX), 2,4-dichlorophenol (DP), and 2,4,5-trichlorophenol (TP). The solid line is the best fit linear regression with 95% confidence intervals denoted with dotted lines.

are significant sorptive differences between various species of wood lignin. The low slope of the individual Douglas fir LFER may have simply been skewed by the analytical uncertainty in determining the *o*-xylene K_{lignin}.

The intercepts of the individual LFERs varied among the different lignin types. These variations may reflect compositional differences between wood species or extraction methods. By analogy, the aromatic carbon content of natural organic matter allows fine tuning of organic carbon partition values (Chin *et al.*, 1997). Since lignin does not have a well defined molecular structure, the carbon content of the lignin may explain the data spread. For example, lignin O had a carbon content of 65.8% and an intercept of 0.18 and lignin A had a carbon content of 57.1% and an intercept of -0.02. If the carbon-normalized partition coefficient was the same for each of these lignins, the lignin-water partition coefficients would be related:

$$\begin{aligned} \log K^{1}_{lignin} &= \log K^{2}_{lignin} + \log \frac{f^{1}_{oc}}{f^{2}_{oc}} \\ &= \log K^{2}_{lignin} + 0.06 \end{aligned} \qquad \textbf{(9)}$$

If lignin O were lignin^1 and lignin A were lignin^2 in Eq. 9, the intercept for lignin O would be greater than the intercept for lignin A by 0.06 as a result of their differing carbon contents. The observed intercept difference of 0.2 was greater, suggesting that more subtle molecular differences may exist between the two lignin types. As a whole, K_{lignin} values in Figure 6.8 showed remarkable consistency despite the physical structure (whole wood *v.* isolated lignin) and the source (organosolv, alkali, Kraft) of the different lignins.

(Note that a prior lignin-octanol LFER published by Severtson and Banerjee (1996) is erroneous. First, they did not report the source of K_{ow} values. In a compilation of values (Mackay *et al.*, 1992), the reported log K_{ow} for 2,4-dichlorophenol generally fell between 3.1 and 3.2 and the log K_{ow} for 2,4,5-trichlorophenol was between 3.7 and 3.8, ranges both greater than the values used by Severtson and Banerjee. Secondly, they plotted the carbon-normalized lignin-water partition coefficients reported by Garbarini and Lion (1986) without noting the change in nomenclature. Finally, the K_{lignin} values measured by Severtson and

Banerjee in their experiment do not appear to be plotted correctly in their LFER. The plotted log K_{lignin} for 2,4-dichlorophenol, with a value greater than 3, is too great even if it also was carbon-normalized. The K_{lignin} value for 2,4-dichlorophenol was reported in the text as 300 by two methods of determination. With an average carbon content of 50%, the carbon-normalized value would be 600, or 2.8 on a log scale. The 2,4,5-trichlorophenol datum was similarly high. The data of Severtson and Banerjee and Garbarini and Lion were plotted with corrected values in Figure 6.8. The individual LFER equation for this data was still similar to Severtson and Banerjee's lignin free energy relationship: Figure 6.8 slope of 0.9 and intercept of -0.32; Severtson and Banerjee (Severtson and Banerjee, 1996) slope of 0.95 and intercept of -0.48. The LFER developed in Figure 6.8 is a better predictor of lignin-water partition coefficients from octanol-water partition coefficients because it incorporates several lignins from several sources and a wider range of sorbate hydrophobicities.)

The results of these sorption experiments with Douglas fir and Ponderosa pine suggest that the sorption of nonpolar compounds to structurally intact softwoods can be predicted by knowing the lignin content and a lignin-octanol LFER. By extension, it is reasonable to assume that hardwood sorption coefficients can also be predicted from the lignin content. Compositional differences are known to exist between hard- and softwood lignins due to varying ratios of the phenylpropanoid precursors (Parham and Gray, 1984); however, the softwood lignin LFER is probably still applicable to hardwoods. The chemical composition of the three monomer compounds are similar, varying only in the number of methoxyl groups. There are about 0.95 methoxy groups per phenylpropanoid unit in hardwoods and 1.3 to 1.7 methoxyl groups in hardwoods (Genco, 1996).

We note again that the prediction of K_{wood} values from lignin-dominated partitioning is applicable only to fully saturated wood. The rate of diffusion of a wetting front into wood is significantly slower than for sorbent molecules (*e.g.*, 18 days to saturate Ponderosa pine chips, less than 9 days to equilibrate toluene). This may be a possible explanation for the low sorptive uptake of benzene observed by Rael *et al.* (1995), although their equilibration time was greater than a day, the time at which our pine shavings were thought to be saturated.

Kinetics of Wood Sorption

Experimental $t_{1/2}$ Values

Compound peak areas in the Douglas fir and Ponderosa pine-containing flasks decreased with time, with apparent bimodal kinetics. A representative time course is shown in Figure 6.5 for toluene (refer to Appendix D for the complete set of all sorbate-sorbent pairs). A similar pattern was also observed for benzene and *o*-xylene. Sorbate peak areas in wood-containing flasks decreased rapidly over the first 1000 min (17 h) of equilibration, followed by a slower decrease in aqueous concentrations. The time courses were developed by repeated monitoring of compound concentrations in single flasks, rather than sacrificing new flasks at each time point. Over time, the headspace in the flasks increased as subsamples were removed for analysis. Between sampling episodes, the volatile sorbates would partition into this headspace and may have been lost while opening and closing the flasks at each sampling point. In order to verify that sorption equilibrium was reached before 10 000 min, the Douglas fir toluene and *o*-xylene sorption isotherms were measured twice, first after 13 000 and 7200 min, respectively, and again after 31 000 min and 21 000 min, respectively. Since there was no change in the aqueous concentrations of these two sorbates between the first and second sampling times, and sorbate concentrations in wood-free controls also began to noticeably decline at time scales approaching 10 000 min, we concluded that the apparent slow kinetics likely reflected loss mechanisms other than sorption. Therefore, the discussion of wood sorption kinetics focusses on the initial, fast kinetics process when the decrease in aqueous concentrations were dominated by sorptive uptake.

Time courses were plotted for wood particles of varied dimensions to determine the rate limitations to sorptive uptake by this sorbent (Figures 6.9 and 6.10). Wood shavings were hypothesized to have the fastest time to sorptive equilibrium because the lignin in these broken cell wall fragments was accessible to the aqueous solution. Indeed, the fastest uptake of toluene by Ponderosa pine and Douglas fir was observed for the shaved particles (Figures 6.9 and 6.10, Table 6.2). After 30 min of equilibration, toluene peak areas in the aqueous phase remained constant (Douglas fir, Figure 6.10) or decreased at the same rate as the wood-free controls (Ponderosa pine, Figure 6.9), indicating that sorptive uptake was

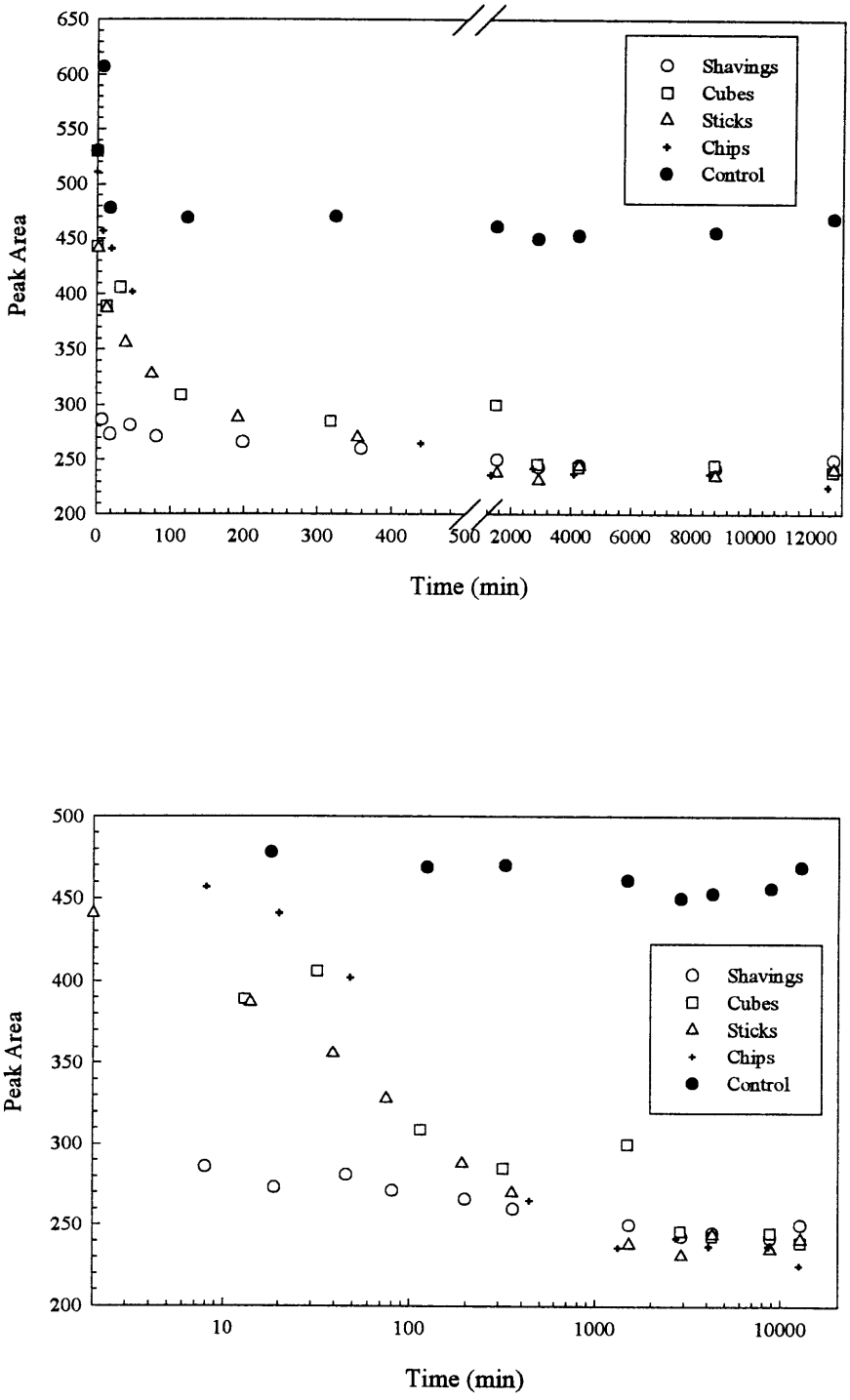

Figure 6.9. Decrease in aqueous peak areas of toluene as a function of time for varied sizes of Ponderosa pine wood particles.

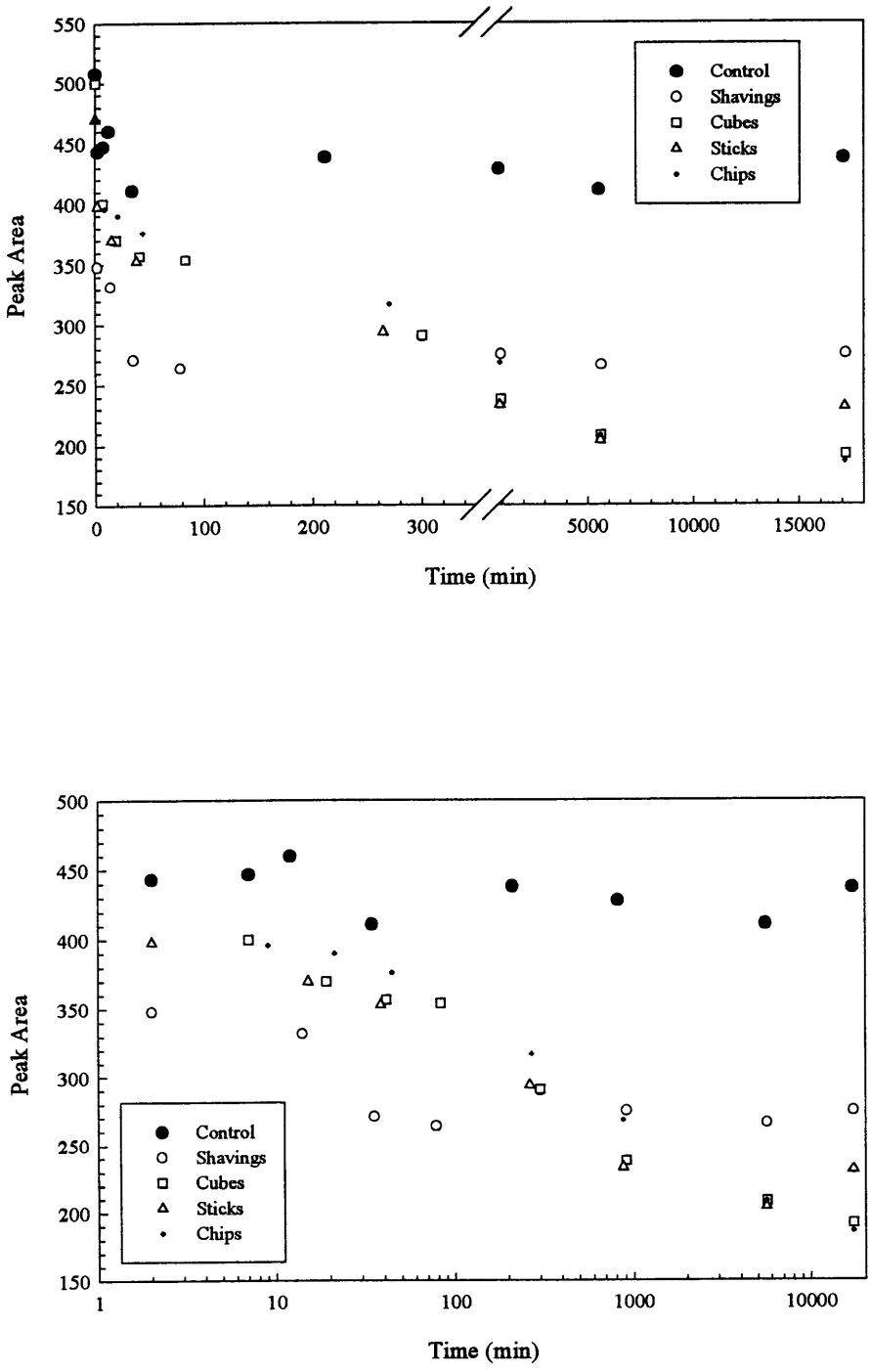

Figure 6.10. Decrease in aqueous peak areas of toluene as a function of time for varied sizes of Douglas fir wood particles.

not important after this time. In contrast, sorptive uptake of toluene by the other wood particles remained an important process for greater than 1000 min. The apparently greater equilibrium peak areas for the Douglas fir and Ponderosa pine shavings, relative to the other wood particles, was a consequence of differing solid-to-water ratios. The solid-to-water ratio in the shavings flasks were lower by a factor of 2 than the other flasks, and hence the fraction of compound mass in the aqueous phase at equilibrium was greater for the wood shavings than the other wood particles.

The Ponderosa pine cubes, sticks and chips all had similar time scales at which 50% of the sorbed mass had been removed from solution (Table 6.2). The values reported in Table 6.2 were from single flasks. The variability among single replicate measures of $t_{1/2}$ was quantified by monitoring duplicate and triplicate kinetic time courses during the sorption isotherm experiments. The time scales to reach 50% uptake for toluene and benzene were between 90 and 120 minutes and 30 and 90 minutes, respectively (Table 6.3). From the range in $t_{1/2}$ values calculated from the multiple time course measurements, individual single point estimates of $t_{1/2}$ were thought to vary by 20 to 50%. Thus, the toluene uptake times for cubes, sticks, and chips were likely not significantly different from one another. Because there was little difference in the uptake times for these particles, and these particles all had a common tangential length scale of 1 to 2 mm, we concluded that the toluene uptake kinetics in Ponderosa pine cubes, chips and sticks was limited by tangential diffusion. If longitudinal diffusion had been important, the uptake times for the sticks and the chips would have been 25 times greater than for the cubes according to Eq. 7 since these particles had longitudinal lengths 5 times greater than the cubes.

The time scale of the fast kinetic process was determined for Douglas fir with data points collected in the first 1000 min of equilibration (Table 6.2). Only the cubes appeared to have reached constant aqueous peak areas by this time (Figure 6.10). The aqueous toluene concentrations for the sticks and chips continued to decrease beyond this time. The sticks were known to reach equilibrium sorptive uptake within 13 000 min from the isotherm experiments so the continued decrease in toluene concentrations in the kinetic time course was probably a result of headspace losses. The time scales for the fast kinetic uptake by the

Table 6.2. Kinetic uptake of toluene by wood particles of various shapes. Reported values are the times, in minutes, at which half of the sorbed mass was taken up by the particles.

	Shavings	Cubes	Sticks	Chips
Douglas fir	2	150	100	270
Ponderosa pine	< 8	60	50	120

Table 6.3. Kinetic uptake by Ponderosa pine chips.

	Benzene	Toluene	*o*-Xylene
$t_{1/2}$ (min)	30 80 90	90 120	110
$r_{bulk}K_d$	0.7	1.1	1.1
D_w (cm^2/s)†	1.06×10^{-5}	9.4×10^{-6}	8.5×10^{-6}
R	7	12	18

†Calculated from Hayduk and Laudie (Schwarzenbach *et al.*, 1993).

Table 6.4. Kinetic uptake by Douglas fir sticks.

	Benzene	Toluene	*o*-Xylene
$t_{1/2}$ (min)	62	100	250
$r_{bulk}K_d$	0.6	0.8	1.2
D_w (cm^2/s)†	1.06×10^{-5}	9.4×10^{-6}	8.5×10^{-6}
R	14	19	27

†Calculated from Hayduk and Laudie (Schwarzenbach *et al.*, 1993).

cubes and sticks were not significantly different within the variability of individual $t_{1/2}$ values, but the chips may have exhibited longer toluene uptake times than the smaller particles.

The effect of compound hydrophobicity on the $t_{1/2}$ values was investigated by comparing the uptake times for each of the isotherm sorbates. In order to compare the kinetics of sorbing compounds, the product of the bulk solid-to-water ratio, r_{bulk}, and the partition coefficient, K_d, must be constant (Wu and Gschwend, 1988; Crank, 1979). This product was near 1 for each of the sorption isotherms and so intercomparisons were made between the uptake times (Tables 6.3 and 6.4). There was no difference in the $t_{1/2}$ values for benzene, toluene, and *o*-xylene and Ponderosa pine. There appeared to be only a slight effect of sorbate hydrophobicity on $t_{1/2}$ times for Douglas fir because *o*-xylene exhibited slightly slower uptake kinetics than benzene and toluene.

Characteristic Diffusion Times - Physically Hindered Diffusion

The measured isotherm $t_{1/2}$ values were compared to characteristic times estimated for the physically hindered and the homogeneous retarded diffusion models. The characteristic times were calculated with Eq. 7 using length scales and diffusion coefficients tuned to our experimental system. First, the characteristic length scale was half the tangential thickness of the wood particles, 0.05 cm. This length scale was used for the homogeneous porous sorbent model because the ratio surface areas in the longitudinal and tangential directions are proportional to the area ratios, and thus wood uptake would be dominated by diffusion in the tangential direction. Secondly, retardation factors were calculated from Eq. 2 (Tables 6.3 and 6.4). The internal solid-to-water ratio was determined from the moisture content of the wood. The values were 0.78 g/mL for sorption of all sorbates to Douglas fir, and 0.65, 0.63 and 0.52 g/mL, respectively, for benzene, toluene and *o*-xylene sorption to pine. The bulk wood partition coefficients (Table 6.1) were used for K_{wood}. Detailed calculations of the diffusion coefficients follow.

Wood diffusion coefficients were first calculated with Stamm's resistance model, accounting for the physical structure of the wood. The individual resistance values for tangential diffusion were calculated with values for Douglas fir from Behr *et al.* (1953) (Appendix C). The resistance model is depicted in Figure 6.11a with values reported as

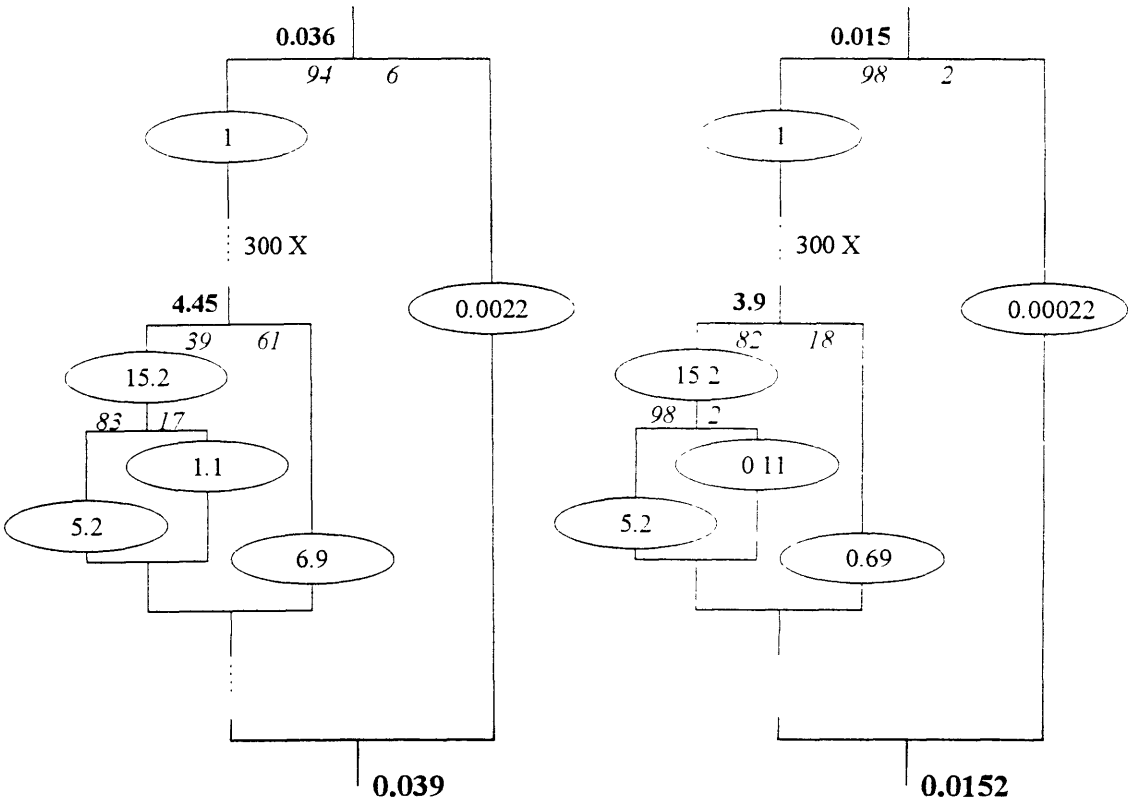

(a) Stamm's diffusion model

(b) Stamm's diffusion model with retarded cell wall diffusion

Figure 6.11. Calculation of tangential Douglas fir conductance with Stamm's resistance model for wood. Conductance values from Behr *et al.* (1953) are noted in the ovals. The conductance of each branch with multiple conductances is noted in bold at each node, and the total conductance is noted in bold at the bottom node. Percentage conductances of each branch are noted in italics.

relative (to aqueous solution) conductances. The overall relative conductance of this "circuit" is 0.04, that is, the tangential wood diffusion coefficient is 0.04 times the aqueous diffusion coefficient. This tangential diffusion coefficient was also applied to Ponderosa pine, but may overestimate the characteristic times for this wood species. Theoretical calculations of the relative tangential conductances for various pine species have yielded 0.03 for Tamarack (Behr *et al.*, 1953) and Western white pine (Burr and Stamm, 1947).

The characteristic times for physically hindered diffusion through wood are reported in Table 6.5. These values were calculated using the wood tangential diffusion coefficient and the aqueous diffusivities reported in Table 6.4. The estimated characteristic times were of the same order of magnitude as the measured $t_{1/2}$ times. The $t_{1/2}$ value for *o*-xylene uptake by Douglas fir was greater than estimated by the hindered diffusion model.

The wood diffusion coefficient was recalculated accounting for sorption to cell wall tissue. In this case, the relative conductances through the pit membranes and cell walls was decreased by a factor of 10, an order of magnitude representation of the wood retardation factors. (The overall conductance was insensitive to the factor of 3 variation in retardation factors between benzene, toluene and *o*-xylene.) The overall conductance was about one third of the value without tissue retardation, yielding characteristic times greater than the measured values (Table 6.5).

The wood sorption kinetics for benzene, toluene and *o*-xylene had $t_{1/2}$ times that fell between estimates with solely hindered diffusion and hindered diffusion with cell tissue retardation. From our isotherm experiments, these compounds are known to sorb to the wood cell wall tissue. It is not known how the tendency to sorb affects the diffusional mechanism for these sorbates. For example, if surface diffusion is important, times may be faster than required for retarded cell tissue diffusion which assumed free liquid diffusion. The low heats of sorption and the noncompetitiveness of sorption to wood (Severtson and Banerjee, 1996) suggest an absorptive partitioning to wood; however, there is adsorptive compound uptake by wood at high sorbate concentrations. Sorption isotherms for stearic acid and phenol have been used to estimate internal surface area of sugar pine (Stamm and Millet, 1941). If wood sorption

Table 6.5. Estimated characteristic mass transfer times (min) for hindered and retarded diffusion.

Diffusion Model	Benzene	Toluene	*o*-Xylene
Stamm's model (Figure 6.11a)	100	110	130
Stamm's model with retardation (Figure 6.11b)	260	300	330
Homogeneous porous sorbent with retarded diffusion	60	80	330

was an adsorptive process, surface diffusion may be an important internal mass transfer process.

Characteristic Diffusion Times - Homogeneous Retarded Diffusion

The second model for sorbate uptake by wood assumed a homogeneous porous sorbent with retarded diffusion. The sorbate aqueous diffusivities were divided by the Douglas fir retardation factors to give the characteristic diffusion coefficients used in Eq. 7. The characteristic times for retarded diffusion were of the same order of magnitude as the measured values with the exception of underestimating the Douglas fir-*o*-xylene $t_{1/2}$ time.

The applicability of a physically hindered diffusion model or a homogeneous retarded diffusion model for wood diffusion kinetics can not be concluded from these experimental results. For the sorbates used, the characteristic times calculated with both of these models were the same, and in general agreement with the experimental observations. The sorption kinetics of a more hydrophobic compound may suggest which model better describes the uptake of sorbing compounds by wood. For example, a compound such as pentamethylbenzene, with a K_{ow} of $10^{4.6}$ (Hansch *et al.*, 1995), has a retardation factor of 165 (assuming the Ponderosa pine lignin-octanol LFER, f_{lignin} of 0.3, and r_{sw} of 0.6 g/mL). Stamm's diffusion model with cell wall retardation reaches an asymptotic relative conductance of 0.012 for compounds of this hydrophobicity. The corresponding characteristic diffusion time for pentamethylbenzene (370 min) is much less than the characteristic time of 750 min for retarded diffusion of this compound. If the measured $t_{1/2}$ value for pentamethylbenzene were closer to the values obtained for BTX, we would conclude that diffusion into wood is not adequately represented by assuming wood is a homogeneous porous sorbent. Further investigation into the mechanism for diffusion of sorbing compounds into wood was beyond the scope of this investigation.

Environmental Relevance

The results of our equilibrium sorption study have implications with respect to the transport of groundwater contaminants at industrial sites with wood present in the aquifer solids. At these sites, plume movement of organic compounds would be underestimated using an organic carbon-based retardation model. The fraction of lignin in the solids must be

quantified and a lignin LFER used to predict the wood partition coefficient. The applicability of our softwood lignin-octanol free energy relationship to hardwoods was not investigated in this study, but, as noted, softwoods may be the dominant species of woods at industrial sites due to their prevalence in construction lumber. Wood and paper products are also found in landfills. From 1 to 4% by weight of municipal refuse is wood, although this percentage is greater for landfills that accept demolition wastes and paper products compose 30 to 60% of refuse by weight (Niessen, 1977). Estimates of leachate transport through these fill solids must account for the high fraction of cellulose carbon which exhibits almost no sorption of organic contaminants.

The timescale for kinetic exchange of contaminants between wood and groundwater may be fast relative to other environmental processes. The actual timescale is a function of the average wood particle size, but for cm-sized wood chips, sorption kinetics were much faster than slow diffusion from natural organic matter (Ball and Roberts, 1991; Steinberg *et al.*, 1987). Thus, diffusive exchange from wood would not be rate-limiting relative to the timescales of pump-and-treat remediation technologies.

References

Ball, W. P.; Roberts, P. V. (1991). "Long-term sorption of halogenated organic chemicals by aquifer materials. Part 2. Intraparticle diffusion." *Environmental Science and Technology* **25**: 1237-1249.

Barton, A. F. M. (1975). "Solubility parameters." *Chemical Reviews* **75**: 731-753.

Barton, A. F. M. (1983). *CRC Handbook of Solubility Parameters and Other Cohesion Parameters*. Boca Raton, FL, CRC Press, Inc.

Behr, E. A.; Briggs, D. R.; Kaufert, F. H. (1953). "Diffusion of dissolved materials through wood." *Journal of Physical Chemistry* **57**: 476-480.

Bodig, J. (1982). "Moisture Effect on Structural Use of Wood." In *Structural Use of Wood in Adverse Environments*. R. W. Meyer ,R. M. Kellogg, Eds.. New York, Van Nostrand Reinhold Co.

Burr, H. K.; Stamm, A. J. (1947). "Diffusion in wood." *Journal of Physical and Colliod Chemistry* **51**: 240-261.

Cady, L. C.; Williams, J. W. (1935). "Molecular diffusion into wood." *Journal of Physical Chemistry* **39**: 88-103.

Chin, Y.-P.; Aiken, G. R.; Danielson, K. M. (1997). "Binding of pyrene to aquatic and commercial humic substances: The role of molecular weight and aromaticity." *Environmental Science and Technology* **31**: 1630-1635.

Chiou, C. T.; Peters, L. J.; Freed, V. H. (1979). "A physical concept of soil-water equilibria for nonionic compounds." *Science* **206**: 831-932.

Crank (1979). *The Mathematics of Diffusion*. Oxford, Clarendon Press.

Dellicoli, H. T. (1977). "Controlled Release of Pesticides from Kraft Lignin Carriers." In *Controlled Release Pesticides*. H. B. Scher, Ed. Washington, DC, American Chemical Society.

Fengel, D. (1971). "The distribution of aqueous solutions within wood." *Journal of Polymer Science, Part C* **36**: 141-152.

Garbarini, D. R.; Lion, L. W. (1986). "Influence of the nature of soil organics on the sorption of toluene and trichloroethylene." *Environmental Science and Technology* **20**: 1263-1269.

Genco, J. M. (1996). "Pulp." In *Encyclopedia of Chemical Technology*. J. I. Kroschwitz, Ed. New York, Wiley.

Hansch, C.; Leo, A.; Hoekman, D. (1995). *Exploring QSAR: Hydrophobic, Electronic and Steric Constants*. Washington, DC, American Chemical Society.

Higuchi, T. (1980). "Lignin Structure and Morphological Distribution in Plant Cell Walls." In *Lignin Biodegradation: Microbiology, Chemistry and Potential Applications*. T. K. Kirk, T. Higuchi ,H.-M. Chang, Eds.. Boca Raton, FL, CRC Press. **1**.

Karickhoff, S. W.; Brown, D. S.; Scott, T. A. (1979). "Sorption of hydrophobic pollutants on natural sediments." *Water Research* **13**: 241-248.

Kopinke, F.-D.; Porschmann, J.; Stottmeister, U. (1995). "Sorption of organic pollutants on anthropogenic humic matter." *Environmental Science and Technology* **29**: 941-950.

Kumada, K. (1987). *Chemistry of Soil Organic Matter*. Tokyo, Japan Scientific Societies.

Luthy, R. G.; Dzombak, D. A.; Peters, C. A.; Roy, S. B.; Ramaswami, A.; Nakles, D. V.; Nott, B. R. (1994). "Remediating tar-contaminated soils at manufactured gas plant sites." *Environmental Science and Technology* **28**: 266A-276A.

Mackay, D.; Shiu, W. Y.; Ma, K. C. (1992). *Illustrated Handbook of Physical-Chemical Properties and Environmental Fate of Organic Chemicals*. Boca Raton, FL, Lewis Publishers.

Niessen, W. R. (1977). "Properties of Waste Materials." In *Handbook of Solid Waste Management*. D. G. Wilson, Ed. New York, Van Nostrand Reinhold.

Parham, R. A.; Gray, R. L. (1984). "Formation and Structure of Wood." In *The Chemistry of Solid Wood*. R. Rowell, Ed. Washington, DC, The American Chemical Society. **207:** 3-56.

Pearl, I. A. (1967). *The Chemistry of Lignin*. New York, Marcel Dekker.

Petterson, R. C. (1984). "The Chemical Composition of Wood." In *The Chemistry of Solid Wood*. R. Rowell, Ed. Washington, DC, The American Chemical Society. **207:** 59-126.

Rael, J.; Shelton, S.; Dayaye, R. (1995). "Permeable barriers to remove benzene: Candidate media evaluation." *Journal of Environmental Engineering* **121**: 411-415.

Rutherford, D. W.; Chiou, C. T.; Kile, D. E. (1992). "Influence of soil organic matter composition on the partition of organic compounds." *Environmental Science and Technology* **26**: 336-340.

Schwarzenbach, R. P.; Gschwend, P. M.; Imboden, D. M. (1993). *Environmental Organic Chemistry*. New York, NY, John Wiley & Sons, Inc.

Schwarzenbach, R. P.; Westall, J. (1981). "Transport of nonpolar organic compounds from surface water to groundwater: Laboratory sorption studies." *Environmental Science and Technology* **15**: 1360-1367.

Severtson, S. J.; Banerjee, S. (1996). "Sorption of chlorophenols to wood pulp." *Environmental Science and Technology* **30**: 1961-1969.

Siau, J. F. (1984). *Transport Processes in Wood*. New York, Springer-Verlag.

Stamm, A. J. (1964). *Wood and Cellulose Science*. New York, The Ronald Press Company.

Stamm, A. J.; Millet, M. A. (1941). "The internal surface area of cellulosic materials." *Journal of Physical Chemistry* **45**: 43-54.

Steinberg, S. M.; Pignatello, J. J.; Sawhney, B. L. (1987). "Persistence of 1,2-dibromoethane in soils: Entrapment in intraparticle micorpores." *Environmental Science and Technology* **21**(12): 1201-1208.

Thompson, N. S. (1996). "Hemicellulose." In *Encyclopedia of Chemical Technology*. J. I. Kroschwitz, Ed. New York, Wiley.

Wegner, T. H.; Baker, A. J.; Bendtsen, B. A.; Brenden, J. J.; Eslyn, W. E.; Harris, J. F.; Howard, J. L.; Miller, R. B.; Petersen, R. C.; Rowe, J. W.; Rowell, R. M.; Simpson, W. T.; Zinkel, D. F. (1992). "Wood." In *Kirk-Other Encyclopedia of Chemical Technology*. J. I. Kroschwitz ,M. Howe-Grant, Eds.. New York, John Wiley and Sons.

Wu, S.-C.; Gschwend, P. M. (1988). "Numerical modeling of sorption kinetics of organic compounds to soil and sediment particles." *Water Resources Research* **24**: 1373-1383.

Xing, B.; McGill, W. B.; Dudas, M. J. (1994). "Cross-correlation of polarity curves to predict partition coefficients of nonionic organic contaminants." *Environmental Science and Technology* **28**: 1929-1933.

Chapter 7.

SUMMARY OF RESULTS AND FUTURE STUDY OF INDUSTRIAL SITES

Introduction

This thesis was undertaken with the broad goal of understanding the unique characteristics of contaminated sites with a history of industrial activity that has resulted in significant anthropogenic reworking of the subsurface solids. A former manufactured gas plant with a 150 year history of industrial operation was investigated as a representative example of such sites. Characterization of the unique properties of the subsurface solids and groundwater transport processes proceeded on several fronts involving both laboratory and field work. In this chapter, the reverse process is followed and the various lines of investigation are drawn together to predict the transport of contaminants at this coal tar site. These calculations demonstrate that the anthropogenic fill solids have transport properties that vary significantly from natural aquifers. The scope of the discussion is then broadened to discuss areas of further investigation which would enhance our understanding of groundwater transport and reaction processes at industrial sites. A general approach for remedial investigations at these sites is also outlined.

Summary of Results

The groundwater transport of organic contaminants is a function of both the mobile contaminant load and individual compound interactions with the solid phase. At Site YYZ, a former manufactured gas plant with subsurface coal tar contamination, the source of aromatic hydrocarbons in the groundwater was found to be equilibrium coal tar dissolution. Evidence of colloid-enhanced groundwater solubilization and biodegradation of compounds were found by quantifying groundwater concentrations of individual compounds from this multi-component source. The subsurface solids, a mixture of manufactured gas production wastes and anthropogenic fill, contained various organic carbon-containing materials in addition to natural organic matter. These fill solids exhibited solid-water partition coefficients that were unique from natural organic matter.

The solid-water partitioning of monoaromatic compounds to wood was investigated further. A linear free energy relationship was developed to enable prediction of wood partition coefficients from octanol water partition coefficients. The sorption kinetics of wood

particles similar in size to those found at Site YYZ were fast relative to groundwater advection.

Application of Results to Transport Calculations at Site YYZ

The effect of colloid-enhanced solubility and the presence of various organic carbon-containing fill solids on groundwater transport at Site YYZ were quantified by calculating retardation factors for these two cases. The calculated retardation factors were compared to estimates of retardation with no colloid-association of contaminants and natural organic matter-dominated solid-water partitioning. These calculations are a hypothetical demonstration of the importance of accurately characterizing groundwater phase transfer and reaction processes at other industrial sites. As discussed in Chapter 2, the groundwater at Site YYZ is saturated with respect to coal tar constituents. Thus, predictions of transport, such as the travel time for a contaminant from to impact a sensitive receptor (*e.g.*, a drinking water well), are not applicable to the anthropogenic fill at this coal tar site. The following retardation factor calculations assume groundwater transport away from the source into a water-bearing unit not already impacted by contaminants.

The influence of colloids on the rate at which a breakthrough front of hydrophobic aromatic hydrocarbons travels relative to the rate with no colloidal transport depends upon the model for contaminant exchange between the colloid, solid and aqueous phases and the model for colloid exchange between the mobile and immobile phases (Corapcioglu and Jiang, 1993). Under the assumption of linear equilibrium partitioning of the contaminant to the colloid and solid phases, and linear equilibrium partitioning of the colloids to the solid phase, and a constant groundwater colloid concentration, the retardation factor is given as (Corapcioglu and Jiang, 1993):

$$R = 1 + \frac{r_{sw} K_d}{1 + (COLL) K_{COLL}}. \qquad (1)$$

where r_{sw} (g/mL) is the solid-to-water ratio; K_d (mL/g) is the solid-water partition coefficient; (COLL) (g/mL) is the concentration of colloids in the groundwater, and K_{COLL} (mL/g) is the colloid-water partition coefficient. This equation is applicable to suspended organic matter

colloids which have a lesser tendency to partition to the immobile solid phase than do polycyclic aromatic hydrocarbons (Magee *et al.*, 1991). For PAHs, the product of the solid-to-water ratio and the partition coefficient is generally much greater than 1 so the retardation factor for these compounds in colloid-containing groundwater is reduced by a factor of $(1 + (COLL)K_{COLL})$ relative to a system with no colloids. This factor is equal to the enhancement factor calculated by taking the ratio of enhanced solubilities (observed groundwater concentrations, Chapter 2) to compound solubilities with no colloids present (measured tar-water equilibrium, Chapter 2). The enhancement factors for benzo(a)pyrene at well W40M ranged from 4 to 16. In a hypothetical groundwater aquifer with similar colloid characteristics, the retardation factor for benzo(a)pyrene would be reduced by a factor of 4 to 16 relative to predictions assuming no colloids. For a typical natural aquifer ($f_{oc} = 10^{-3}$ g/g), the benzo(a)pyrene retardation factor would decrease from about 1000 to about 100 with this magnitude of colloid-enhanced solubility. This colloid-impacted retardation factor for benzo(a)pyrene is still high, but if the industrial site that was the source of this groundwater contamination had been in operation for over 100 years, sufficient time may have elapsed for benzo(a)pyrene to have been transported to sensitive receptors, even with a retardation factor of 100.

Note that the retardation factor was used here as a convenient comparator for assessing colloid-facilitated groundwater contaminant transport. The retardation factor does not account for the increased flux (over the only dissolved case) of contaminants away from the source facilitated by colloid-association of a population of contaminant molecules. To predict the true impact of colloidal transport on contaminant mobility a set of coupled transport equations are required - one transport equation for the dissolved contaminant and one transport equation for the colloid phase (Corapcioglu and Jiang, 1993).

Naphthalene retardation factors were calculated for particular depths in the fill solids at which only one type of organic carbon-containing material was found. For the purposes of demonstration, this calculation did not account for the presence of nonaqueous phase liquids (NAPL) in the solids. At all depths, solid-water partitioning was dominated by tar-water partitioning. In Chapter 5, natural organic matter-based partition coefficient calculations were

Table 7.1. Naphthalene retardation factors as a function of depth at Site YYZ.

Depth	Sorbent	f_{oc}*	R† ($K_d = f_{oc}K_{oc}$)	R‡ ($K_d = \Sigma f_i K_i$)
3.0 m	wood chips	0.04	170	36
3.7 m	coke	0.54	2300	1
6.7 m	natural solids	0.001	5	5

* Fraction organic carbon calculated by subtracting the nonaqueous phase liquid content determined by residue on evaporation of solvent extraction, assuming 80% carbon content, from the total organic carbon at the depth (values reported in Figure 5.1, Chapter 5).

† $R = 1 + r_{sw}K_{trad}$
where r_{sw} (g/mL) is the solid-to-water ratio, here assumed 5 g/mL
and $K_{trad} = f_{oc}K_{oc}$ (mL/g)
where f_{oc} (g/g) is the fraction organic carbon and K_{oc} = 850 mL/g for naphthalene (Chapter 5).

‡ $R = 1 + r_{sw}K_d$
where $K_d = \Sigma f_i K_i$ (mL/g)
and $f_{lignin} = 0.3\ f_{oc}$, K_{lignin} = 580 (mL/g), and K_{coke} = 0 (mL/g) (Chapter 5).

shown to underestimate the solid-water partition coefficients, and hence retardation factors, in NAPL-containing solids. Here, natural organic matter-based partition coefficients are shown to overpredict retardation in aquifer solids composed of other organic-carbon containing materials (Table 7.1). Retardation factors were underestimated by factors of 5 (wood) and 2300 (coke). Therefore, sorbent-specific partition coefficients are required to estimate contaminant transport through organic carbon-containing aquifer solids.

Areas of Further Investigation

Further investigation into understanding groundwater fate processes is required in order to predict which mechanisms would be operative at other industrial sites as a result of the history of industrial processes at those sites. An important fate process that requires further investigation is the conditions under which organic colloids are present in groundwater. Organic colloids in contaminant plumes show an increased capacity to sorb hydrophobic contaminants over organic colloids in pristine environments (Hawley, 1996; Backhus and Gschwend, 1990), but the source and composition of these colloids are not known. It has been suggested that organic colloids are contaminant molecules that have been partially metabolized by microbes (Hawley, 1996). In fill solids at industrial sites, organic colloids may also be generated by microbial degradation of the fill materials, such as wood. A understanding of the sources of organic colloids in contaminant plumes may also help to explain the temporal (Chapter 2, Backus (1990)) and spatial (Chapter 2) variability in colloid presence in groundwater.

The occurrence of biodegration at industrial sites is a second fate process that is not well understood. Microbes have been shown to degrade a variety of different organic contaminants with many different terminal electron acceptors. Industrial sites have great potential for increased bioattenuation over natural aquifers because of the wide variety of fill materials and wastes that may have been disposed. For example, at Site YYZ buried pipes may have been a source for methane, iron-containing minerals were buried in the subsurface and the groundwater contained high levels of sulphate. With a better understanding of the primary mechanisms of microbial degradation, predictions of the potential for contaminant

bioattenuation at an industrial site may be made with knowledge of the industrial processes and the possible waste products that could be buried on site.

There is a need to incorporate multiple-component contaminant sources in transport models. The relative distributions of compounds with varied physical-chemical properties in space (site investigation monitoring wells) and time (pump tests) can give information about potential rate limitations or natural attenuation processes before remediation technologies are implemented. Remedial approaches can then be designed to account for these processes.

Better methods are required to quantify the various organic-carbon-containing fill solids in anthropogenic fill materials. Selective digestions were proposed as a method to quantify various sorbent materials in a mixture. The presence of nonaqueous phase liquids in aquifer are not well quantified. NAPLs that are less dense than water can be quantified by absorption with a foam plug after release from the solids in an aqueous medium (Cary *et al.*, 1991). No similar method exists for the quantification of nonaqueous phase liquid mixtures, such as coal tar, that are denser than water. These NAPLs are quantified by bulk solvent extraction that also includes sorbed compounds. A method that tries to assess the presence of NAPL by subsequently calculating whether the aqueous solubility of a compound would have been exceeded in the pore water requires prior knowledge of the NAPL composition and may mistake small concentrations of NAPL as no NAPL (Feenstra *et al.*, 1991). These small concentrations may still be abundant enough to limit pump-and-treat based remediation (MacKay *et al.*, 1996).

General Approach to Remedial Investigations of Contaminated Sites with a History of Industrial Activity

The groundwater contaminants and the subsurface solids at a particular industrial site are unique to the history and manufacture of operations that occurred at the site. A general guideline to remedial investigation at an industrial site must begin with a review of the history of manufacture to know possible reagents and starting materials, products and wastes that were used or generated on the site. These are the most likely materials to compose on-site anthropogenic fill and groundwater contaminants. While the actual investigation and remediation approaches will be unique to the property, it is necessary to gather concentration

data for compounds with varied physical-chemical properties (*e.g.*, octanol water partition coefficient, Henry's law constant, and approriate others) to help understand groundwater fate processes. Individual compound analyses require better analytical precision than bulk measures of contamination (*e.g.*, total petroleum hydrocarbons, total volatile organic compounds); however, this added expense at strategic sample locations (in space or time) may help to save remediation costs. For example, remediation costs may be lowered by identifying rate-limitations to clean-up before remediation systems are designed. At sites where nonaqueous phase liquids are present, calculations of the expected equilibrium aqueous phase concentrations should be made using Raoult's Law. These values will provide a comparison case for groundwater monitoring to gather information about dominant groundwater processes and sampling artifacts. Finally, the future clean-up of other industrial sites will benefit from the dissemination of information about unique obstacles to remediation and innovative approaches used at industrial sites. There are many classes of sites which have similar groundwater contaminants and waste products (*e.g.*, coal tar sites), and thus publication of case studies in peer-reviewed literature will increase the body of knowledge about these industrial sites and aid the design of investigative and remediation approaches at other similar sites.

References

Backhus, D. A. (1990). *Colloids in Groundwater: Laboratory and Field Studies of Their Influences on Hydrophobic Organic Contaminants.* Ph.D. Thesis, Massachusetts Institute of Technology.

Backhus, D. A.; Gschwend, P. M. (1990). "Fluorescent polycyclic aromatic hydrocarbons as probes for studying the impact of colloids on pollutant transport in groundwater." *Environmental Science and Technology* **24**: 1214-1223.

Cary, J. W.; McBride, J. F.; Simmons, C. S. (1991). "Assay of organic liquid contents in predominantly water-wet unconsolidated porous media." *Journal of Contaminant Hydrology* **8**: 135-142.

Corapcioglu, M. Y.; Jiang, S. (1993). "Colloid-facilitated groundwater contaminant transport." *Water Resources Research* **29**: 2215-2226.

Feenstra, S.; Mackay, D. M.; Cherry, J. A. (1991). "A method for assessing residual NAPL based on organic chemical concentrations in soil samples." *Ground Water Monitoring Review* **11**(Spring): 128-136.

Hawley, C. M. (1996). *A Field and Laboratory Study of the Mechanisms of Facilitated Transport of Hydrophobic Organic Contaminants.* M.S. Thesis, University of Colorado.

MacKay, A. A.; Chin, Y.-P.; MacFarlane, J. K.; Gschwend, P. M. (1996). "Laboratory assessment of BTEX soil flushing." *Environmental Science and Technology* **30**: 3223-3231.

Magee, B. R.; Lion, L. W.; Lemley, A. T. (1991). "Transport of dissolved organic macromolecules and their effect on the transport of phenanthrene in porous media." *Environmental Science and Technology* **25**: 323-331.

Appendix A.

AQUEOUS SOLUBILITY OF AROMATIC HYDROCARBONS IN EQUILIBRIUM WITH COAL TAR

Introduction

The expected equilibrium groundwater concentrations of organic contaminants are often of interest at sites with nonaqueous phase liquids (NAPLs) present. Contaminants will dissolve from the NAPL source until individual compound fugacities are equal in the groundwater and the nonaqueous phase. The equilibrium aqueous compound concentrations can be predicted with knowledge of the NAPL composition and theoretical expressions for the ratio of phase fugacities (Schwarzenbach *et al.*, 1993; Prausnitz *et al.*, 1986). For multi-component nonaqueous phase mixtures, dissolution of individual compounds is expected to obey Raoult's Law:

$$C_w = \gamma_N X_N C_{sat}(L) \qquad (1)$$

where C_w (mg/L) is the equilibrium aqueous concentration, γ_N is the activity coefficient in the NAPL phase, X_N is the compound mole fraction in the NAPL phase, and C_{sat} (L) (mg/L) is the saturated aqueous phase solubility of the pure liquid compound.

Raoult's Law for mixtures of organic compounds is modified by the inclusion of a nonaqueous phase activity coefficient, γ_N. This variable accounts for differences in molecular size, shape and intermolecular forces between the solute compound and the solvent NAPL phase. The magnitude of these solution nonidealities cannot easily be predicted, although empirical expressions for activity coefficients have been developed (Prausnitz *et al.*, 1986). Generally, organic liquid phases in the environment are mixtures of similar compounds (*e.g.*, chlorinated solvents, aliphatic hydrocarbons, etc.) and thus ideal solubility of individual components in the NAPL phase is assumed (*i.e.*, $\gamma_N = 1$).

The equilibrium aqueous phase concentration of a compound, C_w, is proportional to its saturated aqueous solubility as a pure liquid compound. For compounds that are liquids at environmental temperatures, C_{sat} (L) is the compound aqueous solubility. For compounds which are solids, C_{sat} (L) is the aqueous solubility of the subcooled liquid. Solids which are dissolved in nonaqueous phase mixtures have freedom to rotate as if they were in a liquid state at the system temperature. A subcooled liquid is a theoretical thermodynamic phase. Pure compounds cannot exist as subcooled liquids, but the subcooled liquid solubility of a

compound can be estimated from the aqueous solubility of the pure solid, corrected for the enthalpic cost of melting:

$$C_{sat}(L) = C_{sat}(s) \exp\left(\frac{\Delta H_m}{RT_m}\left(\frac{T_m}{T} - 1\right)\right) \quad (2)$$

where C_{sat} (s) (mg/L) is the pure solid aqueous solubility, ΔH_m (J/mol) is the enthalpy of melting, R (J/mol·K) is the gas constant, T_m (K) is the compound melting temperature, and T (K) is the system temperature. Eq. 2 only considers the energy cost of the solid-to-liquid phase change and neglects heat capacity terms. These additional terms which account for the enthalpy of heating the solid and cooling the liquid, before and after the phase change, are usually insignificant (Prausnitz *et al.*, 1986). When they are not, they can lead to large errors in C_{sat} (L) calculations because they change the exponential term (Mukherji *et al.*, 1997).

Raoult's Law (γ_N = 1) calculations of aqueous compound concentrations in the presence of complex NAPL mixtures have shown good agreement with aqueous concentrations measured in batch equilibrations. In a study of seven coal tars, measured concentrations of aromatic hydrocarbons varied by less than a factor of 2 from predicted values (Lee *et al.*, 1992). Coal tars are 40 to 100% aromatic compounds by weight (Nelson *et al.*, 1996), thus NAPL activity coefficients for aromatic hydrocarbons would likely be near 1. Aqueous equilibrium with dissimilar NAPL mixtures could also be predicted with γ_N = 1 for alkylated benzenes dissolving from crude oil (Eganhouse *et al.*, 1996). Nonideal solution behavior might be expected for aromatic hydrocarbons dissolved in this aliphatic nonaqueous phase. For example, the activity coefficient for benzene in hexane is 2 (Schwarzenbach *et al.*, 1993).) These batch equilibrations of water and nonaqueous phase liquids suggest that Raoult's Law can be used to predict equilibrium groundwater concentrations at sites with complex nonaqueous phase liquids present, if the NAPL composition is known.

The source of groundwater contamination at Site YYZ was equilibrium coal tar dissolution (Chapter 2). To investigate the groundwater fate of aromatic hydrocarbons at this site, compound concentrations were compared to measured aqueous concentrations from a tar-

water batch equilibration. In this appendix, the measured aqueous concentrations are compared to Raoult's Law calculations of equilibrium aqueous concentrations.

Methods

Measurements of aqueous aromatic hydrocarbon concentrations in equilibrium with Site YYZ coal tar were made according to the methods detailed in Chapter 2 for tar-water equilibration.

Calculated aqueous concentrations of aromatic hydrocarbons in equilibrium with Site YYZ coal tar were made with Eq. 1, assuming ideal solubility. Compound mole fractions were calculated from analysis of the tar phase (Chapter 2):

$$X_N = C_{tar}\left(\frac{10^{-6}}{\rho_{tar}}\right)\left(\frac{MW_{tar}}{MW_i}\right) \qquad (3)$$

where C_{tar} (mg/L) is the compound concentration in the tar, ρ_{tar} (g/mL) is the measured tar density, 10^{-6} (L·g/mL·mg) is a unit conversion, and MW_{tar} and MW_i are the molecular weights of the tar and the compound, respectively. C_{tar} values are reported in Table 2.2 (Chapter 2). The tar density was measured to be 1 g/mL. The tar molecular weight was assumed to be 160 g/mol (EA Engineering Science and Technology Inc, 1993). This value was representative of tars isolated from other monitoring wells in the vicinity of the MIT monitoring wells and is consistent with other liquid tars (Lee *et al.*, 1992). Subcooled liquid solubilities were taken from Miller *et al.* (1985). Only solid solubilities were reported for 2-methylnaphthalene, chrysene, and benzo(ghi)perylene. Subcooled liquid solubilities were calculated for these compounds with an enthalpy of melting equal to 56.5 J/mol·K × T_m (Schwarzenbach *et al.*, 1993).

Results and Discussion

Calculated equilibrium concentrations were compared to measured aqueous concentrations of coal-tar equilibrated aromatic hydrocarbons (Figure A.1). Error bars representative of the analysis methods and concentration calculations are also included. The measurement error for the volatile compounds was taken as the variability in internal purge standards (10%, Chapter 2). Polycyclic aromatic hydrocarbon concentrations had a measurement error of 28% determined from internal standard recoveries in the solvent extraction method.

There were a number of sources of error in the Raoult's Law calculation of compound aqueous concentrations. First, the tar molecular weight was chosen from wells in the vicinity of the MIT monitoring wells because these values were thought to be representative of tar in the study area. Tar molecular weights across the site varied with an average value of 195 ± 45 g/mol (n = 7) (EA Engineering Science and Technology Inc, 1993). Thus, tar molecular weight values could be in error by 23%.

Subcooled liquid solubilities are the major source of error in calculations with Eq. 1. First, as detailed in Eq. 2, good measurements of the pure compound solubilities are required to calculate C_{sat} (L). A wide range of solubility values have been reported for low solubility polycyclic aromatic hydrocarbons (PAHs) (Mackay *et al.*, 1992). Mukherji *et al.* (1997) estimated a range of ± 25% in reported solubility values for PAHs. Secondly, a major assumption in calculating subcooled solubilities is the assumption of a constant entropy (and hence enthalpy) of melting for these rigid molecules (Schwarzenbach *et al.*, 1993). Entropies of melting for PAHs vary from 59 to 38 J/mol·K while a constant value of 56.5 J/mol·K is assumed (Miller *et al.*, 1985). For pyrene (38J/molK, Wauchope and Getzen, 1972) C_{sat} (L) values are overestimated by a factor of 3 by assuming a constant entropy value for all PAHs.

The errors in tar molecular weight and pure compound solubilities were propagated to give an error of 40% in the calculated C_w values. Errors due to phase change calculations (ΔH_m, omission of heat capacity terms) were omitted because of the good agreement of other experimental data with Raoult's Law calculations using Eq. 2 with ΔH_m = 56.5 J/mol·K × T_m.

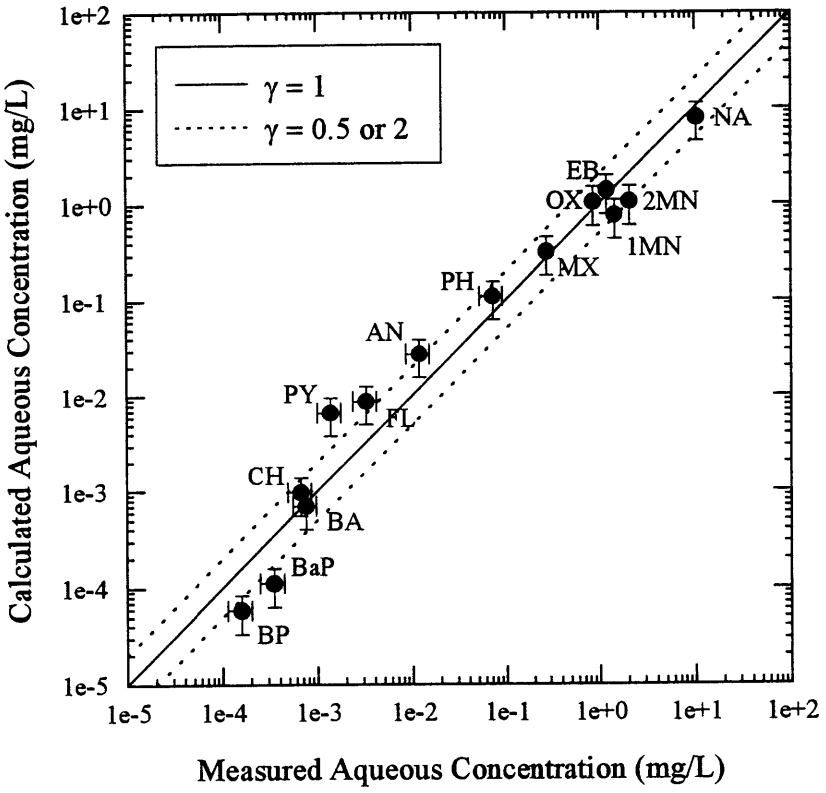

Figure A.1. Comparison of calculated and measured aqueous mono- and polycyclic aromatic hydrocarbon concentrations in equilibrium with W40M coal tar. Compound identities are abbreviated in Table 2.2. Error bar calculations are detailed in the text. Where not visible, error bars are smaller than symbols.

Within the measurement and estimation errors, measured aqueous concentrations were within a factor of 2 of Raoult's Law calculations for Site YYZ coal tar. Pyrene, benzo(a)pyrene and benzo(ghi)perylene showed the greatest deviation from the ideal solubility line. If the source of disagreement between the calculated and observed concentrations was an incorrect tar molecular weight value used in Eq. 3, all of the data points would have fallen above the $\gamma_N = 1$ line. (The value of 160 g/mol was less than the site average suggesting that if this value was not representative of W40M tar, the true molecular weight of this tar would have been greater.) Data points fall above and below the ideal solubility line so poor estimates of the tar molecular weight likely do not explain differences between calculated and measured solubilities.

The differences in calculated and measured aqueous concentrations likely result from inexact estimates of compound subcooled liquid solubilities. Calculations of pyrene aqueous concentrations could be improved by use of its measured enthalpy of melting. As noted earlier, the subcooled liquid solubility used to calculate C_w may have overestimated pyrene solubility by factor of 3. It is difficult to measure accurate saturated aqueous concentrations of benzo(a)pyrene and benzo(ghi)perylene because of the low solubilities of these compounds. Deviations from ideal solubility ($\gamma_N = 1$ line) may result from low values of C_{sat} (s) or measurement error in this tar-water equilibration.

The measured concentrations of aromatic hydrocarbons were compared to observed groundwater concentrations, rather than comparing Raoult's Law estimates because of the uncertainties in C_{sat} (L) values. Also, any systematic errors in our analytical method would cancel one another when comparing groundwater observations to measured tar-water equilibrium concentrations.

In conclusion, Site YYZ coal tar is another example of a complex environmental organic mixture for which Raoult's Law predicts the equilibrium aqueous concentrations of its component compounds. Given the sources of uncertainty in the calculation of subcooled liquid solubilities and the difficulty in measuring aqueous concentrations of low solubility organic compounds, agreement of Raoult's Law calculations within a factor of 2 of aqueous concentrations in batch equilibrations is reasonable.

References

EA Engineering Science and Technology Inc (1993). *Site Characterization Report for the BG&E Spring Gardens Facility.*

Eganhouse, R. P.; Dorsey, T. F.; Phinney, C. S.; Westcott, A. M. (1996). "Processes affecting the fate of monoaromatic hydrocarbons in an aquifer contaminated by crude oil." *Environmental Science and Technology* **30**: 3304-3312.

Lee, L. S.; Rao, P. S. C.; Okuda, I. (1992). "Equilibrium partitioning of polycyclic aromatic hydrocarbons from coal tar into water." *Environmental Science and Technology* **26**: 2110-2115.

Mackay, D.; Shiu, W. Y.; Ma, K. C. (1992). *Illustrated Handbook of Physical-Chemical Properties and Environmental Fate of Organic Chemicals.* Boca Raton, FL, Lewis Publishers.

Miller, M. M.; Wasik, S. P.; Huang, G. L.; Shiu, W. Y.; Mackay, D. (1985). "Relationships between octanol-water partition coefficient and aqueous solubility." *Environmental Science and Technology* **19**: 522-529.

Mukherji, S.; Peters, C. A.; Jr, W. J. W. (1997). "Mass transfer of polynuclear aromatic hydrocarbons from complex DNAPL mixtures." *Environmental Science and Technology* **31**: 416-423.

Nelson, E. C.; Ghoshal, S.; Edwards, J. C.; Marsh, G. X.; Luthy, R. G. (1996). "Chemical characterization of coal tar-water interfacial films." *Environmental Science and Technology* **30**: 1014-1022.

Prausnitz, J. M.; Lichtenthaler, R. N.; Azevedo, E. G. d. (1986). *Molecular Thermodynamics of Fluid-Phase Equilibria.* Englewood Cliffs, NJ, Prentice-Hall, Inc.

Schwarzenbach, R. P.; Gschwend, P. M.; Imboden, D. M. (1993). *Environmental Organic Chemistry.* New York, NY, John Wiley & Sons, Inc.

Wauchope, R. D.; Getzen, F. W. (1972). "Temperature dependence of solubilities in water and heats of fusion of solid aromatic hydrocarbons." *Journal of Chemical Engineering Data* **17**: 38-41.

Appendix B.

EVALUATION OF SOLID PHASE EXTRACTION METHODS FOR SEPARATING DISSOLVED AND COLLOID-ASSOCIATED CONTAMINANTS IN GROUNDWATER

Abstract

Reverse phase separation of dissolved and colloid-associated compounds was investigated as a method to isolate *in situ* organic colloid-associated contaminants in groundwater. Sep Pak cartridges (octadecyl bonded silica) removed > 98% of dissolved polycyclic aromatic hydrocarbon (PAH) mass in a 300 mL volume of coal tar-equilibrated water at a flowrate of 12 mL/min. At this flowrate, separation of humic acid-associated PAHs was not quantitative. In addition to dissolved species, from 50% (chrysene) to 30% (benzo(ghi)perylene) of colloid-associated mass was retained on the Sep Pak, suggesting that colloid desorption occurred in the cartridge. Separation with Empore solid phase extraction disks was also hindered by colloid desorption. Sep Pak reverse phase separation was applied to groundwater from a coal tar site. Isolation of colloid-associated PAHs was unsuccessful because of low organic colloid concentrations.

Introduction

Groundwater colloids can significantly enhance the transport of particle reactive organic compounds over the transport of dissolved species. Two general methods have been used to quantify the importance of colloid-mediated contaminant transport. First, researchers have tried to isolate the colloid-phase and quantify the associated contaminant load with separation techniques such as ultrafiltration, and field flow fractionation. These separation methods suffer from many artifacts. For example, hydrophobic compounds are lost to organic membranes and at low colloid concentrations, breakthrough to the dissolved phase occurs. A quiescent colloid collection system has been developed whereby a sampling device collects colloids which flow through the screened monitoring well. This method requires many months for sample collection and it may be difficult to quantify organic contaminant concentrations in the colloids. The second type of colloid characterization methods do not require physical alteration of groundwater samples. Fluorescent probes are added to groundwater samples to quantify colloid-water partition coefficients (Backhus and Gschwend, 1990; Gauthier *et al.*, 1986). While this method demonstrates the potential for colloid-facilitated transport, it provides no measure of colloid-associated contaminant concentrations. Fluorescent probes can also be dynamically quenched by the presence of dissolved species (*e.g.*, copper ions, oxygen (Lakowicz, 1983)) in the water sample, falsely indicating colloid-association. There is a need for nonintrusive separation methods to isolate and quantify the *in situ* colloid-associated contaminants in groundwater samples with a minimum of manipulation artifacts.

Reverse phase separation is a method which allows separation of contaminants sorbed to organic colloids with no sample preconcentration. A water sample flows through a solid phase sorbent which sorbs the dissolved compound species. The colloid-associated contaminants are carried through the sorbent to the effluent with the organic colloids. The concentration of *in situ* colloid-bound contaminants present in the water sample can be quantified by analysis of the effluent fraction.

The partition coefficients of model organic colloids (Landrum *et al.*, 1984) and colloids from natural waters (Backhus and Gschwend, 1990; Gauthier *et al.*, 1986; Landrum *et*

al., 1984) have been quantified by reverse phase separation. In each of these cases, however, a probe compound was added to the water sample before separation. The partition coefficient was then quantified from the ratio of the compound mass in the effluent to that in retained by the solid phase sorbent. Reverse phase separation has not been used to isolate *in situ* colloid-associated contaminants without the addition of a spike compound.

A reverse phase separation method for field applications must satisfy additional criteria not necessary for these lab studies. Radio-labelled spiking compounds were used in the laboratory studies (Gauthier *et al.*, 1986; Landrum *et al.*, 1984), and thus water volumes of order 10 mL were sufficient to achieve separation. Organic compounds for which colloid transport is important have low solubilities and so significantly larger volumes (100s mL) of groundwater would be necessary to detect compounds in the effluent phase. The dissolved compound mass in these large columns cannot exceed the solid phase sorbent capacity and breakthrough to the effluent fraction. Sorbent pores may become clogged by particles and prevent the passage of the organic colloid phase. Finally, the residence time in the column must be short enough that little colloid-associated contaminant mass desorbs from the colloid phase during groundwater contact with the sorbent. Partition coefficients determined by reverse phase separation were shown to vary with organic colloid concentration (Landrum *et al.*, 1984) as a result of these mechanisms (*i.e.*, colloid filtration, compound desorption). These effects are likely to be exacerbated during the separation of large volume field samples. While reverse phase separation may allow isolation of *in situ* colloid-associated contaminants, it may only provide a lower bound of the concentration of colloid-associated contaminants in groundwater samples.

In this study, several reverse phase separation systems were tested for their ability to isolate colloid-associated polycyclic aromatic hydrocarbons (PAHs). Separation efficiencies were evaluated with a humic acid solution containing a known amount of colloid-associated compound mass. The reverse phase method was also applied to groundwater samples from a coal tar site where transport of PAHs by organic colloids was strongly suspected (Chapters 2 and 3).

Methods

Chemicals

Humic acid (Aldrich, Milwaukee, WI) solutions were made up with sodium chloride (Mallinckrodt, Paris, KY), sodium hydroxide and hydrochloric acid (Fisher Scientific, Fairlawn, NJ). Organic carbon standards were made with potassium hydrogen phthalate (Sigma, St. Louis, MO) and acidified with phosphoric acid (Mallinckrodt). Internal standards of *p*-terphenyl, deuterated (d-) perylene, and d-benz(a)anthracene (Ultra Scientific, North Kingstown, RI) were made in methanol (OmniSolve, EM Science, Gibbstown, NJ). OmniSolve methylene chloride and hexane were also used.

Quantitative Breakthrough of Humic Acid

Quantitative passage of humic acid through the solid phase sorbents was first evaluated with a humic acid solution containing no PAHs. The solution chemistry mimicked the groundwater chemistry at Site YYZ, where reverse phase separation would be applied. Aldrich humic acid (about 20 mg) was dissolved in 50 mL of 0.01 N sodium hydroxide. The base solution was neutralized with the addition of an equal volume of 0.01 N hydrochloric acid and diluted to 1.5 L. Sodium chloride salt (1.2 g) was added to bring the solution conductivity to 1.05 mS, within the range of observed groundwater conductivities (Chapter 2). The final solution pH was 7.2 and the organic carbon content was about 10 mg_C/L, representative of the levels of humic acid-like organic matter in the Site YYZ groundwater (Chapter 3).

The solid phase sorbent systems were cleaned as described below. Purified water (18 MΩ, Aries purification system, Vaponics, Rockland, MA) was flushed through the reverse phase separation system until the organic carbon content of the effluent did not differ from the organic carbon of the 18 MΩ water, within measurement error. Humic acid solution (50-100 mL) was passed through the reverse phase system. The organic carbon content of the starting solution and the effluent were measured to quantify the fraction of organic carbon breakthrough for the reverse phase system.

Organic carbon was analyzed with a Shimadzu TOC-5000 Organic Carbon analyzer. Aqueous samples were acidified with phosphoric acid and bubbled with argon or nitrogen for

5 minutes to remove inorganic carbon. The TOC analyzer was calibrated with external standards of potassium hydrogen phthalate.

Reverse Phase Separations

The sorbent capacity and separation efficiency of the reverse phase systems were evaluated with two model solutions containing polycyclic aromatic hydrocarbons. The first solution was 18 MΩ water containing 0.8 g/L sodium chloride. The second was a humic acid solution as described above. Coal tar (3-4 mL) from the W40M monitoring well was added to each of these solutions. The tar-containing solutions were stirred for 4 hours to aid equilibration of PAHs between the tar and the aqueous solution. The solutions were undisturbed for 5 days, allowing tar droplets to settle from the aqueous phase. Aliquots of the tar-equilibrated solutions were then siphoned from the equilibration flasks. A piece of aluminum tubing with a closed valve was primed with 18 MΩ water and inserted in the aqueous phase. The tube inlet was located well above the settled tar layer. The valve was opened and four tube volumes of the equilibrated aqueous phase was allowed to flow to waste before multiple 300 mL samples were taken in foil-wrapped BOD bottles.

One of the 300 mL samples for each tar-equilibrated solution was analyzed by liquid-liquid extraction (LLE) to enable mass balance for the reverse phase separation procedure. The aqueous sample was spiked with an internal standard of *p*-terphenyl and extracted three times with 20 mL of methylene chloride. The extracts were combined and transferred to hexane. The PAH fraction was isolated by silica gel chromatography according to the method for field samples (Chapter 2).

The remaining 300 mL samples were separated with the reverse phase separation systems. The aqueous solution was spiked with p-terphenyl and passed through cleaned solid phase sorbents. The effluent was collected and its PAH content was quantified by the LLE extraction procedure described above. The PAHs retained by the solid phase sorbent were eluted with methylene chloride according to system-specific methods described below. The solid phase extracts (SPE) were then transferred to hexane and underwent silica gel separation of the PAH fraction according to the LLE method.

The PAH fractions for each of the solid-phase and liquid-liquid extracts were analyzed by gas chromatography-mass spectrometry with an HP5890GC and an HP5972MS (Hewlett

Packard, Palo Alto, CA). Injections were made to a heated (280°C) split-splitless injector. The split was opened 0.75 min after injection. The column was a 30 m HP-5 (Hewlett Packard) capillary column with a film thickness of 0.25 μm. Column flow was maintained at 1 mL/min by an electronic flow controller. The ionization voltage was 70 eV. The temperature program began at 70°C with a 20°C/min ramp to 180°C and followed by a ramp to 300°C at 6°C/min. The final temperature was held for 8 min. The detector was held at 280°C. Compounds were quantified with external standards and all peak areas were quantified by selective ion monitoring.

Reverse Phase Separation Systems

Cartridges. Maxi-Clean (Alltech, Deerfield, IL) and Sep Pak Plus (Waters, Milford, MA) solid phase extraction cartridges with octadecyl (C_{18}) bonded silica were evaluated for their efficiency to separate colloid-associated compounds from dissolved species. Aqueous solutions were drawn through each of these cartridges in a vacuum filtration system. The cartridges were inserted through a silicon stopper in the filter flask for collection of the colloid-containing effluent. A 100 mL Luer-tipped syringe barrel served as the sample reservoir. The filter flask was attached to a teflon vacuum pump with an aluminum line. The vacuum was adjusted to maintain a flow rate of 12 mL/min through the cartridge.

The Maxi-Clean cartridges were only evaluated for humic acid breakthrough and did not undergo any cleaning procedure other than flushing with 18 MΩ water to background levels.

The Sep Pak cartridges were initially cleaned with three 10 mL aliquots of methylene chloride, followed by 10 mL of methanol and 20 mL of 18 MΩ water. After sample collection, the Sep Pak was eluted with three 10 mL aliquots of methylene chloride.

Extraction disks. Empore solid phase extraction disks (3M, St. Paul, MN) were also evaluated for use in the reverse phase separation method. These disks contained a C_{18} sorbent phase imbedded in a Teflon matrix. Although Empore disks were shown to retain pesticides in a humic acid solution (Senseman *et al.*, 1995), their low resistance to flow may allow throughput of colloids and associated PAHs at high flowrates. The disks were placed on a fritted glass filter holder and samples were drawn through with the vacuum filtration system described above at a flowrate of 185 mL/min. The disks were cleaned by drawing several

milliliters of methylene chloride through the disk and allowing it to soak for several minutes before a total of 10 mL was pulled through the disk. The methylene chloride was followed by a rinses of methanol (10 mL) and 18 MΩ water (10 mL). After sample separation the extraction disk was dried by drawing air through the disk for 5 min. The disk was then eluted with three 10 mL aliquots of methylene chloride, allowing each to soak for several minutes after passage of 1 mL.

Other Colloid Phases

The ability of the Sep Pak cartridges to pass colloid phases other than organic matter was also investigated. A 1.5 mg/L kaolin (EM Science) solution with a turbidity of 1.2 ± 0.04 NTU was passed through the Sep Pak in 50 mL increments. The effluent turbidity was measured after each increment until a total of 500 mL had been passed. Turbidity measures were made with an HF Scientific (Ft. Myers, FL) turbidimeter. Tar retention by the Sep Pak was also tested by adding a 20 μL droplet to 2 mL of water in the reservoir. This water was pulled through the cartridge, followed by an additional 50 mL.

Field Application

The Sep Pak reverse phase separation method was applied to groundwater samples from Site YYZ to quantify colloid associated contaminants. Triplicate groundwater samples were collected in foil-wrapped 300 mL BOD bottles by slow pumping methods (Chapter 2). One bottle was retained for analysis of the total dissolved plus colloid-associated polycyclic aromatic hydrocarbons by LLE at MIT. The second sample was spiked with an internal standard containing *p*-terphenyl and d_{12}-perylene and separated in the field with a pre-cleaned Sep Pak system. Photodegradation of PAHs was minimized by foil-wrapping the system to the greatest extent possible. After separation, the effluent was transferred to a clean BOD bottle and liquid-liquid extracted at MIT after spiking with a recovery standard of d-benz(a)anthracene. The third groundwater sample was returned to the laboratory for Sep Pak separation in the event that the contamination was introduced during field manipulations. Contamination introduced in the field was quantified by reverse phase separation of a 300 mL aliquot of 18 MΩ water brought from MIT in a BOD bottle.

The vacuum filtration system was cleaned in the laboratory before use in the field. A new filter flask was used for effluent collection at each well. The filter flasks were soaked in

chromic-sulfuric acid solution overnight, followed by rinsing with 18 MΩ water, methanol and methylene chloride. The individual Sep Paks were pre-cleaned in the laboratory and wrapped in foil. The foil-wrapped cartridges were then wrapped with moist paper and placed in a Zip Loc bag to maintain the moisture content in the cartridge until use 48 h later. After sample separation in the field, this same storage procedure was used to return the cartridges to the laboratory. Twenty four hours after collection, the Sep Paks were hand flushed with 4 mL of methanol in a syringe to remove residual water. The Sep Paks were then eluted by gravitational flow of 50 mL of methylene chloride contained in a glass syringe with no headspace.

All methylene chloride extracts from the field samples were transferred to hexane, chromatographed on silica gel, and analyzed by GC/MS.

Results and Discussion

Evaluation of Humic Acid Passage by Reverse Phase Separation Systems

The solid phase extraction systems were first evaluated for their retention of organic humic acid colloids. Only those systems which quantitatively passed humic acid, as measured by the ratios of organic carbon concentration in the effluent to that in the starting solution, were evaluated for reverse phase separation of colloid-associated polycyclic aromatic hydrocarbons. Maxi-Clean cartridges were eliminated from subsequent reverse phase evaluations due to their retention of humic acid (Table B.1). In addition to the low organic carbon concentration, the effluent lacked coloration in comparison to the starting humic acid solution. The retained humic acid was observed as a brown band at the head of the cartridge.

The results of the humic acid evaluation showed the Empore extraction disks and the Sep Pak cartridges to be promising candidates for reverse phase separation of colloid-associated PAHs. High organic carbon breakthrough was observed for the Empore disks, but some disk discoloration was observed, indicating some retention of humic acid. The Sep Pak cartridges had complete passage of organic carbon and showed no discoloration from humic acid retention in the porous sorbent.

The Sep Pak cartridges were also evaluated for their retention of clay particles and tar. After passage of only 50 mL of a 1.5 mg/L kaolin solution (1.2 NTU), the effluent turbidity was 0.2 NTU. The effluent turbidity remained constant at 0.1 NTU for the next 500 mL collected. Therefore, over 90% of clay particles were filtered by the porous sorbent media. Tar was also retained by the Sep Pak, as expected from the hydrophobic nature of the packing material. A 20 μL tar droplet was not forced through the column by additional passage of water. The effect that pore clogging by clay particles or tar droplets might have on the passage of organic carbon macromolecules through the sorbent cartridge was not investigated.

The separated fraction containing the colloid-associated contaminants can be postulated for various colloid types. If the contaminants were sorbed to suspended organic colloids, the contaminant mass retained on the Sep Pak would be less than extracted from an unfractionated water sample of equivalent volume. The difference in contaminant mass between that eluted from the Sep Pak and that contained in the extract of unfractionated water

Table B.1. Humic acid passage through solid phase extraction systems.

Solid phase extraction system	Initial humic acid concentration (mg C/L)	Effluent humic acid concentration (mg C/L)	Humic acid breakthrough (%)
Empore disk	8.7 9	8.3 7.3	95 80
Maxi-Clean cartridge	8.7	4	45
Sep Pak cartridge	12.5	12.8	100

would be found in the effluent extract. If the contaminants were associated with clay particle colloids or tar droplets, they would be retained on the Sep Pak, in addition to the contaminant mass dissolved in the water sample. In this case the mass of compounds eluted from the Sep Pak would by equal to that in an extraction of an equal volume of unfractionated water. No contaminant mass would be detected in the effluent.

Evaluation of Reverse Phase Separation of Colloid-Associated PAHs

Two model solutions were used to evaluate the separation of dissolved and colloid-associated polycyclic aromatic hydrocarbons by the reverse phase separation systems. Tar equilibrated water, containing only dissolved species, was used to evaluate the extraction capacity of the sorbent. While the mass of solid phase sorbent (300 mg) greatly exceeded the total dissolved compound mass (5 mg) in the volumes tested, the flowrates employed may not have allowed sufficient time for uptake of dissolved compounds by the sorbent. Thus, the effluent would also contain dissolved compound mass, an artifact of too fast flow rates. Once certain that dissolved compounds would be sorbed by the solid phase sorbent, a tar-equilibrated humic acid solution was used to quantify the efficiency of separation of the colloid-associated mass from the dissolved mass. The total colloid-associated mass was known by comparison with tar-equilibrated water. Thus, the separation efficiency could be evaluated by comparison of the mass of compounds in the effluent with the known colloid-associated mass in the starting solution.

The concentrations of polycyclic aromatic hydrocarbons in the humic acid solution were enhanced over those in tar-equilibrated water (Table B.2). The solubility enhancement by the humic acid increased with compound hydrophobicity, from no enhancement of pyrene and fluoranthene to an enhancement of 3 for benzo(ghi)perylene. For each compound, the fraction of dissolved mass in the humic acid solution was calculated by dividing the compound concentration in tar-equilibrated water with that in the humic acid solution. This fraction is the portion of total compound mass expected to be eluted from the solid sorbent after reverse phase separation if the separation of the colloid-associated mass is ideal. The remainder of the compound mass would be present with the organic colloids in the effluent.

Table B.2. Polycyclic aromatic hydrocarbon concentrations in tar-equilibrated water and a tar-equilibrated 7 mg_C/L Aldrich humic acid solution. Concentrations were quantified by methylene chloride extractions of unfractionated samples.

Compound	18 MΩ water (mg/L)	Humic acid solution (mg/L)	Ratio: Humic sol'n / 18 MΩ water	Ratio: Dissolved / Diss'd+Colloid
Fluoranthene (FL)	0.012	0.013	1.1	0.9
Pyrene (PY)	0.012	0.0079	0.7	0.4
Benz(a)-anthracene (BA)	0.0021	0.0048	2.3	0.4
Chrysene (CH)	0.0017	0.0038	2.2	0.4
Benzo(e)-pyrene (BeP)	0.00057	0.0016	2.8	0.4
Benzo(a)-pyrene (BaP)	0.001	0.0029	2.9	0.3
Indeno(123-cd)pyrene (IP)	0.00035	0.001	2.9	0.3
Benzo(ghi)-perylene (BP)	0.00029	0.00092	3.2	0.3

Greater than 98% of the dissolved compound mass was sorbed by the Sep Pak cartridges at the flowrate of 12 mL/min. A mass balance was performed for the reverse phase separation by summing the mass of each compound in the solid phase extract (SPE) and the effluent. Sixty to eighty percent of compound mass was recovered in the reverse phase separated fractions in comparison to the liquid-liquid extraction of a duplicate volume of water (Table B.3). The recoveries of benzo(a)pyrene and benzo(ghi)perylene may have been improved with the addition of deuterated perylene internal standard. The fraction of compound mass in the effluent fraction was only 1-2% of the total mass of PAHs in the tar-equilibrated water. Additionally, less than 0.5% of the *p*-terphenyl internal standard added before reverse phase separation was extracted from the effluent fraction. Therefore, the flowrate for reverse phase separation allowed sufficient contact time for the dissolved compound mass to be exchanged from the aqueous solution to the solid sorbent.

A portion of the colloid-associated PAHs in the tar-equilibrated humic acid solution was separated from the dissolved compound mass by reverse phase separation with the Sep Pak cartridges. The mass balance for this system was also close to 100% by comparison with a liquid-liquid extraction of a duplicate sample volume of the humic acid solution (Table B.4). Detectable levels of PAHs were found in the effluent and the compound masses eluted from the solid phase sorbent were greater than the dissolved mass in the humic acid solution. These results demonstrate that colloid-associated compounds were carried through the Sep Pak with the colloid phase. For each compound, the ratio of mass eluted from the solid sorbent (SPE) to the total mass in the humic acid solution (Table B.4) was greater than the calculated fraction of dissolved compound mass in the starting solution (Table B.2). Thus, PAHs that were colloid-associated in the starting solution were retained by the solid sorbent, in addition to the initially dissolved species. The masses of compounds in the Sep Pak in excess of dissolved levels may have been retained with colloids filtered from solution by the porous media or may have desorbed from the colloids in response to the gradient induced by solid phase sorbent uptake of dissolved compounds.

Table B.3. Sep Pak separation of dissolved and colloid-associated polycyclic aromatic hydrocarbons in tar-equilibrated 18 MΩ water.

Compound	SPE (mg/L)	Effluent (mg/L)	Mass Balance[†]	Ratio: $\frac{\text{SPE}}{18\ \text{M}\Omega\ H_2O}$	Break-through[‡]
FL	0.0096	0.000 025	0.8	0.8	0.002
PY	0.0064	0.000 019	0.5	0.5	0.003
BA	0.0015	0.000 014	0.7	0.7	0.01
CH	0.0013	0.000 012	0.8	0.8	0.01
BeP	0.0004			0.7	
BaP	0.0007	0.000 01	0.8	0.7	0.02
IP	0.0002			0.6	
BP	0.000 17	< 0.000 006	0.7	0.6	0.03

[†] (SPE + Effluent)/18 MΩ water
[‡] Effluent/(SPE + Effluent)

Table B.4. Sep Pak separation of dissolved and colloid-associated polycyclic aromatic hydrocarbons in tar-equilibrated humic acid solution.

Com-pound	SPE (mg/L)	Effluent (mg/L)	Mass Balance†	Ratio: $\frac{\text{SPE}}{\text{Humic acid solution}}$	Break-through‡	Fraction colloid-associated mass retained
FL	0.019	0.002	1.6	1.5	0.1	
PY	0.013	0.0016	1.8	1.6	0.1	
BA	0.0037	0.0016	1.1	0.8	0.3	0.5
CH	0.0029	0.0013	1.1	0.8	0.3	0.5
BeP	0.000 92	0.000 78	1.1	0.6	0.5	0.2
BaP	0.0017	0.0013	1	0.6	0.4	0.4
IP	0.000 43	0.000 43	0.9	0.4	0.5	0.3
BP	0.000 43	0.000 42	0.9	0.4	0.5	0.3

† (SPE + Effluent)/Humic acid solution
‡ Effluent/(SPE + Effluent)

The efficiency of reverse phase separation was quantified by calculating the fraction of initially colloid-associated compound mass retained by the Sep Pak (Table B.4). For example, 60% of the total chrysene mass was colloid-associated in the humic acid solution, but only 30% of the total mass was detected in the effluent. Thus, 50% of the initially colloid-associated chrysene was retained by the Sep Pak, in addition to the dissolved chrysene. For PAHs with increasing hydrophobicities, decreasing fractions of the initially colloid-bound masses were retained by the solid sorbent. If colloids with their associated compound mass were strained from solution, a constant retention would have been observed for all PAHs regardless of hydrophobicity. Colloid straining was likely not an important separation artifact because the fractions of colloid-associated mass retained by the Sep Pak were not constant for all PAHs. If cartridge residence times were long enough for colloid-associated compounds to desorb from the colloid phase, greater fractions of compounds with low hydrophobicities would be retained than for compounds with high hydrophobicities. Uptake of dissolved compounds by the solid phase sorbent induces a gradient for desorption from the colloid phase to maintain phase equilibrium. Low hydrophobicity compounds must desorb more mass than do very hydrophobic compounds to maintain this equilibrium. Thus, smaller fractions of the initially colloid-associated mass with increasing compound hydrophobicity would be retained by the solid phase sorbent, as observed for reverse phase separation of the humic acid solution. Therefore, reverse phase separation with Sep Pak cartridges does allow qualitative identification of organic colloid-associated compounds, but quantification of their concentrations is limited by cartridge residence times greater than colloid desorption times.

Reverse phase separation of the humic acid solution with the Empore extraction disks was also limited by desorption of colloid-associated mass. The ratios of SPE masses to total masses in the humic acid solution (Table B.5) were greater than the fraction of dissolved compound mass calculated in the humic acid solution (Table B.2). The fraction of initially colloid-associated mass retained by the extraction disk was not constant for all PAH, but decreased for compounds with increasing hydrophobicity, suggesting colloid desorption.

Table B.5. Empore disk separation of dissolved and colloid-associated polycyclic aromatic hydrocarbons in tar-equilibrated humic acid solution.

Compound	Solid phase extraction (mg/L)	Ratio: $\frac{\text{SPE}}{\text{Humic acid sol'n}}$	Fraction colloid-associated mass retained by disk
PY	0.011	1.4	
BA	0.004	0.8	0.7
CH	0.0026	0.7	0.5
BaP	0.0017	0.6	0.4
IP	0.0056	0.6	0.4
BP	0.0043	0.5	0.3

Although the flowrate was fifteen times higher than through the Sep Paks, the disk in the filter holder remained exposed to the sample reservoir throughout the course of the separation. This also allowed for compound desorption from the colloid phase local to the disk, elevating the masses of compounds sorbed by the sorbent disk above dissolved levels. For all PAHs, the fraction of initially colloid-associated mass retained in this reverse phase separation system was similar to the fractions retained by the Sep Paks.

There was little difference in separation efficiency of colloid-associated PAHs between the Sep Pak cartridge and Empore disk systems, but sample separation was easier with the cartridge system. The extraction disks were difficult to clean and elute in the vacuum filtration system without drying the disks. The Sep Pak sorbent was contained in a cartridge which minimized sorbent contamination by handling and the cartridges also had Luer fittings which enabled elution with a syringe containing no head space. For these reasons the Sep Pak cartridge system was chosen to investigate *in situ* colloid-associated PAHs in groundwater.

Reverse Phase Separation of Colloid-Associated PAHs in Groundwater

The reverse phase separation technique was applied to groundwater samples from a coal tar site in order to isolate the colloid-associated polycyclic aromatic hydrocarbons. Previous investigations at this site had yielded groundwater PAH concentrations greater than dissolved levels in equilibrium with coal tar (Chapter 2). This concentration enhancement suggested the presence of a colloid phase facilitating PAH transport in groundwater at this site and fluorescence quenching studies supported the hypothesis that humic acid-like organic colloids enhanced groundwater PAH solubilities (Chapter 3). Groundwater samples were collected from wells (W20S, W100S, W100M) which had exhibited enhanced PAH concentrations at some time. Monitoring well W40M which always had elevated PAH concentrations could not be investigated due to a large quantity of tar in the well at the time of sampling. Representative groundwater samples could not be taken from this well without the inclusion of tar artifacts.

Polycyclic aromatic hydrocarbon concentrations were not elevated above tar-equilibrium levels at any of the sampled wells (Figure B.1). Thus, reverse phase separations

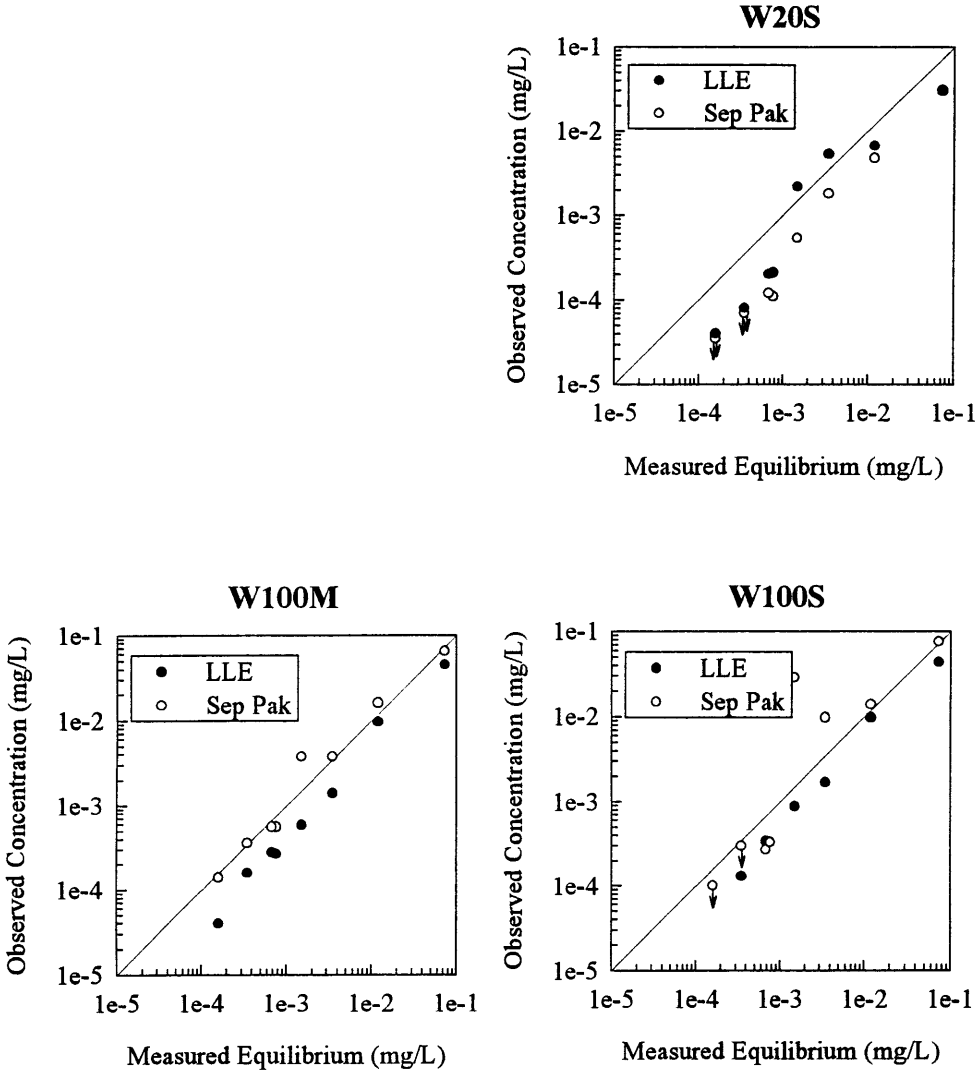

Figure B.1. Polycyclic aromatic hydrocarbon concentrations in groundwater in June 1997. Concentrations determined by liquid-liquid extraction and the Sep Pak extracted concentrations from reverse phase separation are reported. Concentrations that were less than detection limits are indicated with an arrow and a symbol at the detection limit.

of groundwater samples were not expected to contain detectable levels of colloid-associated PAHs in the effluent fraction. The effluent compound mass accounted for less than 0.5% of the total compound mass at all wells (Table B.6a,b,c). From the detection limits of PAHs in the effluent fraction, an upper bound of 1 mg_C/L of organic colloids was estimated to be present to enhance PAH concentrations in the groundwater. For example, if the humic acid colloids were representative of the groundwater organic colloids, only 60% of the colloid-associated benzo(a)pyrene in the initial groundwater sample would be present in the effluent. Assuming groundwater organic colloids had partition coefficients similar to Aldrich humic acid (as suggested by the fluorescence quenching studies (Chapter 3)), the mass of benzo(a)pyrene associated with organic colloids present at levels less than 1 mg_C/L would have been below the detection limits for the effluent analysis. The amount of organic carbon in the effluent which was capable of quenching pyrene fluorescence, and hence enhancing PAH concentrations in equilibrium with tar, was not quantified because the Sep Pak had not been rinsed with 18 MΩ water prior to use, nor was the amount of fluorescence-quenching material leached from the Sep Pak known.

Table B.6a. Sep Pak separation of dissolved and colloid-associated polycyclic aromatic hydrocarbons at monitoring well W20S.

Compound	SPE (mg/L)	Effluent (mg/L)	Breakthrough
FL	0.0018	0.000 04	< 0.001
PY	0.000 54	0.000 02	< 0.001
BA	0.000 11	< 0.000 03	< 0.001
CH	0.000 12	< 0.000 03	<0.002
BaP	< 0.000 07	< 0.0001	
BP	< 0.000 04	< 0.000 05	

Table B.6b. Sep Pak separation of dissolved and colloid-associated polycyclic aromatic hydrocarbons at monitoring well W100S.

Compound	SPE (mg/L)	Effluent (mg/L)	Breakthrough
FL	0.0098	0.000 025	0.001
PY	0.029	0.000 032	0.001
BA	0.000 33	0.000 029	0.002
CH	0.000 27	0.000 028	0.004
BaP	< 0.0003	< 0.000 03	
BP	< 0.000 01	< 0.000 002	

Table B.6c. Sep Pak separation of dissolved and colloid-associated polycyclic aromatic hydrocarbons at monitoring well W100M.

Compound	SPE (mg/L)	Effluent (mg/L)	Breakthrough
FL	0.0038	0.000 026	< 0.001
PY	0.0038	0.000 028	< 0.001
BA	0.000 56	0.000 024	< 0.001
CH	0.000 56	0.000 023	0.001
BaP	0.000 36	< 0.000 02	< 0.05
BP	0.000 14	< 0.000 001	< 0.08

Conclusions

The method development indicates that reverse phase separation may be a promising way to isolate organic colloid-associated compounds from field samples with a minimum of sample manipulation. Presently this method only allows verification of the presence of organic-colloid associated compounds by their detection in the effluent fraction. Quantification of the fraction of colloid-associated mass, and hence groundwater-colloid partition coefficients, is hindered by colloid desorption while the sample is in contact with the solid phase sorbent. Additionally, compound detection limits may restrict the application of reverse phase separation to field sites with high mobile organic colloid concentrations. Further investigation is required to quantify the effects of other colloid phases, such as clays, on reverse phase separation of organic colloids and their associated contaminant loads.

References

Backhus, D. A.; Gschwend, P. M. (1990). "Fluorescent polycyclic aromatic hydrocarbons as probes for studying the impact of colloids on pollutant transport in groundwater." *Environmental Science and Technology* **24**: 1214-1223.

Gauthier, T. D.; Shame, E. C.; Guerin, W. F.; Seitz, W. R.; Grant, C. L. (1986). "Fluorescence quenching method for determining equilibrium constants for polycyclic aromatic hydrocarbons binding to dissolved humic materials." *Environmental Science and Technology* **20**: 1162-1166.

Lakowicz, J. R. (1983). *Principles of Fluorescence Spectroscopy*. New York, Plennum Press.

Landrum, P. F.; Nihart, S. R.; Gardner, W. S. (1984). "Reverse-phase separation method for determining pollutant binding to Aldrich humic acid and dissolved organic carbon of natural waters." *Environmental Science and Technology* **18**: 187-192.

Senseman, S. A.; Lavy, T. L.; Mattice, J. D.; Gbur, E. E. (1995). "Influence of dissolved humic acid and Ca-montmorillinite clay on pesticide extraction efficiency from water using solid-phase extraction disks." *Environmental Science and Technology* **29**: 2647-2653.

Appendix C.

CALCULATION OF THE EFFECTIVE DIFFUSION COEFFICIENT IN DOUGLAS FIR

This appendix details the calculation of the effective diffusion coefficient in Douglas fir (Burr and Stamm, 1947, Figure6.4, Chapter 6). Experimental results of the monoaromatic hydrocarbon uptake in wood suggested that only tangential diffusion was important to overall compound uptake (Chapter 6). Therefore, only calculations of the tangential diffusion coefficient are shown here. The methodology is the same for calculating longitudinal wood diffusion, however, the individual parameters in the resistance terms have different values due to the differing orientation of the wood fibres relative to the diffusion pathway.

The diffusion coefficient of a compound in wood (D_{eff}) is related to its aqueous diffusivity (D_w) by the overall resistance of the physical wood structure:

$$D_{eff} = \left(\frac{1}{R_{TOT}}\right) D_w$$

where R_{TOT} is the overall resistance of the physical wood structure given as the sum of individual resistances (refer Figure 6.4, Chapter 6):

$$\frac{1}{R_{TOT}} = \frac{1}{R_f} + \frac{1}{R_a + \dfrac{n_T}{\dfrac{1}{R_e} + \dfrac{1}{R_b + \dfrac{1}{R_d + R_c}}}} \qquad (2)$$

where R_a is the fibre cavity resistance in the fibre direction;

R_b is the pit cavity resistance;

R_c is the resistance of the pit membrane substance;

R_d is the pit membrane pore resistance;

R_e is the resistance of the overlapping cell walls;

R_f is the resistance of the continuous cell wall, and

n_T is the number of cells per unit length in the fibre direction.

These equations can also be written in terms of conductance (= resistance^{-1}):

$$D_{WOOD} = C_{TOT} D_w \tag{3}$$

$$C_{TOT} = C_f + \frac{1}{\frac{1}{C_a} + \frac{n_T}{C_e + \frac{1}{\frac{1}{C_b} + \frac{1}{C_d + C_c}}}} \tag{4}$$

where the conductances, C_i, are for the physical structures as described for Eq. 2.

The following expressions are used to calculate the individual conductances (Behr *et al.*, 1953):

$$C_a = 1 \tag{5}$$

$$C_b = \frac{q_p}{L_m} \tag{6}$$

$$C_c = \frac{q_m}{L_p} \tag{7}$$

$$C_d = \frac{q_T}{L_p} \tag{8}$$

$$C_e = \frac{Q_T}{L_m} \tag{9}$$

$$C_f = L_m n_T S_T \tag{10}$$

where the parameters are defined in the following table.

Parameter	Description	Value for Douglas fir
n_T	average number of fibres traversed per cm in the tangential direction	300
L_m	average thickness of the double cell walls of swollen wood	0.000 92
L_p	average pit membrane thickness	0.0001
q_p	fractional area of tangential fibre walls covered by pits	0.014
q_m	fractional cross-sectional area of the transient pit membrane-capillaries of solvent-swollen wood for the passage of molecules the size of water molecules, exclusive of permanent pores	0.000 11
q_T	effective fractional cross-sectional area of permanent pit-membrane pores for transverse passage	0.000 52
Q_T	fractional cross-section of the transient cell wall capillaries of solvent-swollen wood effective for the passage of molecules the size of water molecules in the transverse direction from one cavity to another	0.0063
S_T	fractional cross-section of the transient cell wall capillaries of solvent-swollen wood effective for passage of molecules the size of water molecules in the tangential direction	0.0078

These numerical values were used to calculate the individual and overall conductances for Douglas fir shown in Figure 6.11a (Chapter 6). The effect of equilibrium microscale partitioning is hypothesized to increase the effective pathlength through any wood tissue structure. The individual resistances were recalculated in Figure 6.11b with tissue partitioning with lengths L_m and L_p multiplied by a retardation factor of 10.

References

Behr, E. A.; Briggs, D. R.; Kaufert, F. H. (1953). "Diffusion of dissolved materials through wood." *Journal of Physical Chemistry* **57**: 476-480.

Burr, H. K.; Stamm, A. J. (1947). "Diffusion in wood." *Journal of Physical and Colliod Chemistry* **51**: 240-261.

Appendix D.

ADDITIONAL TIME COURSE PLOTS OF MONOAROMATIC COMPOUND UPTAKE BY WOOD

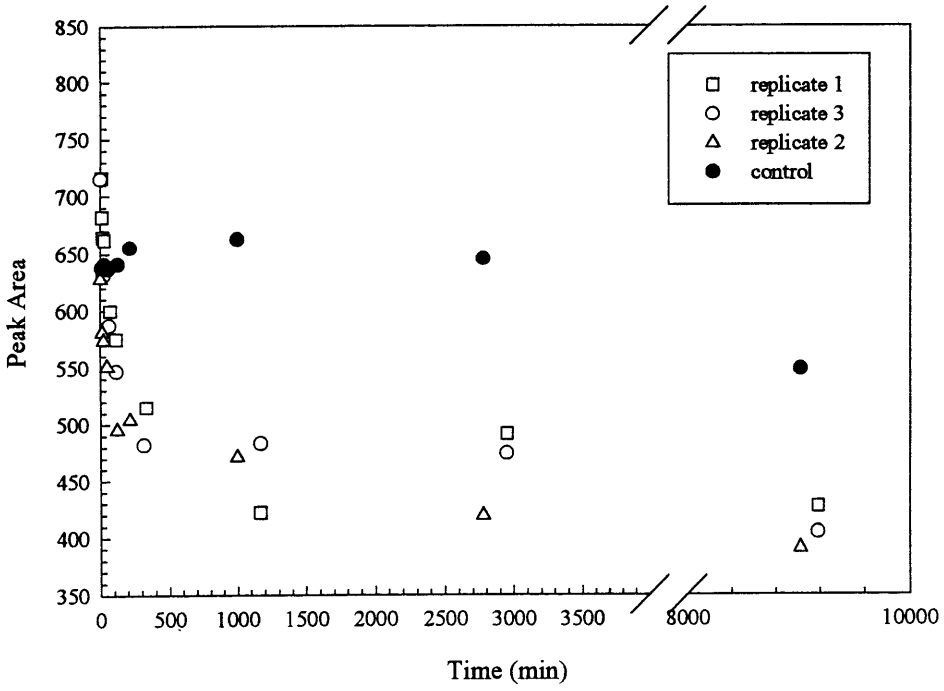

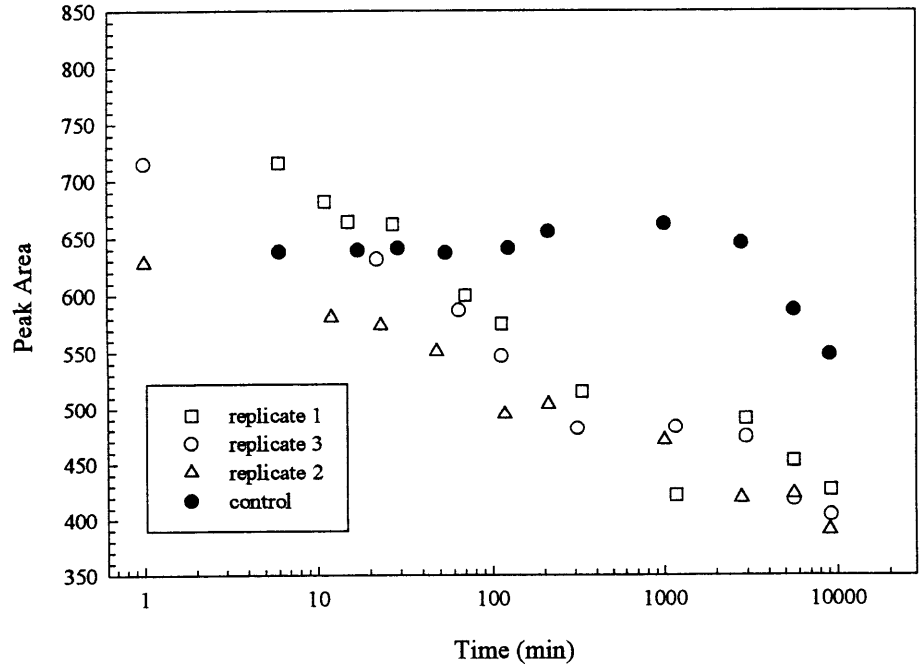

Figure D.1. Benzene uptake by Ponderosa pine chips.

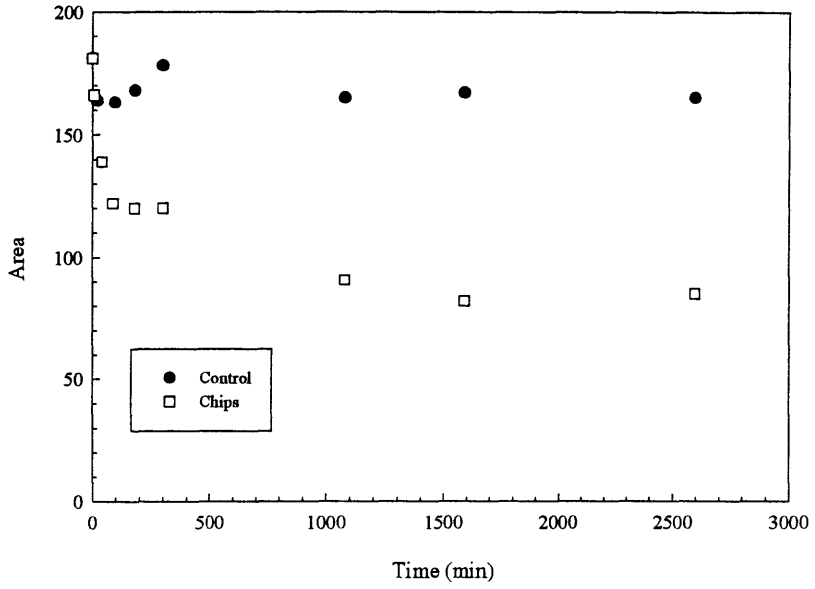

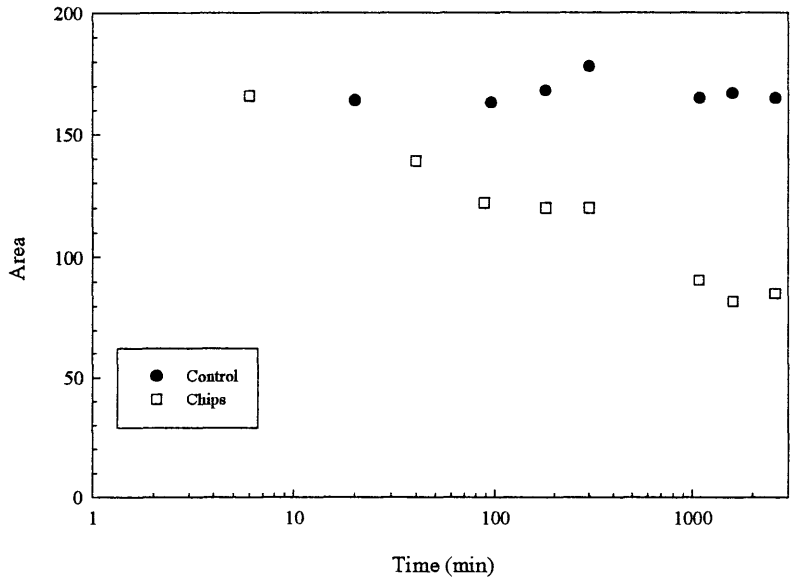

Figure D.2. *O*-xylene uptake by Ponderosa pine chips.

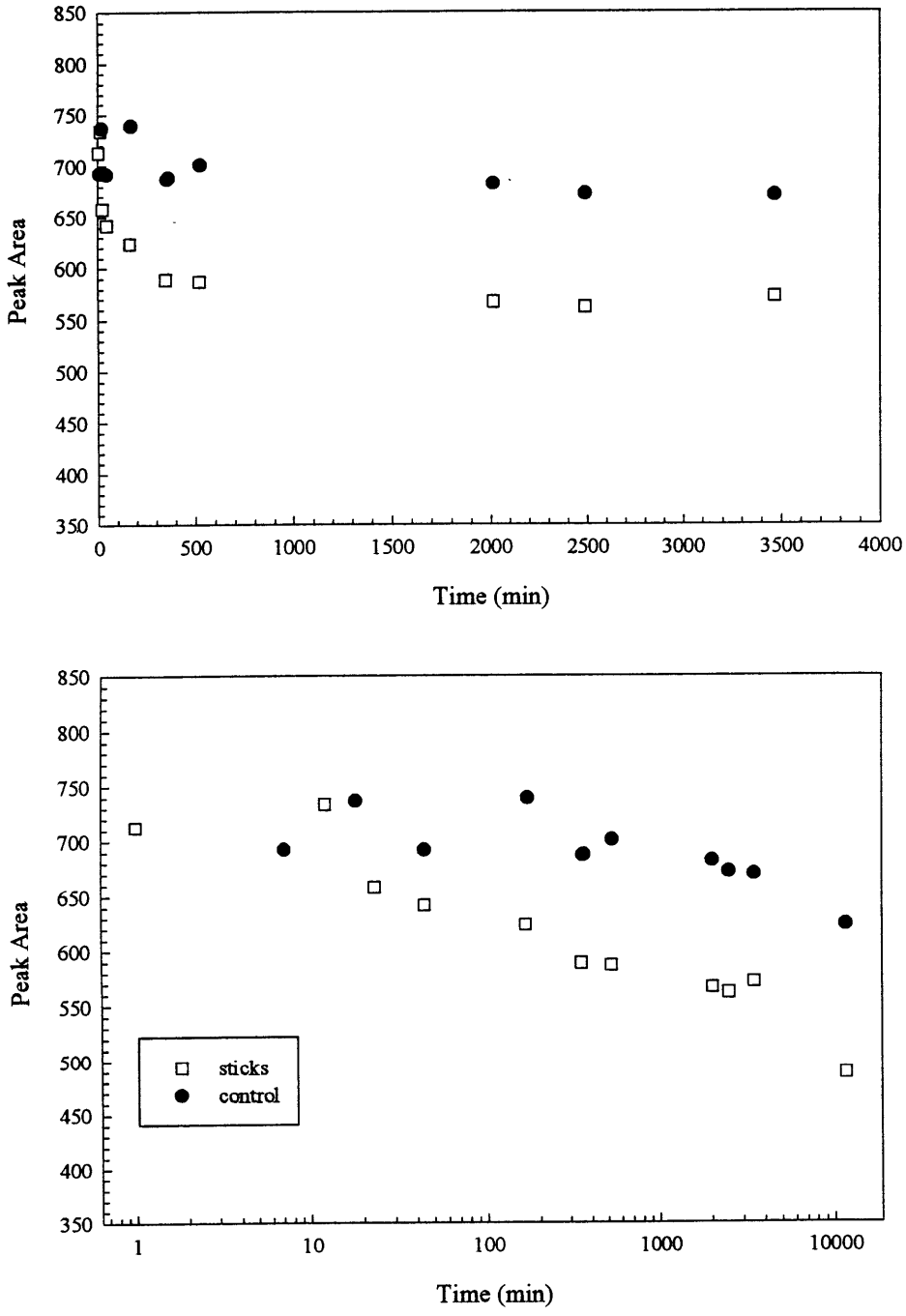

Figure D.3. Benzene uptake by Douglas fir sticks.

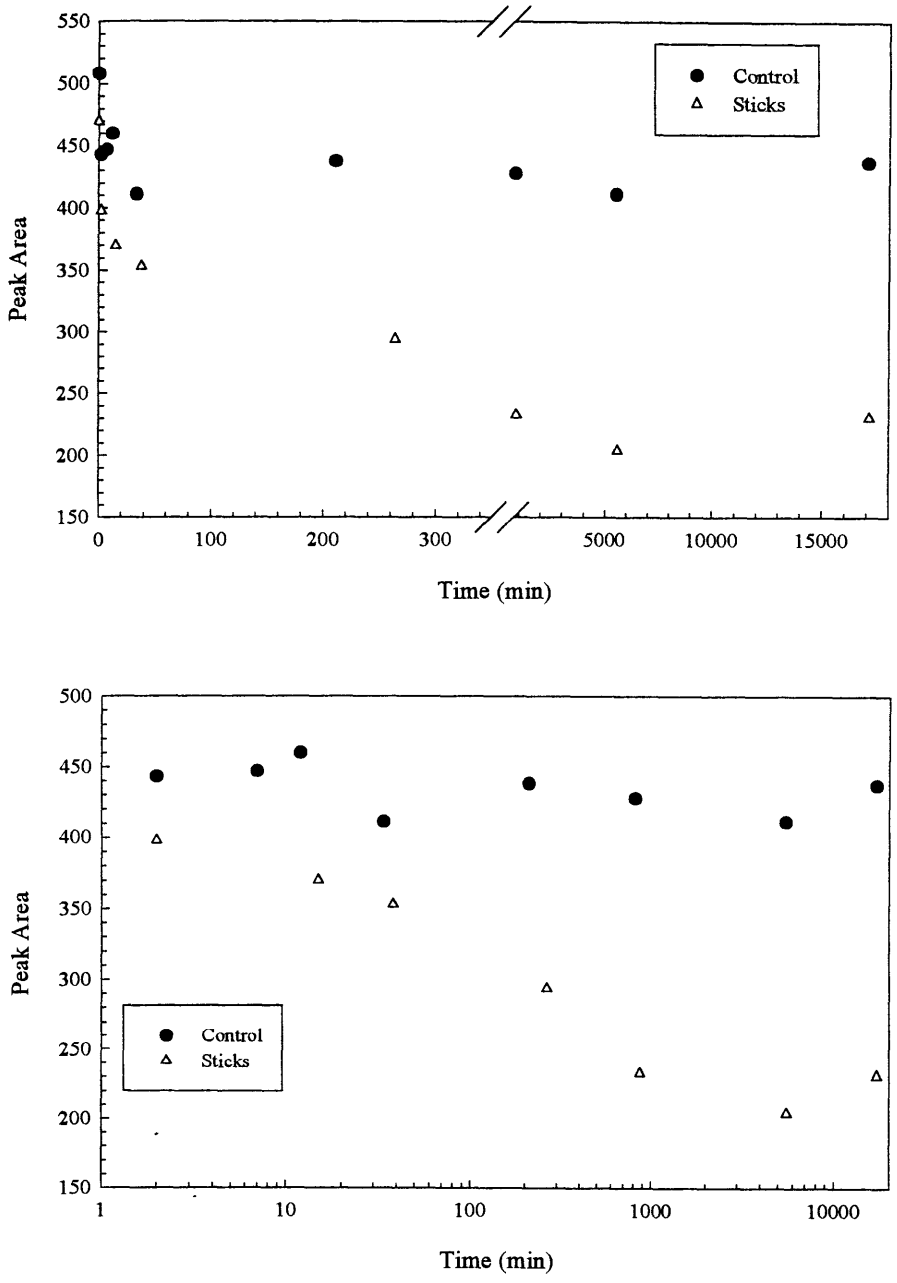

Figure D.4. Toluene uptake by Douglas fir sticks.

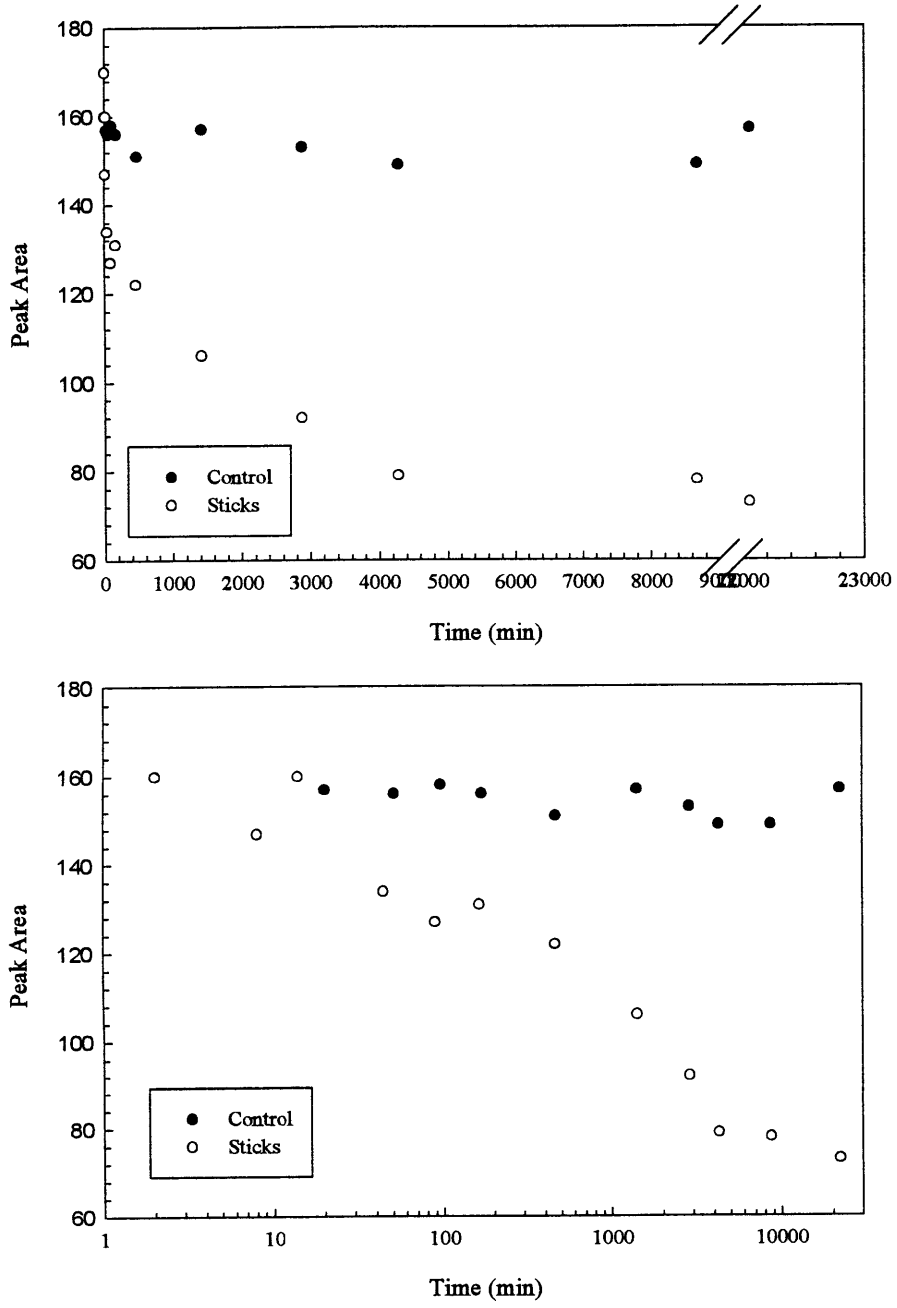

Figure D.5. *O*-xylene uptake by Douglas fir sticks.

Appendix E.

REPRESENTATIVE GAS CHROMATOGRAMS

Figure E.1. W40M coal tar (1/1250 dilution).
Note the attenuation changes during the temperature program.

The pyrene peak corresponds to a tar concentration of 9300 mg/L. Other concentration values are given in Table 2.2 (Chapter 2).

Peaks are identified with the following compound abbreviations:

NA - naphthalene
MeNA - methylnaphthalenes
C_2NA - ethyl and dimethylnaphthalenes
PH - phenanthrene
AN - anthracene
MePH - methylphenanthrenes and methylanthracenes
PY - pyrene
FL - fluoranthene
BA - benz(a)anthracene
CH - chrysene
BaP - benzo(a)pyrene
BeP - benzo(e)pyrene
BP - benzo(ghi)perylene
IP - indeno(123-cd)pyrene

BZ
EB
OX
NA
2-MeNA
1-MeNA
C2NA
PH
AN
MePH
FL
PY
BA
CH
BaP
BeP
IP
BP
4
16
8
4
2
96/06/20 - 4
1mL C2-W1B-S
1/125Z DIS in MeCl2
35 → 300(5) 8°/min TEMP PRDG.

Figure E.2. Oil isolated from the B4 boring.

96/10/22
1/200 dil ~ oil from 12-BDY-5
atten 32

Figure E.3. Pentane/acetone extract from the B4 core. Note the prevalence of polycyclic aromatic hydrocarbon peaks, reflecting the nonaqueous phase liquid coal tar in these solids. Compound abbreviations are given in Figure E.1.

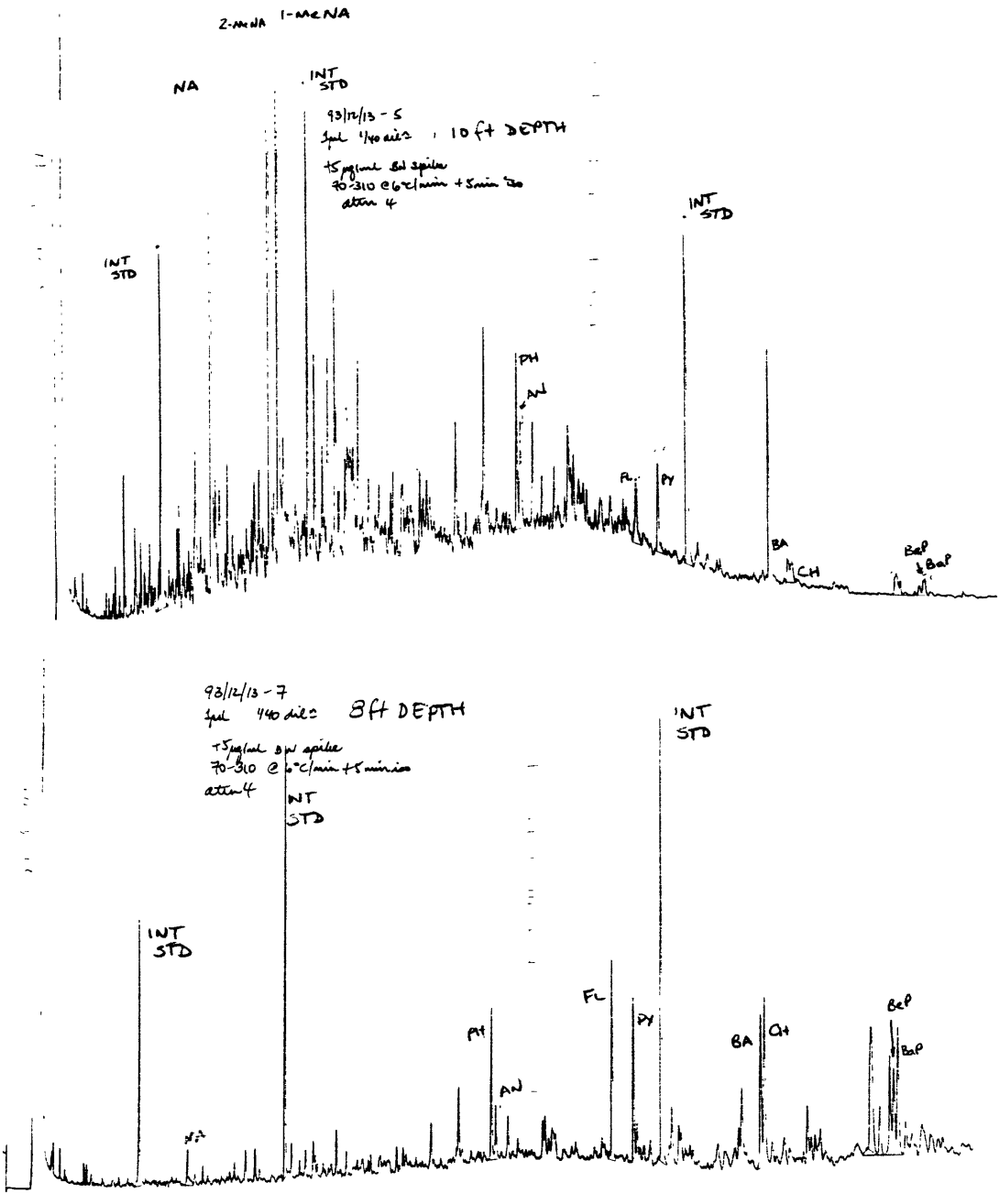
2-MeNA
1-MeNA
NA
INT STD
93/12/13 - 5
1µl 1/40 dil = 10 ft DEPTH
+5 µg/ml Sol spike
70-310 @ 6°C/min + 5min @ 310
attn 4
INT STD
INT STD
PH
AN
FL
PY
BA
CH
BeP
& BaP
93/12/13 - 7
1µl 1/40 dil = 8ft DEPTH
+5 µg/ml Sol spike
70-310 @ 6°C/min + 5 minutes
attn 4
INT STD
INT STD
INT STD
PH
AN
FL
PY
BA
CH
BeP
BaP